Knotted fields and real algebraic links

Benjamin Bode

School of Physics, University of Bristol

A dissertation submitted to the University of Bristol in accordance with the requirements for award of the degree of Doctor of Philosophy in the Faculty of Science

July, 2018

72,934 words

Abstract

This doctoral thesis offers a new approach to the construction of arbitrarily knotted configurations in physical systems. We describe an algorithm that given any link L finds a function $f : \mathbb{C}^2 \to \mathbb{C}$, a polynomial in complex variables u, v and the conjugate $\bar{v}$, whose vanishing set $f^{-1}(0)$ intersects the unit three-sphere S^3 in L. These functions can often be manipulated to satisfy the physical constraints of the system in question. The explicit construction allows us to make precise statements about properties of these functions, such as the polynomial degree and the number of critical points of $\arg f$.

Furthermore, we prove that for any link L in an infinite family, namely the closures of squares of homogeneous braids, the polynomials can be altered into polynomials from $\mathbb{R}^4$ to $\mathbb{R}^2$ with an isolated singularity at the origin and L as the link of that singularity. Links for which such polynomials exist are called real algebraic links and our explicit construction is a step towards their classification.

We also study the crossing numbers of composite knots and relate them to crossing numbers of spatial graphs. The resulting connections are expected to lead to a new approach to the conjecture of the additivity of the crossing number.

To my parents
my sister
my brother

Acknowledgements

I would like to thank my PhD supervisors Mark Dennis and Jonathan Robbins. During the last four years both of them have set a lot of time aside for me and I am very grateful for countless kind words of encouragement and for valuable feedback on earlier drafts of this thesis.

It has been a great experience to be a part of the SPOCK team and I would like to thank everyone involved, especially the other PhD students from the Knots Office.

I would also like to thank De Witt Sumners, Mikami Hirasawa and Seiichi Kamada, all of whom have been very supportive when it came to questions about my academic future. Daniel Peralta-Salas has been very generous during my time in Madrid, where much of the work that led to Chapter 7 was done. I would also like to thank Gareth Alexander for explaining several things about the Biot-Savart construction and liquid crystals to me.

I am grateful to Jon Keating, who asked exactly the right question at the right time, which led to Section 5.5, and Robert King, who showed me how to make pretty pictures of knots in Povray.

Another big thank you goes to the family Bustamante who welcomed me in their home during a conference in LA.

Most of all, I am grateful to my parents, my brother Andi, my sister Jenny and her husband Jake for all their support.

Chapter 4 and parts of Chapter 6 are based on:
Bode B, Dennis MR, Foster D and King R (2017).
Knotted fields and explicit fibrations for lemniscate knots.
Proc R Soc A **475**, 20160829.

Chapter 5 and parts of Chapter 6 are based on:
Bode B and Dennis MR (2016).
Constructing a polynomial whose nodal set is any prescribed knot or link.
(arXiv: 1612.06328).

Parts of Chapter 6 cover material that was originally published in:
Dennis MR and Bode B (2017).
Constructing a polynomial whose nodal set is the three-twist knot 5_2.
J Phys A **50**, 265204.

Chapter 7 is based on:
Bode B (2017).
Constructing links of isolated singularities of polynomials $\mathbb{R}^4 \to \mathbb{R}^2$.
(arXiv:1705.09255).

Chapter 8 is based on:
Bode B (2017).
Crossing numbers of composite knots and spatial graphs.
Topology and its Applications **243**, 33–51.

Author's Declaration

I declare that the work in this dissertation was carried out in accordance with the requirements of the University's Regulations and Code of Practice for Research Degree Programmes and that it has not been submitted for any other academic award. Except where indicated by specific reference in the text, the work is the candidate's own work. Work done in collaboration with, or with the assistance of, others, is indicated as such. Any views expressed in the dissertation are those of the author.

SIGNED: _____ DATE: _____

Benjamin Bode

Contents

List of Figures

1 Introduction

Every hurricane or tornado has at its centre a small region of relatively calm weather. This eye of the storm is the centre around which air rotates with great velocities. Real cyclones are a lot more complicated than this, but for our purposes it is enough to consider winds that are blowing in circles around a common centre point. The quiet weather at this centre, the vortex, is then merely a consequence of the continuity of wind directions. There simply is not any direction that the wind could blow in at that point without breaking this continuity and so it does not blow at all.

Tornadoes are not just winds at the surface of the earth, but they extend in the third dimension, so that the eye of the storm is not just one point at the surface of the earth, but a line that starts at the earth and rises into the sky. A good toy model for this is a cylinder that rotates around its centre axis. Points on the centre axis do not move at all, while all other points move on circles around it.

This dissertation is mostly concerned with the questions of what would happen if we could take this line at the centre of the storm and tie it into a knot, just like we would tie a knot into a piece of string and how we would describe the resulting physical system (air rotating around a knotted line) mathematically.

At first these questions seem absurdly abstract. We simply cannot grab a tornado like a piece of string. However, they originate from a very practical problem, the stability of matter, and continue to be of interest in many areas of physics.

In 1867, Lord Kelvin suggested that atoms were actually knotted vortex lines in the aether and that different chemical elements should correspond to different knot and link types [133]. This theory was largely inspired by experiments on smoke rings. In this case, air is circulating around a line very much like in

the example of the tornado. The difference is that this line does not have any open ends. It is a circle. In contrast to air, the æther was expected to be an incompressible fluid without friction. Kelvin showed that in this case the vortex lines could never pass through each other. Therefore the vortex atoms would -in contrast to the smoke rings in air - preserve their topological shape for all time, which would have explained the stability of matter.

Lord Kelvin's vortex atom theory of course turned out to be false, but it marked the birth of modern knot theory, even though Gauss had already defined the linking integral several years earlier.

Tait began a table of different knot types, believing he was constructing a table of elements. He arranged the knots that he found by the *minimal crossing number*, the minimal number of times a projection of the knotted curve crosses itself in a plane. This is still the convention of modern knot tables today.

Since then, knot theory has grown into a rich subject and has continued strong interactions with physics. Some knot invariants can be interpreted as expectation values in Chern-Simons theory and more general topological quantum field theories [136]. On the other hand, knots and other topologically conserved quantities often provide the physical system in question with a certain stability.

We now give a brief overview of our main results. The actual mathematical definitions can be found in the later chapters. In particular, Chapter 2 provides the reader with the necessary background on mathematical knot theory.

There is a wide range of so-called *knotted fields*, physical systems that contain lines that are in some sense knotted. Like smoke rings, the knots that we talk about here do not have any open ends, similar to a knot in a piece of string whose ends have been glued together.

This great variety of systems is also reflected in the many different mathematical descriptions of configurations in the different physical systems, such as vector fields, director fields or complex scalar fields. This might lead to the conclusion that in order to develop a theory of knotted fields, one would need a different machinery for each physical system. However, it turns out that complex scalar fields, i.e. functions from 3-dimensional space to the complex numbers $\mathbb{C}$, whose zero level set is knotted can also be used to construct knotted configurations in physical systems that are described by vector fields or director

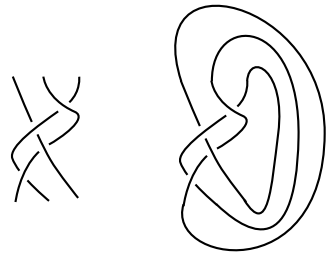

Figure 1.1: The closure of a braid to a knot or link.

fields.

Therefore the problem of constructing knotted fields reduces to the construction of analytic functions $\mathbb{R}^3 \to \mathbb{C}$ whose zero level set is knotted. We give an overview of the known constructions of knots in different physical systems in Chapter 3.

One of these constructions is based on the work of Brauner [27] and Milnor [99], who studied knots as the vanishing sets of polynomials mostly in the context of isolated singularities in four real or two complex dimensions. This has resulted in explicit polynomials for a certain class of knots, the *algebraic links*. The construction can be interpreted as being built around braids that have particularly simple parametrisations in terms of trigonometric functions. Since every knot or link with multiple components is the closure of a braid as in Figure 1.1, it is natural to try to generalise this approach.

In Chapter 4 we discuss a construction of polynomials for *lemniscate links*. These are also built from braids that have nice parametrisations in terms of trigonometric functions. As such they have symmetries that we can employ to prove some properties of knots in this class.

Lemniscate knots have first been constructed as vanishing sets of polynomials and knots in physical systems in [41, 79]. However, there were several misconceptions in the literature that we correct here.

The key observation in the process of generalising the construction of Brauner is that all braids can be parametrised in terms of trigonometric functions. These might be arbitrarily complicated, but in principle we can construct polynomials with an arbitrarily knotted zero level set once we have such a parametrisation. In Chapter 5 we provide the reader with an instruction on how to find such parametrisations for any given braid using trigonometric interpolation. Furthermore, we can give bounds on the degree of the trigono-

metric polynomials that form this parametrisation. We therefore know that the parametrisations that we find are not arbitrarily complicated.

This explicit construction of polynomials with knotted vanishing sets allows us to generate arbitrarily knotted configurations in many physical systems.

We find that we can change our construction such that the resulting functions share nice properties with Brauner's and Milnor's polynomials.

Our construction actually takes place in four real dimensions, exactly like Brauner's and Milnor's. We obtain a function $f : \mathbb{R}^4 \to \mathbb{C}$ such that the intersection of the vanishing set of f with the unit three-sphere results in the desired link. The polynomials from three-dimensional space are then the result of a stereographic projection. Brauner's and Milnor's polynomials are by nature complex. They can be written as polynomials $f : \mathbb{C}^2 \to \mathbb{C}$ in two complex variables u and v. It is a feature of our algorithm that the resulting functions can be written as polynomials in u, v and the complex conjugate $\bar{v}$. They are therefore holomorphic in one of the complex variables, but not in the other. We show in Chapter 5 that we can make some changes to our construction such that it gives complex polynomials $f : \mathbb{C}^2 \to \mathbb{C}$. However, in this case the desired link is only a sublink of $f^{-1}(0) \cap S^3$.

The polynomials that were constructed by Brauner [27] and Milnor [99] have the property that their argument is a fibration of the link complement over the circle. This means that for any of their polynomials $f : \mathbb{C}^2 \to \mathbb{C}$ with a link L the vanishing set $f^{-1}(0) \cap S^3$ of f on the three-sphere $S^3 \subset \mathbb{C}^2$, the map $\arg(f) = f/|f|$ from $S^3 \backslash L$ to the circle S^1 does not have any critical points, so the three space-derivatives do not vanish simultaneously. We show in Chapter 6 that if a braid satisfies some algebraic properties, i.e. if it is *homogeneous*, then we can perform the steps in our construction such that we obtain a polynomial that also gives a fibration of the complement of the corresponding link. The fact that closures of homogeneous braids are fibred was shown by Stallings [127]. More concretely, we introduce a measure of how far a given braid is from being homogeneous and this integer is an upper bound on the number of argument-critical points of our constructed polynomials.

The third desirable property of Brauner's and Milnor's polynomials that we are trying to maintain is the existence of an *isolated singularity*. We find that if a braid is the square of a homogeneous braid, then we can construct polynomials $f : \mathbb{R}^4 \to \mathbb{R}^2$ with the corresponding link around an isolated singularity. This is discussed in Chapter 7. Links for which such polynomials exist are called

real algebraic links and at the moment it is not known which links have this property. Our explicit construction shows that all links corresponding to squares of homogeneous braids are real algebraic. In this case $\arg(f)$ also is a fibration of the link complement. The principle behind the existence of fibrations in the form of arguments of polynomials can also be used to define new braid invariants.

Thus for certain knots and links we can make sure that our polynomials have one or two of the nice properties of Brauner's and Milnor's polynomials: Holomorphicity, the fibration property or the existence of an isolated singularity.

In Chapter 8 we approach the question of how the minimal crossing number of a knot behaves under the connected sum, a binary operation on the set of all knots. It is an old (but still open) conjecture that the crossing number is additive, i.e. the crossing number of the sum of two knots is simply the sum of their crossing numbers.

We prove relations between the crossing numbers of composite knots and spatial graphs and use these to establish conditions that, if satisfied, imply the additivity or at least a lower bound for the crossing number of the sum of two knots in terms of the crossing number of its summands.

While this last chapter differs thematically quite a bit from the earlier chapters, there is an overarching theme of a philosophical nature that connects the different parts of this thesis, namely the worth of explicit constructions. Mathematicians are often satisfied with the existence of objects, while physicists often require explicit functions to work with, making a more constructive approach necessary. However, we find that the applications in Physics are not the only motivation to look for explicit constructions of mathematical objects. An algorithm like in Chapter 5 offers us a deeper understanding of the functions that we construct. This allows us to prove results about these objects that go beyond the previously known existence results. Chapters 4 -7 all discuss explicit constructions of polynomials and properties that the constructed functions must have. Most of the inequalities between crossing numbers of spatial graphs and composite knots in Chapter 8 are derived by constructing a diagram of a certain spatial graph starting from a knot diagram or the other way around. We can then express the number of crossings of the constructed diagram in terms of the number of crossings of the initial diagram and obtain inequalities relating the minimal crossing numbers to each other.

2 Notation and background on Knot Theory

This chapter is an overview of the fundamentals of knot theory. Most of the material can be found in much more detail in [4, 58, 89, 115].

2.1 Knots and links

The central objects of this dissertation are knots and links. Mathematical knots are in many ways similar to the knots in pieces of string or rope that we encounter in our daily lives. The main difference is that knots in the mathematical sense do not have open ends. We can think of this as tying a knot into a piece of string and then gluing the two ends of the string together.

Definition 2.1. *A **knot** is a smooth (i.e. C^∞) embedding of the circle S^1 into the three-sphere S^3.*

This definition is equivalent to saying that a knot is a simple closed curve in S^3. Some authors prefer to define knots as closed curves in $\mathbb{R}^3$, as opposed to S^3, which only leads to very minor differences in the theory. An *n-component link* is a disjoint union of n knots and hence an embedding of n copies of S^1 into S^3.

Knot theorists are interested in the classification of knots. Since intuitively the knottedness of a curve does not change when the curve is moved around in space, we want to consider two knots K_1 and K_2 to be equivalent if one can be deformed into the other without cutting. Even though we have not yet defined what we exactly mean by such a deformation, it already shows the significance of working with closed curves instead of the open knots familiar to us from everyday life. Since every open string can be untied, the resulting theory does not capture any knotting. There is some interest in studying open knotted

curves as well, with knotoids [134], virtual knots [71] and theta curves [70] being the most active areas of research, but they will not be discussed here.

There are multiple things that could be reasonably referred to as a deformation of a knot. We will briefly argue which of these are good choices to take for the definition of an equivalence relation on the set of knots and links.

Definition 2.2. *Two knots K_1 and K_2 are **isotopic** if there is a continuous map $\phi : S^1 \times [0,1] \to S^3$ such that $\phi(S^1, 0) = K_1$, $\phi(S^1, 1) = K_2$ and $\phi(\bullet, t)$ is an embedding for every $t \in [0,1]$.*

This definition captures our intuition about moving a knot around in space. Since the isotopy is continuous, the motion of the knot in space (where we consider t as a time parameter going from 0 to 1) is similar to our experiences and the fact that $\phi(\bullet, t)$ is an embedding implies that the curve never passes through itself, i.e. we never have to make any cuts while we deform the knot.

However, the continuity of ϕ is not enough to give us a theory that captures what it means to be knotted in reality. We could take any knotted curve and shrink the knotted part further and further until we are left with an unknotted circle. Since we can do this with any knot and the shrinking process is continuous, all knots are isotopic to each other. Therefore we have to add an extra condition on the isotopy ϕ.

Definition 2.3. *There is a **smooth isotopy** between two knots K_1 and K_2 if there exists a map ϕ as in Definition 2.2 which is smooth.*

The smoothness condition excludes the possibility of shrinking every knot away and we are indeed left with an equivalence relation that matches our intuition. However, it is not the only reasonable such definition.

Definition 2.4. *There is a **smooth ambient isotopy** between two knots K_1 and K_2 if there is a smooth map $\phi : S^3 \times [0,1] \to S^3$ such that $\phi(K_1, 0) = K_1$, $\phi(K_1, 1) = K_2$ and $\phi(\bullet, t)$ is a homeomorphism for every $t \in [0,1]$.*

When talking about the relation between the two knots, we often say that they are ambient isotopic (dropping the 'smooth'). An ambient isotopy moves all points in S^3 and not only the knot. The knot is merely dragged along, while the points in S^3 are shifted around.

The following equivalence relation is not motivated by the idea of moving knots in space, but has the advantage that it is closer to typical topological equivalence relations.

Definition 2.5. *Two knots K_1 and K_2 are **diffeomorphic** if there is an orientation-preserving diffeomorphism $\phi : S^3 \to S^3$ such that $\phi(K_1) = K_2$.*

It is easy to check that all three definitions give equivalence relations on the set of knots. The same definitions extend trivially to the set of links as well. Fortunately, we do not have to choose between the three different notions of equivalent knots because, while they are different at first sight, they all give rise to the same equivalence relation [58].

The equivalence of Definition 2.3 and Definition 2.4 follows from the Isotopy Extension Theorem. Here we only state the case for smooth maps.

Theorem 2.6. *[60] Let $V \subset M$ be a compact submanifold of a closed manifold M and $\phi : V \times [0,1] \to M$ be a smooth isotopy of V. Then ϕ extends to a smooth ambient isotopy from $\phi(V,0)$ to $\phi(V,1)$.*

In the case of knots we take $V = S^1$, $K_1 = \phi(V,0)$ and $K_2 = \phi(V,1)$.

The central question of knot theory is to determine whether two given knots (or links) K_1 and K_2 are in the same equivalence class with respect to any of the three equivalent equivalence relations defined in Definition 2.3, Definition 2.4 and Definition 2.5. If this is the case, we say K_1 and K_2 have the same knot type and more often we somewhat inexactly say that K_1 and K_2 are the same knot.

While there is no known practical algorithmic solution to the problem of deciding whether two knots are equivalent, the concept of *knot invariants* has proven very effective in telling different knots apart. Generally speaking, a knot invariant is a function from the set of equivalence classes of knots to some class of mathematical objects. We will see some examples of this later, but at the moment we can think of this as associating a mathematical object $V(K)$ (a number or a polynomial or a vector space etc.) to any knot K and if two knots K_1 and K_2 are equivalent, then their corresponding invariants $V(K_1)$ and $V(K_2)$ must be identical too, i.e. $V(K_1) = V(K_2)$. This is very useful, since we know exactly when two numbers (or two polynomials or two vector spaces) are the same.

Note that while we can use knot invariants to find that two knots are different, there typically are knots K_1 and K_2 that are not equivalent, but have the same invariant $V(K_1) = V(K_2)$ nonetheless.

It turns out that all the information about a knot can be captured in knot (or link) diagrams, projections of the space-curve into the plane (cf. Figure 2.1). The image of this projection is some closed curve in the plane potentially with

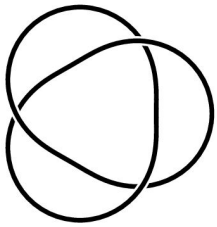

Figure 2.1: A knot diagram representing the trefoil knot 3_1.

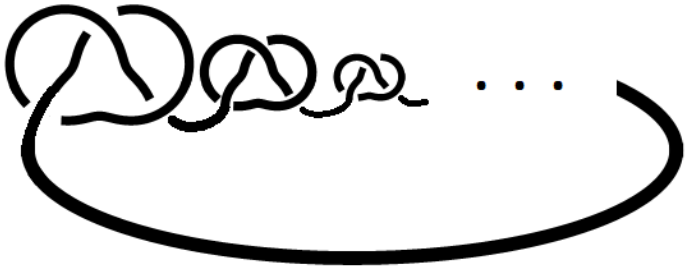

Figure 2.2: A diagram of a wild knot.

some points where the projection is not injective. We call a knot diagram *regular* if the curve has at most double points (i.e. all points where the projection is not injective have exactly two preimage points on the space-curve) and the two parts of the curve that meet at each such point intersect transversally. We call each such double point a crossing. In order to keep track of which of the two preimage points on the space-curve was above the other one in the third space-direction, we erase a bit of the undercrossing strand in a neighbourhood of the crossing as in Figure 2.1.

Occasionally it is advantageous to give links an orientation. Since they are 1-manifolds this simply amounts to drawing an arrow on each component.

Example: The *crossing number* $c(L)$ of a link L is the minimal number of crossings of any link diagram representing L. Even though it is very easy to count the crossings of a link diagram, it is in general very hard to calculate $c(L)$, since there are infinitely many diagrams representing L and in general there is no known method to determine whether a given diagram D is the simplest possible in the sense that all other diagrams representing L must have at least as many crossings as D. The only knot with zero crossing number is the planar embedding of the circle, the *unknot* O. Note that the smoothness in Definition 2.1 is necessary to avoid so-called *wild knots* as in Figure 2.2 with infinitely

many crossings.

There are several other link invariants that are built around the same principle. We associate a number to every link diagram and the minimum taken over all diagrams of one equivalence class will then automatically be a link invariant.

Example: The *bridge number* $br(D)$ of a diagram D is the number of local maxima (or equivalently local minima) of the height function on the diagram D. The bridge number $br(L)$ of a link is then (analogously to the crossing number) defined to be the minimum of the bridge numbers of all diagrams representing the link type L.

The diagram in Figure 2.1 for example has 3 crossings and 2 bridges.

Note that while each link diagram representing a link L contains all information about all properties of L, there are infinitely many diagrams representing L. Reidemeister showed that the equivalence question of two links L_1 and L_2 can be translated into a question about the equivalence of diagrams.

Theorem 2.7. *[114] Two link diagrams represent the same link if and only if they are related by a finite sequence of the Reidemeister moves depicted in Figure 2.3.*

Figure 2.3 should be interpreted as a statement of equivalence of two link diagrams that are identical outside a disc and whose behavior inside that disc is shown in the figures.

Reidemeister moves can be a great help to show that two diagrams represent the same link. We 'simply' have to find a sequence of moves. The problem of course is that there are infinitely many, arbitrarily complicated sequences and we cannot test every single one of them. Some work has been done to find bounds on the possible lengths and patterns of sequences of Reidemeister moves [36, 37, 56], but the bounds are still so large that exhausting the list possible Reidemeister sequences is not a practical approach.

The true value of Reidemeister's theorem is that it makes it easier to show that a quantity associated with a link diagram is a link invariant. Say we have some function from the set of link diagrams to some target set, say the integers or space of polynomials or the set of vector spaces. Then if this function is invariant under the three Reidemeister moves, it is a link invariant.

Example: Let L be an oriented 2-component link with components L_1 and L_2. Then the *linking number* of L_1 and L_2 is denoted by $lk(L_1, L_2)$ and can be

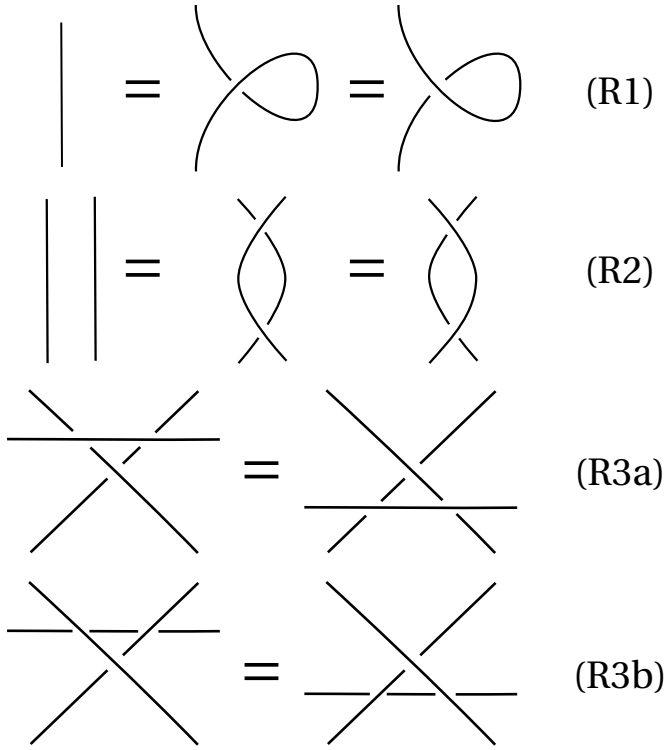

Figure 2.3: The three Reidemeister moves.

calculated by the integral

$$lk(L_1, L_2) = \frac{1}{4\pi} \oint_{L_1} \oint_{L_2} \frac{r_1 - r_2}{|r_1 - r_2|^3} \cdot (dr_1 \times dr_2), \tag{2.1}$$

where r_1 and r_2 are points on L_1 and L_2 respectively, so we integrate along the components L_1 and L_2.

Alternatively, the linking number can be calculated from any diagram by the following rule. We colour L_1 blue and L_2 red and then assign a label to each crossing, where L_1 passes over L_2. The label is either $+1$ or -1 depending on which type of the two crossings in Figure 2.4 it is. Then the linking number is the sum over all the labels for a given diagram.

This means that the integral in Equation (2.1) is always an integer and it is easy to check that the Reidemeister moves do not change the sum of labels. Therefore $lk(L_1, L_2)$ is an invariant of L.

Example: The *Jones Polynomial* $V(L)$ is a Laurent-polynomial-valued link invariant in one variable $t^{1/2}$. For any diagram the Jones polynomial can be

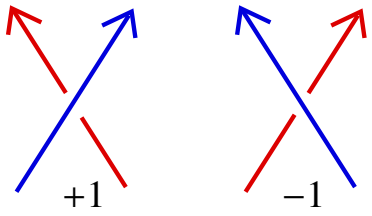

Figure 2.4: The rule for labelling oriented crossings to compute the linking number.

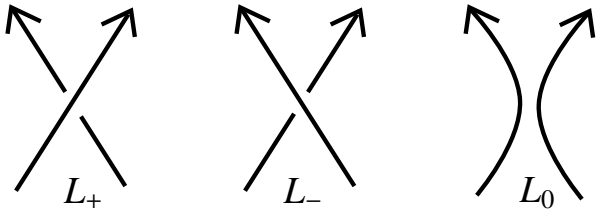

Figure 2.5: The three types of crossings in the skein relation.

calculated recursively with the following rules called skein relations:

$$V(O) = 1$$
$$(t^{1/2} - t^{-1/2})V(L_0) = t^{-1}V(L_+) - tV(L_-), \tag{2.2}$$

where the terms in the last equation should be interpreted as the Jones polynomial of three diagrams that are identical outside a disc in the plane and whose behavior inside that disc is illustrated by Figure 2.5.

Example: The *Alexander polynomial* $\Delta(L)$ is another Laurent-polynomial-valued link invariant. It satisfies the skein relations:

$$\Delta(O) = 1$$
$$(t^{1/2} - t^{-1/2})\Delta(L_0) = \Delta(L_+) - \Delta(L_-). \tag{2.3}$$

In this normalisation the Alexander polynomial satisfies $\Delta(t^{-1}) = \Delta(t)$. Occasionally, a different normalisation is used, where we multiply $\Delta(t)$ by a power of $t^{1/2}$ such that it becomes a polynomial in $t^{1/2}$ with non-zero constant term. In any case, the degree of the Alexander polynomial $\deg \Delta$ refers to the span of Δ, i.e. the difference between its largest and its smallest exponent of t.

Both the Jones polynomial and the Alexander polynomial are graded Euler characteristics of homological link invariants. For example, Khovanov homology [76] associates to each link L a bigraded vector space $Kh(L) = \bigoplus_{i,j} Kh^{i,j}(L)$ and

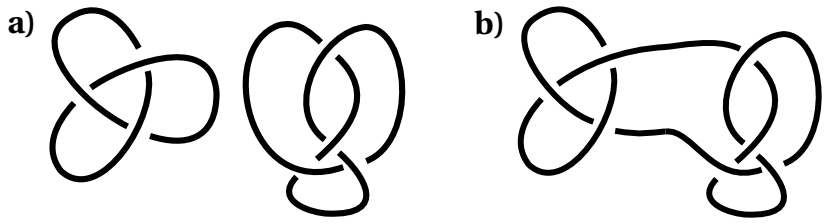

Figure 2.6: The connected sum operation on the level of diagrams. a) A diagram of the trefoil knot 3_1 and the figure eight knot 4_1. b) A diagram of their connected sum $3_1\#4_1$.

the Jones polynomial is

$$V(L)(t) = \frac{1}{t^{1/2} - t^{-1/2}} \sum_{i,j} (-1)^{i+j+1} t^{j/2} \dim Kh^{i,j}(L). \tag{2.4}$$

Similarly, the Alexander polynomial is the graded Euler characteristic of the vector space that is given by the Knot Floer homology of a link [109]. These homological invariants are strictly better in distinguishing knots than their polynomial counterparts, but also harder to compute.

Both the Jones polynomial and the Alexander polynomial are specializations of a two-variable link polynomial, the HOMFLYPT polynomial [53], which turns out to be another graded Euler characteristic of a triply-graded homological link invariant, HOMFLYPT homology [77].

There is a notion of addition on the set of all oriented knot types. Given two oriented knots K_1 and K_2 and a small radius $\epsilon > 0$ we can form the *connected sum* $K_1\#K_2$ by picking a point x_i on each of the curves and deleting an ϵ-ball $B_\epsilon(x_i)$ around each of them. We can then glue $S^3 \backslash B_\epsilon(x_1)$ to $S^3 \backslash B_\epsilon(x_2)$ along their boundaries, identifying the intersection points of K_1 with $B_\epsilon(x_1)$ with the intersection points of K_2 with $B_\epsilon(x_2)$ with matching orientation. This yields an oriented simple closed curve $K_1\#K_2$ in $S^3\#S^3 = S^3$.

It turns out that the connected sum is well-defined, meaning that it does not depend on the specific choice of space curve representative of the knot types, the chosen points x_i or the exact value of ϵ as long as it is small enough. The corresponding process on a diagrammatic level is shown in Figure 2.6.

The connected sum is associative and commutative and the unknot O is an identity, i.e. $O\#K = K\#O = K$ for all knots K. However, there are no inverses with

respect to the connected sum, so the set of knots forms a commutative monoid, but not a group.

Definition 2.8. *A knot K is called **prime** if for all knots K_1 and K_2 with $K = K_1\#K_2$ then either $K_1 = K$ and $K_2 = O$ or $K_1 = O$ and $K_2 = K$.*

If a knot is not prime, it is called composite.

Like in the case of prime numbers, there is a unique (up to reordering of the factors) factorisation of a knot into its factors, i.e. every knot K can be written as $K = K_1\#K_2\#\ldots\#K_n$, where all K_i are prime knots, and if two prime decompositions are equal, $K_1\#K_2\#\ldots\#K_n = K_1'\#K_2'\#\ldots\#K_{n'}'$, then $n = n'$ and $K_i = K'_{\pi(i)}$ for all $i \in \{1, 2, \ldots, n\}$ and some permutation $\pi \in S_n$.

With this notion of addition it is now a natural question how knot invariants behave under the connected sum. The Jones polynomial for example can be shown [64] to satisfy

$$V_{K_1\#K_2}(t) = V_{K_1}(t)V_{K_2}(t) \tag{2.5}$$

and the bridge number [122] satisfies

$$br(K_1\#K_2) = br(K_1) + br(K_2) - 1. \tag{2.6}$$

The crossing number on the other hand is only conjectured to be additive with respect to the connected sum $c(K_1\#K_2) = c(K_1) + c(K_2)$, but it is not known in general. We will return to this problem in Chapter 8.

All the information of a knot diagram can be stored in a sequence of numbers in the following way. Orient the knot diagram D and pick an arbitrary point P on the curve as the starting point. We then follow the curve in the prescribed orientation and label the crossings as we visit them. The first crossing that we encounter gets the label 1. We then travel along the curve until we reach the next crossing. If it has not been labeled yet, it obtains the label 2, or more generally a label that is one greater than the crossing that was last labeled. If the crossing already has a label we simply keep following the curve to the next crossing.

Once all crossings have a label, we can form the *Gauss code* of the diagram D as follows. Again we follow the curve starting at P. This time we keep track of the order in which we encounter the crossing by writing down the label of each crossing that we encounter along with a plus or minus-sign indicating whether we are traversing the crossing by an over- or undercrossing strand.

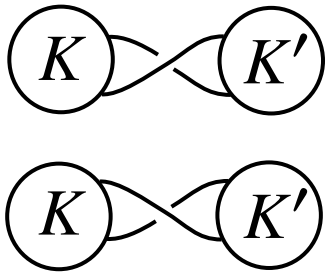

Figure 2.7: Two reducible crossings. K and K' are arbitrary knots with open ends on the boundary of the ball.

Proceeding like this produces a sequence of integers, where each of the numbers $\{\pm 1, \pm 2, \ldots, \pm c(D)\}$ appears exactly once. Furthermore, the first time that a number of absolute value i appears is after the first time that a number of absolute value k appears for all $k = 1, 2, \ldots, i-1$.

Given this sequence one can reconstruct the diagram uniquely. It is however not a knot invariant, since different diagrams or different choices of starting point lead to a different sequence. It also depends on the chosen orientation of the curve. The diagram of the trefoil in Figure 2.1 for example produces the Gauss codes $1, -2, 3, -1, 2, -3$ or $-1, 2, -3, 1, -2, 3$ depending on the starting point and the chosen orientation. We say a diagram is alternating, if it has a Gauss code with alternating signs like in the example of the trefoil diagram. Note that this property is independent of the choice of orientation and starting point. A knot is *alternating* if it can be represented by an alternating diagram.

A knot diagram is called *reduced* if there are no crossings as in Figure 2.7, which can be easily removed. One of the Tait conjectures says that every diagram that is reduced and alternating, is a minimal diagram. This was proven by Thistlethwaite [131, 132], Murasugi [102, 103] and Kauffman [69] and makes it possible to make statements about the minimal crossing numbers of alternating knots. In particular, it is known that for alternating knots the crossing number is additive with respect to the connected sum.

A class of links that is very well studied is the family of *torus links*. These are all the links that can be drawn on the surface of a torus that is trivially embeddded in S^3. These are characterised by their homotopy classes on the torus and thus by two integers p and q, counting the number of times the links go around the longitude and the meridian. The corresponding torus knot is called the (p,q)-torus knot and often denoted $K_{p,q}$.

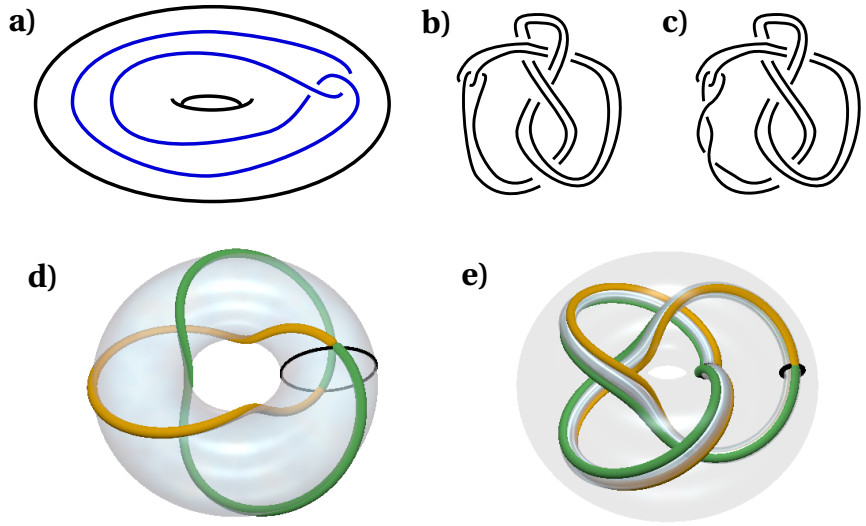

Figure 2.8: The definition of satellite and cable knots. a) An embedding of the unknot into the solid torus. b) The untwisted Whitehead double of the figure-eight knot. c) A twisted Whitehead double of the figure-eight knot. d) The trefoil knot on the surface of an unknotted torus. e) The $(2,3)$-cable of a trefoil knot embedded in an unknotted solid torus.

Besides the connected sum there is another operation that uses two knots to generate a new knot. We embed a knot K_1 into an unknotted solid torus in such a way that there is no ball inside the torus containing K_1 and K_1 is not the central core $0 \times S^1$ of the solid torus. Now take a non-trivial knot K_2 with a framing, i.e. a non-zero normal vector field $\mathbf{n}$ on K_2. For small values of $\epsilon > 0$ this framing provides us with a second simple curve $K_2' = \{p + \epsilon \mathbf{n}(p) : p \in K_2\}$. We remove the tubular neighbourhood $N_\epsilon(K_2)$ of K_2 of radius ϵ from S^3 and glue the torus containing K_1 to the boundary of $S^3 \backslash N_\epsilon(K_1)$ such that the longitude of the torus is identified with K_2'. This means essentially that we tie the solid torus that contains K_1 into a knot K_2 and the knot that one obtains in this way is called the *satellite knot* K. We call K_2 the companion knot of K. The knot K_1 is usually referred to as the pattern.

If K_1 is embedded into the solid torus as in Figure 2.8a), then K is called the *Whitehead double* of K_2. If the linking number of K_2 and K_2' is zero, then we say the satellite is *untwisted*. Otherwise we say it is *twisted*.

If K_1 is a torus knot K_{p_1,q_2}, there is a very natural embedding into the solid torus, namely the one into the boundary. Taking the satellite knot of K_{p_1,q_1} where the companion knot K_{p_2,q_2} is also a torus knot, is called *cabling* K_{p_1,q_1} by K_{p_2,q_2}. The result is not a torus knot, but again there is a very natural embedding

into the solid torus as in Figure 2.8e), which can again be tied into a torus knot. The result of iterating this process is called an *iterated cable of torus knots* and we call the numbers (p_1, q_1), $(p_2, q_2), \ldots (p_n, q_n)$ the cabling coefficients.

The satellite knots form an important family of knots. In fact a given knot belongs to exactly one of the following families: satellite knots, torus knots and hyperbolic knots.

A knot K is called *hyperbolic* if there exists a hyperbolic metric on the knot complement $S^3 \backslash K$ and there appear to be close connections between the volume of the knot complement with this hyperbolic metric and the Jones polynomial [67].

Changing the signs of all crossings (over to under and under to over) in a diagram D of a link L results in a diagram of the mirror image of L, denoted by $m(L)$. Some link invariants have trouble discriminating them, for example the Alexander polynomial satisfies $\Delta_L(t) = \Delta_{m(L)}(t)$, but in general the two links are not isotopic.

If L is ambient isotopic to its mirror image, we say L is *achiral* or *amphichiral*. The precise definition is that L is achiral if there exists an orientation-reversing homeomorphism T of S^3 to itself that maps L to itself. If L carries an orientation, we can ask whether T changes that orientation or not. If T^2 is the identity and $T(L)$ is isotopic to L as oriented links, then we say L is *strongly positively amphichiral*. If T^2 is the identity and $T(L)$ is isotopic to L with flipped orientation, we say L is *strongly negatively amphichiral*.

The trefoil knot in Figure 2.1 is chiral. It is not isotopic to its mirror image. However, it possesses a different symmetry. Rotating the diagram by $2\pi/3$ results in the same diagram again, so it has a cyclic symmetry of order 3. In general we call a link L *r-periodic* if it has a diagram that misses the origin and is mapped to itself by a $2\pi/r$-rotation.

Murasugi [101] studied Alexander polynomials of periodic knots and found conditions on their reductions mod r and on their degrees if r is a prime power. His results are very useful even when r is not a prime power though, since an r-periodic link is by definition also a q-periodic link for all divisors q of r.

2.2 Fibred Links

The following notions are crucial in the discussion of differentiable functions and their relation to knots in the later chapters. Let $f : M \to N$ be a differentiable

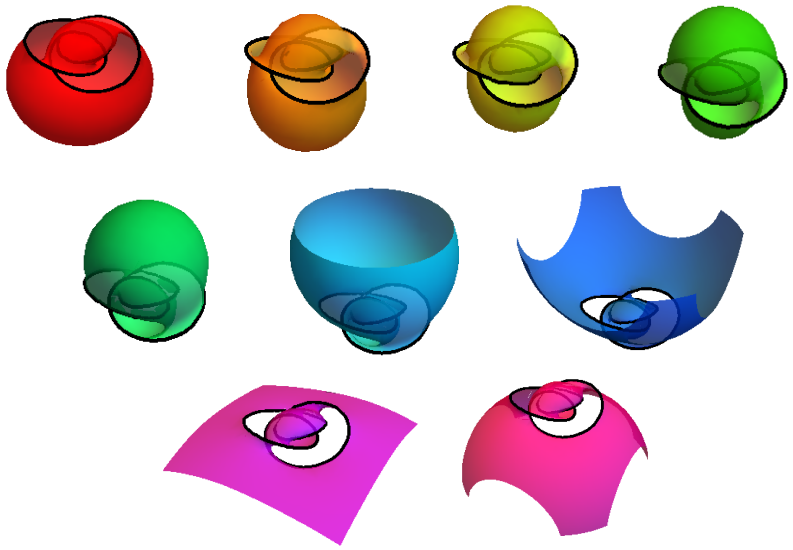

Figure 2.9: A fibration of the complement of the figure eight knot. Each subfigure shows the level set of a fibration map, a Seifert surface. In this case the fibration map is the argument of a polynomial constructed as Chapters 4-6.

map between manifolds M and N. Then we say that $x \in M$ is a *regular point* if the gradient $\nabla_M f(x)$ has full rank. Note that while the gradient ∇_M on M is defined in terms of local coordinates, whether the matrix has full rank or not does not depend on the choice of coordinates. A point that is not regular is called a *critical point.*

If x is a critical point of f, we say $f(x) \in N$ is a *critical value.* If a value $y \in f(M) \subset N$ is not critical, it is a *regular value*

Definition 2.9. *A **Seifert surface** S of a link L is an oriented 2-manifold in S^3 whose boundary ∂S is equal to L.*

Every link L admits infinitely many Seifert surfaces S and the minimal genus $g(S)$ of all these surfaces is by definition the *genus of the link* $g(L)$. We have $g(K_1 \# K_2) = g(K_1) + g(K_2)$ for all knots K_1 and K_2. This and the fact that the unknot is the only knot with genus equal to zero shows that the connected sum operation does not allow for any inverses.

Definition 2.10. *An n-component link L is called **fibred** if there is a map $\phi : S^3 \backslash L \to S^1$ that is a fibration and in a tubular neighbourhood $T(L) = (\bigcup_{j=1}^{n} S^1) \times D \backslash \{0\}$ of L is the projection of $D \backslash \{0\}$ onto S^1.*

Figure 2.10: A fibration of a knot complement in a neighbourhood of a segment of the knot.

Note that the condition on the behaviour of the fibration map ϕ in the tubular neighbourhood $T(L)$ means that the level sets of ϕ look like Figure 2.10.

Theorem 2.11 (Ehresmann's Fibration Theorem)**.** *[43] Let M and N be compact smooth manifolds and let $\phi : M \to N$ be a smooth map. Then ϕ is a locally trivial fibration if ϕ is surjective and does not have any critical points.*

By the Ehresmann Fibration Theorem 2.11 the definition of a fibred link L is equivalent to the existence of a map $\phi : S^3\backslash L \to S^1$ (with the correct property in $T(L)$) which does not have any critical points, i.e. there are no points in $S^3\backslash L$ where all three first partial derivatives vanish simultaneously. This follows directly from Theorem 2.11 with $M = S^3\backslash T(L)$, $N = S^1$ and $T(L)$ an open tubular neighbourhood of the link L as in Definition 2.10.

If a link L is fibred and ϕ is a fibration, then the level sets of ϕ are Seifert surfaces, all of which are homeomorphic to each other. For fibred knots the genus of any Seifert surface must be at least the genus of this fibring Seifert surface [72]. Therefore the earlier definition of the genus of a knot implies that the genus of a fibred knot is equal to the genus of the fibre surface.

The commutator subgroup $[\pi_1(S^3\backslash L), \pi_1(S^3\backslash L)]$ of the fundamental group of the link complement $\pi_1(S^3\backslash L)$ is finitely generated if and only if L is fibred [127], but this condition is again quite hard to check. There are connections between fibredness and certain knot invariants, for example the Alexander polynomial of a fibred link is monic. However, there are also plenty of unfibred links whose Alexander polynomial is monic as well. The categorification of the Alexander polynomial, Knot Floer homology, does detect fibred knots [105].

Fibredness is another example of a property that behaves well under the connected sum. If K_1 and K_2 are fibred, then $K_1\#K_2$ is also fibred.

2.3 Braids and tangles

For a more detailed overview of the mathematics of braids, we point the reader to [68], [17] and [19] or the original work of Artin [8].

A braid B on s strands is the union of s disjoint parametric curves in $\mathbb{R}^3$, parametrised by their z-coordinate between 0 and 2π. This means that each strand is given by

$$(X_j(t), Y_j(t), t), \quad j = 1, 2, \ldots, s, 0 \leq t \leq 2\pi, \tag{2.7}$$

where each X_j and each Y_j is a smooth function $[0, 2\pi] \to \mathbb{R}$.

Additionally, we demand that there is a permutation $\pi_B \in S_s$, such that $X_j(0) = X_{\pi_B(j)}(2\pi)$ and $Y_j(0) = Y_{\pi_B(j)}(2\pi)$ for all $j \in \{1, 2, \ldots, s\}$. Given these equalities, we can identify the $z = 0$ plane and the $z = 2\pi$ plane, which closes the braid to a link $L \subset \mathbb{R}^2 \times S^1$. Since L is actually in $D_\rho \times S^1$, where D_ρ is the disk of some radius $\rho > 0$, the link L can be easily embedded into $\mathbb{R}^3$ in a natural way such as

$$\Big((R + X_j(t))\cos(t), (R + X_j(t))\sin(t), Y_j(t)\Big), \quad j = 1, 2, \ldots, s, 0 \leq t \leq 2\pi, \tag{2.8}$$

where $R > \rho$. This parametrisation of L is obtained by embedding $D_\rho \times S^1$ as the unknotted solid torus in $\mathbb{R}^3$. We call L the *closure* of the braid B. Note that there is a one-to-one correspondence between the cycles in the cycle notation of π_B and the components of the link L. Furthermore, the length of each cycle is equal to the number of strands making up the corresponding link component.

If we make an arbitrary choice of what the coordinates of the s strands at $t = 0$ should be, for example $(X_j(0), Y_j(0)) = (j, 0)$, the set of isotopies of braids on s strands (with fixed endpoints) forms a group B_s, where the group operation is simply the stacking of braids, expressed by concatenation and rescaling of the parametrisations.

For all values of t for which the strands all have different x-coordinates, we can order the strands by their x-coordinate. We say the strand with the lowest x-coordinate at a fixed t is in the first position at t, the strand with the next highest x-coordinate is in second position and so on. If we write σ_j for a positive twist of the strand in the jth position with the strand that is in position $j + 1$ (as in Figure 2.11a)), the group B_s is generated by σ_j, $j = 1, 2, \ldots, s - 1$ subject to the relations $\sigma_i\sigma_j = \sigma_j\sigma_i$ if $|i - j| > 1$ and $\sigma_i\sigma_{i+1}\sigma_i = \sigma_{i+1}\sigma_i\sigma_{i+1}$ for all $i \in \{1, 2, \ldots, s - 2\}$. The identity of the group is the empty word e, which geometrically is a braid where all strands remain in their initial position at all

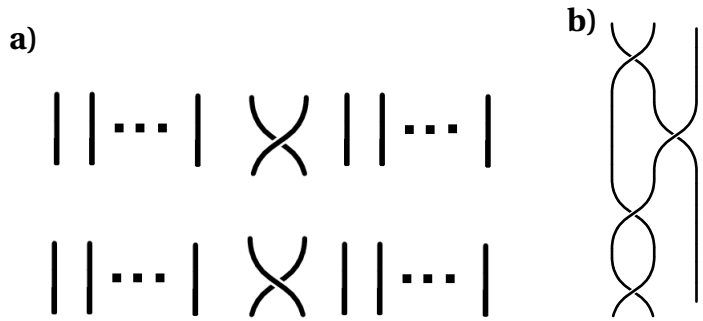

Figure 2.11: The definition of the braid group. a) The generator σ_i and its inverse σ_i^{-1}. b) The braid representing the word $\sigma_1\sigma_1\sigma_2\sigma_1$.

times t, i.e. $(X_j(t), Y_j(t)) = (X_j(0), Y_j(0))$ for all t. In this presentation the braid group is also called the Artin Braid group and σ_i is called an Artin generator.

Projecting the strands $(X_j(t), Y_j(t), t)$ of a braid B on the $y = 0$ plane will typically result in a braid diagram that allows to read off the braid word of B, that is the element of the braid group on s strands B_s corresponding to B in terms of the Artin generators σ_j. There are different conventions, but we will read the braid word from the bottom ($t = 0$) to the top ($t = 2\pi$). Furthermore, we choose the signs of the generators as follows. A crossing at time t is positive (σ_j rather than σ_j^{-1}) if at the crossing the y-coordinate of the strand coming from the jth position is larger than the y-coordinate of the strand that is coming from the $j+1$-position. This means that when we parametrise the closure of B as in Equation (2.8), then an overpassing arc in the corresponding link diagram (large z-coordinate) corresponds to an overpassing strand in the original braid diagram.

The permutation $\pi_B \in S_s$ that is associated to a braid B and tells how B permutes the strands is now seen to be the image of a braid group representation $h : B_s \to S_s$ that sends σ_i to the transposition $(i\ i+1)$. We often call this representation h the permutation representation. Elements of the kernel of this group homomorphism are called *pure braids*.

As mentioned before, identifying the $z = 0$ and the $z = 2\pi$ plane results in a collection of simple closed curves, a link consisting of as many components as π_B has cycles, called the closure of the braid. Alexander proved that the converse is also true [6].

Theorem 2.12. *Every link is the closure of some braid.*

Alexander's theorem means that as in the case of diagrams we can define link invariants by simply assigning numbers to braids and taking the invariant to be the minimum of all the numbers associated to braids that close to the given link type. For example the braid index $b_{\text{ind}}(L)$ of a link L is the minimal number of strands s of any braid B that closes to L. The minimal length of any braid word closing to a link L is also a link invariant. Gittings went numerically through all possible braid words of certain lengths to find the minimal braid words for many knots [55].

The close connection between braids and links is already reflected in the group relations. The obvious relation $\sigma_i\sigma_i^{-1} = \sigma_i^{-1}\sigma_i = e$ corresponds to the second Reidemeister move, while the relation $\sigma_i\sigma_{i+1}\sigma_i = \sigma_{i+1}\sigma_i\sigma_{i+1}$ is the third Reidemeister move.

The first Reidemeister move can be realised as in Figure 2.12. This process is called stabilization (if the crossing number increases) and destabilization (if it decreases). In terms of the braid word this means that the braids B, $B\sigma_s$ and $B\sigma_s^{-1}$ all close to the same link for all $B \in B_s$.

Markov answered the natural question of when two braids close to the same link.

Theorem 2.13. *[95] Two braids $B_1 \in B_s$ and $B_2 \in B_{s'}$ close to the same link if and only if they are related by a finite sequence consisting of the following moves: Braid isotopies (corresponding to the braid relations), conjugation and (de)stabilization.*

Markov's theorem has a big influence on the search for link invariants. Suppose we have a braid group representation $\rho_s : B_s \to GL(V)$ for every positive s such that $tr(\rho_s(B)) = tr(\rho_{s+1}(B\sigma_s)) = tr(\rho_{s+1}(B\sigma_s^{-1}))$ for all $B \in B_s$. Then the trace of this representation is a link invariant. This can be seen as follows. Isotopic braids in B_s obviously have the same image under ρ_s, conjugate braids have conjugate images and therefore give rise to the same trace and braids that are related by stabilization/destabilization give the same result by assumption. Therefore the value of the trace does not change under a finite sequence of Markov moves, the moves specified in Theorem 2.13. Many link invariants including the Jones polynomial can be interpreted this way [64].

Definition 2.14. *A braid B on s strands is called **homogeneous** if for every $j \in \{1, 2, \ldots, s-1\}$, the generator σ_j appears in its braid word if and only if σ_j^{-1} does not appear.*

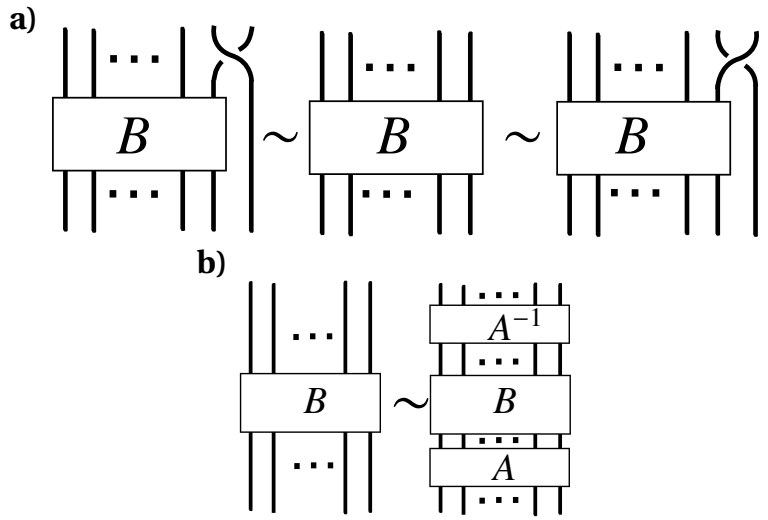

Figure 2.12: The Markov moves. a) The stabilization and destabilization moves. b) Conjugation of braid words.

The braid word $\sigma_1\sigma_2\sigma_1^{-1}\sigma_2$ for example is not homogeneous because both σ_1 and σ_1^{-1} appear in it. The 3-strand braid $\sigma_1\sigma_2^{-1}\sigma_1\sigma_2^{-1}$ which closes to the figure-eight knot is homogeneous. Some authors call the braids in Definition 2.14 strictly homogeneous, but it seems like the term homogeneous is now commonly used. It is easy to see that all torus knots are closures of homogeneous braids. In fact they are closures of *positive* braids, where every generator always appears with a positive sign.

Stallings showed that homogeneity of braids is related to the fibredness of their closures.

Theorem 2.15. *[128] Let B be a homogeneous braid and L be its closure. Then L is fibred.*

Note that the converse of this theorem does not hold. Mark Bell [12] gives the example of the knot 8_{20} which is fibred, but is not the closure of any homogeneous braid.

The notion of homogeneity generalises that of positivity, where all generators in the braid word are required to carry a positive sign. Another way to generalise positivity is by allowing conjugates of positive generators.

Definition 2.16. *A braid B is called **quasipositive** if its braid word is a product of conjugates of positive Artin generators, i.e. $B = \prod_{j=1}^{\ell} w_j\sigma_{i_j}w_j^{-1}$ for some braid*

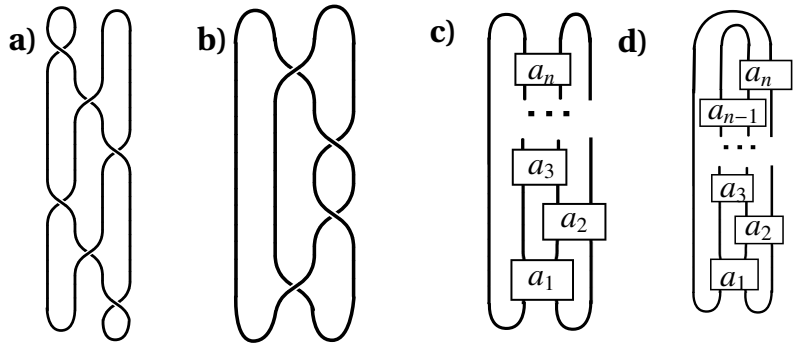

Figure 2.13: The definition of the plat closure. a) The plat closure of a braid with four strands. b) The same link as the plat closure of a braid with one passive strand. c) The general form of a 4-plat with one passive strand. d) A tangle $[a_1, a_2, \ldots, a_n]$ with n even can be interpreted as a 4-strand braid with an alternative closure.

words w_j and $\ell > 0$.
A link is called quasipositive if it is the closure of a quasipositive braid.

Braids are usually closed by identifying the top and the bottom plane, thereby gluing each bottom end of a strand to a top end of a strand. If we have an even number of strands, we can also connect pairs of bottom ends and pairs of top ends as in Figure 2.13. This type of closed braid is usually referred to as a plat. Note that with this different closure type Markov's theorem does not hold anymore, so there are different rules for when two braids close to the same link.

Plats with 4 strands are called 4-plats or in the original German Viergeflechte. All Viergeflechte can be brought into a form where one strand, the *passive strand* is not crossing any of the others as in Figure 2.13b), so that the braid is characterized by the sequence of integers signifying the number of twists between a pair of neighbouring strands before the next twist of the remaining pair of neighbouring strands that does not involve the passive strand. This means that the 4-plat given by the sequence of numbers $a_1, a_2, \ldots, a_n$ can be constructed from four parallel strands by twisting the strands in position 2 and 3 exactly a_1 times (respecting the sign of the twists), then twisting the strands in position 3 and 4 exactly $-a_2$ times, then again the strands in position 2 and 3 exactly a_3 times and so on. Once the end of the sequence is reached the ends of the strands are connected as in Figure 2.13. For example the plat in Figure 2.13b) is given by the sequence $a_1 = 1$, $a_2 = 2$, $a_3 = 1$.

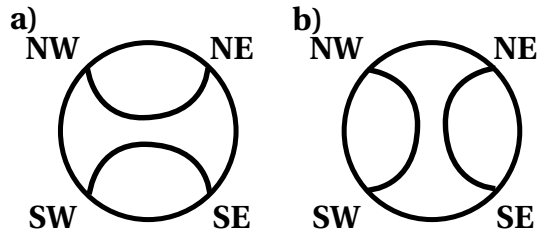

Figure 2.14: The two most basic tangles. a) The 0-tangle. b) The ∞-tangle.

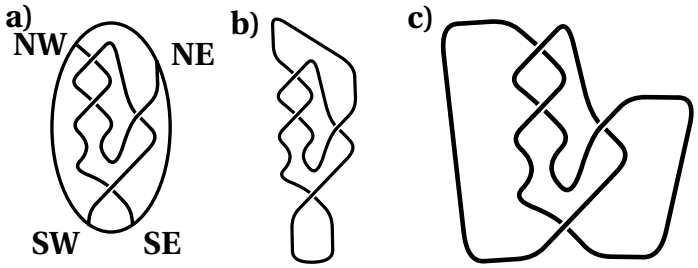

Figure 2.15: The definition of the closure of a tangle. a) The tangle $[2,-1,1]$. b) Its numerator closure. c) Its denominator closure.

In an equivalent description due to Conway [35], one could start with two curves trivially embedded into a disk such that each curve intersects the boundary exactly twice and these intersections occur at the ends of the curves. Such an embedding is called a *tangle*. We label the intersection points as in Figure 2.14 by NE, SE, SW and NW in clockwise orientation. There are thus four possible neighbouring ends of curves that can be twisted. The link described by $a_1, a_2, \ldots, a_n$ is then the result of twisting NE and SE exactly a_1 times, then SE and SW exactly a_2 times, then again NE and SE exactly a_3 times and so on. Once we reach the end of the sequence, the tangle is closed as in Figure 2.15. Closures of tangles are called rational links and the above remarks should make it clear that a link is rational if and only if it is a 4-plat.

The sequence $a_1, a_2, \ldots, a_n$, often written as $[a_1, a_2, \ldots, a_n]$, that describes the link type L of the closed tangle uniquely is the *Conway notation* of L. It is not a link invariant, but it is known exactly when two Conway notations describe the same link type [123].

Every 4-plat has a bridge number equal to 2. It is thus a so-called 2-bridge knot. It turns out that the converse is also true, so that the set of 4-plats is identical to the set of 2-bridge knots.

2.4 Algebraic links

The material in this section is a very brief summary of material from [99], [124] and [44].

Let $f \in \mathbb{C}[u,v]$ be a complex polynomial in two variables corresponding to a complex plane curve. As such it is a smooth map $\mathbb{C}^2 \to \mathbb{C}$. We refer to the set $f^{-1}(0) = \{x \in \mathbb{C}^2 : f(x) = 0\}$ as the nodal set of f and sometimes as the zero level set or the vanishing set of f. By definition $f^{-1}(0)$ is a complex hypersurface.

A point $x \in f^{-1}(0)$ is a *singular* point or a *singularity* if the matrix of first partial derivatives, the Jacobian, is the zero matrix, i.e. $\left(\frac{\partial f}{\partial u}(x), \frac{\partial f}{\partial v}(x)\right) = (0,0)$. We denote the set of singular points of $f^{-1}(0)$ by f_{sing}.

Note that $f^{-1}(0)\backslash f_{sing}$ is a manifold. A singular point x is called *isolated* if there exists a neighbourhood of x such that it is the only point in that neighbourhood where the Jacobian is the zero matrix.

In this case the intersection $f^{-1}(0) \cap S^3_\rho(x)$ of the vanishing set with the three-sphere of radius $\rho > 0$ around x is a closed 1-dimensional manifold for small enough ρ. As such it is a link L in a three-sphere. Furthermore, the link type of L does not depend on ρ as long as ρ is small enough. The link L is then called the *link of the singularity*. The following theorem can be found in [99].

Theorem 2.17. *Let f be a complex plane curve and $x \in \mathbb{C}^2$ be an isolated singular point of f. Then there exists a link L and $\varepsilon > 0$ such that $f^{-1}(0) \cap S^3_\rho(x) = L$ for all $\rho < \varepsilon$.*

Furthermore, $\arg f = f/|f| : S^3_\rho(x)\backslash L \to S^1$ *is a fibration as long as ρ is small enough.*

Theorem 2.17 shows that not every link can arise as the link of an isolated singularity, since it has to be fibred. The links that are links of some singularity are called *algebraic links*. From now on we assume without loss of generality that the isolated singularity is the origin.

The branches of $f^{-1}(0)$ in a neighbourhood of the singular point at the origin can be parametrised in terms of v. Brauner found that in this case

$$u = c_1 v^{m_1/n_1} + c_2 v^{m_2/n_1 n_2} + \dots, \tag{2.9}$$

where $c_i \in \mathbb{C}\backslash\{0\}$, $m_1/n_1 < m_2/n_2 < \cdots$ and each pair (m_i, n_i) is a coprime pair of integers [27]. These are called the Puiseux pairs. In principle, this parametrisation is an infinite sum. However, we can remove all but finitely many terms

without changing the topology. It turns out that the topology of $f^{-1}(0)$ is entirely characterised by these remaining pairs of integers. We can write Equation (2.9) as

$$u = v^{q_1/p_1}(a_1 + v^{q_2/p_1p_2}(a_2 + \ldots(a_{s-1} + v^{q_s/p_1\cdots p_s}(a_s + \cdots)\cdots))), \tag{2.10}$$

with $p_i, q_i > 0$ and (p_i, q_i) coprime for all i. The so-called Newton pairs (p_i, q_i) are determined by the Puiseux pairs by $p_i = n_i$, $q_1 = m_1$ and $q_i = m_i - m_{i-1}n_i$ for all i. The curves parametrised by Equation (2.10) form the (p_s, α_s)-cable of the (p_{s-1}, α_{s-1})-cable of the $\cdots(p_1, \alpha_1)$-torus link, where $\alpha_1 = q_1$ and $\alpha_{i+1} = q_{i+1} + p_ip_{i+1}\alpha_i$. Therefore all algebraic links must be iterated cables of torus links and all iterated cables of torus links whose (p_i, α_i) give rise to Puiseux pairs satisfying $m_1/n_1 < m_2/n_2 < \cdots$ and (m_i, n_i) coprime for all i are algebraic.

Theorem 2.18. *[27], [29], [30], [65], [83] The set of algebraic links is identical to the set of iterated cables of torus links subject to the conditions on the cable numbers and Puiseux pairs as outlined above.*

From Equation (2.10) we can easily find the complex plane curve that corresponds to the (p, q)-torus link, which is the link with Puiseux pairs $(p_1, q_1) = (p, q)$ and $(a_i, b_i) = (0, 0)$ for all $i > 1$. The (p, q)-torus link is the vanishing set of

$$f(u, v) = u^p - v^q \tag{2.11}$$

on small three-spheres around the isolated singularity at the origin. This was originally shown by Brauner [27].

Note that in this case the p branches given by Equation (2.9) can be interpreted as the p strands of a braid closing to the (p, q)-torus link. If we set $|v|$ in Equation (2.9) to be constant and do not identify the zero and 2π-value of $\arg v$, the explicit parametrisation describes a braid whose strands lie on a cylinder $S^1 \times [0, 2\pi]$. We revisit this point of view in Chapters 3 and 4.

Instead of complex plane curves we can consider polynomial maps $f : \mathbb{R}^4 \to \mathbb{R}^2$, i.e. $f = (f_1, f_2)$ with $f_1, f_2 \in \mathbb{R}[x_1, x_2, x_3, x_4]$. With slight misuse of notation we write f for the real map as well as for the complex-valued polynomial (in real variables) that is given by $f_1 + \mathrm{i}f_2 : \mathbb{R}^4 \to \mathbb{C}$. We call a point $x \in \mathbb{R}^4$ a *singular* point or a singularity of f if the Jacobian matrix $\nabla f(x)$ is zero. If the rank of ∇f at x is less than two, we call x a *critical point*. The Cauchy-Riemann equations imply that if one considers a complex plane curve as a polynomial map $\mathbb{R}^4 \to \mathbb{R}^2$, then a point is singular if and only if it is critical. In general, the singular points are by definition a subset of the critical points.

Singular points of polynomial maps $f : \mathbb{R}^4 \to \mathbb{R}^2$ can be isolated in two different ways. A singular point x of f is called *weakly isolated* if it has an ϵ-neighbourhood B_ϵ such that x is the only critical point in B_ϵ that is also part of the vanishing set. The link type of the intersection of three-spheres of small enough radius around x with the vanishing set of f is then, exactly as in the case of complex plane curves, independent of the radius and we call the resulting 1-manifold the link of the singularity. The links that arise in this way are called *weakly algebraic links*. Weak isolation is not a very strong condition and Akbulut and King showed that every link is weakly algebraic [5].

Theorem 2.19. *[5] All links are weakly algebraic.*

The situation changes if we impose stricter conditions. A singular point x of f is called *isolated* if it has an ϵ-neighbourhood B_ϵ such that x is the only critical point in B_ϵ. Again we define the link of the singularity to be the intersection of $f^{-1}(0)$ with S^3_ϵ and call the links that arise in this way *real algebraic links*.

Unfortunately, the terms 'real algebraic knots' and 'algebraic knots' are used in several different contexts. Closures of compositions of rational tangles are called algebraic knots [35] as well as the links of isolated singular points of complex plane curves. Additionally, in our terminology the title of Akbulut and King's paper 'All knots are algebraic' [5] translates to 'All knots are weakly algebraic'. Oleg Viro and others have developed a branch of knot theory called real algebraic knot theory where the knots of interest are sets of real points on (projective) algebraic varieties [135] and isotopies are replaced by *rigid isotopies* through such 'real algebraic links'. Our use of the term 'real algebraic' goes back to Perron's paper [111] whose French title translates to 'The figure-eight knot is real algebraic'. We find this fitting, since it stresses the analogy to the case of complex plane curves.

Compared to weak isolation, the stronger notion of isolation is much more restrictive. In particular, Milnor proved the following result.

Theorem 2.20. *[99] Let L be a real algebraic link. Then L is fibred.*

This led Benedetti and Shiota to conjecture that the two sets of links are actually identical.

Conjecture 2.21. *[13] A link L is real algebraic if and only if it is fibred.*

This conjecture is to our knowledge still open. Naturally, all algebraic links are real algebraic and some examples of non-algebraic links have been shown

to be real algebraic, including the figure-eight knot and the Borromean links by Perron [111] and Rudolph [118]. Furthermore, Looijenga showed that if K is fibred, then the connected sum $K\#K$ is real algebraic [90]. The proofs by Perron, Rudolph and Looijenga illustrate a difficulty of the conjecture, namely that there does not seem to be any way of proving that a given link is real algebraic other than constructing a corresponding polynomial f explicitly.

Knots and links have also been considered as vanishing sets of polynomials in different contexts from isolated singularities. Lee Rudolph defined the class of transverse $\mathbb{C}$-links [121]. These are all the links L for which there exists a complex plane curve $f : \mathbb{C}^2 \to \mathbb{C}$ such that the vanishing set of f intersects the unit three-sphere transversely and this intersection is the link L.

These polynomials do not necessarily have an isolated singularity at the origin and the intersections of the nodal set with two three-spheres of different radii in general have two different link types.

Theorem 2.22. *[25], [116] The set of transverse $\mathbb{C}$-links is identical to the set of quasipositive links.*

This class obviously contains all algebraic links, but also so-called links of divides [3] and links at infinity [26].

Dennis generalized the idea of transverse $\mathbb{C}$-links to the study of *semiholomorphic* polynomials, functions $f : \mathbb{C}^2 \to \mathbb{C}$ that are polynomials in complex variables u, v and the complex conjugate $\bar{v}$, and transverse intersections of their vanishing set with the unit three-sphere. Dennis and King found such a polynomial for the figure-eight knot, which is not quasipositive, and some other knots and links [41, 79]. They used the polynomials for the engineering of knots in laser light [41].

In the next chapter we review several physical systems for which knotted configurations have been found. For physical applications one usually requires a function from 3-dimensional space to some target space, not a polynomial in two complex or four real variables. However, composing the stereographic projection

$$u = \frac{x^2 + y^2 + z^2 - 1 + 2\mathrm{i}z}{1 + x^2 + y^2 + z^2}, \quad v = \frac{2(x + \mathrm{i}y)}{1 + x^2 + y^2 + z^2} \tag{2.12}$$

with the restriction $f|_{S^3} : S^3 \to \mathbb{R}^2$ of a polynomial $f : \mathbb{R}^4 \to \mathbb{R}^2$ with a knotted vanishing set L on the unit three-sphere S^3, we obtain a rational map $\mathbb{R}^3 \to \mathbb{C}$ in real variables x, y and z.

Since the denominator is some multiple of a power of $1 + x^2 + y^2 + z^2$, we can multiply through by the denominator without changing the vanishing set and obtain a polynomial $\mathbb{R}^3 \to \mathbb{C}$ that vanishes exactly on the desired link L.

3 Knotted fields in physics

Recent years have seen a growing interest in configurations of physical systems that contain knots and links. Knots have been found in very diverse areas such as quantum mechanics [14], optics [15], [41], non-linear field theories in particle physics [129], topological fluid dynamics [46, 47, 88, 100], and liquid crystals [91], [92], [66]. In physics the term 'field' describes a function from $\mathbb{R}^3$ to some target space. Different physical systems require different target spaces, so that we are for example confronted with complex scalar fields $\mathbb{R}^3 \to \mathbb{C}$, vector fields $\mathbb{R}^3 \to \mathbb{R}^3$ or director fields $\mathbb{R}^3 \to \mathbb{RP}^2$.

In scalar complex fields knots arise as the nodal set of the field, while systems that are described by 3d vector fields can contain knotted flow lines or vortex knots. There are two main approaches to the study of knotted fields: the statistical analysis of the knots that occur in these fields naturally [130] and the constructive approach, that aims to construct such field configurations for given knot types [41]. The remarkable thing is that despite the great variety of different physical systems, all of the known constructions are in one way or another based on finding maps from 3-dimensional space to the complex numbers whose vanishing set is a given knot, such as the complex plane curves for algebraic links studied by Brauner [27] and Milnor [99] composed with a stereographic projection.

If the system is not taken to be static, these maps can be used as initial conditions for the time evolution of the system. The dynamics of the system is then governed by a differential equation or a given energy functional that needs to be minimized. As the system evolves, so does the knot. Typically, intersections occur, parts of the knotted curve pass through each other and the knot type changes and potentially disappears altogether. Either through statistical analysis of random field configurations or through the study of final

stable knotted configurations one obtains topological information about the physical system. For example, one might find that certain knots arise much more often than others or that some do not appear at all. Both cases indicate a connection between the properties of the physical system and properties of knots.

In this chapter we review some of the physical systems in which knotted initial configurations have been constructed and the methods that were applied. We also discuss the role of fibred knots in some of these systems.

Recall that in the case of a fibration map $\phi : S^3 \backslash L \to S^1$ the level sets of ϕ are disjoint Seifert surfaces that fill the whole space around the link L. The situation that surfaces fill the whole space apart from some set, in this case a knot, arises in physics for example as layers of materials, layers of molecules in liquid crystals or as surfaces of constant phase in any complex scalar field, for example a quantum wavefunction.

This chapter is outlined as follows. In Section 3.1 we review vortex knots in superfluids and electromagnetism. The case of scalar optical fields with knotted vortex lines is discussed in Section 3.2. Knots have also been found in the Skyrme-Faddeev model, a non-linear field theory, that is used as a model in particle physics and treated in Section 3.3. Section 3.4 describes the construction of vector fields with knotted flow lines that can be applied to fluids and electromagnetic fields. Section 3.5 studies knotted disclination lines in the area of smectic and nematic liquid crystals. A concluding summary can be found in Section 3.6.

3.1 Superfluids and Biot-Savart

Superfluids, such as helium at very low temperatures, are fluids without any viscosity. Despite being many-body systems, they can in a lot of cases (for example Bose-Einstein condensates) be described by a single wavefunction $\Psi : \mathbb{R}^3 \to \mathbb{C}$. This quantum description contains information about classical properties of the superfluid, for example the gradient of the phase $\nabla \arg \Psi$ is a good approximation for the expectation value of the local velocity and $|\Psi|^2$ is the classical density.

The zero level set $\Psi^{-1}(0)$ typically forms a set of curves, that can be knotted or linked, and isolated points. If the flow field $\nabla \arg \Psi$ circulates around these knotted lines as in Figure 3.1, we call them vortex knots.

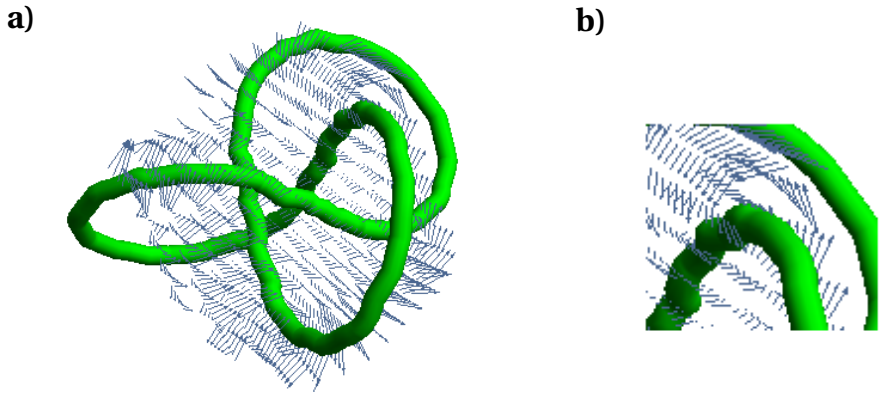

Figure 3.1: Magnetic fields induced by knotted wires. a) The magnetic field around a wire in the form of a trefoil knot. b) A close-up of how the vector field circulates around the wire in a tubular neighbourhood

We can use a complex-valued function Ψ with knotted zero level set, say the restriction of a polynomial f as in Section 2.4, $\Psi = f|_{S^3} : S^3 \to \mathbb{C}$, to generate an initial configuration of a superfluid with a knotted vortex line of the desired knot type. Typically polynomials do not give rise to minimal energy conformations, so as the superfluid evolves towards a more stable configuration as the function Ψ changes. Kleckner, Kauffman and Irvine studied the dynamics of vortex knots in superfluids numerically, using initial configurations of all prime knots and links with 9 or fewer crossings, and found an overwhelming tendency to untie [80]. Their initial configurations are not polynomials, but constructed as follows.

Figure 3.1 cannot only be interpreted as the velocity field of a superfluid around a vortex knot. It also illustrates the following phenomenon in electromagnetism. If we let a constant electric current run through a closed thin wire that is a knotted curve K, then the electric current induces a magnetic field $\mathbf{B} : \mathbb{R}^3 \backslash K \to \mathbb{R}^3$ around the wire that is given by the Biot-Savart law

$$\mathbf{B}(x,y,z) = \frac{I\mu_0}{4\pi} \int_K \frac{d\mathbf{l} \times (\mathbf{r} - \mathbf{l})}{|\mathbf{r} - \mathbf{l}|^3}, \tag{3.1}$$

where μ_0 is the magnetic constant, I is the electric current, $\mathbf{r} = (x,y,z)$ and $\mathbf{l}$ is a point moving along the wire. It has been suggested to use magnetic fields that result from such knotted wires in magnetic confinement devices [61].

Setting all constants to 1, the line integral of B around a second loop γ

$$lk(\gamma, K) = \frac{1}{4\pi} \oint_\gamma \oint_K \frac{\mathbf{r_1} - \mathbf{r_2}}{|\mathbf{r_1} - \mathbf{r_2}|^3} \cdot (d\mathbf{r_1} \times d\mathbf{r_2}) = \oint_\gamma \mathbf{B}(\mathbf{r_1}) d\mathbf{r_1}, \tag{3.2}$$

is an integer for any closed loop γ in $S^3 \backslash K$, namely the linking number of γ with K. Hence the integral of $\mathbf{B}$ along any closed loop in $S^3 \backslash K$ is an integer.

Therefore

$$\int_\gamma \mathbf{B}(\mathbf{r})d\mathbf{r} \mod 1, \tag{3.3}$$

where γ is a path, does not depend on the choice of path γ, but only on the start and end point.

Thus the magnetic field is the gradient field of a circle-valued function $P : S^3\backslash K \to S^1$. This means that for a given knot K (given as a parametric curve), we get a 3d vector field with K as a vortex knot. This vector field could be interpreted as the velocity field $\nabla \arg \Psi$ of a superfluid or a magnetic field. Kleckner et al used this construction to obtain the phase field $P = \arg \Psi$. For the density field $\rho = |\Psi|^2$ they used the following ansatz:

$$\rho(r) = \frac{\frac{11}{32}r^2 + \frac{11}{384}r^4}{1 + \frac{1}{3}r^2 + \frac{11}{384}r^4}, \tag{3.4}$$

where r is the minimal distance from the point (x, y, z) to the vortex knot.

The Biot-Savart law also tells us that in a tubular neighbourhood of K the level sets of $P = \arg \Psi$ look exactly like in Figure 2.10.

Since $\nabla \arg \Psi : \mathbb{R}^3\backslash K \to \mathbb{R}^3$ is effectively the velocity away from the vortex knot, critical points of $\arg \Psi$ correspond to stagnation points of the superfluid. Since there must always be critical points in the complements of unfibred knots, there must always be stagnation points for a vortex line in the form of an unfibred knot.

Studying the existence of stagnation points in superfluids could hence give insight into whether fibred vortex knots are more common than unfibred knots.

Likewise in the case of magnetic fields, if P does not have any critical points, P is a fibration of the complement of K over S^1 and K must be fibred. At a critical point we have that $\mathbf{B} = \nabla P = 0$ and it follows that if K is not fibred, then the induced magnetic field in the knot complement must vanish at some point. The existence of critical points of maps from the knot complement to the circle are discussed in greater detail in Chapter 6.

Strictly speaking, every magnetic field $\mathbf{B}$ defined by the Biot-Savart law vanishes at infinity, but it turns out that if the knot is in braid form, say braided around the z-axis, then we can slightly perturb the field to get a nowhere vanishing vector field that is still the gradient field of a circle-valued function.

This can be seen as follows. Consider the unknot in a planar embedding, say as $(\cos(t), \sin(t), 0)$, $t \in [0, 2\pi]$. Then the magnetic field $\mathbf{B}$ induced around this curve is $C \cdot \nabla p$, where $C : S^3\backslash K \to \mathbb{R}_{\geq 0}$ vanishes only at $(0, 0, 0, 1)$, corresponding

to the point at infinity in $\mathbb{R}^3$, and $p : S^3\backslash K \to S^1$ is the fibration around the unknot. We can thus slightly perturb $\mathbf{B}$, by perturbing C, in a neighbourhood of infinity to obtain a nowhere vanishing vector field around the unknot in the whole of S^3.

Assume now we have a knot K in braid form around the z-axis. Then in a neighbourhood of infinity the induced vector field $\mathbf{B}$ is arbitrarily close to the one that we obtained for the unknot (potentially with a different electric current through the knot). We can thus again apply a small perturbation to get rid of the zero at infinity. Thus if we call the resulting vector field $\mathbf{B}'$, there is a circle-valued function $P : S^3\backslash K \to S^1$ with $\nabla P = \mathbf{B}'$ without any critical points. Thus P is a fibration and K must be fibred.

We have thus shown that for unfibred knots in braid form the induced magnetic field must vanish somewhere in $\mathbb{R}^3$. This raises the following question: If K is a fibred knot, is there a parametrisation of K such that the induced magnetic field does not vanish anywhere in $\mathbb{R}^3$?

At the moment, we are unsure if the answer to the question above is positive, but we discuss in Chapter 6 why at least for knots that are closures of homogeneous braids there are indications that such a parametrisation exists. Gareth Alexander has found knot parametrisations that lead to such Biot-Savart fibrations for all fibred knots with less than 8 crossings [16].

We have seen that the Biot-Savart integral and an ansatz like the one in Equation (3.4) are enough to find an initial configuration of a superfluid or magnetic field with a given vortex knot. The only input that is needed for this calculation is a parametric curve in the shape of the desired knot. Different parametrisations of the same knot type lead to different fields and it is not obvious which knot parametrisations lead to field configurations that are physically favourable. A large part of this dissertation (Chapters 4, 5 and 6) is devoted to an alternative construction that involves complex-valued polynomials. Not only is an explicit polynomial somewhat more aesthetically pleasing, but it is also expected to be numerically less expensive than the Biot-Savart, which after all requires a two-dimensional integral to obtain the phase $\arg\Psi$ and a way to find the closest point on the knot for each point in space to obtain the ansatz for $|\Psi|$. Furthermore, we will see in Chapter 6 that the construction allows a certain control of the number of critical points of $P = \arg\Psi$, i.e. the number of stagnation points of the superfluid or the number of points, where the magnetic field vanishes.

There are also settings where a holomorphic function is explicitly needed, so a Biot-Savart approach seems out of question, since that requires a construction of ρ different from Equation (3.4) that makes $\Psi = \sqrt{\rho}\,\mathrm{e}^{\mathrm{i}P}$ holomorphic.

Instead of focusing on vortex knots in a magnetic field, we can study vortex knots in the whole electromagnetic field. An electromagnetic field can be describe the Riemann-Silberstein vector $\mathbf{F}$, a function $\mathbf{F} = \mathbf{E} + \mathrm{i}\mathbf{B} : \mathbb{R}^4 \to \mathbb{C}^3$, where $\mathbf{E} : \mathbb{R}^4 \to \mathbb{R}^3$ is the time-dependent electric field and $\mathbf{B} : \mathbb{R}^4 \to \mathbb{R}^3$ is the time-dependent magnetic field. Together they satisfy Maxwell's equations in free space:

$$\nabla \cdot \mathbf{B} = 0, \tag{3.5}$$

$$\nabla \times \mathbf{E} + \partial_t \mathbf{B} = 0, \tag{3.6}$$

$$\nabla \cdot \mathbf{D} = 0, \tag{3.7}$$

$$\nabla \times \mathbf{H} - \partial_t \mathbf{D} = 0, \tag{3.8}$$

where $\mathbf{H} = \frac{1}{\mu_0}\mathbf{B}$, $\mathbf{D} = \frac{1}{\varepsilon_0}\mathbf{E}$, μ_0 and ε_0 are the electric and magnetic permittivity respectively and t is the time coordinate and ∇ only involves the three spatial derivatives.

A vortex knot in an electromagnetic field is a vortex knot in both the electric and the magnetic field at a given time t, i.e. $K = \mathbf{F}^{-1}(0,0,0) \cap (\mathbb{R}^3 \times \{t\})$. De Klerk et al. describe a construction of electromagnetic vortex knots for all algebraic knots in [39].

They consider the following versions of the inverse stereographic projection formula (2.12) from $\mathbb{R}^3 \cup \{\infty\}$ to S^3_ε

$$u = \varepsilon \frac{x^2 + y^2 + z^2 - t^2 - 1 + 2\mathrm{i}z}{x^2 + y^2 + z^2 - (t - \mathrm{i})^2} \qquad \text{and} \qquad v = \varepsilon \frac{2(x - \mathrm{i}y)}{x^2 + y^2 + z^2 - (t - \mathrm{i})^2}, \tag{3.9}$$

where x, y and z are the three spatial coordinates, t represents time and $\varepsilon > 0$.

Let L be an algebraic link and f_L be the polynomial with an isolated singularity with link type L. Then it is not hard to see that

$$\mathbf{F}_L := f_L(u, v)\nabla u \times \nabla v \tag{3.10}$$

has L as a vortex knot at the time $t = 0$, since the three components of $\nabla u \times \nabla v$ never vanish simultaneously. Furthermore, the link type of $\mathbf{F}_L$ does not change as t changes, i.e. for every fixed time t, the field $\mathbf{F}_L$ has L as a vortex knot.

What is even more remarkable is that $\mathbf{F}_L$ as a time-dependent field satisfies Maxwell's equations. The proof of de Klerk et al actually does not need the fact

that L is algebraic. What is required is that there is a holomorphic polynomial f that intersects a three-sphere of some radius transversally in L, i.e. L has to be a transverse $\mathbb{C}$-link. By Theorem 2.22 this means that the construction suggests that a field F_L with L as an electromagnetic vortex link and satisfying Maxwell's equations exists for every quasipositive link L. However, in order to construct the corresponding electromagnetic fields we need to know how to find the complex plane curve f with $f^{-1}(0) \cap S^3 = L$ for a given quasipositive link L.

3.2 Optical complex scalar fields

In the previous section we discussed electromagnetic fields as functions $\mathbf{F} = \mathbf{E} + \mathrm{i}\mathbf{B} : \mathbb{R}^4 \to \mathbb{C}^3$ that satisfy Maxwell's equations (3.5)-(3.8). There are however physical settings where this description can be significantly simplified. First note that when we take the curl of (3.6) and substitute into (3.5), we see that Maxwell's equations imply

$$\begin{aligned} \nabla^2\mathbf{E} - c^{-2}\ddot{\mathbf{E}} &= 0, \\ \nabla^2\mathbf{B} - c^{-2}\ddot{\mathbf{B}} &= 0, \end{aligned} \tag{3.11}$$

where $\nabla^2 = \frac{\partial^2}{\partial x^2} + \frac{\partial^2}{\partial y^2} + \frac{\partial^2}{\partial z^2}$ is the Laplacian with respect to the three spatial coordinates x, y and z, and $c = \sqrt{\mu_0\varepsilon_0}$ is the speed of light.

We want to focus on monochromatic solutions of Equation (3.11) for $\mathbf{E}$. These are fields whose time dependence is based on a single frequency ω. Therefore they can be written as

$$\mathbf{E}(x, y, z, t) = \mathrm{Re}(\mathrm{e}^{-\mathrm{i}\omega t}\,\mathcal{E}(x, y, z)), \tag{3.12}$$

where $\mathcal{E} : \mathbb{R}^3 \to \mathbb{C}^3$ is the complex amplitude of the electric field, which is static. Note that if $\mathrm{Re}(-\mathrm{e}^{i\omega t}\,\mathcal{E}(x, y, z))$ satisfies Equation (3.11), so does $\mathrm{e}^{-\mathrm{i}\omega t}\,\mathcal{E}(x, y, z)$. Since $\mathrm{e}^{-\mathrm{i}\omega t} \neq 0$, we obtain the Helmholtz vector wave equation

$$\nabla^2\mathcal{E} + k^2\mathcal{E} = 0, \tag{3.13}$$

where $k = \frac{\omega}{c}$ is the constant wavenumber.

We are interested in beams of light, like that of a laser. It is convention to choose the z-direction as the direction of propagation and only consider one component of $\mathcal{E}$ that is perpendicular to that. We are hence left with a complex scalar field $\Psi : \mathbb{R}^3 \to \mathbb{C}$ that satisfies the scalar Helmholtz equation

$$\nabla^2\Psi + k^2\Psi = 0. \tag{3.14}$$

Substituting the ansatz $\Psi(x,y,z) = \psi(x,y,z)\,\mathrm{e}^{\mathrm{i}kz}$ into (3.14) yields

$$\left(\frac{\partial^2}{\partial x^2} + \frac{\partial^2}{\partial y^2}\right)\psi(x,y,z) + \frac{\partial^2}{\partial z^2}\psi(x,y,z) + 2\mathrm{i}k\frac{\partial}{\partial z}\psi(x,y,z) = 0. \tag{3.15}$$

Assuming that the paraxial approximation

$$\left|\frac{\partial^2\psi}{\partial z^2}\right| \ll k\left|\frac{\partial\psi}{\partial z}\right| \tag{3.16}$$

holds, we get the paraxial wave equation

$$\left(\frac{\partial^2}{\partial x^2} + \frac{\partial^2}{\partial y^2}\right)\psi(x,y,z) + 2\mathrm{i}k\frac{\partial}{\partial z}\psi(x,y,z) = 0. \tag{3.17}$$

This derivation can also be found in [79] and [82].

We will now briefly review what the scalar field $\Psi(x,y,z) = \psi(x,y,z)\,\mathrm{e}^{\mathrm{i}kz}$ represents physically. Shining a laser pointer on a wall does not result in a single bright point on the wall. Looking closely enough, one can make out a pattern of brighter and darker regions. This is because in this regime the optical field can be described by the complex scalar function $\Psi : \mathbb{R}^3 \to \mathbb{C}$. What we see on the wall is a 2-dimensional slice of the optical field, bright points corresponding to points where the intensity $|\Psi|^2$ is large and dark points corresponding to points of low intensity.

If we plot $\arg(\Psi)$ as in Figure 3.2 on the wall (a 2-dimensional slice of $\mathbb{R}^3$), we find points where $\Psi = 0$ and $\arg(\Psi)$ is not defined. These are called vortices or phase singularities and the argument $\arg(\Psi)$ rotates by an integer multiple of 2π around them.

In $\mathbb{R}^3$ the set of points with zero intensity, $\Psi^{-1}(0)$, then forms a number of curves. As such these optical vortex lines can be knotted or linked.

The field assigns to every point away from these curves a phase $\arg(\Psi) \in S^1$ and the surfaces of constant phase $\arg(\Psi) = \chi \in S^1$ can be interpreted as wavefronts. Extending Figure 3.2a) to the third dimension we see that the wavefronts rotate around the phase singularities not unlike in the case of Figure 2.10 and the closures of the surfaces of constant phase intersect on the vortex lines.

The polynomials $f : \mathbb{C}^2 \to \mathbb{C}$ from Brauner [27], Milnor [99] and Dennis [41] have been used to explicitly construct optical fields $\Psi : \mathbb{R}^3 \to \mathbb{C}$ with a knotted vortex line in the shape of a torus knot or a lemniscate knot [41], a family which will be defined in the next chapter.

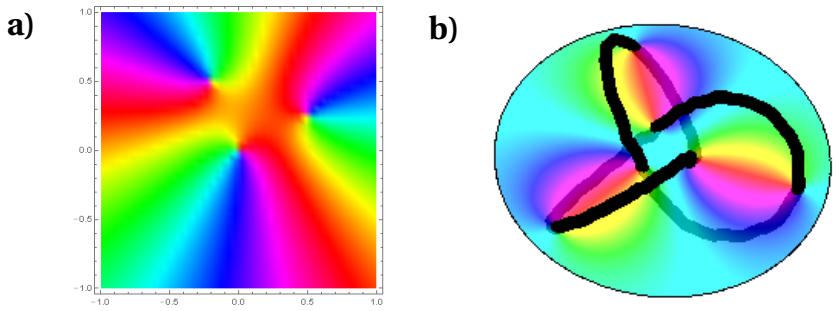

Figure 3.2: An optical vortex knot. a) A two-dimensional phase field. The phase rotates around the three vortices by multiples of 2π. b) A knotted optical vortex line in the shape of a trefoil knot. The coloured disk indicates the values of the phase of the complex scalar field in the $z = 0$-plane, with different colours corresponding to different phase values between 0 and 2π.

We first apply an inverse stereographic projection to the polynomial f, making the identification

$$u = \frac{x^2 + y^2 + z^2 - 1 + 2iz}{x^2 + y^2 + z^2 + 1}, \quad v = \frac{2(x + iy)}{x^2 + y^2 + z^2 + 1}. \tag{3.18}$$

This results in a rational function, whose denominator is a non-zero multiple of an integer power of $x^2 + y^2 + z^2 + 1$. Thus by multiplying by the denominator, we do not change the zero level set of the function. Call the resulting function F. Since the zero level set of f on the unit three-sphere is some given knot, the vanishing set of F is that same knot.

Not every complex-valued function describes an optical field and a polynomial function almost certainly does not. In order to obtain a function that satisfies the necessary wave equation, we multiply F by a Gaussian factor $e^{-(x^2+y^2)/w}$, where w is the beam width, and evolve the $z = 0$-plane of the resulting function according to the paraxial wave equation (3.17), i.e. we take $\psi(x, y, 0) = F(x, y, 0)\, e^{-(x^2+y^2)/w}$ as a boundary condition to solve Equation (3.17). We should point out that this construction refers to the paraxial field ψ. The actual optical field is then given by $\Psi = \psi\, e^{ikz}$.

This procedure does not guarantee that the topology of the zero level set is preserved. We do not know in general if $\psi^{-1}(0)$ is isotopic to $f^{-1}(0) \cap S^3$, but in simple cases, such as the trefoil or the figure eight knot, parameters can be chosen in such a way that the nodal set of the resulting optical field is ambient isotopic to the one of the polynomial map [41]. These 'simple cases' only include fibred links, but the paraxial wave equation does not explicitly exclude critical

points of the argument. We thus expect that optical fields with non-fibred knots as vortices should also be possible to construct.

An optical field with a knotted vortex line in the shape of a trefoil knot has been created experimentally in [41] using the polynomial $u^2 - v^3$.

In order to construct links that are not in the very restricted families of links accessible to us from Brauner's or Dennis's construction, we have to find corresponding polynomials for them, which can then potentially be used analogously to the polynomials of the trefoil or the figure-eight knot. These polynomials do not need a singularity at the origin or to be holomorphic, but should be $\mathbb{R}^4 \to \mathbb{R}^2$ and have a vanishing set that intersects the unit three-sphere in the given link.

3.3 The Skyrme-Faddeev model

The Skyrme-Faddeev model is a non-linear field theory [49] with connections to QCD and condensed matter physics. It is sometimes used as a model of nuclei in particle physics. We briefly review its basics following the summary in [129].

The objects of this theory are maps $\phi = (\phi_1, \phi_2, \phi_3) : \mathbb{R}^3 \to S^2$, i.e. $\phi \cdot \phi = 1$. The energy functional of the model is given by

$$E(\phi) = \frac{1}{32\pi\sqrt{2}} \int \partial_i\phi \cdot \partial_i\phi + \frac{1}{2}(\partial_i\phi \times \partial_j\phi) \cdot (\partial_i\phi \times \partial_j\phi) d^3x, \tag{3.19}$$

where we use (x_1, x_2, x_3) as coordinates of $\mathbb{R}^3$ and denote $\frac{\partial}{\partial x_i}$ by ∂_i. We make use of Einstein's summation convention, where repeated indices are summed over.

In order to have a finite energy, ϕ has to take a well-defined value at infinity. We can choose this value as a boundary condition, say $\phi(\infty) = (0, 0, 1)$. This compactifies $\mathbb{R}^3$ to S^3 and turns ϕ into a map from S^3 to S^2.

Since $\pi_3(S^2) = \mathbb{Z}$, every such map ϕ is associated with an integer $Q(\phi)$, called the Hopf charge, which represents its homotopy class. If we assume that the evolution of a field is governed by the gradient flow, i.e. every field configuration evolves continuously until its energy is stationary, then this integer does not change over time.

The Hopf charge $Q(\phi)$ has another topological interpretation. If $x \in S^2$ is a regular value, its preimage $\phi^{-1}(x)$ is a link in S^3. Then $Q(\phi)$ is equal to the linking number of the link $\phi^{-1}(x)$ and the link $\phi^{-1}(y)$, where $y \in S^2$ is any regular value of ϕ.

It was first suggested by Faddeev and Niemi [50] that there could be minimal energy configurations ϕ where the *position curve* $\phi^{-1}((0, 0, -1))$ is knotted.

Sutcliffe constructed (local) minimal energy configurations ϕ where the preimage set $\phi^{-1}((0,0,-1))$ is the (p,q)-torus link [129]. His approach uses Brauner's polynomial $u^p + v^q$ to construct the rational map

$$W(u,v) = \frac{v^\alpha u^\beta}{f(u,v)} = \frac{v^\alpha u^\beta}{u^p + v^q}, \tag{3.20}$$

where α is a positive integer and β is any integer. Note that $W^{-1}(\infty)$ is the desired (p,q)-torus link.

Defining ϕ via

$$W(u,v) = \frac{\phi_1 + \mathrm{i}\phi_2}{1+\phi_3}, \tag{3.21}$$

which is essentially just an inverse stereographic projection, Sutcliffe obtained a map ϕ of the desired form. We can use the (non-standard) stereographic projection

$$v = (x_1 + \mathrm{i}x_2)\frac{\sin(f)}{R}, \qquad u = \cos(f) + \frac{\sin(f)}{R}\mathrm{i}x_3, \tag{3.22}$$

where $R^2 = x^2 + y^2 + z^2$ and f is a monotonically decreasing function of the radius $R > 0$, satisfying the boundary conditions $f(0) = \pi$ and $f(\infty) = 0$, whose explicit derivation can be found in [129]. With this definition ϕ satisfies the boundary condition $\phi(\infty) = (0,0,1)$, since (u,v) goes to $(1,0)$ as R goes to infinity. It is a simple calculation to show that $Q(\phi) = \alpha p + \beta q$.

Using ϕ as an initial condition for a numerical energy minimization, Sutcliffe obtained several minimal energy configurations where the preimage of $(0,0,-1)$ is the (p,q)-torus link. Note however that in general, the link type of configuration could change in the process of energy minimization as there is no restriction that $(0,0,-1)$ has to be a regular value at all times, i.e. the link could pass through itself at some time.

Paul Jennings extended Sutcliffe's construction to algebraic links essentially by simply replacing $u^p + v^q$ in the denominator of W in Equation (3.20) by the complex polynomial corresponding to the desired algebraic link [63]. These initial conditions gave rise to minimal energy conformations that are torus links and cables of torus links, but also the hyperbolic knot 10_{139}.

If we want to generalise this further to obtain initial conditions containing arbitrarily complicated links, we need (like in the other physical systems discussed so far) to find a way to construct a polynomial from $\mathbb{R}^4$ to the complex numbers which vanishes on S^3 exactly on the desired link L and could then be used to define W as in Equation (3.20) and ϕ as in Equation (3.21).

3.4 Knotted field lines in electromagnetism

Fields with knotted field lines have been suggested as an explanation for the little-understood phenomenon of ball-lightning [113]. The fact that ball-lightning has a lifespan that is much longer than that of regular lightning could then be attributed to the stability that is forced on the system by topological constraints.

For any rational map W defined as in Equation 3.20 we can (following [74] and [75]) define the vector field

$$\mathbf{B} = \frac{\nabla\overline{W} \times \nabla W}{2\pi i(1 + W\overline{W})^2} \tag{3.23}$$

on $\mathbb{R}^3$.

Direct calculations show that $\mathbf{B}$ is smooth, divergence-free and that the value of W is constant along the flow lines of $\mathbf{B}$. Note that $W^{-1}(z) \cap S^3$ is isotopic to $W^{-1}(\infty) \cap S^3 = L$ for all $z \in \mathbb{C}$ whose modulus is large enough. Since none of the points on W's level set of z is a stationary point of this flow, it follows that there are flow lines that are exactly $W^{-1}(z)$ and hence the desired link L.

This gives a method of constructing a vector field with flow lines of link type L for any algebraic link. The helicity

$$Q(B) = \int \mathbf{A} \cdot \mathbf{B} d^3\mathbf{r}, \tag{3.24}$$

where $\mathbf{A}$ is a vector potential of $\mathbf{B}$, i.e. $\mathbf{B} = \nabla \times \mathbf{A}$ is a topological invariant that measures how flow lines that are close twist around each other. It is precisely their linking number and therefore equal to $Q(\phi)$ as defined in the previous section. For torus links we thus have a helicity $Q(\mathbf{B}) = \alpha p + \beta q$ that we can control by varying the positive integer α and the integer β.

Physical examples of systems where knotted flow lines of vector fields play a role are topological fluid dynamics and electromagnetism. However, the vector fields usually need to satisfy some differential equation, for example Maxwell's equations in the case of electromagnetic fields. Vector fields as in (3.23) have been used as initial configurations to construct knotted time-dependent electromagnetic fields [112, 7].

While it is often extremely challenging to see which steps of the construction have to be modified in order to obtain vector fields with knotted flow lines that actually describe physical systems, Kedia et al. [73] managed to do this for electromagnetic fields with torus links. They explicitly constructed electromagnetic fields $\mathbf{F} = \nabla u^p \times \nabla v^q$, where $(u, v) \in S^3$ is identified with $(x, y, z) \in \mathbb{R}^3$ via Equation

(3.9) with $\varepsilon = 1$, that contain magnetic flow lines and electric flow lines that form the (p,q)-torus link at the time $t = 0$. Furthermore, their fields satisfy Maxwell's equations and the links remain stable for all time.

Extending their construction to more general links remains an open problem, but we can see that if we can construct a complex-valued polynomial f that vanishes on a given link L, we can define W as in Equation (3.20) and B as in (3.23) and at least have a vector field with the desired topology, albeit it does not satisfy any of the physical constraints. Kedia et al [75] showed that if $\mathbf{B}$ and a corresponding electric field $\mathbf{E}$ satisfy certain PDEs at the time $t = 0$, then the time-dependent electromagnetic field that results from taking $\mathbf{E} + \mathrm{i}\mathbf{B}$ as initial condition for Maxwell's equations has flow lines of the same link type as $\mathbf{E} + \mathrm{i}\mathbf{B}$ for all time.

3.5 Knotted defect lines in liquid crystals

A liquid crystal is a state of matter where elongated molecules fill a three-dimensional space. Ignoring details from chemistry we can describe a configuration by a director field $\mathbf{n} : D \to \mathbb{RP}^2$ in some domain $D \subset \mathbb{R}^3$. This director field describes the orientation of the long axis of the molecules at each point in space. There are two different types of liquid crystal phases that we discuss here: the nematic phase and the smectic A phase. Our exposition follows [66, 91, 92, 93].

For a nematic liquid crystal the orientation of the molecules is a smooth function of their position. Nematic liquid crystals possess many desirable optical properties, which make them useful as LCDs (liquid crystal displays) in several modern devices. There is a rich theory of defects in liquid crystals, points and lines where the director field cannot be continuously defined. We are particularly interested in knotted defect lines, or knotted disclination lines as they are also called.

Recall from Section 3.1 that from a knotted parametric curve K we can calculate an electromagnetic potential $P : \mathbb{R}^3 \backslash K \to S^1 = [0, 2\pi]/0 \sim 2\pi$. Alexander uses this function to construct a nematic liquid crystal with defect knot K [16] via

$$\mathbf{n}(x, y, z) = (\cos(P/2), \sin(P/2), 0) \tag{3.25}$$

The function P satisfies some nice properties, it is for example harmonic, and for low crossing numbers the knotted defects constructed in this manner

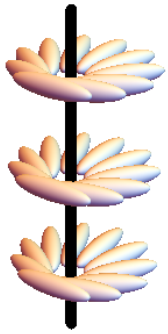

Figure 3.3: Ellipsoid modeling the molecules of a nematic liquid crystal in the tubular neighbourhood of a disclination line. The director field **n** is pointing in the direction of the long axis of each ellipsoid.

turn out to be stable. When the director field **n** as in Equation (3.25) is taken as an initial configuration for an energy minimization, the knot type does not change during the energy minimization process.

One might wonder about alternative approaches, that do not involve the brute force Biot-Savart integral and of course in (3.25) there is nothing special about the choice of P, any smooth function $\mathbb{R}^3\backslash K \to S^1$ will do. Machon and Alexander [91, 92, 93] consider the argument $\arg f$ of Milnor's polynomials $u^p - v^q$ to construct knotted defects in the shape of torus knots in an analogous fashion to (3.25). Again a generalisation of this approach to arbitrarily complicated knots requires a construction of polynomials with arbitrarily knotted zero level sets.

The molecules in a liquid crystal in a smectic A phase tend to align themselves such that their long axes are orthogonal to layers. We can for example consider a vector field $\mathbf{B} : S^3\backslash K \to \mathbb{R}^3$ such as the one obtained from the Biot-Savart formula (3.1). Then restricting B to the subset of $S^3\backslash K$ where it is non-vanishing and composing this map with the projection from $\mathbb{R}^3$ to $\mathbb{RP}^2$ results in a director field with line defect K and point defects at the points where **B** vanishes. The layers of molecules are then the level sets of the potential function $P : S^3\backslash K \to S^1$ such that $\mathbf{B} = \nabla P$ and **n** is the composition of **B** with the projection from $\mathbb{R}^3\backslash\{(0,0,0)\}$ to $\mathbb{RP}^2$. Where $\mathbf{B} = (0,0,0)$, **n** is not defined. This corresponds to point defects at points where **B** vanishes.

Similarly, we could take a complex-valued polynomial $f : \mathbb{R}^3 \to \mathbb{C}$ that vanishes on a given link L and compose $\nabla \arg f$ with the projection map from

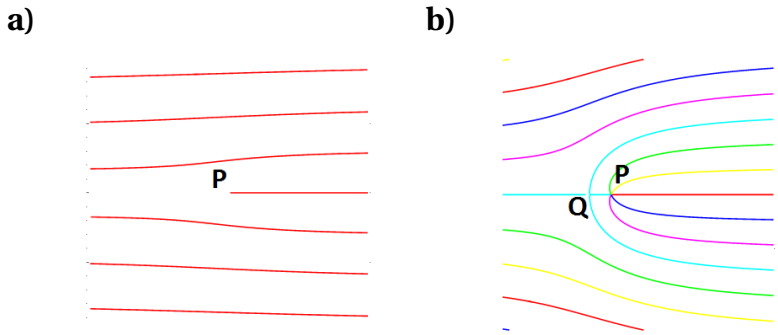

Figure 3.4: A 2-dimensional slice of a smectic liquid crystal with an edge dislocation. a) The red lines are the level sets of a circle-valued function. All surfaces meet at the point P, the intersection of the knotted dislocation line with the slice. b) A closer look at the neighbourhood of P. Different layers meet at P such that no normal direction is defined. The point Q is a saddle point of the cyan surface.

$\mathbb{R}^3\backslash\{(0,0,0)\}$ to $\mathbb{RP}^2$. Therefore, an algorithmic construction of complex-valued polynomials with given knotted vanishing sets offers (again) an approach to the construction of topological defects in liquid crystals, alternative to the brute force Biot-Savart calculation.

In Figure 3.5a) we show a sketch of a 2-dimensional slice of a liquid crystal with a typical edge dislocation, a line defect intersecting the slice in a point P. The red lines indicate the layers of molecules, which are oriented orthogonal to these layers. Figure 3.5b) offers a closer look at the region around the intersection point P of the defect line with the slice. In P the different surfaces (indicated by differently-coloured lines) meet, so that there is no well-defined orthogonal direction. Moreover, around the intersection point P of K with the slice the normals to the surfaces rotate around K as required in a fibration. At the point Q the normal direction (in 2D) is not well-defined either. However, it is not a critical point, but simply a saddle point, where the normal to the cyan surface is orthogonal to the slice.

In a tubular neighbourhood of the knot, the constructions outlined above, be it the Biot-Savart calculation or the polynomial approach, result in layers as in Figure 2.10. We therefore obtain a close connection between the existence of knot fibrations in liquid crystals and the existence of point defects. If K is not fibred, then P (or $\arg f$) must have critical points. These are then by construction defect points of the resulting liquid crystal configuration. In other words, fibred knots are the only defect lines that can exist in a liquid crystal (constructed with the methods above) without additional point defects.

The introduction of these extra defect points comes with a price in terms of the energy of the liquid crystal. The free energy of the ground state of a liquid crystal can be written as an integral over second orders of gradients of the director field $\mathbf{n}$,

$$F = \frac{1}{2}\int K_{11}(\nabla\cdot\mathbf{n})^2 + K_{22}(\mathbf{n}\cdot(\nabla\times\mathbf{n}))^2 + K_{33}(\mathbf{n}\times(\nabla\times\mathbf{n}))^2 dV, \tag{3.26}$$

where the K_{ii} are the Frank constants depending on the particular liquid crystal. The three terms in the energy are known as bend $B = (\mathbf{n}\times(\nabla\times\mathbf{n}))^2$, splay $S = (\nabla\cdot\mathbf{n})^2$ and twist $T = (\mathbf{n}\cdot(\nabla\times\mathbf{n}))^2$. The bend measures the local rate of change of the director $\mathbf{n}$ along its axis, while the splay S measures the change of $\mathbf{n}$ perpendicular to its axis and the twist T is the rotation of $\mathbf{n}$ about an axis perpendicular to its axis.

We consider the following setting. We delete a tubular neighbourhood of the defect line in the shape of a knot K from $\mathbb{R}^3$ and demand that on the boundary the director twist by 2π as one follows a meridian of the toroidal boundary (i.e. normal to the surfaces in Figure 2.10). Furthermore, the director field should be constant at the point at infinity (or equivalently after rescaling on the boundary of a ball D in $\mathbb{R}^3$). We can now study all possible smectic liquid crystals that satisfy these boundary conditions and have a defect line ambient isotopic to K. Let $E(K)$ be the minimal energy of all director fields satisfying these boundary conditions and $\mathbf{n}(K)$ be a director field with $E(\mathbf{n}(K)) = E(K)$.

Since the energy is an expansion in terms of the gradient of the director and $\nabla\mathbf{n}$ diverges around a critical point, we expect critical points to be energetically unfavourable. We thus expect that the minimal energy configurations $\mathbf{n}(K)$ of liquid crystals with line defects in the form of fibred knots under the given boundary conditions give fibrations in the sense that the layers of molecules are the fibres of a fibration of the knot complement over S^1. This argument is based on the assumption that the divergence of $\nabla\mathbf{n}$ around a critical point leads to a larger energy than that of a configuration, where $\nabla\mathbf{n}$ is bounded. From a mathematical perspective this does not always have to be the case.

Besides the existence of point defects, the length of the line defect, the radius of the tube around the knot that is removed and the radius of the ball D also affect the energy of the configuration.

This shows that fibred knots play a special role in the study of knotted defect lines in smectic liquid crystals, since they are the only knots that do not need additional point defects in the constructions outlines above. Furthermore, we

expect their minimal energy configurations under given boundary conditions to be without point defects and thus to explicitly describe fibrations.

3.6 Discussion

We have seen that knotted configurations have been theoretically constructed for many diverse physical systems. Even though these are mathematically quite different, including scalar fields, director fields and vector fields, the methods of the past approaches fall easily into only two categories. There is a brute-force approach, that for any given knot given as a parametric curve finds knotted configurations based on the Biot-Savart integral. This approach works in principle for any knot, but it is computationally quite expensive.

The other method of construction is based on complex-valued polynomial functions that vanish on the desired link, such as Brauner's polynomials for torus links. This approach is perhaps mathematically more elegant, but it has been quite restrictive with respect to the class of links that it can access, since it requires the knowledge of an explicit polynomial for a given link. For algebraic links that is of course the case, but for more general links we lack a machinery to construct such polynomials.

Chapters 4, 5 and 6 are devoted to the development of such a generalised construction.

Once we know how to find a polynomial for any link, we can explicitly write down a knotted initial configuration for all systems discussed in this chapter. These initial configurations then typically evolve with time, which allows physicists to study the dynamics of knots in these systems and the topological properties of minimal energy configurations.

Lemniscate Knots

4

The construction of polynomial maps $f : \mathbb{R}^3 \to \mathbb{C}$ where the nodal lines form torus links was briefly sketched in Chapter 2. In this chapter, we generalise these ideas to a larger class of links, which we call the lemniscate links and lemniscate knots. Most of the material is based on the author's contribution to [23].

Definition 4.1. *Let s, r and ℓ be positive integers with s and ℓ coprime. Then the (s,r,ℓ)-lemniscate link $L(s,r,\ell)$ is defined to be the closure of the braid, whose s strands are parametrised by*

$$(X_j^{s,r}(t), Y_j^{s,r,\ell}(t), t) := \left(\cos\left(\frac{rt+2\pi j}{s}\right), \sin\left(\frac{\ell(rt+2\pi j)}{s}\right), t\right), \quad t \in [0,2\pi],\ j = 1,2,\ldots,s. \tag{4.1}$$

*We say that a link L is a **lemniscate link** if there are s, r and ℓ as above such that $L = L(s,r,\ell)$.*

While a torus link is the closure of a braid whose strands lie on a cylinder $S^1 \times [0,2\pi]$, a lemniscate link is the closure of a braid whose strands can be taken to lie on the cartesian product of a generalized lemniscate figure (cf. Figure 4.1) and an interval in a highly symmetric fashion. Dennis and King [41, 79], who first defined this class of links, realised that this leads again to a rather simple parametrisation of the strands in terms of a single trigonometric function.

Projecting the braid that is given by Equation (4.1) in the xy-plane gives a generalized lemniscate figure with ℓ lobes. The numbers s and r refer to the number of strands and the number of repeats of a basic braid, respectively.

Note that if $\ell = 1$, Equation (4.1) reduces to Equation (4.2), so that the (s,r)-torus link is the $(s,r,1)$-lemniscate link.

The condition that s and ℓ have to be coprime guarantees that different strands do not intersect.

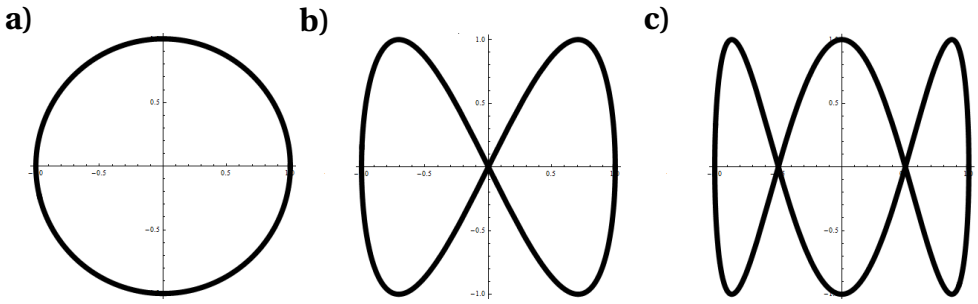

Figure 4.1: Generalised lemniscate curves with ℓ lobes parametrised by $(\cos(t), \sin(\ell t))$. a) $\ell = 1$ gives a circle. b) $\ell = 2$ is the lemniscate of Gerono. c) The $\ell = 3$ lemniscate curve with 3 lobes.

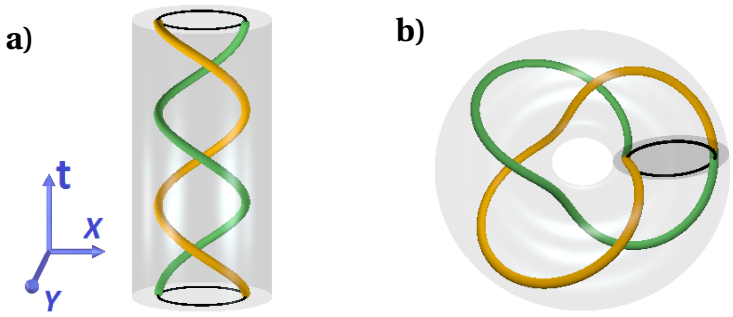

Figure 4.2: Closing a helical braid on a cylinder to a torus knot. a) The strands of the 2-strand braid σ_1^{-3} form a three-crossing double helix inside a cylinder. X, Y and t increase in the direction of the corresponding arrow. b) Gluing the top and bottom of the cylinder together closes the braid, yielding a trefoil knot inside a torus. This process identifies the height coordinate t in the space of the braid with $\arg(v)$.

The symmetries of these trigonometric functions force certain symmetries on the braid and thus its closure, the lemniscate link, that allow us in some cases to derive explicit formulas for certain knot invariants, such as the minimal crossing number, the braid index or the Alexander polynomial of lemniscate links.

4.1 Polynomials for lemniscate knots

As a basis for our later construction, it is helpful to formalise the procedure for torus links and the figure-8 knot, generalising to arbitrary lemniscate braids. Consider the (s, r)-torus link. Since it can be drawn on a torus, it is the closure of a braid B, whose s strands can be taken to lie on a cylinder $S^1 \times [0, 2\pi]$, undergoing r/s full twists as in Figure 4.2.

The s strands can thus be parametrised as

$$(X_j^{s,r}(t), Y_j^{s,r,1}(t), t) := \left(\cos\left(\frac{rt + 2\pi j}{s}\right), \sin\left(\frac{rt + 2\pi j}{s}\right), t\right), \quad t \in [0, 2\pi],\ j = 1, 2, \ldots, s. \tag{4.2}$$

This corresponds to the s strands being symmetrically arranged on a circle at every height t. Note that the projection of the braid in the xy-plane is the unit circle.

We now define a family of complex polynomials $g_t \in \mathbb{C}[u]$ through

$$g_t(u) = \prod_{j=1}^{s} \left(u - X_j^{s,r}(t) - \mathrm{i}Y_j^{s,r}(t)\right), \tag{4.3}$$

such that the s roots of g_t are the positions of the s strands of the braid B at height t, where we have identified the horizontal plane (orthogonal to the braid height) at $z = t$ with the complex plane.

Thus the function $g : \mathbb{C} \times [0, 2\pi] \to \mathbb{C}$ given by $g(u, t) := g_t(u)$ is a polynomial in u and vanishes exactly on the braid B, parametrised as in Equation (4.2).

We can write $\frac{1}{2}(\mathrm{e}^{\mathrm{i}t} + \mathrm{e}^{-\mathrm{i}t})$ for $\cos(t)$ and $\frac{1}{2\mathrm{i}}(\mathrm{e}^{\mathrm{i}t} - \mathrm{e}^{-\mathrm{i}t})$ for $\sin(t)$ in Equation (4.2). Then expanding the product in Equation (4.3) results in

$$g(u, t) = u^s - \mathrm{e}^{r\mathrm{i}t}. \tag{4.4}$$

Note that Brauner's polynomial $f(u, v) = u^s - v^r$ now can be obtained from Equation (4.4) by replacing $\mathrm{e}^{\mathrm{i}t}$ by v. This way we identify the braid height t with the angular coordinate of a second complex variable v. Note that f is then well-defined on all of $\mathbb{C}^2$ and on $\mathbb{C} \times S^1$, i.e. when $v = \mathrm{e}^{\mathrm{i}t}$, we have $f(u, \mathrm{e}^{\mathrm{i}t}) = g(u, t)$ and therefore $f^{-1}(0) \cap (\mathbb{C} \times S^1)$ is the (s, r)-torus link. As we know from Brauner's work, the vanishing set of f on the unit three-sphere is that same link.

We now describe the construction of a polynomial for the figure-eight knot 4_1 as outlined in [41]. The figure-eight knot is not a torus knot and therefore we cannot use the braid parametrisation from Equation (4.2), but it is the closure of the pigtail braid given by the braid word $\sigma_1\sigma_2^{-1}\sigma_1\sigma_2^{-1}$, whose symmetry allows a comparatively simple parametrisation, too.

It is the basis of the constructions of both Perron [111] and Dennis [41] that the three strands of this braid can be parametrised as

$$(X_j^{3,2}(t), Y_j^{3,2,2}(t), t) := \left(\cos\left(\frac{2t + 2\pi j}{3}\right), \sin\left(\frac{2(2t + 2\pi j)}{3}\right), t\right), \quad t \in [0, 2\pi],\ j = 1, 2, 3. \tag{4.5}$$

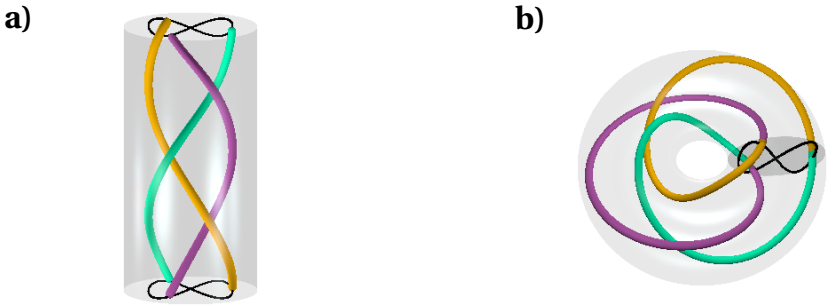

Figure 4.3: The lemniscate braid with braid word $(\sigma_1\sigma_2^{-1})^2$, closing to the figure-8 knot. a) The strands of the braid $(\sigma_1\sigma_2^{-1})^2$ drawn in a cylinder. The strands are parametrised such that they lie on the '∞' figure times $[0, 2\pi]$ (the pigtail braid). b) Gluing the the ends of the cylinder yields a torus enclosing the figure-8 knot.

The figure-eight knot is therefore the $(3, 2, 2)$-lemniscate link.

While in the case of torus links the strands are arranged symmetrically on the unit circle, here the three strands are placed symmetrically (relative to the parameter t) on a lemniscate figure $(\cos(t), \sin(2t))$, $t \in [0, 2\pi]$. Projecting the braid into the xy-plane results in this lemniscate figure. At $t = 0$, the strands have the coordinates $(1, 0, 0)$, $(-1/2, -\sqrt{3}/2, 0)$ and $(-1/2, \sqrt{3}/2, 0)$. As the value of t increases, the strands move on the lemniscate figure until at $t = \pi$ the positions of the strands on the lemniscate figure have been cyclically permuted, i.e. the strand that went through the point $(1, 0, 0)$ $(j = 1)$ is now at $(-1/2, -\sqrt{3}/2, \pi)$, which (projected on the lemniscate figure) is the position that the second strand $(j = 2)$ started at, while the second strand is now at the initial position of the third strand $(j = 3)$, which itself is at $(1, 0, \pi)$, the initial position of the first strand.

As t increases further to 2π, the strands move again on the lemniscate figure until at $t = 2\pi$ the strands have again been cyclically permuted, so that the first strand ends up at $(-1/2, \sqrt{3}/2, 2\pi)$, which (again projected on the lemniscate figure) is the initial position of the third strand and so on.

The two cyclic permutations correspond to two repeats of the basic braid word $\sigma_1\sigma_2^{-1}$ that is repeated twice in the braid word of the pigtail braid.

In order to make the construction work for the figure-eight knot, we need two additional real, positive parameters a and b. Note that since Equation (4.5)

is a parametrisation of the pigtail braid, so is

$$(aX_j^{3,2}, bY_j^{3,2,2}, t) = \left(a\cos\left(\frac{2t+2\pi j}{3}\right), b\sin\left(\frac{2(2t+2\pi j)}{3}\right), t\right), \quad t \in [0, 2\pi],\ j = 1,2,3 \tag{4.6}$$

for every positive value of a and b. Here a and b are simply scaling parameters, that stretch or shrink the braid in the x- and the y-direction, respectively, which clearly does not affect the braid word or the link type of its closure.

Note that switching the sign of either a or b to a negative number results in a mirrored braid.

For each positive choice of a and b, we can define the family of functions g_t as in the case of torus links:

$$g_t(u) := \prod_{j=1}^{3} \left(u - aX_j^{3,2}(t) - \mathrm{i}bY_j^{3,2,2}(t)\right). \tag{4.7}$$

Again the roots of g_t for a given value of t correspond to the positions of the strands of the pigtail braid in the parametrisation in Equation (4.6) at height t. Then again $g : \mathbb{C} \times [0, 2\pi] \to \mathbb{C}$ with $g(u,t) := g_t(u)$ is a polynomial in u which has the pigtail braid as its vanishing set.

Expanding the product in Equation (4.7) gives

$$\begin{aligned} g(u,t) = u^3 &- \frac{3}{4}u(b^2 - a^2 - ab(\mathrm{e}^{2\mathrm{i}t} - \mathrm{e}^{-2\mathrm{i}t})) \\ &- \frac{1}{8}(a^3(\mathrm{e}^{2\mathrm{i}t} + \mathrm{e}^{-2\mathrm{i}t}) + b^3(\mathrm{e}^{4\mathrm{i}t} - \mathrm{e}^{-4\mathrm{i}t}) + 3ab^2(\mathrm{e}^{2\mathrm{i}t} + \mathrm{e}^{-2\mathrm{i}t})). \end{aligned} \tag{4.8}$$

Note that g is now not only a polynomial in u, but also in $\mathrm{e}^{\mathrm{i}t}$ and $\mathrm{e}^{-\mathrm{i}t}$, so that replacing $\mathrm{e}^{\mathrm{i}t}$ by a complex variable v and $\mathrm{e}^{-\mathrm{i}t}$ by its complex conjugate $\overline{v}$ results in a polynomial $f : \mathbb{C}^2 \to \mathbb{C}$ in u, v and $\overline{v}$, that like in the case of torus links satisfies $f(u, \mathrm{e}^{\mathrm{i}t}) = g(u,t)$. We do not obtain a polynomial holomorphic in u and v, since g depends on both $\mathrm{e}^{\mathrm{i}t}$ and $\mathrm{e}^{-\mathrm{i}t}$. We call such functions that are polynomials in u, v and $\overline{v}$ *semiholomorphic*.

By construction $f^{-1}(0) \cap (\mathbb{C} \times S^1)$ is the figure-eight knot, but what we are interested in is the nodal set on the unit three-sphere.

So far we have not used the scaling parameters a and b that we introduced earlier. In order to stress the dependence of f on a and b, we henceforth denote it by $f_{a,b}$.

It turns out that for small values of a and b (e.g. $a = 1$ and $b = 1/2$) the vanishing set of $f_{a,b}$ on the unit three-sphere is the desired figure-eight knot, while for others (e.g. $a = b = 1$), it is not. This is proved in more generality in Chapter 5.

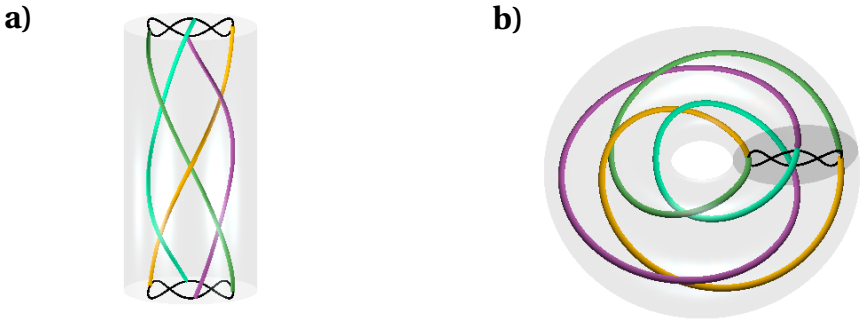

Figure 4.4: A braid with an $\ell = 3$ lemniscate trajectory, and its closure. a) The trigonometric braid with parameters $(s, r, \ell) = (4, 2, 3)$. b) Closure of the braid, isotopic to the link $L6a1$.

The successful construction of the figure-eight knot motivated the definition of the family of lemniscate links (Definition 4.1) and the generalization of the procedure outline above to this family.

Knotted curves parametrised by trigonometric functions have been studied before, most notably in the case of Lissajous knots [24] and Lissajous-toric knots [126]. In the case of lemniscate links however, we require a braid parametrisation in terms of one single trigonometric term for x and y-coordinate respectively.

The construction of the (s, r, ℓ)-lemniscate link as the vanishing set of a semiholomorphic polynomial on the unit three-sphere can now be done completely analogously to that of the figure-eight knot.

We define a family of complex polynomials

$$g_t(u) = \prod_{j=1}^{s} (u - aX_j^{s,r}(t) - \mathrm{i}bY_j^{s,r,\ell}(t)), \qquad t \in [0, 2\pi], \tag{4.9}$$

whose roots encode the positions of the strands of the desired braid at each height t.

Defining $g(u, t) := g_t(u)$ as before and expanding the product results in a polynomial in u, $\mathrm{e}^{\mathrm{i}t}$ and $\mathrm{e}^{-\mathrm{i}t}$. This polynomial expression is unique once we require that there are no occurrences of $\mathrm{e}^{\mathrm{i}t}\,\mathrm{e}^{-\mathrm{i}t}$, which can obviously be canceled. Replacing every instance of $\mathrm{e}^{\mathrm{i}t}$ by v and every instance of $\mathrm{e}^{-\mathrm{i}t}$ by the conjugate $\overline{v}$ results in a semiholomorphic polynomial f in u, v and $\overline{v}$ with $f(u, \mathrm{e}^{\mathrm{i}t}) = g_t(u)$, or more accurately a family of semiholomorphic polynomials $f_{a,b}$.

By construction the vanishing set of $f_{a,b}$ on $\mathbb{C} \times S^1$ is the closure of the braid parametrised by Equation (4.1) and hence the (s, r, ℓ)-lemniscate link $L(s, r, \ell)$.

We show in Theorem 5.1 that for small enough a and b, the same is true for the vanishing set on the unit-three sphere S^3. More precisely, for every a and b there is a $\lambda > 0$ such that $f_{\lambda a,\lambda b}^{-1}(0) \cap S^3 = L(s,r,\ell)$.

Some polynomials for lemniscate links with low values for s, r and ℓ have been calculated with fixed $a = 1$ and $b = 1/\ell$ in [41]. While these choices are sufficient for the examples, it is not clear if this is always the case or if there are lemniscate links for which a and b have to be chosen smaller. The original construction in [41] does not use a and b as flexible parameters, which is necessary for the construction to be guaranteed to work.

Note that how small a and b have to be chosen to make the construction work depends on s, r and ℓ. Suppose that g is the polynomial derived from Equation (4.9) for the (s,r,ℓ)-lemniscate link. Then multiplying all exponents of $\mathrm{e}^{\mathrm{i}t}$ and $\mathrm{e}^{-\mathrm{i}t}$ in the polynomial expression of g by a positive integer n gives the g-polynomial for the (s,nr,ℓ)-lemniscate link.

Let $f_{a,b}$ be the semiholomorphic polynomial with a and b such that $f_{a,b}^{-1}(0)\cap S^3$ is the (s,r,ℓ)-lemniscate link. Then it is in general not true that multiplying all exponents of v and $\overline{v}$ in $f_{a,b}$ by a positive integer n results in a semiholomorphic polynomial $\widetilde{f_{a,b}}$ such that the nodal set of $\widetilde{f_{a,b}}$ on the unit three-sphere is the (s,nr,ℓ)-lemniscate link. This is because even though a and b are small enough to give the (s,r,ℓ)-lemniscate link, they might not be small enough for the (s,nr,ℓ)-lemniscate link and a different choice a' and b' might be required such that (s,nr,ℓ)-lemniscate link is the vanishing set of $f'_{a',b'}$ on the unit three-sphere.

Like in the case of the lemniscate links, known symmetries can also be used to find (comparatively) simple trigonometric parametrisations of braids whose strands do not follow lemniscate figures, but figures that are built of lemniscates, such as braids where the strands follow a *rotating* lemniscate figure. The s strands of a rotating lemniscate braid are then parametrised by

$$Z_j^{s,r,\ell,n}(t) = e^{\mathrm{i}tn}(X_j^{s,r}(h) + \mathrm{i}Y_j^{s,r,\ell}(t)), \tag{4.10}$$

where $X_j^{s,r}$ and $Y_j^{s,r,\ell}$ are as in Equation (4.1) and $n \in \mathbb{Z}$ is the number of full clockwise rotations that the lemniscate figure performs as t increases from 0 to 2π. Again the function $g_{\lambda,\lambda}(u,t) = \prod_{j=1}^{s}(u - \lambda Z_j^{s,r,\ell,n}(t))$ is a polynomial in u, $\mathrm{e}^{\mathrm{i}t}$ and $\mathrm{e}^{-\mathrm{i}t}$ and the proof of Theorem 5.1 implies that for small enough λ, replacing $e^{\mathrm{i}t}$ by v and $e^{-\mathrm{i}t}$ by $\overline{v}$ results in a semiholomorphic polynomial f_λ whose nodal set on S^3 is ambient isotopic to the closure of the braid with strands defined by (4.10).

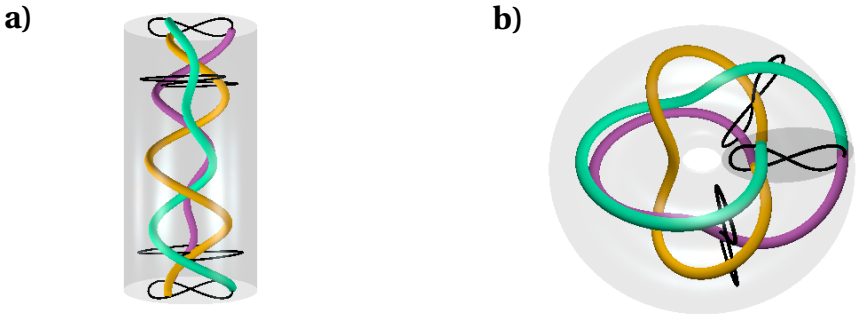

Figure 4.5: Rotating lemniscate braid closing to the composite of two trefoil knots. a) Braid executing a rotating lemniscate, $(s, r, \ell, n) = (3, 2, 2, 1)$, with braid word $(\sigma_1^{-1}\sigma_2)^2(\sigma_1\sigma_2\sigma_1)^{-2}$. b) Closure of the braid forming the composite of two trefoil knots (with same chirality), with minimum braid word $\sigma_1^{-3}\sigma_2^{-3}$.

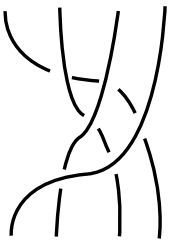

Figure 4.6: A diagram of the half-twist Δ_4.

In the case of $s = 3$, $r = 2$, $\ell = 2$ and $n = 1$, this results in the connected sum of two trefoil knots as can be seen in Figure 4.5. A half twist of a braid on s strands is shown in Figure 4.6 and given by $\Delta_s = (\sigma_1)(\sigma_2\sigma_1)(\sigma_3\sigma_2\sigma_1)\dots(\sigma_{s-1}\dots\sigma_1)$. Therefore rotating the braid which closes to the $L(s, r, \ell)$ by n turns, is isotopic to the braid with word $w^{s,r,\ell}\Delta_s^{-2n}$ where $w^{s,r,\ell}$ is the braid word of the (s, r, ℓ)-lemniscate braid.

Alternatively, more complicated braids can be built by a generalisation of the notion of cabling as was originally done for iterated torus links by Brauner [27]. Rather than considering braids where single strands execute generalised lemniscate trajectories, a single strand/root in the polynomial may be replaced by a cluster of strands/roots, executing their own smaller lemniscate figure which we call an 'epicycle'. This idea and terminology is due to Mark Dennis. This process can be iterated. However, closures of such braids typically have many crossings, so this does not generate tabulated knots.

4.2 Properties of lemniscate knots

The fact that lemniscate links are closures of braids parametrised by single trigonometric functions means that there are certain symmetries that every lemniscate braid has to satisfy. The first observation is that the particular parametrisation makes it comparatively easy to extract a braid word for any (s, r, ℓ)-lemniscate braid.

Projecting the braid parametrisation (4.1) into the xz-plane and keeping track of the signs results in a braid diagram of the (s, r, ℓ)-lemniscate braid. It is made up of the curves $(X_j^{s,r}(t), t)$. Crossings occur when $(X_j^{s,r}(t'), t') = (X_{j'}^{s,r}(t'), t')$ for some $t = t'$ and some j, j' with $j \neq j'$. We can check using the expression for $X_j^{s,r}(t)$ in (4.1) that this requirement is satisfied if and only if $tr = 0 \mod 2\pi$ or $tr = \pi \mod 2\pi$. By Markov's theorem conjugate braids close to the same link. Hence we can place the crossings occurring simultaneously at $t = 0$ and $t = 2\pi$ either at the end or at the beginning of the braid word without changing the braid closure. We choose to place them at the beginning.

Note that the crossings that occur at t with $tr = 0 \mod 2\pi$, $\sigma_k^{\varepsilon_k}$ with k odd, $\varepsilon = \pm 1$, are simultaneous in t, as are the crossings at t with $tr = \pi \mod 2\pi$ with k even.

Our convention (as discussed in Chapter 2) is that the strand labelled by j crosses over j' at t if $Y_j^{s,r,\ell}(t) > Y_{j'}^{s,r,\ell}(t)$.

For $r = 1$, we obtain the basic braid word

$$\begin{aligned} w^{(s,r=1,\ell)} &= \sigma_1^{\varepsilon_1}\sigma_3^{\varepsilon_3}\sigma_5^{\varepsilon_5}\cdots\sigma_2^{\varepsilon_2}\sigma_4^{\varepsilon_4}\sigma_6^{\varepsilon_6}\cdots \\ &= \prod_{\substack{j=1 \\ j \text{ odd}}}^{s} \sigma_j^{\varepsilon_j} \prod_{\substack{j=1 \\ j \text{ even}}}^{s} \sigma_j^{\varepsilon_j}, \end{aligned} \tag{4.11}$$

and for general r, we have r repeats of this basic braid word, i.e. $w^{(s,r,\ell)} = (w^{(s,1,\ell)})^r$. The signs of the crossings ε_k are determined by ℓ and s and depend on the parity of the lobe of the generalised lemniscate figure in which the crossing occurs. Since the strands cannot intersect, s and ℓ must be coprime (so there is no t for which $(X_j^{s,r}(t), Y_j^{s,r,\ell}(t), t) = (X_{j'}^{s,r}(t), Y_{j'}^{s,r,\ell}(t), t)$ for some $j \neq j'$). We choose $s > \ell$, since for any knot with $s < \ell$, there is $\ell' < s$ which gives rise to the same braid word. It is straightforward to see that the crossing signs, for $j = 1, \ldots, s-1$, and

s and ℓ coprime, are determined by the following rule:

$$\varepsilon_{s-1} = -\operatorname{sign} b \qquad \text{and } \varepsilon_j = \begin{cases} -\varepsilon_{j+1} \text{ if there is an integer } m \text{ with } \frac{j}{s} < \frac{m}{\ell} < \frac{j+1}{s}, \\ +\varepsilon_{j+1} \text{ otherwise.} \end{cases} \tag{4.12}$$

For $\ell = 1$, this implies that the crossings all have the same sign, as expected for braid representations of torus links. For $\ell = 2$, s must be odd, and so all crossings $j < s/2$ are negative, and $j > s/2$ are positive if $b > 0$. Thus the $(3,2,2)$-lemniscate braid representation of the figure-8 knot is $(\sigma_1\sigma_2^{-1})^2$. Note that for negative values of b the vector $\boldsymbol{\varepsilon} = (\varepsilon_1, \varepsilon_2, \ldots, \varepsilon_{s-1})$ is exactly the negative of the $\boldsymbol{\varepsilon}$ for positive b. In general, the lemniscate braid representation is not the minimal braid representation of the knot or link as found by Gittings [55].

Lemniscate links are in the more general family of *spiral knots* (or links). A spiral knot (or link) is defined as the closure of the rth power of a braid word w in which every generator σ_k appears exactly once, either as positive or negative power $\varepsilon_k = \pm 1$ [28]. The braid word (4.11) clearly satisfies this condition and hence all lemniscate knots are spiral, but in general spiral knots are not subject to Equation (4.12). Following [28], the spiral knot with s strands, r repeats with signs determined by $\boldsymbol{\varepsilon}$ is denoted $S(s, r, \boldsymbol{\varepsilon})$, and the lemniscate knot with s strands, r repeats with ℓ lobes by $L(s, r, \ell)$; therefore $L(s, r, \ell) \simeq S(s, r, \boldsymbol{\varepsilon})$ for $\boldsymbol{\varepsilon}$ satisfying (4.12). Spiral knots have several remarkable properties, which do not depend on $\boldsymbol{\varepsilon}$.

Theorem 4.2. *The spiral knot/link $S = S(s, r, \boldsymbol{\varepsilon})$ satisfies the following properties.*

(i) If $r = 1$, S is the unknot;

(ii) S is an m-component link iff $\gcd(s, r) = m$, and in particular S is a knot when s and r are relatively coprime;

(iii) If $r = 2$, then S is a 2-bridge knot (i.e. rational);

(iv) Every spiral knot is a periodic knot [89] with period r;

(v) Every spiral knot is fibred [128];

(vi) If S is the closure of w^r for some basic braid word $w = \prod_{j=1}^{s-1} \sigma_{i_j}^{\varepsilon_{i_j}}$ with $i_j \neq i_k$ for all $j \neq k$, then S is also the closure of $\pi(w)^r$, where $\pi(w)$ is any anagram of w;

(vii) If r is a prime power, $r = p^k$, and S a 1-component link, then the Alexander polynomial $\Delta_S(t) \equiv (1 + t + \ldots + t^{s-1})^{r-1} \mod p$;

(viii) If S is a knot, the genus g of S satisfies $\frac{1}{2}\deg \Delta_S \leq g \leq \frac{1}{2}(s-1)(r-1)$;

(ix) If r is a prime power and S a knot, $\deg \Delta_S = (s-1)(r-1)$ and the genus g of S satisfies $g = \frac{1}{2}(s-1)(r-1)$;

(x) *If r is a prime power, the minimal crossing number c of S satisfies* $(s-1)(r-1) < c \leq (s-1)r$.

The proofs of all of these but parts (iii) and (v) are given in [28] (or are straightforward generalisations. Part (vii) is based on Murasugi's theorem [101]). Part (vi) is what allows a spiral knot to depend only on s, r and $\boldsymbol{\varepsilon}$, and not on the specific ordering of the basic word, which justifies the notation $S(s,r,\boldsymbol{\varepsilon})$. This means that we are free to choose the order in which the generators appear in the basic braid word, where some choices might be more natural than others. In the case of lemniscate knots it might be preferable to stick with the original braid word found in Equation (4.11). In [28] the authors prefer to arrange the generators with ascending indices, i.e. each basic braid word is $\prod_{j=1}^{s-1}\sigma_j^{\varepsilon_j}$. Part (iii) follows from considering a braid as the union of parametric curves in cylindrical coordinates as in Equation (4.1) with $a=b=1$, with angle t, radius $2+Y_j^{s,r,\ell}(t)$ and height $X_j^{s,r}(t)$; with $X_j^{s,r}$ as the height function, there are r maxima and r minima, so S is 2-bridge if $r=2$. More generally, this representation shows the r-fold periodicity as a cyclic symmetry generated by a $2\pi/r$ rotation about the axis of cylindrical coordinates. Part (v) follows from Theorem 2.15 by Stallings [128], saying that a knot is fibred if it is the closure of a homogeneous braid. This follows directly since the braid words of spiral knots are powers of braid words w, where every generator appears exactly once. Thus whenever a generator appears in the braid word w^r of a spiral knot it appears with the same unique sign with which it appears in the basic braid word w.

Strictly speaking there are two lemniscate knots $L(s,r,\ell)$ for every choice of s, r and ℓ, one for a positive value of b and one for a negative b. The two knots are mirror images, so that some invariants like the Alexander polynomial, the crossing number, the braid index and the genus do not distinguish them. In particular, the statements of Theorem 4.2 are valid for both cases.

Lemniscate knots have the additional symmetry that the ε of (4.12) is a palindromic vector if ℓ is odd, and anti-palindromic if ℓ is even, that is $\varepsilon_j=(-1)^{\ell+1}\varepsilon_{s-j}$. As we show below, this seems to give rise to symmetric tangle representations of rational lemniscate knots, and similarly palindromic minimal braid words (where known), although we do not have a general proof which covers all values of s, ℓ and r. In common with other studies of spiral knots [78], families of lemniscate knots and links seem to have common properties regarding their Alexander polynomial coefficients, Jones polynomial coefficients and tangle notation (when $r=2$), implying they are worthy of study in general, not simply

as the knots simply realisable as nodal sets of complex scalar functions. Dennis and King [79, 23] identified the lemniscate links for low values of s, r and ℓ using standard tabulations [10, 31] and polynomial invariants. Since these knot tables stop after minimal crossing number $c = 14$, there are not many lemniscate links with $r > 3$ and $s > \ell + 1$ that can be identified.

When $\ell = 1$, we have the torus knots, with $L(s, r, 1)$ being the (s, r) torus knot (which is isotopic to the (r, s) torus knot). Since all crossings in the braid words for these have the same sign, the braid words generating the knots are not only homogeneous, but strictly positive or strictly negative. The properties of torus knots are well-known [72], and we do not consider them further here.

King and Dennis [23] showed that the lemniscate knot $L(s = 2n + 1, r = 2, \ell = 2)$ has minimal braid word $\sigma_1\sigma_2^{-n}\sigma_1^n\sigma_2^{-1}$ and Alexander polynomial

$$\Delta_L(t) = t^{-n} - 3t^{-n+1} + 5t^{-n+2} \ldots + (-1)^n s + \ldots + t^n = \sum_{k=-n}^{n} (-1)^{n+k}(2(n-|k|)+1)t^k. \quad (4.13)$$

Combining these results with Theorem 4.2, we see that these knots are rational, with minimal crossing number $c = s + 1$ (whereas the original generating braid has $2s - 2$ crossings), braid index $b_{\text{ind}} = 3$, $\deg \Delta_L = 2n$ and genus n.

Furthermore, all identified $L(s = 2n + 1, r = 2, \ell = 2)$ lemniscate links with $n > 2$ have a tangle notation of the form $[n,\ 1,\ 1,\ n]$. We prove this and a more general pattern in the tangle notations of lemniscate links with $r = 2$ in Proposition 4.3. The symmetries of the braid word for even ℓ imply that these knots are achiral, i.e. isotopic to their own mirror image, and hence their Jones polynomials $V(t)$ satisfy $V(t) = V(t^{-1})$ with alternating signs of coefficients and the coefficient of the constant term always positive. Since 2-bridge knots are alternating [57], the span of the Jones polynomial is equal to the crossing number [69, 102, 131]. Further patterns in how the coefficients of the Jones polynomial change as s increases have been suggested in [23], but have not been proven yet.

There are similar patterns in these link invariants for other families of lemniscate links, such as those with $(s, r = 2, \ell = 3)$. As in the $r = 2, \ell = 2$ case considered above, the tangle representations are all symmetric; for $s \geq 7$ and $b > 0$ they follow the same pattern $[-n,\ -1,\ -1,\ -(n - 2 + m),\ -1,\ -1,\ -n]$ where $s = 3n + m$ (and $m \in \{1, 2\}$). The sequence for $b < 0$ is simply the negative of that.

The patterns in crossing numbers, braid index and Conway tangle notation indicated above generalise to the following result, which holds in general for spiral knots and links.

Proposition 4.3. *Let L be a spiral link with $r = 2$. Then it is rational and if we write the vector*

$$\boldsymbol{\varepsilon} = (\varepsilon_{1,1}, \varepsilon_{1,2}, \ldots, \varepsilon_{1,n_1}, \varepsilon_{2,1}, \ldots, \varepsilon_{2,n_2}, \ldots, \varepsilon_{\ell,n_\ell})$$

with $\varepsilon_{i,j} = \varepsilon_{i,k}$ for all $j, k \in \{1, \ldots, n_i\}$ and $\varepsilon_{i,n_i} = -\varepsilon_{i+1,1}$, then the Conway tangle notation of L is

$$[\varepsilon_{1,1}n_1,\ \varepsilon_{1,1},\ \varepsilon_{1,1},\ \varepsilon_{1,1}(n_2-1),\ \varepsilon_{1,1},\ \varepsilon_{1,1},\ \varepsilon_{1,1}(n_3-1),\ldots\ \varepsilon_{1,1}(n_{\ell-1}-1),\ \varepsilon_{1,1},\ \varepsilon_{1,1},\ \varepsilon_{1,1}n_\ell].$$

Furthermore, the minimal crossing number is $c(L) = s + \ell - 1$ and if L is a knot, then the braid index is $b_{\text{ind}}(L) = \ell + 1$.

Proof. Let L be a spiral knot with $r = 2$. Then it is the closure of a braid word of the form w^2, where $w = \sigma_1^{\varepsilon_1}\sigma_2^{\varepsilon_2}\ldots\sigma_{s-1}^{\varepsilon_{s-1}}$. We write the vector $\boldsymbol{\varepsilon} = (\varepsilon_1, \varepsilon_2, \ldots, \varepsilon_{s-1})$ as $(\varepsilon_{1,1}, \varepsilon_{1,2}, \ldots, \varepsilon_{1,n_1}, \varepsilon_{2,1}, \ldots, \varepsilon_{2,n_2}, \ldots, \varepsilon_{\ell,n_\ell})$ with $\varepsilon_{i,j} = \varepsilon_{i,k}$ for all $j, k \in \{1, \ldots, n_i\}$ and $\varepsilon_{i,n_i} = -\varepsilon_{i+1,1}$.

Figure 4.7 b) shows a diagram of the closed braid. Any closing arc connecting the bottom end of one strand with the top end of another can be taken, and placed either on top or below the braid as shown in Figure 4.7 (c), which can be done so that it cancels all crossings on the top. The resulting diagram can be easily brought into the form of a 4-plat as in Figure 4.7(d), so L is rational. Note that by placing the closing arcs such that they cancel the crossings on the top, they also cancel the crossings on the bottom if $\varepsilon_i = \varepsilon_{i+1}$. With our sign conventions this gives a 4-plat (Figures 4.7 (d), (e)) with Conway notation $[\varepsilon_{1,1}(n_1 + 1),\ 2\varepsilon_{2,1},\ \varepsilon_{2,1}n_2,\ 2\varepsilon_{3,1},\ \ldots\ \varepsilon_{\ell-1,1}n_{\ell-1},\ 2\varepsilon_{\ell,1},\ \varepsilon_{\ell,1}n_\ell]$. Note that the tangle sign convention means that the ith entry in the Conway notation is $(-1)^i$ times the number in the *ith* box from the left in the diagram.

For the following it is convenient to work with a different notation, where we define $\{b_1,\ b_2,\ b_3,\ \ldots\ b_n\} = [-b_1,\ b_2,\ -b_3,\ \ldots\ (-1)^n b_n]$ using the usual Conway notation. With this notation the numbers b_i exactly correspond to the numbers in the boxes in 4.7. In Chapter 10 of his book [38], Cromwell describes a move (Figure 4.8) that shows that a link with notation $\{b_1,\ \ldots\ b_i,\ b_{i+1}\ \ldots\}$ is equivalent to both $\{b_1,\ \ldots b_i - 1,\ -1,\ b_{i+1} - 1\ \ldots\}$ and $\{b_1,\ \ldots b_i + 1,\ 1,\ b_{i+1} + 1\ \ldots\}$. This move requires us to fix the ith box with one hand and rotate everything that is on the right of this box (excluding the passive strand and the closing arcs) by 180 degrees, so that all boxes b_j with $j > i$ that were in the bottom row are now in the middle row and vice versa. As shown in Figure 4.8 this moves three crossings to

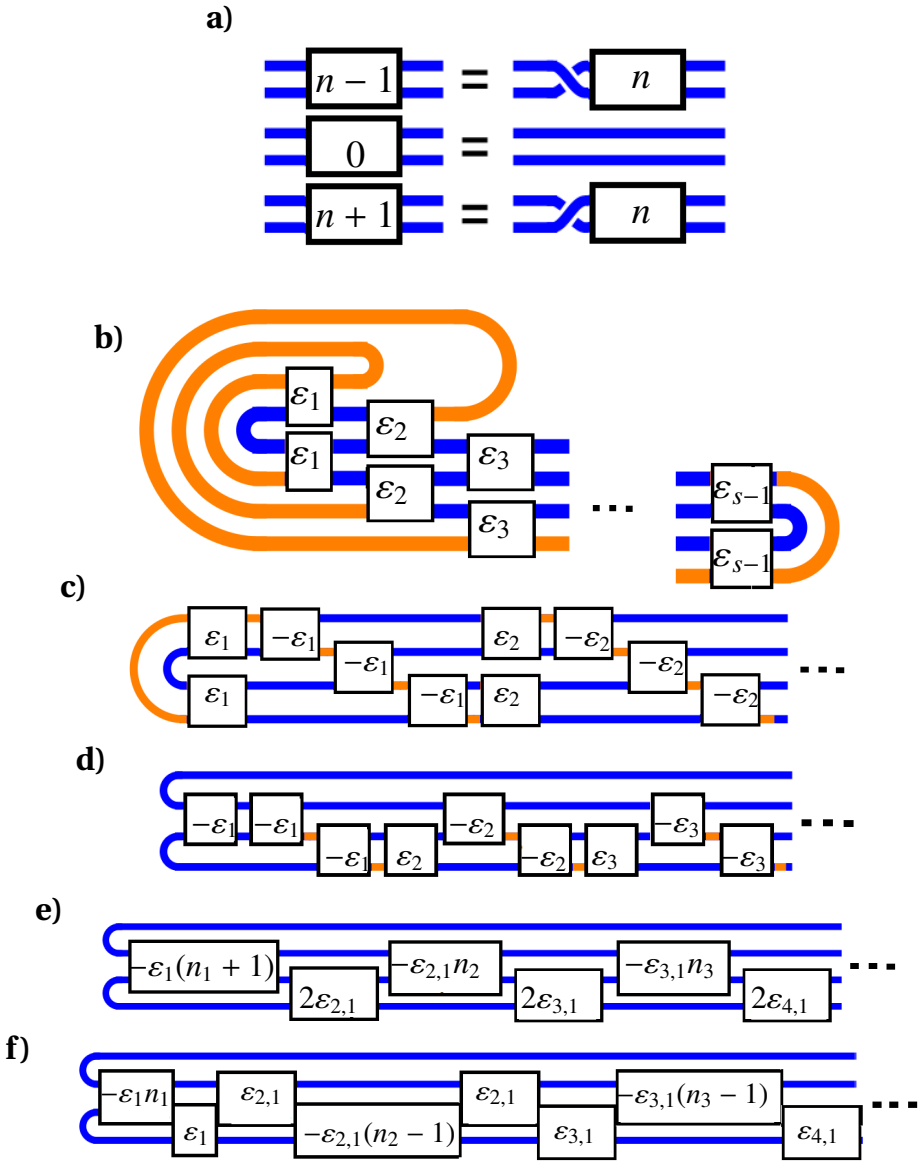

Figure 4.7: Sequence of diagrams from the closed braid to a minimal diagram in 2-bridge form. a) Definition of crossing notation. b) Knot diagram of the spiral braid closure. Arcs which are part of the braid are blue and closing arcs are orange. (c) Placing orange arcs either above or below the braid diagram, gives a new diagram. (d) With the right choice of 'above' or 'below', all crossings in the top row cancel, resulting in the diagram of a closed tangle. The bottom left crossing in (c) (with sign ε_1) has been moved into the middle row (now with sign $-\varepsilon_1$). (e) The knot diagram that results from canceling the crossings in the bottom row when possible. (f) Applying Cromwell's move allows neighbouring boxes with entries a and b to be transferred to boxes with entries $a-1$, -1 and $b-1$ or $a+1$, 1 and $b+1$. A sequence of these moves leads to the depicted diagram, which is reduced and alternating and hence minimal.

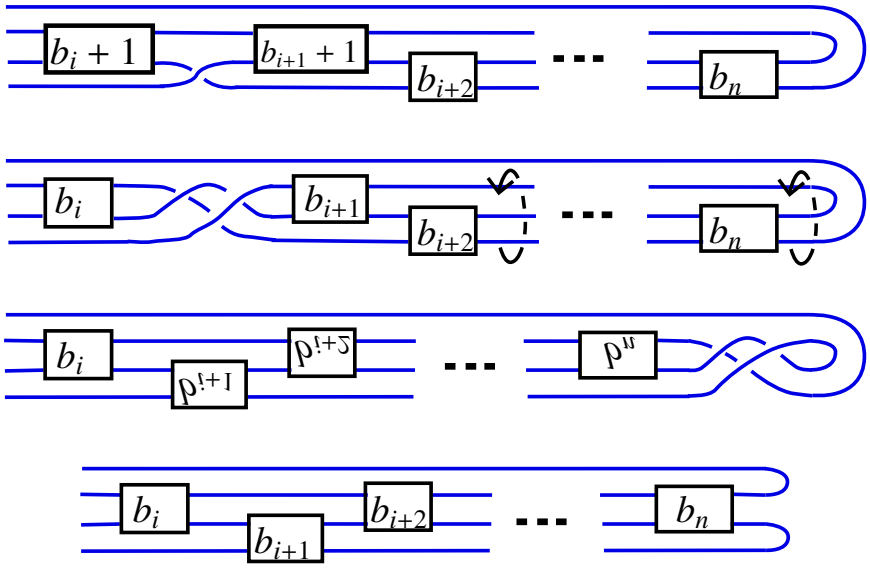

Figure 4.8: Cromwell's move. In order to go from the second to the third picture we rotate the bottom three strands to the right of the ith box as indicated by the black arrow.

the right end of the knot, where they can be removed using Reidemeister moves. If before Cromwell's move the tangle is closed as in Figure 2.13c), then removing the three crossings on the right changes the type of closure to that of Figure 2.13b) and vice versa. Note that this is consistent with the definition of closures of tangles depending on the parity of the number of boxes with twists given by Figure 2.13b) and Figure 2.13c).

With this relation

$$\{-\varepsilon_{1,1}(n_1+1),\ 2\varepsilon_{2,1},\ -\varepsilon_{2,1}n_2,\ 2\varepsilon_{3,1},\ \ldots\ -\varepsilon_{\ell-1,1}n_{\ell-1},\ 2\varepsilon_{\ell,1},\ -\varepsilon_{\ell,1}n_\ell\}$$

is equivalent to

$$\{-\varepsilon_{1,1}n_1,\ \varepsilon_{1,1},\ \varepsilon_{2,1},\ -\varepsilon_{2,1}(n_2-1),\ \varepsilon_{2,1},\ \varepsilon_{3,1},\ -\varepsilon_{3,1}(n_3-1),\ \varepsilon_{3,1},\ \varepsilon_{4,1},\ldots$$
$$\ldots\ -\varepsilon_{\ell-1,1}(n_{\ell-1}-1),\ \varepsilon_{\ell-1,1},\ \varepsilon_{\ell,1},\ -\varepsilon_{\ell,1}n_\ell\}.$$

Going back to the usual tangle notation, from the definition of $\boldsymbol{\varepsilon}$ in (4.12), this is equal to the desired Conway notation and the corresponding diagram has crossing number $s+\ell-1$. It is easy to check that the diagram is reduced and alternating and thus by the proof of one of Tait's conjectures by Kauffman [69], Thistlewaite [131, 132] and Murasugi [102, 103] the diagram is minimal. Hence we have $c(L) = s+\ell-1$. Since L is alternating and fibred by Theorem 4.2(v), it

follows from [104] that $b_{\text{ind}}(L) = s + \ell - 1 - (s-1) + 1 = \ell + 1$ if L is a knot. We believe the formula for the braid index could alternatively have been proven using Theorem B from [104] as well, but it is not immediately obvious that spiral links with $r = 2$ satisfy the conditions stated in that Theorem. □

Recall that a lemniscate knot is just a special case of a spiral knot and note that the number of loops ℓ is equal to the number ℓ defined implicitly in the proposition. Note that Proposition 4.3 confirms the pattern indicated by the list of identified lemniscate knots with $\ell = 2$ or 3 and $r = 2$.

While the proof of Proposition 4.3 gives a formula for the braid index $b_{\text{ind}}(L)$, it does not provide a form of a braid on $b_{\text{ind}}(L)$ strands.

We speculate that for any spiral knot with small r (hence for any such lemniscate knot), $c = (r-1)(s+\ell-1)$, which would generalise the formulas for the crossing numbers of torus knots (with $\ell = 1$) and the spiral links in Proposition 4.3. If the knot is alternating and r is a prime power, using [104] and [28], the braid index then should be of the form $b_{\text{ind}} = (r-1)\ell + 1$. While examples for low r are consistent with these formulas, a theorem by Lee and Seo [84] implies that if $r > \max\{n_1, n_2 \ldots, n_\ell\}$, then $b(L(s,r,\boldsymbol{\varepsilon})) = s$, where n_i is defined as in Proposition 4.3. Hence if $r > \max\{n_1, n_2 \ldots, n_\ell\}$ is a prime power and $L(s,r,\boldsymbol{\varepsilon})$ is alternating, the crossing number is of the form $c = r(s-1)$. This means that in this case the braid diagram in its spiral form minimises both the braid index and the crossing number.

A theorem by Lee [85] gives $r \leq 2g+1$ where g is the genus. Combining this with Theorem 4.2(ix) and Proposition 4.3 it can be shown that 6_2 (the closure of $(\sigma_1\sigma_2\sigma_3\sigma_4^{-1})^2$) is spiral, but not lemniscate and 8_5 (the closure of $(\sigma_1^3\sigma_2^{-1})^2$) is the closure of a homogeneous braid, but not spiral. Therefore all of the following inclusions are proper inclusions:

$$\left\{\begin{array}{l}\text{torus}\\ \text{links}\end{array}\right\} \subset \left\{\begin{array}{l}\text{lemniscate}\\ \text{links}\end{array}\right\} \subset \left\{\begin{array}{l}\text{spiral}\\ \text{links}\end{array}\right\} \subset \left\{\begin{array}{l}\text{closures of}\\ \text{homogeneous}\\ \text{braids}\end{array}\right\} \subset \left\{\begin{array}{l}\text{fibred}\\ \text{links}\end{array}\right\}. \tag{4.14}$$

Suppose 6_2 were the (s,r,ℓ)-lemniscate knot. Then since $g(6_2) = 2$, we have $r \leq 5$, in particular r is a prime power. Then by Theorem 4.2 we have $4 = 2g = (s-1)(r-1)$. Since 6_2 is not a torus knot, s is at least 3, so the only possibilities for (s,r) are $(3,3)$ or $(5,2)$. Note that s and r have to be coprime to give a knot, so it

has to be $(5,2)$. However, in this case Proposition 4.3 says that $2 = b_{\text{ind}}(6_2) = \ell + 1$, so $\ell = 1$, which would imply that 6_2 is a torus knot. Hence 6_2 is not lemniscate.

The considerations for 8_5 are similar, but a bit more involved. First note that it follows from Lee's result that $r \leq 7$. If it is a spiral knot with r being a prime power, then Theorem 4.2 and Proposition 4.3 (in the case of $r = 2$) give us quite strong restrictions on the values that s and ℓ can take. We can simply generate the spiral knots with these values and note that 8_5 is not among them. If r is not a prime power, then $r = 6$. We now use one of Murasgi's results on Alexander polynomials of periodic knots [101], which here implies that $6 = \deg \Delta(8_5) \geq (q-1)(s-1)$, where q is a prime power such that 8_5 is q-periodic. If 8_5 is 6-periodic, then it is also 3-periodic and so $s \leq 4$, but then s and $r = 6$ are not coprime. Therefore 8_5 cannot be spiral.

4.3 Discussion

With the outlined construction of semiholomorphic polynomials $f : \mathbb{C}^2 \to \mathbb{C}$ whose vanishing set on the unit-three sphere is any given lemniscate link, we can construct initial configurations containing lemniscate links in various physical systems as outlined in Chapter 3. Like in the case of torus links, the construction makes use of the fact that by definition lemniscate links are closures of braids that have particularly simple parametrisations in terms of trigonometric functions.

These simple parametrisations result in polynomials that have comparatively few terms, which makes them more accessible for applications, in particular the construction of knotted fields as outlined in Chapter 3. Lemniscate vortex links in laser light have been experimentally realised [41]. Furthermore, Dave Foster used some of the constructed polynomials for lemniscate links as initial configurations for energy minimizations in the Skyrme-Faddeev model and found that they decay to torus links [23].

The symmetries of the trigonometric functions are reflected in symmetries of the resulting braid word. Lemniscate braids are determined by three natural numbers s, r and ℓ. For low values of these numbers, the corresponding links have been identified with knot and link invariants. These lists of lemniscate links seem to indicate that the symmetries imply several patterns in classical knot invariants, such as the crossing number, the braid index and the Conway tangle notation. While we were able to prove some of these patterns for $r = 2$,

others, such as patterns in the coefficients of Jones polynomials, still remain conjectural.

5 Constructing polynomials with knotted zero level sets

In Chapter 4 we described the construction of semiholomorphic polynomials $f : \mathbb{C}^2 \to \mathbb{C}$ such that the nodal set of f on the unit-three sphere is the (s, r, ℓ)-lemniscate link $L(s, r, \ell)$. Lemniscate links have special symmetries and are fibred, so that it is clear that the construction in Chapter 4 does not cover all links.

In this chapter we prove that the method from Chapter 4 can be extended to all links.

Theorem 5.1. *For every link L there exists a semiholomorphic polynomial $f : \mathbb{C} \times \mathbb{R}^2 \to \mathbb{C}$ such that $f^{-1}(0) \cap S^3 = L$.*

The overall idea is still identical to the one discussed earlier. We use certain trigonometric parametrisations of a given braid B to define a family of functions from $\mathbb{C} \times [0, 2\pi]$ to $\mathbb{C}$ whose zero level set is B. Identifying the 2π-periodic variable with the argument of a complex number v allows us to close the braid and define a 1-parameter family of functions whose zero level set is the closure of B for appropriate choices of a scaling parameter. The parametrisation of the braid is chosen in such a way that the resulting function is a polynomial in u, v and $\overline{v}$.

As in Section 2.3 we consider a braid as the union of s disjoint parametric curves in $\mathbb{R}^3$, parametrised by their z-coordinate between 0 and 2π as in Equation (2.7).

We want to describe an algorithm that for any given link L constructs a semiholomorphic polynomial $f : \mathbb{C} \times \mathbb{R}^2 \to \mathbb{C}$ such that $f^{-1}(0) \cap S^3 = L$. This algorithm is a generalisation of the methods used in [111], [41] and [23]. Let L be the link we want to construct and B be a braid on s strands that closes to L.

The first step of the algorithm is to find a parametrisation of the braid B as

in Equation (2.7). Then we can define a family of functions $g_{a,b} : \mathbb{C} \times [0, 2\pi] \to \mathbb{C}$,

$$g_{a,b}(u,t) = \prod_{j=0}^{s-1}(u - aX_j(t) - ibY_j(t)) \tag{5.1}$$

which has the braid B as its zero level set $g_{a,b}^{-1}(0)$ for any $a > 0$, $b > 0$.

Every $g_{a,b}$ is by definition a polynomial in the complex variable u, but its dependence on t is determined by the parametrisation. In Section 5.1 we show that if the braid parametrisation is of a certain form, $g_{a,b}$ is a polynomial in u, $\mathrm{e}^{\mathrm{i}t}$ and $\mathrm{e}^{-\mathrm{i}t}$. As such it is the restriction of a semiholomorphic polynomial $f_{a,b} : \mathbb{C}^2 \to \mathbb{C}$ to $\mathbb{C} \times S^1$. Note that $f_{a,b}$ can be obtained from $g_{a,b}$ simply by replacing every instance of $\mathrm{e}^{\mathrm{i}t}$ by a complex variable v and $\mathrm{e}^{-\mathrm{i}t}$ by $\overline{v}$, the complex conjugate of v. In the case of lemniscate links it is the particular parametrisation in terms of single trigonometric functions that implies that this substitution results in a semiholomorphic polynomial f. In Section 5.1 we show that it is sufficient to find a braid parametrisation in terms of trigonometric polynomials. Section 5.2 shows that for small $\lambda > 0$ the zero level set of $f_{\lambda a,\lambda b}$ on the unit three-sphere is ambient isotopic to L, i.e. $f_{\lambda a,\lambda b}^{-1}(0) \cap S^3 = L$.

In Section 5.3 we introduce an algorithm to find a trigonometric braid parametrisation for any braid word, making our method of constructing f fully algorithmic.

In Section 5.4 we use this algorithmic nature to derive bounds of the polynomial degree of f in terms of the number of strands s and the number of crossings of the parametrised braid.

Section 5.5 discusses a slightly modified construction that yields complex plane curves that intersect the unit three-sphere in a link that contains any given link as a sublink.

The material of Sections 5.1-5.4 can be found in [22].

5.1 Trigonometric braid parametrisations

In this section we describe a braid parametrisation as in Equation (2.7) of a certain form that guarantees that $g_{a,b}$ defined by Equation (5.1) can be written as a polynomial in u, $\mathrm{e}^{\mathrm{i}t}$ and $\mathrm{e}^{-\mathrm{i}t}$ for all a and b.

Recall that we can associate to every braid B with s strands an element π_B of the symmetric group S_s on s elements. The cycles of π_B correspond to the link components of the closure of B. We will denote the set of cycles of π_B, or

equivalently the set of components of L, by $\mathscr{C}$. For a given cycle $C \in \mathscr{C}$ let s_C denote the length of C or equivalently the number of strands that form the link component C.

The condition that $X_j(0) = X_{\pi_B(j)}(2\pi)$ and $Y_j(0) = Y_{\pi_B(j)}(2\pi)$ for all j ensures that the projection of the braid on the xy-plane is a collection of closed curves, one for each link component. Thus for each link component C there exist 2π-periodic, continuous real functions F_C and G_C such that for every strand j in C we have $X_j(t) = F_C\left(\frac{t+2\pi k}{s_C}\right)$, $Y_j(t) = G_C\left(\frac{t+2\pi k}{s_C}\right)$, $X_{\pi_B(j)}(t) = F_C\left(\frac{t+2\pi(k+1)}{s_C}\right)$ and $Y_{\pi_B(j)}(t) = G_C\left(\frac{t+2\pi(k+1)}{s_C}\right)$ for some $C \in \mathscr{C}$ and $1 \leq k \leq s_C$.

Let F_C and G_C be trigonometric polynomials, i.e.

$$F_C(t) = \sum_{k=-N_C}^{N_C} a_{C,k}\, \mathrm{e}^{\mathrm{i}kt} \text{ and } G_C(t) = \sum_{k=-M_C}^{M_C} b_{C,k}\, \mathrm{e}^{\mathrm{i}kt} \tag{5.2}$$

with $a_{C,-k} = \overline{a}_{C,k}$ and $b_{C,-k} = \overline{b}_{C,k}$ for all $C \in \mathscr{C}$ and all k. Suppose

$$\bigcup_{C\in\mathscr{C}} \bigcup_{j=0}^{s_C-1} \left(F_C\left(\frac{t+2\pi j}{s_C}\right), G_C\left(\frac{t+2\pi j}{s_C}\right), t\right), \quad t \in [0, 2\pi] \tag{5.3}$$

is a parametrisation of the braid B as in Equation (2.7). Then as in Equation (5.1) this parametrisation with $X_j(t) = F_C\left(\frac{t+2\pi k}{s_C}\right)$ and $Y_j(t) = G_C\left(\frac{t+2\pi k}{s_C}\right)$ for some (C,k) leads to a function $g_{a,b} : \mathbb{C} \times [0,2\pi] \to \mathbb{C}$

$$g_{a,b}(u,t) = \prod_{C\in\mathscr{C}} \prod_{j=1}^{s_C} \left(u - aF_C\left(\frac{t+2\pi j}{s_C}\right) - \mathrm{i}bG_C\left(\frac{t+2\pi j}{s_C}\right)\right) \tag{5.4}$$

with B as its zero level set for all $a > 0$, $b > 0$ and we claim that it is in fact a polynomial.

Lemma 5.2. *The function $g_{a,b}$ can be written as a polynomial in u, $\mathrm{e}^{\mathrm{i}t}$ and $\mathrm{e}^{-\mathrm{i}t}$.*

Proof. Obviously all exponents of u are natural numbers, so we only have to show that after expanding the product in Equation (5.4) all exponents of $\mathrm{e}^{\mathrm{i}t}$ are integers.

We are going to show this for knots, so there is only one cycle in π_B, equivalently for one component $C \in \mathscr{C}$. Since $g_{a,b}$ is the product over the functions associated with each component, this will show that $g_{a,b}$ is a product of polynomials and hence a polynomial itself for any braid. We now write s for s_C, the number of strands of the component C that we focus on.

Since $g_{a,b}$ has exactly s factors, every term of $g_{a,b}$ after expanding the product consists of exactly s terms which can each be u or $c_m \, \mathrm{e}^{\frac{\mathrm{i}m(t+2\pi j)}{s}}$ for some non-zero integer m and $c_m \in \mathbb{C}$. Hence every summand has the form

$$u^{s-k} T^{m_1,\dots,m_k}_{j_1\dots,j_k} = u^{s-k} \prod_{p=1}^{k} c_{m_p} \, \mathrm{e}^{\frac{\mathrm{i}m_p(t+2\pi j_p)}{s}} \tag{5.5}$$

with $j_p \neq j_r$ if $p \neq r$.

Moreover, if $T^{m_1,\dots,m_k}_{j_1,\dots,j_k}$ appears with the factor u^{s-k}, so do all $T^{m_1,\dots,m_k}_{\widetilde{j_1},\dots,\widetilde{j_k}}$ with $\widetilde{j_i} \in \{0,\dots,s-1\}$, $\widetilde{j_i} \neq \widetilde{j_r}$ if $i \neq r$. Note that if $m_i = m_w$, then $T^{m_1\dots,m_i,\dots,m_w,\dots,m_k}_{j_1,\dots,j_i,\dots,j_w,\dots,j_k} = T^{m_1\dots,m_i,\dots,m_w,\dots,m_k}_{j_1,\dots,j_w,\dots,j_i,\dots,j_k}$. This turns the proof of the lemma into a combinatorial problem. Summing over all summands with the same m_i becomes summing over all possibilities of choosing p distinct values j_p between 1 and s.

We will use induction on $k = s - l$, where l is the exponent of u in the relevant term, to show that all terms $T^{m_1,\dots,m_k}_{j_1,\dots,j_k}$ with $s \nmid \sum_{i=1}^{k} m_i$ cancel each other, i.e. $\sum_{\substack{(j_1,j_2,..,j_k)\\ \in(\mathbb{Z}/s\mathbb{Z})^k \\ j_i \text{ disjoint}}} T^{m_1,\dots,m_k}_{j_1,\dots,j_k} = 0$.

Note that this implies that all summands that involve non-integer exponents of $\mathrm{e}^{\mathrm{i}t}$ enter the sum with a factor equal to zero. Hence $g_{a,b}$ can be written as a polynomial in u, $\mathrm{e}^{\mathrm{i}t}$ and $\mathrm{e}^{-\mathrm{i}t}$.

Consider a term T^m_j which comes with a factor of u^{s-1}, so there is only one term which is not u (i.e. $k = 1$), so $T^m_j = c_m \, \mathrm{e}^{\frac{\mathrm{i}m(t+2\pi j)}{s}}$ for some $j = 0,\dots,s-1$. Then T^m_j must appear with the factor u^{s-1} for all values of j. We get

$$\sum_{j=0}^{s-1} T^m_j = c_m \, \mathrm{e}^{\mathrm{i}mt/s} \sum_{j=0}^{s-1} \mathrm{e}^{2\pi \mathrm{i} m j/s}, \tag{5.6}$$

where the last sum is 0 if $s \nmid m$ which shows the statement for $k = 1$.

Assume now there is a $k \in \{1,2,\dots,s-1\}$ such that all terms $T^{m_1,\dots,m_k}_{j_1,\dots,j_k}$ with $s \nmid \sum_{i=1}^{k} m_i$ cancel each other, i.e

$$\sum_{j_1=1}^{s} \sum_{\substack{j_2=1 \\ j_2\neq j_1}}^{s} \cdots \sum_{\substack{j_k=1 \\ j_k\neq j_1,j_2,\dots,j_{k-1}}}^{s} T^{m_1,\dots,m_k}_{j_1,\dots,j_k} = 0. \tag{5.7}$$

Let $T^{m_1,\dots,m_{k+1}}_{j_1\dots,j_{k+1}}$ be a term with $s \nmid \sum_{i=1}^{k} m_i$. Summing over all terms with the same $(m_1,\dots,m_{k+1})$, but different choices of $(j_1,\dots,j_{k+1})$ yields

$$\sum_{\substack{(j_1,j_2,..,j_{k+1})\\ \in(\mathbb{Z}/s\mathbb{Z})^{k+1} \\ j_i \text{ disjoint}}} T^{m_1,..,m_{k+1}}_{j_1,..,j_{k+1}} = \mathrm{e}^{\mathrm{i}t\sum_{p=1}^{k+1}\frac{m_p}{s}} \left(\prod_{p=1}^{k+1} c_{m_p}\right) \sum_{\substack{(j_1,j_2,..,j_{k+1})\\ \in(\mathbb{Z}/s\mathbb{Z})^{k+1} \\ j_i \text{ disjoint}}} \prod_{p=1}^{k+1} \mathrm{e}^{\frac{2\pi \mathrm{i} m_p j_p}{s}}. \tag{5.8}$$

There is at least one m_p which is not divisible by s. Otherwise $s \mid \sum_{p=1}^{k+1} m_p$. Without loss of generality, we can assume that $s \nmid m_{k+1}$. Then $\sum_{j=1}^{s} \mathrm{e}^{\frac{2\pi \mathrm{i} m_{k+1} j}{s}} = 0$ and hence $\mathrm{e}^{\frac{2\pi \mathrm{i} m_p j_p}{s}} = -\sum_{p=1}^{k} \mathrm{e}^{\frac{2\pi \mathrm{i} m_{k+1} j_p}{s}} - \sum_{\substack{w=1 \\ w \neq j_1 \ldots, j_{k+1}}}^{s} \mathrm{e}^{\frac{2\pi \mathrm{i} m_{k+1} w}{s}}$. Thus Equation (5.8) is equivalent to

$$\mathrm{e}^{\mathrm{i}t \sum_{p=1}^{k+1} \frac{m_p}{s}} \left(\prod_{p=1}^{k+1} c_{m_p} \right) \sum_{\substack{(j_1, j_2, \ldots, j_{k+1}) \\ \in (\mathbb{Z}/s\mathbb{Z})^{k+1} \\ j_i \text{ disjoint}}} \left(\prod_{p=1}^{k} \mathrm{e}^{\frac{2\pi \mathrm{i} m_p j_p}{s}} \times \left(-\sum_{p=1}^{k} \mathrm{e}^{\frac{2\pi \mathrm{i} m_{k+1} j_p}{s}} - \sum_{\substack{w=1 \\ w \neq j_1 \ldots, j_{k+1}}}^{s} \mathrm{e}^{\frac{2\pi \mathrm{i} m_{k+1} w}{s}} \right) \right)$$

$$= T_1 + T_2, \tag{5.9}$$

with

$$T_1 = -\mathrm{e}^{\mathrm{i}t \sum_{p=1}^{k+1} \frac{m_p}{s}} \left(\prod_{p=1}^{k+1} c_{m_p} \right) \sum_{\substack{(j_1, j_2, \ldots, j_{k+1}) \\ \in (\mathbb{Z}/s\mathbb{Z})^{k+1} \\ j_i \text{ disjoint}}} \sum_{r=1}^{k} \mathrm{e}^{2\pi \mathrm{i}(m_r + m_{k+1}) j_r} \prod_{\substack{p=1 \\ p \neq r}}^{k} \mathrm{e}^{\frac{2\pi \mathrm{i} m_p j_p}{s}} \tag{5.10}$$

and

$$\begin{aligned} T_2 &= -\mathrm{e}^{\mathrm{i}t \sum_{p=1}^{k+1} \frac{m_p}{s}} \left(\prod_{p=1}^{k+1} c_{m_p} \right) \sum_{\substack{(j_1, j_2, \ldots, j_{k+1}) \\ \in (\mathbb{Z}/s\mathbb{Z})^{k+1} \\ j_i \text{ disjoint}}} \sum_{\substack{w=1 \\ w \neq j_1 \ldots, j_{k+1}}}^{s} \mathrm{e}^{\frac{2\pi \mathrm{i} m_{k+1} w}{s}} \prod_{p=1}^{k} \mathrm{e}^{\frac{2\pi \mathrm{i} m_p j_p}{s}} \\ &= -\mathrm{e}^{\mathrm{i}t \sum_{p=1}^{k+1} \frac{m_p}{s}} \left(\prod_{p=1}^{k+1} c_{m_p} \right) \sum_{\substack{(j_1, j_2, \ldots, j_{k+1}, w) \\ \in (\mathbb{Z}/s\mathbb{Z})^{k+2} \\ w, j_i \text{ all disjoint}}} \mathrm{e}^{\frac{2\pi \mathrm{i} m_{k+1} w}{s}} \prod_{p=1}^{k} \mathrm{e}^{\frac{2\pi \mathrm{i} m_p j_p}{s}} \\ &= -(s - (k+1))\, \mathrm{e}^{\mathrm{i}t \sum_{p=1}^{k+1} \frac{m_p}{s}} \left(\prod_{p=1}^{k+1} c_{m_p} \right) \sum_{\substack{(j_1, j_2, \ldots, j_k, w) \\ \in (\mathbb{Z}/s\mathbb{Z})^{k+1} \\ w, j_i \text{ all disjoint}}} \mathrm{e}^{\frac{2\pi \mathrm{i} m_{k+1} w}{s}} \prod_{p=1}^{k} \mathrm{e}^{\frac{2\pi \mathrm{i} m_p j_p}{s}}, \end{aligned} \tag{5.11}$$

where the last equality follows from the fact that the summand

$$\mathrm{e}^{\frac{2\pi \mathrm{i} m_{k+1} w}{s}} \prod_{p=1}^{k} \mathrm{e}^{\frac{2\pi \mathrm{i} m_p j_p}{s}} \tag{5.12}$$

in Equation (5.11) does not depend on j_{k+1} and for each $(j_1, j_2, \ldots, j_k, w)$, there are $s - (k+1)$ choices for j_{k+1}.

For every fixed r the first term T_1 describes $-\sum_{\substack{(j_1, j_2, \ldots, j_k) \\ \in (\mathbb{Z}/s\mathbb{Z})^k \\ j_i \text{ disjoint}}} T^{m_1, \ldots, m_r + m_{k+1}, \ldots, m_k}_{j_1, \ldots, j_k}$, which vanishes by the induction hypothesis (5.7), since

$$s \nmid \sum_{p=1}^{k+1} m_p = (m_r + m_{k+1}) + \sum_{\substack{p=1 \\ p \neq r}}^{k} m_p \tag{5.13}$$

for all r.

We find from Equation (5.9) that

$$\sum_{\substack{(j_1,j_2,..j_{k+1})\\ \in(\mathbb{Z}/s\mathbb{Z})^{k+1}\\ j_i\text{disjoint}}} T^{m_1,...,m_{k+1}}_{j_1,...,j_{k+1}} = T_2 = -(s-(k+1)) \sum_{\substack{(j_1,j_2,..j_{k+1})\\ \in(\mathbb{Z}/s\mathbb{Z})^{k+1}\\ j_i\text{disjoint}}} T^{m_1,...,m_{k+1}}_{j_1,...,j_{k+1}}, \tag{5.14}$$

where the last equality follows from simply relabeling w in Equation (5.11) as j_{k+1}.

We have $k+1 \leq s$ and hence

$$\sum_{j_1=1}^{s} \sum_{\substack{j_2=1\\ j_2\neq j_1}}^{s} \cdots \sum_{\substack{j_{k+1}=1\\ j_{k+1}\neq j_1,...,j_k}}^{s} T^{m_1,...,m_{k+1}}_{j_1,...,j_{k+1}} = 0. \tag{5.15}$$

This completes the proof for $k+1$ and proves the lemma by induction.

Hence all terms of $g_{a,b}$ where e^{it} has a non-integer exponent cancel each other when we expand the product. Therefore $g_{a,b}$ is a polynomial in u, e^{it} and e^{-it}. □

As a polynomial in u, e^{it} and e^{-it}, the function $g_{a,b}$ is the restriction of a semiholomorphic polynomial $f_{a,b} : \mathbb{C}^2 \to \mathbb{C}$ in u, v and $\overline{v}$ to $\mathbb{C} \times S^1$. Thus $f_{a,b}(u, e^{it}) = g_{a,b}(u,t)$ and by construction the zero level set of $f_{a,b}$ on $\mathbb{C} \times S^1$ is equal to the closure of the braid $g^{-1}_{a,b}(0)$ for every $a > 0$, $b > 0$. The polynomial $f_{a,b}$ can be constructed from $g_{a,b}$ in the following way. We expand the product in Equation (5.4), so that $g_{a,b}$ is in the form of a polynomial in u, e^{it} and e^{-it}. This expression is unique once all occurrences of $e^{it}\,e^{-it}$ have been canceled. Then we replace every instance of e^{it} by v and every instance of e^{-it} by $\overline{v}$. Since $f_{a,b}(u, e^{it}) = g_{a,b}(u,t)$ for all $u \in \mathbb{C}$ and $t \in [0, 2\pi]$, the zero level set of $f_{a,b}$ on $\mathbb{C} \times S^1$ is the closure of the braid B parametrised by Equation (5.3). Performing this substitution in Equation (5.4) before the product is expanded results in a different function, which is typically not a polynomial in u, v and $\overline{v}$.

Note that substituting t by rt in F_C and G_C for some $r \in \mathbb{N}$ results in a parametrisation of r repeats of the original braid. Thus if $f_{a,b}$ has a zero level set on $\mathbb{C} \times S^1$ which is of the form of the closure of a braid B, then multiplying each exponent of v and $\overline{v}$ by r gives a family of semiholomorphic polynomials with zero levels set on $\mathbb{C} \times S^1$ which are the closure of B^r.

The classes of knots that were discussed in Chapter 4 and [23] can now be seen as particularly simple examples, since lemniscate knots are exactly the

closures of repeats of braids given by parametrisations of the form of Equation (5.3) with $F(t) = \cos(t)$ and $G(t) = \sin(\ell t)$ for some $\ell \in \mathbb{N}$ coprime to the number of strands s, generalising the torus knots with $\ell = 1$. The spiral knots, first introduced in [28], are exactly the closures of repeats of braids that can be parametrised by Equation (5.3) with $F(t) = \cos(t)$ and $G(t)$ some trigonometric polynomial.

By Alexander's Theorem [6] every link is the closure of a braid and since trigonometric polynomials are dense in the set of continuous 2π-periodic functions from $\mathbb{R}$ to $\mathbb{R}$, every braid can be parametrised as in Equation (5.3). Hence for every link L there exists a family of semiholomorphic polynomials $f_{a,b}$ with $f_{a,b}^{-1}(0) \cap (\mathbb{C} \times S^1) = L$ for all $a > 0$, $b > 0$.

In Section 5.2 we show that for small enough a and b, it is in fact $f_{a,b}^{-1}(0) \cap S^3 = L$ as desired.

5.2 The proof of Theorem 5.1

Let $f_{a,b} : \mathbb{C}^2 \to \mathbb{C}$ be the polynomial constructed from $g_{a,b}$, so $f_{a,b}^{-1}(0) \cap (\mathbb{C} \times S^1)$ is the closure of the braid that is $g_{a,b}^{-1}(0)$. We will make this statement more precise. Consider the map $\Psi : \mathring{D} \times (\mathbb{C}\backslash\{0\}) \to S^3$, $\Psi(u, r\,\mathrm{e}^{\mathrm{i}t}) = (u, \sqrt{1-|u|^2}\,\mathrm{e}^{\mathrm{i}t})$, where $\mathring{D}$ is the interior of the unit disk in the complex plane. We think of $f_{a,b}$ as a family of polynomials in one complex variable u, parametrised by $v = r\,\mathrm{e}^{\mathrm{i}t}$, a and b. In the following we set $a = \lambda a_1$ and $b = \lambda b_1$, leave a_1 and b_1 as real constants and only vary the real parameter λ. With this notation we write f_λ instead of $f_{a,b}$, slightly abusing notation. For fixed r, t and λ, we denote the s roots of $f_\lambda(\bullet, r\,\mathrm{e}^{\mathrm{i}t})$ by $u_{\lambda,j}(r,t)$. Note that by definition $u_{\lambda,j,}(r,t) = \lambda u_{1,j}(r,t)$, $j = 1, 2, \ldots, s$. Thus if λ is small enough, all roots $u_{\lambda,j}(1, \mathrm{e}^{\mathrm{i}t})$ of $f_\lambda(\bullet, \mathrm{e}^{\mathrm{i}t})$ lie in $\mathring{D}$. It is intuitively clear and can be shown that $\Psi(f_\lambda^{-1}(0) \cap (\mathbb{C} \times S^1)) = \Psi((u_{\lambda,j}(1, \mathrm{e}^{\mathrm{i}t}), \mathrm{e}^{\mathrm{i}t}))$ is the closure of $B = g_{a,b}^{-1}(0)$, which is L. This idea can be found among others in [111].

In order to show that $f_\lambda^{-1}(0) \cap S^3$ is L as well, we need to show that there is an ambient isotopy between $L_1 = \Psi(f_\lambda^{-1}(0) \cap (\mathbb{C} \times S^1))$ and $L_2 = f_\lambda^{-1}(0) \cap S^3$ as defined in Chapter 2.

In fact by the Isotopy Extension Theorem (Theorem 2.6), it is enough to construct a smooth isotopy between the two sets of curves.

For fixed λ, j and t we think of the roots $u_{\lambda,j}(r,t)$ as functions of r. Note that the union of the intersection points of the roots $u_{\lambda,j}(r,t)$ with S^3 is equal to the zero level set of f_λ on S^3. We would like to see that for every fixed λ, j and t there

is a unique intersection point of the curve $(u_{\lambda,j}(r,t), r\,\mathrm{e}^{\mathrm{i}t})$ with S^3, so that there is a $1-1$ correspondence between the points in $f_\lambda^{-1}(0)\cap S^3$ and $f_\lambda^{-1}(0)\cap(\mathbb{C}\times S^1)$. To do this we first need to restrict the range of r to a domain where all the roots are distinct. This allows us to treat the roots $u_{\lambda,j}(r,t)$ as smooth functions of r.

Lemma 5.3. *There is a $\delta>0$ independent of λ such that if $u_{\lambda,j}(r_1,t)=u_{\lambda,k}(r_2,t)$ with $r_1,r_2\in[1-\delta,1]$, then $j=k$.*

Proof. Note that it is enough to show the lemma for $\lambda=1$, since $u_{\lambda,j}(r,t)=\lambda u_{1,j}(r,t)$, so that $u_{\lambda,j}(r_1,t)=u_{\lambda,k}(r_2,t)$ if and only if $u_{1,j}(r_1,t)=u_{1,k}(r_2,t)$. In particular the value that we find for δ when $\lambda=1$ will be sufficient for any choice of $\lambda>0$.

Since for every fixed t and every $\lambda>0$ the roots of $g_{\lambda a,\lambda b}(\cdot,t)$ are by definition distinct, the roots $u_{\lambda,j}(1,t)$ of $f_\lambda(\cdot,\mathrm{e}^{\mathrm{i}t})$ are distinct. By continuity of the roots of a polynomial with respect to its coefficients, they remain distinct on an open neighbourhood of $r=1$ for all λ and t.

Let R be the biggest value of $r\le 1$ for which different strands intersect for $\lambda=1$, that is $R=\max_{t\in[0,2\pi],\ j\neq k}\{r|\ u_{1,j}(r,t)=u_{1,k}(r,t),\ r\le 1\}$. Since $u_{\lambda,j}(r,t)=\lambda u_{1,j}(r,t)$ for all λ, j, r and t, all the roots $u_{\lambda,j}(r,t)$ are simple roots of $f_\lambda(\bullet, r\,\mathrm{e}^{\mathrm{i}t})$ as long as $r\in[R,1]$ and hence $\mathrm{Re}(u_{\lambda,j}(r,t))$ and $\mathrm{Im}(u_{\lambda,j}(r,t))$ are differentiable functions with respect to $r\in[R,1]$. Note that by the remark above $R<1$, so $[R,1]$ is a proper interval.

The Implicit Function Theorem allows us to calculate these derivatives in terms of $\frac{\partial f_a(\cdot,r\,\mathrm{e}^{\mathrm{i}t})}{\partial u}$ and $\frac{\partial f_a(\cdot,r\,\mathrm{e}^{\mathrm{i}t})}{\partial r}$. Let

$$D_1(\delta)=\max_{\substack{t\in[0,2\pi]\\ j\\ r\in[1-\delta,1]}}\left\{\left|\frac{\partial\,\mathrm{Re}(u_{1,j}(r,t))}{\partial r}\right|\right\} \tag{5.16}$$

and

$$D_2(\delta)=\max_{\substack{t\in[0,2\pi]\\ j\\ r\in[1-\delta,1]}}\left\{\left|\frac{\partial\,\mathrm{Im}(u_{1,j}(r,t))}{\partial r}\right|\right\} \tag{5.17}$$

for $\delta\in[0,1-R]$.

Take $\widetilde{\delta}$ to be $\frac{1}{2}\min_{\substack{t\in[0,2\pi]\\ j\neq k}}\{|u_{1,j}(1,t)-u_{1,k}(1,t)|\}$ and choose $\delta<\frac{\widetilde{\delta}}{\sqrt{D_1(\delta)^2+D_2(\delta)^2}}$. Note that as δ approaches zero, the right hand side of the inequality converges to a

non-zero value. Hence such a δ always exists. The Lemma follows then from

$$\begin{aligned}|u_{1,j}(r_1,t)-u_{1,k}(r_2,t)| &\geq |u_{1,j}(1,t)-u_{1,k}(1,t)| - |u_{1,j}(1,t)-u_{1,j}(r_1,t)| \\ &\quad - |u_{1,k}(1,t)-u_{1,k}(r_2,t)| \\ &\geq |u_{1,j}(1,t)-u_{1,k}(1,t)| - 2\delta|D_1(\delta)+\mathrm{i}D_2(\delta)| \\ &> |u_{1,j}(1,t)-u_{1,k}(1,t)| - 2\widetilde{\delta} \geq 0 \end{aligned} \tag{5.18}$$

for all $r_1, r_2 \in [1-\delta, 1]$ and $j \neq k$. □

We use the following lemma to show that for every fixed λ, j and t the intersection point of the curve $(u_{\lambda,j}(r,t), r\,\mathrm{e}^{\mathrm{i}t})$ with S^3 is unique if λ is small enough.

Lemma 5.4. *There exists $\varepsilon_1 > 0$ such that for every fixed $\lambda < \varepsilon_1$ and all fixed j and t there is at most one intersection of $(u_{\lambda,j}(r,t), r\,\mathrm{e}^{\mathrm{i}t})$ with S^3 where $1-\delta \leq r \leq 1$ with δ as in Lemma 5.3.*

Proof. Lemma 5.3 implies that the roots $u_{\lambda,j}(r,t)$, $j = 1, 2, \ldots, s$ are distinct for $r \in [1-\delta, 1]$. As simple roots of the polynomial $f_\lambda(\bullet, r\,\mathrm{e}^{\mathrm{i}t})$, they depend smoothly on its coefficients, in particular $u_{\lambda,j}(r,t)$ is a smooth function of r for all $r \in [1-\delta, 1]$.

Consider the function $|u_{\lambda,j}(r,t)|^2 + r^2 - 1 = \lambda^2|u_{1,j}(r,t)|^2 + r^2 - 1$. This is a smooth function of r on $[1-\delta, 1]$ and its zeros correspond to intersection points of $u_{\lambda,j}(r,t)$ with S^3.

Now suppose a curve $(u_{\lambda,j}(r,t), r\,\mathrm{e}^{\mathrm{i}t})$ with fixed λ, j and t has multiple intersection points with S^3 while $r \in [1-\delta, 1]$. Then between the corresponding values of r the function $|u_{\lambda,j}(r,t)|^2 + r^2 - 1$ must have an extremum.

We can choose λ small enough such that the derivative $\frac{d}{dr}(\lambda^2|u_{1,j}(r,t)|^2 + r^2 - 1)$ is strictly positive for all $r \in [1-\delta, 1]$. Hence for small λ, there is a unique intersection point with r in that interval.

In fact we can find a sufficient value for ε_1 as follows.

We need to make sure that $\frac{d}{dr}(\lambda^2|u_{1,j}(r,t)|^2 + r^2 - 1) > 0$ for all $r \in [1-\delta, 1]$ and all $\lambda < \varepsilon_2$.

Since $f_\lambda(\bullet, r\,\mathrm{e}^{\mathrm{i}t})$ is a polynomial in the first variable u, we may write $f_\lambda(u, r\,\mathrm{e}^{\mathrm{i}t}) = \sum_{j=0}^{s} c_j \lambda^{s-j} u^j$, where $c_j \in \mathbb{C}$ depends on r and t. Note that it follows from Rouché's Theorem that

$$U = \max_{\substack{r\in[1-\delta,1] \\ j=0,1,\ldots,s-1 \\ t\in[0,2\pi]}} \{1, \sum_{j=0}^{s-1} |c_j|\} \tag{5.19}$$

is a bound on the modulus of all roots of all polynomials $f_1(\bullet, r\,\mathrm{e}^{\mathrm{i}t})$ with $r \in [1-\delta, 1]$. Hence λU is an upper bound on the modulus of all roots of all polynomials $f_\lambda(\bullet, r\,\mathrm{e}^{\mathrm{i}t})$, which are by definition $u_{\lambda,j}(r,t)$. Define $\widetilde{D}_1 = \max_{\substack{t\in[0,2\pi]\\ j=0,1,\dots,s-1\\ r\in[1-\delta,1]}} \left\{\left|\frac{\partial|\operatorname{Re}(u_{1,j}(r,t))|}{\partial r}\right|\right\}$ and $\widetilde{D}_2 = \max_{\substack{t\in[0,2\pi]\\ j=0,1,\dots,s-1\\ r\in[1-\delta,1]}} \left\{\left|\frac{\partial|\operatorname{Im}(u_{1,j}(r,t))|}{\partial r}\right|\right\}$.

With $\varepsilon_1 = \sqrt{\frac{(1-\delta)}{U(\widetilde{D}_1+\widetilde{D}_2)}}$ we find

$$\frac{d}{dr}(\lambda^2|u_{1,j}(r,t)|^2 + r^2 - 1) > 2r - \lambda^2 2U(\widetilde{D}_1 + \widetilde{D}_2) > 0, \tag{5.20}$$

as long as $\lambda < \varepsilon_1$ and $r \in [1-\delta, 1]$. □

Recall that δ from Lemma 5.3 does not depend on λ. This allows us to prove the following lemma.

Lemma 5.5. *There exists $\varepsilon_2 > 0$ such that for all $\lambda < \varepsilon_2$ all intersections of the curves $(u_{\lambda,j}(r,t), r\,\mathrm{e}^{\mathrm{i}t})$ with S^3 occur with $r \in [1-\delta, 1]$.*

Proof. With the definition of U above we can make sure that all intersection points of the roots $u_{\lambda,j}(r,t)$ with S^3 happen in the region where $r \in [1-\delta, 1]$ if λ is small enough. We set $\varepsilon_2 = \frac{\sqrt{\delta(2-\delta)}}{U}$. Then for all $\lambda < \varepsilon_2$, we have

$$|u_{\lambda,j}(r,t)|^2 + r^2 < \lambda^2 U^2 + (1-\delta)^2 < 1 \tag{5.21}$$

for all $r < 1-\delta$ and hence all intersections with S^3 happen for $r \in [1-\delta, 1]$. □

Note that Equation (5.21) also shows that for every $\lambda < \varepsilon_2$ and every fixed j and t, the curve $u_{\lambda,j}(r,t)$ intersects S^3, since $|u_{\lambda,j}(r,t)|^2 + r^2 \geq 1$ at $r = 1$. Combining this with Lemma 5.4 means that this intersection point is unique for every curve $(u_{\lambda,j}(r,t), r\,\mathrm{e}^{\mathrm{i}t})$. Denote the value of r at which the intersection occurs by $r_{\lambda,j}(t)$.

Recall the definition of the map

$$\Psi : \mathring{D} \times (\mathbb{C}\backslash\{0\}) \to S^3, \quad \Psi(u, r\,\mathrm{e}^{it}) = (u, \sqrt{1-|u|^2}\,\mathrm{e}^{\mathrm{i}t}). \tag{5.22}$$

We now define a smooth isotopy between $\Psi(f_\lambda^{-1}(0) \cap (\mathbb{C} \times S^1))$, which we know to be the desired link, and $f_\lambda^{-1}(0) \cap S^3$.

Let $I : (\underbrace{S^1 \cup \ldots \cup S^1}_{|\mathscr{C}| \text{ copies}}) \times [0,1] \to S^3$ be defined by

$$I(\Psi((u_{\lambda,j}(1,t), \mathrm{e}^{\mathrm{i}t})), s) = \Psi(u_{\lambda,j}(1-s+sr_{\lambda,j}(t), t), (1-s+sr_{\lambda,j}(t))\,\mathrm{e}^{\mathrm{i}t}). \tag{5.23}$$

Lemma 5.6. *There is an $\varepsilon > 0$ such that for all $\lambda < \varepsilon$ the function I is a smooth isotopy from $\Psi(f_\lambda^{-1}(0) \cap (\mathbb{C} \times S^1))$ to $f_\lambda^{-1}(0) \cap S^3$.*

Proof. We have to show that for every s the function $I(\bullet, s)$ is an embedding and that I is smooth. Suppose there is an s such that $I(\bullet, s)$ is not an embedding, then there exist complex numbers $u_{\lambda,j}(1 - s + sr_{\lambda,j}(t), t) = u_{\lambda,k}(1 - s + sr_{\lambda,k}(t), t)$ with $j \neq k$, but Lemma 5.3 and Lemma 5.5 tell us that this does not happen if $\lambda < \min\{\varepsilon_1, \varepsilon_2\}$. Furthermore, since simple roots of a polynomial depend smoothly on its coefficients and the map Ψ is smooth, I is a smooth isotopy.

Note that

$$I(\Psi((u_{\lambda,j}(1,t), e^{it})), 0) = \Psi(u_{\lambda,j}(1,t), e^{it}) = \Psi(f_\lambda^{-1}(0) \cap (\mathbb{C} \times S^1)) \tag{5.24}$$

and

$$I(\Psi((u_{\lambda,j}(1,t), e^{it})), 1) = \Psi(u_{\lambda,j}(r_{\lambda,j}(t), t), r_{\lambda,j}(t)\, e^{it}) = f_\lambda^{-1}(0) \cap S^3 \tag{5.25}$$

which finishes the proof. Note that I is well-defined if $\lambda < \min\{\varepsilon_1, \varepsilon_2\}$, so we can set $\varepsilon = \min\{\varepsilon_1, \varepsilon_2\}$. □

The Isotopy Extension Theorem 2.6 says that I extends to an ambient isotopy. Thus $f_\lambda^{-1}(0) \cap S^3$ is ambient isotopic to the desired link if λ is small enough.

Since every link is the closure of a braid by Alexander's Theorem [6] and for every braid B there is a family of functions f_λ, this concludes the proof of Theorem 5.1. We have shown that for every link L there is a function $f : \mathbb{C}^2 \to \mathbb{C}$ such that $f^{-1}(0) \cap S^3 = L$ and f is a polynomial in complex variables u, v and $\overline{v}$, i.e. f is a semiholomorphic polynomial.

In [40] we describe the constructed semiholomorphic polynomials for several links and all knots of six or fewer crossings. It turns out that in practice λ can be chosen to be a lot larger than the bound $\varepsilon = \min\{\varepsilon_1, \varepsilon_2\}$ which is given in the proof.

5.3 Finding Fourier parametrisations

In this section we present an algorithm that generates a parametrisation as in Equation (5.3) for any given braid.

For every link component $C \in \mathscr{C}$ we obtain F_C and G_C by trigonometric interpolation of data points that can be obtained from a presentation of the braid diagram. For background on trigonometric interpolation we point the

reader to [9].

Step 1: Finding the data points for the trigonometric interpolation for F_C

We need to perform a trigonometric interpolation for F_C for each link component $C \in \mathscr{C}$. The data points for this interpolation are chosen such that they contain the information about the position of every strand of C between two crossings in the braid diagram.

Let s denote the number of strands and ℓ the length of the braid word. The given braid word allows us to draw a braid diagram of B. For convenience we draw the strands as piecewise linear curves with all crossing points evenly distributed along the t-axis as in Fig. 5.1 a). If we neglect the signs of the crossings, the diagram consists of s curves $(D_{C,j}(t), 0, t)$, $t \in [0, 2\pi]$, $C \in \mathscr{C}$, $j = 0, 1, \ldots, s_C$ in the tx-plane, each of which can be interpreted as the graph of a function $D_{C,j}(t)$ (Fig. 5.1 b)). Since the crossing points are evenly distributed, they occur at $t_k = 2\pi(2k-1)/(2\ell)$ with $k = 1, 2, \ldots \ell$. The braid diagram is drawn in such a way that the value of $D_{C,j}(2\pi)$ is equal to $D_{C,k}(0)$ for some k, say $k = j+1$. This way each strand obtains a label (C, j). This label is unique once for each component C an arbitrary strand of that component is chosen as the strand $(C, 1)$. We can draw the graph of the piecewise-linear function $D_C : [0, 2\pi] \to \mathbb{R}$, $D_C(\frac{t+2\pi j}{s_C}) = D_{C,j}(t)$ as in Fig. 5.1 c).

We can now perform a trigonometric interpolation through the points $(t_k/s_C - 2\pi/(2s_C\ell), D_C(t_k - 2\pi/(2\ell)))$, $k = 1, 2, \ldots, s_C\ell$ (shown in Fig. 5.1 d)) for every component C to obtain $|\mathscr{C}|$ trigonometric polynomials F_C that satisfy $F_C(t_k/s_C - 2\pi/(2s_C\ell)) = D_C(t_k - 2\pi/(2\ell))$ for every $k = 1, 2, \ldots s_C\ell$ and every link component $C \in \mathscr{C}$ (cf. Fig. 5.1 e)).

Step 2: Trigonometric interpolation for F_C

The trigonometric polynomials F_C can be explicitly constructed by using the discrete Fourier transform

$$\widetilde{D}_{C,k} = \frac{1}{s_C\ell} \sum_{n=0}^{s_C\ell-1} D_C\left(t_n - \frac{2\pi}{2s_C\ell}\right) \mathrm{e}^{-\mathrm{i}\left(\frac{t_n}{s_C} - \frac{2\pi}{2s_C\ell}\right)k}. \tag{5.26}$$

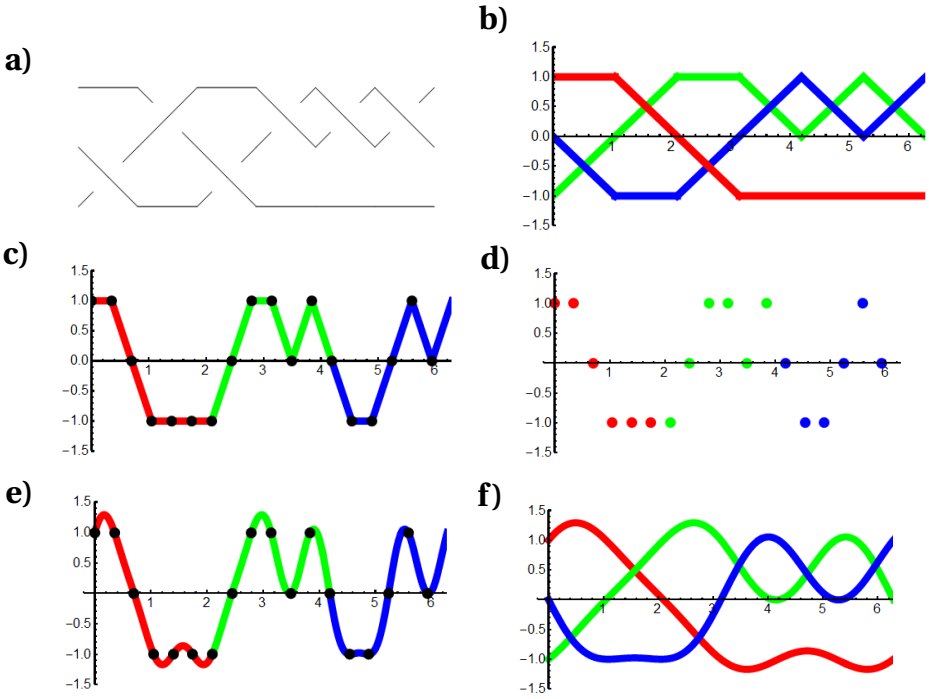

Figure 5.1: The trigonometric interpolation for F_C. a) The braid diagram of a minimal braid of 5_2. b) The projection of strands of the braid as piecewise linear curves in a coordinate system. c) The graph of the function D_C. d) The data points for the trigonometric interpolation. These can be read off from the graph of D_C. e) The graph of F, the trigonometric polynomial interpolating the data points. f) The graphs of the different X_j, when F is used to parametrise the x-coordinate of the braid. The crossing points in this plot give rise to the data points for the interpolation for G.

We get

$$F_C(t) = \begin{cases} \widetilde{D}_{C,0} + \sum_{k=1}^{s_C\ell/2-1} 2\,\mathrm{Re}(\widetilde{D}_{C,k})\cos(kt) - \sum_{k=1}^{s_C\ell/2-1} 2\,\mathrm{Im}(\widetilde{D}_{C,k})\sin(kt) \\ \qquad +\widetilde{D}_{C,s_C\ell/2}\cos\left(\frac{s_C\ell}{2}t\right), \qquad \text{if } s_C\ell \text{ is even,} \\ \\ \widetilde{D}_{C,0} + \sum_{k=1}^{(s_C\ell-1)/2} 2\,\mathrm{Re}(\widetilde{D}_{C,k})\cos(kt) - \sum_{k=1}^{(s_C\ell-1)/2} 2\,\mathrm{Im}(\widetilde{D}_{C,k})\sin(kt), \\ \qquad\qquad\qquad\qquad \text{if } s_C\ell \text{ is odd.} \end{cases} \tag{5.27}$$

Since the example in Fig. 5.1 is the knot 5_2, there is only one link component. Figure 5.1 e) shows the graph of the trigonometric polynomial F_C. The graphs of $F_C\left(\frac{t+2\pi j}{s_C}\right)$ in Fig. 5.1 f) form a braid diagram B' with unspecified signs of crossing. Note that in contrast to usual braid diagrams there might in general be more than two strands involved in a crossing and crossing strands might not be transverse.

Since the trigonometric polynomials F_C are interpolating the data points, there is a bijection between the strands of B' and the strands of the original braid B and for every k there is a crossing of B' in the interval $[t_k - 2\pi/(2\ell), t_{k+1} - 2\pi/(2\ell)]$ that involves the same strands as the crossing of B at t_k. This crossing might not be unique. However, for every pair of strands of B that is not crossing at t_k, there is an even number of crossings in the diagram B' between them in the interval $[t_k - 2\pi/(2\ell), t_{k+1} - 2\pi/(2\ell)]$ (counting multiplicities if a crossing is not transverse). For the pair of strands of B that is crossing at t_k, the corresponding strands of B' cross an odd number of times in the interval $[t_k - 2\pi/(2\ell), t_{k+1} - 2\pi/(2\ell)]$ (counting multiplicities). This is due to the choice of data points for the trigonometric interpolation that store the information about the position of every strand of B between two crossings.

Step 3: Finding the data points for the trigonometric interpolation for G_C

Again we need to perform a trigonometric interpolation for each link component $C \in \mathscr{C}$. Recall that Step 2 resulted in B', a braid diagram whose signs of crossings are not specified. By choosing data points whose t-coordinates are the positions of crossings in the braid diagram B' and choosing the y-coordinate appropriately, we attach signs to the crossings of B' in such a way that it becomes the diagram of a braid isotopic to B.

This can be achieved as follows. For every $k = 1, 2, \dots \ell$ we choose a bijection w_k between the strands of B' and a set of s distinct real numbers such that the strand corresponding to the strand of B which is overcrossing at t_k gets assigned a larger number than the strand corresponding to the strand of B which is undercrossing at t_k.

This time the t-coordinate of the data points used for the trigonometric interpolation for G_C are the positions of the crossings that the strands $F_C\left(\frac{t}{s_C} + \frac{2\pi j}{s_C}\right)$ are involved in. Let the strand (C, j) be involved in a crossing of B' at $t = t_*$, i.e. $F_C\left(\frac{t_*}{s_C} + \frac{2\pi j}{s_C}\right) = F_{C'}\left(\frac{t_*}{s_{C'}} + \frac{2\pi m}{s_{C'}}\right)$ for some $C' \in \mathscr{C}$ and $m \in \{0, 1, \dots, s_{C'} - 1\}$. Then $\left(\frac{t_*+2\pi j}{s_C}, w_k((C, j))\right)$ is a data point. Note that if a strand is not involved in a crossing in the kth interval, then there is no data point for this strand in this interval and hence its image under w_k does not affect the result at all. We denote the data points by (t'_k, y_k). The number of data points for G_C depends on the number of crossings of B' that involve strands of the link component C.

Each crossing creates a data point for each strand involved in the crossing.

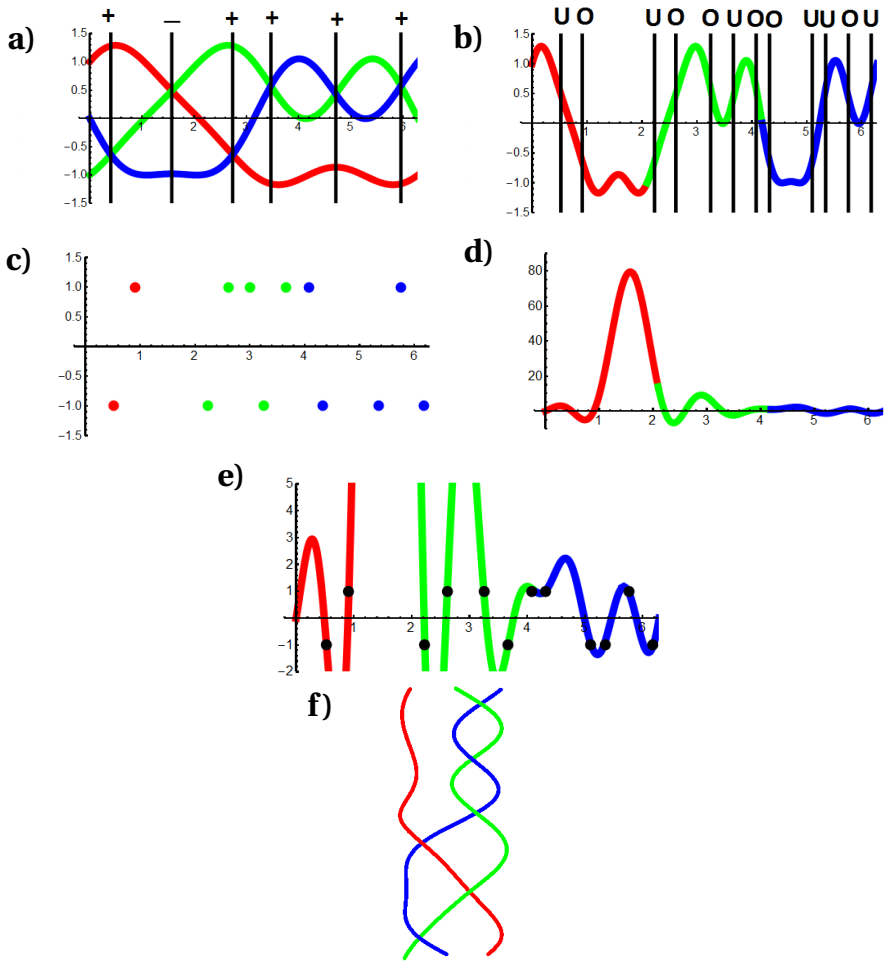

Figure 5.2: The trigonometric interpolation to get G_C. a) The x-coordinate of s strands parametrised by F_C with marked positions of crossings and signs of crossings. b) The graph of F_C with marked positions of crossings and a label indicating whether the corresponding strand is the overpassing (O) or the underpassing (U) strand. c) The set of data points to be interpolated by G_C. Overpassing strands should have value +1 at the position of the crossings and underpassing strands the value −1. d) The graph of the interpolating trigonometric polynomial G_C. e) The graph of G_C passes through all data points. f) The braid parametrised by F_C and G_C (plotted in a left-handed coordinate system)

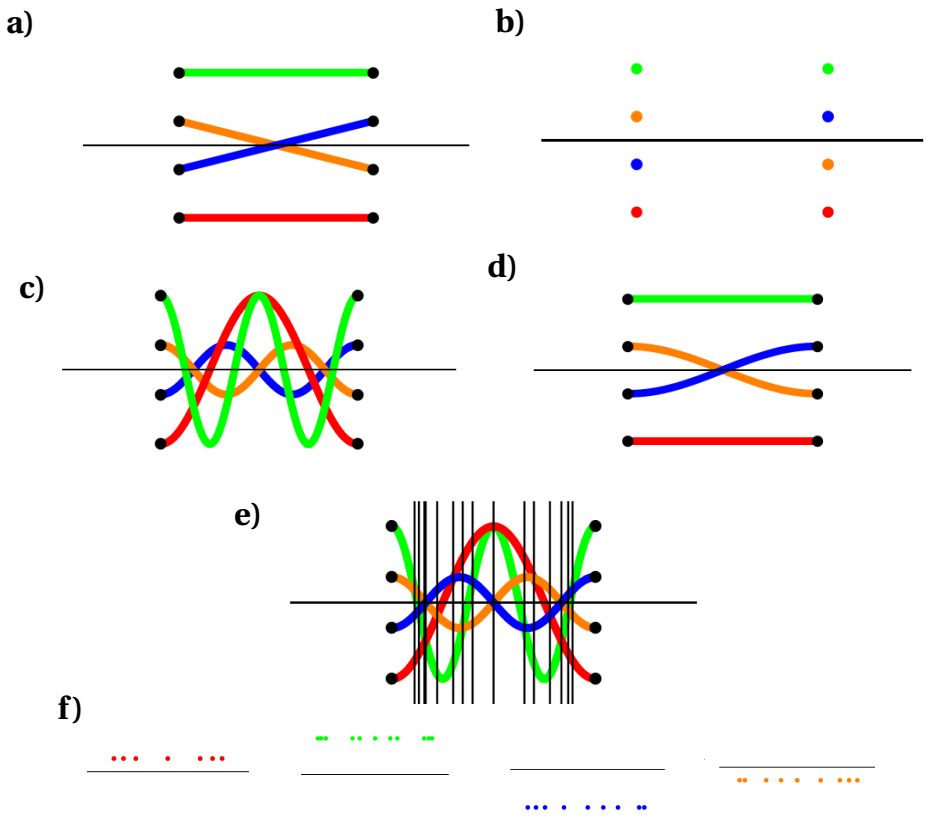

Figure 5.3: An example of creating data points from an interval with additional crossings. a) The piecewise linear braid diagram (without crossing signs) in some interval. b) The strands parametrised by the interpolating trigonometric polynomial F_C must pass through the shown points, where the colours indicate which strands pass through which points. c) An example of strands parametrised by trigonometric polynomials that pass through the data points in the desired points, but have additional crossings and not only the one desired crossing. d) If for example the green strand lies above all other strands throughout the entire interval, the red one above blue and orange, and orange above blue, then the braid can be straightened to look like the shown braid. e) A plot of the strands parametrised by the interpolating trigonometric polynomial F_C with marked positions where crossings occur. We create data points such that at all crossing positions that involve the green strand, it is on top; in all remaining crossings that involve the red strand, that should be on top and so on. f) The set of data points from the exemplary interval that should be interpolated by G_C.

This choice of data points implies that any family of trigonometric polynomials G_C that interpolates these together with F_C from Step 1 gives a parametrisation of a braid as in Equation (5.3) and this braid is braid isotopic to B. This can be seen as follows. Since the y-coordinate of the data points only depends on the strand and on k, all crossings between one pair of strands in the interval $[t_k - 2\pi/(2\ell), t_{k+1} - 2\pi/(2\ell)]$ in B' have the same strand as an overpassing strand (and the other as the underpassing strand). This and the previous observation about the parity of numbers of crossings between strands means that in every interval $[t_k - 2\pi/(2\ell), t_{k+1} - 2\pi/(2\ell)]$ all crossings but one can be canceled. The two strands that are involved in the remaining crossing correspond to the two strands of B crossing at t_k and by definition of w_k they cross with the required sign.

Step 4: Trigonometric interpolation for G_C

Since the positions of the crossings of B' are in general not equidistributed, the trigonometric interpolation does not directly translate to a discrete Fourier Transform.

Finding a trigonometric polynomial that interpolates the data points (t'_k, y_k) is equivalent to finding a function $q(z) = \sum_{k=-M_C}^{M_C} c_k z^k$ with $q(\mathrm{e}^{\mathrm{i}t'_k}) = y_k$ for all k, which is equivalent to finding a polynomial $\widetilde{q}(z) = \sum_{k=0}^{2M_C} c_{k-K} z^k$ such that $q(\mathrm{e}^{\mathrm{i}t'_k}) = y_k \, \mathrm{e}^{\mathrm{i}Kt'_k}$ for all k and $c_{-k} = \overline{c}_k$ for all k.

We can find such a function by using the Lagrange formula for polynomial interpolation. This allows us to explicitly calculate G_C. If the number N of data points (t'_k, y_k) is odd, say $2K+1$, we get

$$q(\mathrm{e}^{\mathrm{i}t}) = G_C(t) = \sum_{k=1}^{N} y_k \, \mathrm{e}^{-\mathrm{i}Kt + \mathrm{i}Kt'_k} \prod_{\substack{m=1 \\ m \neq k}}^{N} \frac{\mathrm{e}^{\mathrm{i}t} - \mathrm{e}^{\mathrm{i}t'_m}}{\mathrm{e}^{\mathrm{i}t'_k} - \mathrm{e}^{\mathrm{i}t'_m}}. \tag{5.28}$$

If N is even, say $N = 2K$, the result is

$$q(\mathrm{e}^{\mathrm{i}t}) = G_C(t) = \sum_{k=1}^{N} y_k \, \mathrm{e}^{-\mathrm{i}Kt + \mathrm{i}Kt'_k} \frac{\mathrm{e}^{\mathrm{i}t} - \mathrm{e}^{\mathrm{i}\alpha_k}}{\mathrm{e}^{\mathrm{i}t'_k} - \mathrm{e}^{\mathrm{i}\alpha_k}} \prod_{\substack{m=1 \\ m \neq k}}^{N} \frac{\mathrm{e}^{\mathrm{i}t} - \mathrm{e}^{\mathrm{i}t'_m}}{\mathrm{e}^{\mathrm{i}t'_k} - \mathrm{e}^{\mathrm{i}t'_m}}, \tag{5.29}$$

where α_k is a free parameter that can be chosen to be 0 for all k.

Writing $q(\mathrm{e}^{\mathrm{i}t}) = \sum_{k=-K}^{K} c_k \, \mathrm{e}^{\mathrm{i}kt}$ as a power series in $\mathrm{e}^{\mathrm{i}t}$ allows to compute the coefficients c_k of G_C for every link component $C \in \mathscr{C}$.

Then Equation (5.3) with the trigonometric polynomials F_C and G_C obtained by trigonometric interpolation is a finite Fourier parametrisation of the desired braid.

In this construction there are several choices to be made, each of which leads to a different trigonometric polynomial. There is first of all the choice of braid. We will see in Section 5.4 how the choice of braid affects the possible degrees of the resulting trigonometric polynomials. It is not true in general that the simplest braid (in terms of number of crossings ℓ or number of strands s) leads to the simplest trigonometric polynomials (in terms of degree). However, we compute bounds for the degree of the trigonometric polynomials in terms of ℓ and s and these are strictly increasing with ℓ and s.

Analogous to Gittings's work [55] on minimal braid words we used a numerical algorithm to identify the closures of all rth powers of braid words of length $\ell < 6$, number of strands $s < 6$ and number of repeats r depending on s and ℓ. We only find four links where the shortest 'basic braid word' is shorter than Gittings's minimal braid word for the same link: 6_2 $((\sigma_2\sigma_4^{-1}\sigma_3\sigma_1)^2)$, 6_3 $((\sigma_2^{-1}\sigma_4\sigma_3\sigma_1^{-1})^2)$, 7_6 $((\sigma_2^{-1}\sigma_4\sigma_3\sigma_1)^2)$ and 7_7 $((\sigma_2^{-1}\sigma_4\sigma_3^{-1}\sigma_1)^2)$.

Secondly, there is the choice of embedding the piecewise linear braid diagram in $\mathbb{R}^2$, which corresponds to the functions $D_{C,j}$. Demanding that between crossings the strands are equidistant and are arranged symmetrically around $x = 0$ seem like reasonable conditions, since a rather symmetric arrangement of data points suggests an interpolating trigonometric polynomial with few terms. The choice of function D_C also means that we choose a first strand for each link component. The algorithm works for any such choice.

Furthermore, the choice of functions w_k that are used to determine the data points for the interpolation for G_C do not affect the topology of the braid parametrised by the obtained trigonometric polynomials. Like in the choice of the piecewise linear braid embedding it appears reasonable to place the strands that are involved in crossings in the relevant interval symmetrically and with equal distances around $y = 0$.

The two families of knots that are described in Chapter 4 and [23], lemniscate knots and spiral knots, have particularly symmetric braid words that allow comparatively simple trigonometric braid parametrisations.

Figure 5.1 and Figure 5.2 illustrate our method for the example of the knot 5_2, which is the simplest knot (in terms of minimal crossing number) that is

not a lemniscate knot or a spiral knot. For this example we choose the braid $\sigma_1\sigma_2^{-1}\sigma_1\sigma_2^3$ (Fig. 5.1 a)) which closes to the knot 5_2. In fact it is a minimum braid word of 5_2 [55]. To make the step from braid diagram to graphs of real functions more intuitive, we draw braid diagrams horizontally from now on. We read off braid words from braid diagrams from left to right and strand positions are numerated from top to bottom. Since σ_j should correspond to the strand with the jth lowest x-coordinate passing over the strand with the next highest x-coordinate, the labeling of the strand positions is a bit counter-intuitive. A positive crossing σ_i corresponds to the strand in position i (counted from the bottom of the picture) passing over the strand in position $i+1$.

Since 5_2 is a knot, there is only one component. To find F_C, we interpolate the data points $(\widetilde{t_k}, x_k)$ for $k = 0, 1, \ldots, 17$, where $\widetilde{t_k} = 2\pi k/18$ and x_k is the kth entry of $x = (1, 1, 0, -1, -1, -1, -1, 0, 1, 1, 0, 1, 0, -1, -1, 0, 1, 0)$. These data points can be read off from Fig. 5.1 c) and are displayed in Fig. 5.1 d).

The resulting interpolating trigonometric polynomial is

$$\begin{aligned} F(t) &= 0.108784\,\mathrm{e}^{-8\mathrm{i}t} + 0.0846189\mathrm{i}\,\mathrm{e}^{-7\mathrm{i}t} + 0.24365\mathrm{i}\,\mathrm{e}^{-5\mathrm{i}t} - 0.0886815\,\mathrm{e}^{-4\mathrm{i}t} \\ &\quad + 0.479898\,\mathrm{e}^{-2\mathrm{i}t} - 0.129644\mathrm{i}\,\mathrm{e}^{-\mathrm{i}t} + 0.129644\mathrm{i}\,\mathrm{e}^{\mathrm{i}t} + 0.479898\,\mathrm{e}^{2\mathrm{i}t} \\ &\quad - 0.0886815\,\mathrm{e}^{4\mathrm{i}t} - 0.24365\mathrm{i}\,\mathrm{e}^{5\mathrm{i}t} - 0.0846189\mathrm{i}\,\mathrm{e}^{7\mathrm{i}t} + 0.108784\,\mathrm{e}^{8\mathrm{i}t} \\ &= -0.259288\sin(t) + 0.959796\cos(2t) - 0.177363\cos(4t) + 0.4873\sin(5t) \\ &\quad + 0.169238\sin(7t) + 0.217568\cos(8t). \end{aligned} \tag{5.30}$$

The coefficients were computed numerically, so they are not necessarily exact. However, this small change in the parametrisation does not change the braid type. The graph of F is plotted in Fig. 5.1 e). In order to find the data points for the trigonometric interpolation of G, we need to compute the values of t for which $F(t + 2\pi j/3) = F(t + 2\pi k/3)$ for some $j, k \in \{0, 1, 2\}$.

There is only one crossing between the red strand ($j = 0$) and the green strand ($j = 1$), namely at $t = 0.523599$. Since this crossing corresponds to the crossing σ_1^{-1} in the original braid word, the green strand is supposed to pass over the red strand. Hence the points $(0.523599, -1)$ (for the red strand) and $(0.523599 + 2\pi/3, 1)$ (for the green strand) will be included in the list of data points used for the interpolation of G. Note that this corresponds to a bijection w_1 that sends the red strand to -1 and the green strand to 1.

Similarly, we compute the intersection points of the other pairs of strands and obtain the list of data points $(0.523599, -1)$, $(0.912415, 1)$, $(0.134782+2\pi/3, -1)$,

$(0.523599 + 2\pi/3, 1)$, $(1.15567 + 2\pi/3, 1)$, $(1.5708 + 2\pi/3, -1)$, $(1.98592 + 2\pi/3, 1)$, $(0.134782 + 4\pi/3, 1)$, $(0.912415 + 4\pi/3, -1)$, $(1.15567 + 4\pi/3, -1)$, $(1.5708 + 4\pi/3, 1)$, $(1.98592 + 4\pi/3, -1)$.

Performing a trigonometric interpolation through these points yields

$$\begin{aligned} G(t) = {} & 19.0248 - 0.823358\cos(t) + 17.1048\sin(t) - 15.2722\cos(2t) - 0.13139\sin(2t) \\ & - 0.454434\cos(3t) - 12.8637\sin(3t) + 11.9691\cos(4t) - 1.02332\sin(4t) \\ & - 0.823379\cos(5t) + 8.6227\sin(5t) - 4.10823\cos(6t) - 0.818417\sin(6t), \end{aligned} \tag{5.31}$$

whose graph is shown in Figure 5.2d).

Using F and G in Equation (5.3) results in a Fourier parametrisation of the desired braid, closing to 5_2. This allows us to construct $g_{a,b}$ and then $f_{a,b}$.

As discussed in [40] braids whose words are identical up to signs, i.e. $B_1 = \sigma_{i_1}^{\varepsilon_{i_1,1}}\sigma_{i_2}^{\varepsilon_{i_2,1}}\dots\sigma_{i_\ell}^{\varepsilon_{i_\ell,1}}$ and $B_2 = \sigma_{i_1}^{\varepsilon_{i_1,2}}\sigma_{i_2}^{\varepsilon_{i_2,2}}\dots\sigma_{i_\ell}^{\varepsilon_{i_\ell,2}}$ with all $\varepsilon_i \in \{\pm 1\}$, can be parametrised using the same F_C. For example the function F computed above can also be used to parametrise the x-coordinate of the braid $\sigma_2\sigma_1^{-1}\sigma_2\sigma_1^{-3}$, which closes to the knot 6_2.

The described algorithm finds a trigonometric parametrisation for every braid. While we will see in the next section that there is a bound on the degree of the trigonometric polynomials that are constructed this way, we cannot expect this algorithm to give us the simplest (i.e the minimal number of terms and lowest degree) trigonometric parametrisation for a given braid. For links with few crossings it is often sufficient to make some educated guesses to find Fourier parametrisation that are much simpler than the one found by the algorithm.

For example, in [40] we find that the knot 5_2 for which the algorithm found trigonometric polynomials with 6 (respectively 13) terms and degree equal to 8 (respectively 6), can also be realised as the closure of the braid parametrised by

$$\begin{aligned} (X_j(t), Y_j(t), t) = \Bigg(& -\cos\left(\frac{2(t+2\pi j)}{3}\right) - \cos\left(\frac{5(t+2\pi j)}{3}\right), \\ & \frac{1}{2}\sin\left(\frac{t+2\pi j}{3}\right) + \sin\left(\frac{4(t+2\pi j)}{3}\right), t\Bigg). \end{aligned} \tag{5.32}$$

This parametrisation is found through geometric considerations alone. The parametrisation found by our algorithm is significantly more complicated than the one in Equation (5.32) ([40]). However, the procedure in [40] is not algorithmic and in general very time consuming.

In [40] we use geometric inspection to find a finite Fourier parametrisation for the braid word $\sigma_1^{-1}\sigma_2\sigma_1^3\sigma_2$, which is also a minimal braid word for the knot 5_2, since it differs from the one given above only by conjugation by σ_2. There are some fundamental differences between the approach in [40] and the algorithm described here. The method from [40] requires a lot of testing. Choosing a braid representative which is as symmetric as possible typically allows us to parametrise the braid using only few terms and low spatial frequencies. Geometric considerations give us a rough idea of a possible range of coefficients and spatial frequencies, so that it becomes feasible to find a finite Fourier parametrisation for the given braid. The desire for symmetry makes $\sigma_1^{-1}\sigma_2\sigma_1^3\sigma_2$ a better choice of braid word, in particular if we place the crossings at equal distances along the t-axis and have the first crossing at $t = 0$. Note that this is different from the positions of the crossings in the description of our algorithm. In order to calculate the trigonometric interpolation efficiently by using the discrete Fourier transform, we want the data points to be equally distributed along the t-axis starting at $t = 0$. Since the data points should lie between crossings, we explicitly do not want a crossing at $t = 0$.

For short and symmetric braids with few strands the method from [40] might lead to simpler polynomials in the sense of fewer terms and lower orders, for example the parametrisation for the knot 5_2 in (5.32) only has two terms for F and G each and the highest order is five. However, since the method is not algorithmic, it is in general not a good way of finding parametrisations for more complicated braids.

With the described algorithm we can find a finite Fourier parametrisation for any braid B. Then $g_{a,b}$ defined as in Equation (5.1) can be written as a polynomial in u, $\mathrm{e}^{\mathrm{i}t}$ and $\mathrm{e}^{-\mathrm{i}t}$ by Lemma 5.2. Constructing $f_{a,b}$ as in Section 5.1 gives a semiholomorphic polynomial which by the results from Section 5.2 has the closure of B as its zero level set on the three-sphere of radius one if a and b are small enough. This makes our proof of the existence of semiholomorphic polynomials with knotted zero level sets fully algorithmic.

5.4 Properties of the constructed polynomials

In this section we prove some properties of the constructed polynomials obtained from the algorithm described in the last section. We use the notation from Section 5.2, in particular the symbol f_λ will always denote a polynomial

that was constructed using the method described in Sections 5.1-5.3.

Corollary 5.7. *If λ is small enough, 0 is a regular value of $f_\lambda|_{S^3}$.*

Proof. Let $(u_*, v_*) \in S^3$ be a point on the link, so $f_\lambda(u_*, v_*) = 0$. Then for fixed $v = v_*$, the function f_λ is a polynomial in u with u_* being a simple root. Hence $\frac{\partial f_\lambda}{\partial u}(u_*, v_*) \neq 0$, so in particular the 2×4-matrix $\nabla f_\lambda(u_*, v_*)$ has full rank.
Furthermore, for small fixed λ a straightforward calculation shows that the intersections of the curves $(u_{\lambda,j}(r,t), r\,\mathrm{e}^{\mathrm{i}t})$, $j = 1, 2, \ldots, s$, $t \in [0, 2\pi]$ fixed, with S^3 are transverse. Hence (u_*, v_*) is a regular point of $f|_{S^3}$. □

This corollary is important for applications which focus on functions $\mathbb{R}^3 \to \mathbb{C}$. In order to make the functions satisfy extra physical conditions, which depend on the individual setting, coefficients might have to be slightly changed. The fact that 0 is a regular value offers a certain stability under small perturbations of the originally constructed polynomial. This means that if we do not change the coefficients too much, the zero set of interest will remain the desired link.

Recall from Chapter 2 the definition of Rudolph's transverse $\mathbb{C}$-links as the transverse intersection of a complex plane curve with the unit three-sphere. A link is a transverse $\mathbb{C}$-link if and only if it is quasipositive (cf. Theorem 2.22). Corollary 5.7 shows that if we relax the condition from f being a complex polynomial to being semiholomorphic, then every link can be realised as the transverse intersection of the zero level set of such a polynomial with S^3.

Corollary 5.8. *The polynomial f_λ is harmonic, that is $(\partial_u \partial_{\overline{u}} + \partial_v \partial_{\overline{v}}) f_\lambda = 0$.*

Proof. This is immediate from the construction. Since f_λ is a polynomial in u, there is no dependence on $\overline{u}$. Recall that f_λ was obtained from $g_{a,b}$ by replacing $\mathrm{e}^{\mathrm{i}t}$ by v and $\mathrm{e}^{-\mathrm{i}t}$ by $\overline{v}$ and $g_{a,b}$ is a polynomial in u, $\mathrm{e}^{\mathrm{i}t}$ and $\mathrm{e}^{-\mathrm{i}t}$. Now suppose there was a monomial containing both v and $\overline{v}$, say $v^n \overline{v}^m$, as a factor. Then in the polynomial expression of $g_{a,b}$ these would have simplified to $\mathrm{e}^{\mathrm{i}t(n-m)}$, which would give v^{n-m} or $\overline{v}^{m-n}$ depending on whether n or m is larger. In either case, there is no monomial with v and $\overline{v}$ as a factor. Thus $\partial_{\overline{v}} f_\lambda$ does not depend on v which proves the corollary. □

Not every polynomial of the form constructed in Sections 5.1-5.3 will be of practical use. In particular with regard to the engineering of physical knotted fields, a polynomial with too many terms or of too high degree might be too

hard to control to be applicable to some of the systems described in Chapter 3. This is also a reason why a naive algebraic approximation of a link given as a parametric curve is not particularly useful.

An advantage of our construction is that it allows for an upper bound of the degree of the constructed polynomial f_λ in terms of braid data.

We use the notation from Section 5.2. The algorithm in Section 5.3 finds a finite Fourier parametrisation (5.3) of a braid B that closes to the desired link L. Using trigonometric interpolation to find such a parametrisation allows us to give a bound on the highest order $D_C = \max_{C\in\mathscr{C}}\{N_C, M_C\}$, where N_C and M_C are the trigonometric degrees of F_C and G_C respectively, in terms of the length ℓ of the braid and the number of strands s_C in each link component C.

Lemma 5.9. *Let $\mathscr{C}$ be again the set of all link components of L, s_C be the number of strands that form $C \in \mathscr{C}$, ℓ be the length of the braid word and $s = \sum_{C\in\mathscr{C}} s_C$ the number of strands of the braid. Then*

$$D_C \leq \left\lfloor \frac{(s_C+1)(s_C\ell-1) + \ell s_C(s-s_C) - 1}{2} \right\rfloor. \tag{5.33}$$

Proof. The degrees of the trigonometric polynomials F_C and G_C can be directly calculated from the number of data points used for the interpolation. Note that the number of data points needed for the trigonometric interpolation of each of the polynomials F_C is equal to $s_C\ell$. Thus N_C is equal to $\lfloor \frac{s_C\ell-1}{2} \rfloor$, where $\lfloor x \rfloor$ denotes the largest integer less than or equal to x.

The union of the graphs of $F_C\left(\frac{t+2\pi j}{s_C}\right)$ form a braid diagram B' with unspecified signs of crossings. We can choose the signs in such a way that the resulting braid is identical to the input braid B, although the braid word might be different. The number of crossings of B' is equal to the length ℓ' of its braid word and hence by the discussion in Section 5.3 at least ℓ.

For the trigonometric interpolation of one trigonometric polynomial G_C we need n data points for every crossing that involves n strands of C. The crossings of B' correspond to intersections of certain trigonometric polynomials related to the different F_C. Since the trigonometric polynomials can be be associated with complex polynomials on the unit circles, by the fundamental theorem of algebra their number of intersections can be bounded in terms of their degree.

Let $C \in \mathscr{C}$ be a component consisting of s_C strands. We first consider the number of intersections between different strands of the same component C. Recall that for a trigonometric polynomial $F_C(t) = \sum_{k=-N_C}^{N_C} c_{k,C}\, \mathrm{e}^{\mathrm{i}kt}$ we can

construct a complex polynomial $p_C(z)$ of degree $2N_C$ with $p_C(\mathrm{e}^{\mathrm{i}t}) = \mathrm{e}^{\mathrm{i}tN_C} F_C(t)$ by defining $p_C(z) = z^{N_C} \sum_{k=-N_C}^{N_C} c_{k,C} z^k$. Note that an intersection point of a strand with index j and a strand with index $j+1$ corresponds to a number $t \in [0, 2\pi]$ such that $F_C(t) = F_C(t + 2\pi/s_C)$, which is equivalent to $p_C(\mathrm{e}^{\mathrm{i}t}) = p_C(\mathrm{e}^{\mathrm{i}t}\,\mathrm{e}^{\mathrm{i}2\pi/s_C})\,\mathrm{e}^{-\mathrm{i}2\pi N_C/s_C}$.

Therefore the sum of the number of intersections between strands with index j and $j+1 \mod s_C$ is exactly the number of points on the unit circle where the complex polynomials $p_C(z)$ and $p_C(z\,\mathrm{e}^{\frac{\mathrm{i}2\pi}{s_C}})\,\mathrm{e}^{-\mathrm{i}2\pi N_C/s_C}$ are equal. Since both are polynomials in z of degree $2N_C$, this number is at most $2N_C \le s_C\ell - 1$. In general the sum of intersections between strands with index j and $j+k$ correspond to points on the unit circle where $p_C(z)$ and $p_C(z\,\mathrm{e}^{\frac{\mathrm{i}2\pi k}{s_C}})\,\mathrm{e}^{-\mathrm{i}2\pi k N_C/s_C}$ coincide. Thus there are again at most $2N_C \le s_C\ell - 1$ many of these. In order to capture all pairs of strands in the component C, we have to sum over k from 1 to $\lfloor \frac{s_C+1}{2} \rfloor$. Thus there are at most $\lfloor \frac{s_C+1}{2} \rfloor (s_C\ell - 1)$ many intersection points between two different strands of the same component C. Hence the number of data points needed to achieve the correct signs for these crossings are at most $2\lfloor \frac{s_C+1}{2} \rfloor (s_C\ell - 1) \le (s_C + 1)(s_C\ell - 1)$.

Intersections involving two different link components, especially if the components consist of different numbers of strands, are more complicated to count. We denote by $\mathrm{lcm}(s_C, s_{C'})$ the least common multiple of s_C and $s_{C'}$ and by $\gcd(s_C, s_{C'})$ their greatest common divisor. A crossing between a strand of the component C with a strand of component C' is equivalent to the existence of t_1, $t_2 \in [0, 2\pi]$ such that $F_C(t_1) = F_{C'}(t_2)$ and $t_1 s_C \equiv t_2 s_{C'} \mod 2\pi$. This is equivalent to

$$p_C\left(\left(\mathrm{e}^{\frac{\mathrm{i}t_1 s_C}{\mathrm{lcm}(s_C,s_{C'})}}\right)^{\mathrm{lcm}(s_C,s_{C'})/s_C}\right)\mathrm{e}^{-\mathrm{i}N_C t_1} = p_{C'}\left(\left(\mathrm{e}^{\frac{\mathrm{i}t_2 s_{C'}}{\mathrm{lcm}(s_C,s_{C'})}}\right)^{\mathrm{lcm}(s_C,s_{C'})/s_{C'}}\right)\mathrm{e}^{-\mathrm{i}N_{C'} t_2} \quad (5.34)$$

and also

$$\begin{aligned} &p_C\left(\left(\mathrm{e}^{\frac{\mathrm{i}(t_1+2\pi m)s_C}{\mathrm{lcm}(s_C,s_{C'})}}\right)^{\mathrm{lcm}(s_C,s_{C'})/s_C}\right)\left(\mathrm{e}^{\frac{-\mathrm{i}N_C(t_1+2\pi m)s_C}{\mathrm{lcm}(s_C,s_{C'})}}\right)^{\mathrm{lcm}(s_C,s_{C'})/s_C} \\ &\quad = p_{C'}\left(\left(\mathrm{e}^{\frac{\mathrm{i}(t_2+2\pi n)s_{C'}}{\mathrm{lcm}(s_C,s_{C'})}}\right)^{\mathrm{lcm}(s_C,s_{C'})/s_{C'}}\right)\left(\mathrm{e}^{\frac{-\mathrm{i}N_{C'}(t_2+2\pi n)s_{C'}}{\mathrm{lcm}(s_C,s_{C'})}}\right)^{\mathrm{lcm}(s_C,s_{C'})/s_{C'}} \end{aligned} \quad (5.35)$$

for some $m = 0, 1, \ldots, \frac{\mathrm{lcm}(s_C,sC')}{s_C} - 1$ and $n = 0, 1, \ldots, \frac{\mathrm{lcm}(s_C,s_{C'})}{s_{C'}} - 1$.

We want again a one-to-one correspondence between crossings and the zeros of a polynomial on the unit circle. We can turn Equation (5.35) in an equation of two polynomials by multiplying both sides by $z^{\mathrm{lcm}(s_C,s_{C'})\max\{N_C/s_C, N_{C'}/s_{C'}\}}$.

Then Equation (5.35) says that there are points $z_1 = e^{i(t_1+2\pi m)s_C/\mathrm{lcm}(s_C,s_{C'})}$ and $z_2 = e^{i(t_2+2\pi m)s_{C'}/\mathrm{lcm}(s_C,s_{C'})}$ where the two polynomials

$$p_C(z^{\mathrm{lcm}(s_C,s_{C'})/s_C})z^{\mathrm{lcm}(s_C,s_{C'})(\max\{N_C/s_C,N_{C'}/s_{C'}\}-N_C/s_C)} \tag{5.36}$$

and

$$p_{C'}(z^{\mathrm{lcm}(s_C,s_{C'})/s_{C'}})z^{\mathrm{lcm}(s_C,s_{C'})(\max\{N_C/s_C,N_{C'}/s_{C'}\}-N_{C'}/s_{C'})} \tag{5.37}$$

agree.

Therefore the common roots of the two polynomials above are in one-to-one correspondence with crossings between strands (C, j) and (C', k) such that there are m, n with

$$\begin{aligned}(t_1 + 2\pi m)s_C/\mathrm{lcm}(s_C, s_{C'}) = (\tfrac{t+2\pi j}{s_C} + 2\pi m)s_C/\mathrm{lcm}(s_C, s_{C'})\\ = (\tfrac{t+2\pi k}{s'_C} + 2\pi n)s_{C'}/\mathrm{lcm}(s_C, s_{C'}) = (t_2 + 2\pi n)s_{C'}/\mathrm{lcm}(s_C, s_{C'}) \bmod 2\pi,\end{aligned} \tag{5.38}$$

which is equivalent to the existence of m, n with

$$j - k = ns_{C'} - ms_C \bmod \mathrm{lcm}(s_C, s_{C'}). \tag{5.39}$$

Such m and n exists if and only if $j - k = 0 \bmod \gcd(s_C, s_{C'})$.

In general this means that the crossings of (C, j) with (C', k) with $j - k = M \bmod \gcd(s_C, s_{C'})$ are in one-to-one correspondence with the points on the unit circle where

$$\begin{aligned}&p_C\left(z^{\mathrm{lcm}(s_C,s_{C'})/s_C}\right)z^{\mathrm{lcm}(s_C,s_{C'})(\max\{N_C/s_C,N_{C'}/s_{C'}\}-N_C/s_C)}\\ =&p_{C'}\left(z^{\mathrm{lcm}(s_C,s_{C'})/s_{C'}}\, e^{-i2\pi\frac{M}{\gcd(s_C,s_{C'})}}\right)z^{\mathrm{lcm}(s_C,s_{C'})(\max\{N_C/s_C,N_{C'}/s_{C'}\}-N_C/s_C)}.\end{aligned} \tag{5.40}$$

The degrees of the polynomials are $\mathrm{lcm}(s_C, s_{C'})(N_C/s_C + \max\{N_C/s_C, N_{C'}/s_{C'}\})$ and $\mathrm{lcm}(s_C, s_{C'})(N_{C'}/s_{C'} + \max\{N_C/s_C, N_{C'}/s_{C'}\})$ respectively. Using $N_C \le s_C\ell/2$ and $N_{C'} \le s_{C'}\ell/2$ there are at most $\ell\mathrm{lcm}(s_C, s_{C'})$ crossings between strands with $j - k = M \bmod \gcd(s_C, s_{C'})$ for each M.

Summing over M from 1 to $\gcd(s_C, s_{C'})$ we get that there are at most

$$\gcd(s_C, s_{C'})\ell\mathrm{lcm}(s_C, s_{C'}) = \ell s_C s_{C'} \tag{5.41}$$

crossings that involve exactly one strand of the component C and one strand of the component C'. Therefore the total number of crossings that involve exactly one strand from the link component C is at most $\ell s_C \sum_{\substack{C'\in\mathscr{C}\\ C'\neq C}} s_{C'} = \ell s_C(s - s_C)$

Thus the total number of data points needed for G_C is at most $(s_C+1)(s_C\ell-1)+\ell s_C(s-s_C)$ and hence the degree of G_C is at most

$$M_C \leq \left\lfloor \frac{(s_C+1)(s_C\ell-1)+\ell s_C(s-s_C)-1}{2} \right\rfloor. \tag{5.42}$$

Thus

$$\begin{aligned} D_C &= \max\{N_C, M_C\} \\ &\leq \max\left\{ \left\lfloor \frac{s_C\ell-1}{2} \right\rfloor, \left\lfloor \frac{(s_C+1)(s_C\ell-1)+\ell s_C(s-s_C)-1}{2} \right\rfloor \right\} \\ &= \left\lfloor \frac{(s_C+1)(s_C\ell-1)+\ell s_C(s-s_C)-1}{2} \right\rfloor, \end{aligned} \tag{5.43}$$

where the last equality holds because s, ℓ and s_C are all positive integers. □

Lemma 5.10. *The degree of f_λ is equal to $\sum_{C\in\mathscr{C}} \max\{D_C, s_C\}$.*

Proof. The polynomial degree of f_λ is equal to the degree of $g_{\lambda a,\lambda b}$, when considered as a polynomial in u, $\mathrm{e}^{\mathrm{i}t}$ and $\mathrm{e}^{-\mathrm{i}t}$. Since $g_{\lambda a,\lambda b}$ is defined as the product of polynomials that one obtains for each component, its degree is the sum of the degrees of its factors

$$g_C(u,t) := \prod_{j=0}^{s_C} \left(u - \lambda a F_C\left(\frac{t+2\pi j}{s_C}\right) - \mathrm{i}\lambda b G_C\left(\frac{t+2\pi j}{s_C}\right)\right). \tag{5.44}$$

The degree with respect to u of the factor corresponding to the component C is s_C. Note that the total degree of a monomial of $g_C(u,t)$ for which the degree with respect to u is k is at most $\frac{D_C}{s_C}(s_C-k)+k$. If $D_C \geq s_C$, then $\frac{D_C}{s_C}(s_C-k)+k \leq D_C + k(1-\frac{D_C}{s_C}) \leq D_C$. If $D_C < s_C$, then $\frac{D_C}{s_C}(s_C-k)+k \leq (s_C-k)+k = s_C$.

Note that there are monomials of degree s_C and D_C respectively, so the degree of g_C is $\max\{s_C, D_C\}$. □

Using the bound we have for D_C, we get:

Proposition 5.11. *The degree of f_λ is bounded above by*

$$\deg(f_\lambda) \leq \sum_{C\in\mathscr{C}} \max\left\{ \left\lfloor \frac{(s_C+1)(s_C\ell-1)+\ell s_C(s-s_C)-1}{2} \right\rfloor, s_C \right\}. \tag{5.45}$$

Note that for knots $|\mathscr{C}| = 1$, $s = s_C$ and hence for non-trivial knots $\deg(f_\lambda) \leq \lfloor \frac{(s+1)(s\ell-1)-1}{2} \rfloor$, since in this case $s \geq 2$ and $\ell \geq 3$.

Also note that the bound given in Proposition 5.11 holds for all semiholomorphic polynomials constructed using the algorithm described in Sections 5.1-5.3, in particular using trigonometric interpolation to find the trigonometric braid parametrisation as described in Section 5.3. Proposition 5.11 is not a statement about the non-existence of polynomials of a certain degree.

We can also give a lower bound for the polynomial degree, which holds for all semiholomorphic polynomials constructed as in Sections 5.1 and 5.2, whether trigonometric interpolation as in Section 5.3 is used or not. For any braid parametrisation of the form (5.3) the degree of the trigonometric polynomials is bounded below in terms of the number of crossings between pairs of strands. Again we can write the trigonometric polynomials as complex polynomials restricted to the unit circle such that crossings of strands correspond to points on the unit circle where the two corresponding polynomials share the same value. As before we have to sum over all possible pairs of strands and obtain the following bound.

Lemma 5.12. *Let C' be the component of the braid B such that the degree $N_{C'}$ of the trigonometric polynomial $F_{C'}$ used to parametrise B as in Equation (5.3) is* $\max\{N_C : C \in \mathscr{C}\}$. *Then*

$$N_{C'} \geq \frac{\ell}{|\mathscr{C}|^2 s_{\widetilde{C}} + |\mathscr{C}|}, \tag{5.46}$$

where ℓ is the length of the braid word (i.e. the number of crossings) and $\widetilde{C}$ is the component such that $s_{\widetilde{C}} = \max\{s_C : C \in \mathscr{C}\}$.

Proof. We only give a sketch of the proof here, since it is the same principle as the proof of Lemma 5.9. In order for the F_C to provide a parametrisation of the x-coordinate of the braid B as in Equation (5.3), each pair of strands has to cross at least a prescribed number of times. The values of $t \in [0, 2\pi]$ where these crossings occur, correspond to points on the unit circle where two complex polynomials agree. This yields a lower bound for the degrees of these polynomials, which are related to the different N_C. □

If the braid closes to a knot, there is only one component, so $N_{C'} \geq \frac{\ell}{s+1}$,

where ℓ is the length of the braid word. Lemma 5.12 implies that

$$\begin{aligned}\deg(f_\lambda) &\geq \max\{s, N_{C'} + s - s_{C'}\} \\ &\geq \max\left\{s, \frac{\ell}{|\mathscr{C}|^2 s_{\widetilde{C}} + |\mathscr{C}|} + s - s_{\widetilde{C}}\right\}. \end{aligned} \tag{5.47}$$

For knots this inequality is $\deg(f_\lambda) \geq \max\{s, (\ell-1)/s\}$.

From the polynomials we have constructed, we find that the bounds given by Lemma 5.12 and Corollary 5.11 are typically not tight bounds [40]. The proofs can explain this, since the degree is determined by the number of data points which in turn is determined by the number of points on the unit circle where two complex polynomials agree. This number is bounded by the degree of these complex polynomials, but of course in general a complex polynomial does not have all of its roots on the unit circle.

We have proven the existence of a semiholomorphic polynomial f of bounded degree, whose zero level set on the unit three-sphere is a given link. Applying the standard stereographic projection

$$u = \frac{x^2 + y^2 + z^2 - 1 + 2\mathrm{i}z}{x^2 + y^2 + z^2 + 1}, \quad v = \frac{2(x + \mathrm{i}y)}{x^2 + y^2 + z^2 + 1} \tag{5.48}$$

to f results in rational function, whose denominator is a constant times some power of $(x^2 + y^2 + z^2 + 1)$. Hence multiplying by the common denominator yields a polynomial $\mathbb{R}^3 \to \mathbb{C}$ in x, y and z, whose zero level set is L. It follows from Lemma 5.7 that the coefficients of this polynomial can be taken to be Gaussian integers. This shows:

Corollary 5.13. *Let B be a braid of length ℓ and let L denote its closure. Let $\mathscr{C}$ denote the set of components of L and let s_C denote the number of strands that the component $C \in \mathscr{C}$ consists of. Then there exist $F_1, F_2 \in \mathbb{Z}[x,y,z]$ such that the vanishing set of (F_1, F_2) over the reals $\{(x,y,z) \in \mathbb{R}^3 : F_1(x,y,z) = F_2(x,y,z) = 0\}$ is ambient isotopic to L. Furthermore*

$$\begin{aligned}&\max\{\deg(F_1), \deg(F_2)\} \leq \\ &\qquad 2\sum_{C\in\mathscr{C}} \max\left\{\left\lfloor \frac{(s_C+1)(s_C\ell - 1) + \ell s_C(s - s_C) - 1}{2}\right\rfloor, s_C\right\},\end{aligned} \tag{5.49}$$

where $s_{\widetilde{C}}$ is the number of strands of the link component $\widetilde{C} \in \mathscr{C}$ that consists of the most strands.

In Section 3 we describe how semiholormophic polynomials with knotted nodal sets can be used for the engineering of knotted physical systems. The

algorithm from Section 5.3 is therefore a way to create initial configurations in physical systems that contain an arbitrary given knot or link. What the term 'initial configuration' means here depends on the physical system in question, but in most examples from Chapter 3 the system comes with an energy functional whose minimization describes the time evolution of the system. We can use the constructed configuration as the starting point of this minimization procedure and study if the knot persists in the stable configuration, the result of the energy minimization process.

The knots in paraxial laser light are static. Here 'initial configuration' means something else. Recall from Section 3 that the optical fields that describe the laser beam are obtained from the construction polynomial, by propagating the evaluation of the polynomial in the $z = 0$-plane (after multiplication by a Gaussian) according to the paraxial wave equation. While in the case of simple torus and lemniscate links this procedure results in optical fields with optical vortices in the shape of the desired link [41], this is in general not the case. It remains an open question what it is exactly that governs whether the propagation results in a field that contains the desired knot.

The fact that the constructed polynomials are semiholomorphic plays an important role in the context of vector fields with knotted flow lines and the Skyrme-Faddeev model. As in Section 3 we can construct a rational map $W : \mathbb{C}^2 \to \mathbb{C} \cup \{\infty\}$ via

$$W(u,v) = \frac{v^\alpha u^\beta}{f(u,v)}, \tag{5.50}$$

where $\alpha, \beta \in \mathbb{Z}$, $\alpha > 0$ and f is the constructed polynomial for a given link L. From this we obtain a Skyrme-Faddeev field $\phi = (\phi_1, \phi_2, \phi_3) : S^3 \to S^2$ by stereographic projection

$$W = \frac{\phi_1 + \mathrm{i}\phi_2}{1 + \phi_3}. \tag{5.51}$$

Note that with this construction $\phi^{-1}(0,0,-1) = L$.

Sutcliffe used Milnor's polynomials $f(u,v) = u^p + v^q$ to construct fields of this form for (p,q)-torus links [129]. These fields are not energy minimizer, but can be taken as an initial ansatz for a recursive energy minimization procedure. Furthermore, Sutcliffe showed that the topological degree of ϕ and hence the Hopf charge Q is equal to $\alpha p + \beta q$. Since $\alpha \in \mathbb{Z}_{>0}$ and $\beta \in \mathbb{Z}$ can be chosen arbitrarily, this gives a construction of Skyrme-Faddeev fields that allows us to control the Hopf charge of the resulting fields.

Sutcliffe's calculation relies on the fact that both the numerator $v^\alpha u^\beta$ and the denominator $u^p - v^q$ of W are holomorphic. Since the degree of ϕ is equal to that of $(v^\alpha u^\beta, u^p - v^q) : \mathbb{B}^4 \subset \mathbb{C}^2 \to \mathbb{C}^2$, the Hopf charge Q is simply the number of preimages of a regular value.

If we mimic Sutcliffe's construction and use the constructed semiholomorphic polynomial $f(u,v)$ as the denominator of W, then Q is still equal to the degree of $(P_1,P_2,P_3,P_4) := (v^\alpha u^\beta, f(u,v)) : \mathbb{B}^4 \to \mathbb{R}^4$, but since f is not holomorphic, it is not enough to count the preimages of a regular value. We have to take the sign of the determinant of the Jacobian at these preimage points into account too.

Proposition 5.14. *If $\beta = 0$, then the topological degree of W and hence the Hopf charge of ϕ is equal to $Q = \alpha \deg_u f = \alpha s$*

Proof. If we choose $\beta = 0$, then the Jacobian at any point has the form

$$\begin{pmatrix} \frac{\partial P_1}{\partial \mathrm{Re}(v)} & \frac{\partial P_1}{\partial \mathrm{Im}(v)} & \frac{\partial P_1}{\partial \mathrm{Re}(u)} & \frac{\partial P_1}{\partial \mathrm{Im}(u)} \\ \frac{\partial P_2}{\partial \mathrm{Re}(v)} & \frac{\partial P_2}{\partial \mathrm{Im}(v)} & \frac{\partial P_2}{\partial \mathrm{Re}(u)} & \frac{\partial P_2}{\partial \mathrm{Im}(u)} \\ \frac{\partial P_3}{\partial \mathrm{Re}(v)} & \frac{\partial P_3}{\partial \mathrm{Im}(v)} & \frac{\partial P_3}{\partial \mathrm{Re}(u)} & \frac{\partial P_3}{\partial \mathrm{Im}(u)} \\ \frac{\partial P_4}{\partial \mathrm{Re}(v)} & \frac{\partial P_4}{\partial \mathrm{Im}(v)} & \frac{\partial P_4}{\partial \mathrm{Re}(u)} & \frac{\partial P_4}{\partial \mathrm{Im}(u)} \end{pmatrix} = \begin{pmatrix} a & -b & 0 & 0 \\ b & a & 0 & 0 \\ \frac{\partial \mathrm{Re}(f)}{\partial \mathrm{Re}(v)} & \frac{\partial \mathrm{Re}(f)}{\partial \mathrm{Im}(v)} & c & -d \\ \frac{\partial \mathrm{Im}(f)}{\partial \mathrm{Re}(v)} & \frac{\partial \mathrm{Im}(f)}{\partial \mathrm{Im}(v)} & d & c \end{pmatrix} \tag{5.52}$$

for some $a,b,c,d \in \mathbb{R}$, since f is holomorphic in u and v^α is holomorphic in v and does not depend on u.

Thus the sign of the determinant of the Jacobian is always positive and Q is equal to the number of preimages of a regular value. Note that, since $f_{\lambda a,\lambda b}(u,\mathrm{e}^{\mathrm{i}t}) = g_{\lambda a,\lambda b}(u,t)$ and the roots of g are distinct, $(1-\varepsilon,0) \in (P_1,P_2,P_3,P_4)(\mathbb{B}^4)$ for some small $\varepsilon > 0$ is a regular values of P if the scaling parameter λ is small enough. The number of its preimages is $\alpha \deg_u f = \alpha s$, where s is the number of strands of the braid that was used to construct f. □

We see that just as in Sutcliffe's construction we have control over the topological degree, i.e. the Hopf charge, by changing the parameter $\alpha \in \mathbb{Z}_{>0}$ or taking different braids with different numbers of strands as the input of the algorithm from Section 5.3.

We still have to check that the field ϕ defined by the rational map W with $\beta = 0$ actually satisfies the boundary condition $\phi(\infty) = (0,0,1)$. This is true because if we use the same projection map as Sutcliffe (Equation 3.22), then (u,v) as a function of (x,y,z) goes to $(1,0)$ as $R = \sqrt{x^2+y^2+z^2}$ goes to infinity. Note that $f(1,0)$ is some complex number, so $W(1,0) = 0$, since $\alpha > 0$.

As in Section 3.4 we can use the rational map W to define a vector field

$$B = \frac{\nabla\overline{W} \times \nabla W}{2\pi i(1 + W\overline{W})^2}, \tag{5.53}$$

which has a flow line in the shape of $W^{-1}(\infty) = L$. Since the Hopf charge $Q = \alpha s$ is equal to the linking number of preimage lines of close regular values and the topological helicity

$$Q(B) = \int A \cdot B d^3 r, \tag{5.54}$$

with $B = \nabla \times A$ is the linking number of close flow lines, we immediately find that $Q(B) = \alpha s$ as well. We have thus a way to construct knotted and linked vector fields with tunable helicity.

5.5 Transverse $\mathbb{C}$-links

Recall from the earlier sections that the semiholomorphic polynomial $f_{a,b}$ resulted from the braid polynomial $g_{a,b}$ by replacing every instance of $\mathrm{e}^{\mathrm{i}t}$ in the polynomial expression of $g_{a,b}$ by the complex variable v and every instance of $\mathrm{e}^{-\mathrm{i}t}$ by the complex conjugate $\overline{v}$. For small enough $\lambda > 0$ the zero level set $f^{-1}_{\lambda a,\lambda b}(0)$ intersects the unit three-sphere transversely in the desired link L.

Before we move on, we should briefly recapitulate what can go wrong if λ is not small enough. For every $r \in [0,1]$ and $t \in [0, 2\pi]$ the s (not necessarily distinct) roots of the complex polynomial $f_{\lambda a,\lambda b}(u, r\,\mathrm{e}^{\mathrm{i}t})$ are denoted by $u_{\lambda,j}(r,t)$ and for every fixed t the roots $(u_{\lambda,j,t}(r), r\,\mathrm{e}^{\mathrm{i}t}) = (u_{\lambda,j}(r,t), r\,\mathrm{e}^{\mathrm{i}t})$ form parametric curves in $\mathbb{C}^2$ parametrised by r. Note that $u_{\lambda,j,t}(r) = \lambda u_{1,j,t}(r)$.

There are three different problems that can occur (cf. Figure 5.4).

- One such curve $(u_{\lambda,j,t}(r), r\,\mathrm{e}^{\mathrm{i}t})$ does not intersect S^3 at all (cf. the remark after Lemma 5.5).
- Both $(u_{\lambda,j,t}(r), r\,\mathrm{e}^{\mathrm{i}t})$ and $(u_{\lambda,k,t}(r), r\,\mathrm{e}^{\mathrm{i}t})$ with j and k distinct intersect S^3, say at values r_1 and r_2, but their u-coordinates intersect each other at a value $r \in [\min\{r_1, r_2\}, 1]$ (cf. Lemma 5.3).
- One curve $(u_{\lambda,j,t}(r), r\,\mathrm{e}^{\mathrm{i}t})$ intersects S^3 more than once (cf. Lemma 5.4 and 5.5).

All of these problems can be resolved by making λ small (cf. Lemma 5.4-5.5).

Now we consider a slightly different construction, where instead of replacing every instance of $\mathrm{e}^{\mathrm{i}t}$ in $g_{a,b}$ by v and every instance of $\mathrm{e}^{-\mathrm{i}t}$ by $\overline{v}$, we replace $e^{\mathrm{i}t}$ by v and $e^{-\mathrm{i}t}$ by $\frac{1}{v}$. We call the resulting function $p_{\lambda a,\lambda b}$. In contrast to $f_{\lambda a,\lambda b}$, the

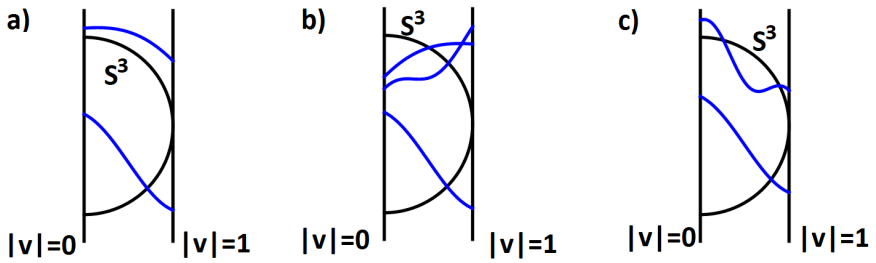

Figure 5.4: 2-dimensional sketches of the three different problems that can arise when λ is not small enough. The vertical lines represent the planes in $\mathbb{C}^2$ where $|v| = 0$ and $|v| = 1$ respectively and a fixed value of $\arg v = t$. The half circle is the intersection of S^3 with $\arg v = t$ for a fixed t. The blue curves show the curves $u_{\lambda,j,t}(r)$. a) One of the curves $u_{\lambda,j,t}(r)$ does not intersect S^3. b) The u-coordinate of two curves coincide between their intersection points with S^3 and with $|v| = 1$. c) One of the curves $u_{\lambda,j,t}(r)$ intersects S^3 multiple times.

function $p_{\lambda a,\lambda b}$ is not a semiholomorphic polynomial, but a rational function, where the denominator is some power of v and its numerator $\widetilde{f}_{\lambda a,\lambda b}$ is a complex plane curve.

The largest power of v and $\overline{v}$ in $f_{a,b}$ is $\sum_{C\in\mathscr{C}}\{D_C\}$ (cf. Lemma 5.10) and the degree of that monomial with respect to u is 0. It follows that $\widetilde{f}_{\lambda a,\lambda b}(u,v) \neq 0$ if $v = 0$ and therefore the zero level set of $\widetilde{f}_{\lambda a,\lambda b}$ is identical to the zero level set of $p_{\lambda a,\lambda b}$. We know that the intersection of the zero level set of $\widetilde{f}_{\lambda a,\lambda b}$ and S^3 is a transverse $\mathbb{C}$-link (or equivalently quasipositive) as long as the intersection is transverse (which it is for appropriate values of λ), since $\widetilde{f}_{\lambda a,\lambda b}$ itself is a complex plane curve. In particular, if we started with the parametrisation of a braid that does not close to a quasipositive link, then $p^{-1}_{\lambda a,\lambda b}(0) \cap S^3$ is not the desired link even when λ is small.

This might be a bit surprising at first, since $p_{\lambda a,\lambda b}$ shares many crucial properties of $f_{\lambda a,\lambda b}$, of which we know that $f^{-1}_{\lambda a,\lambda b}(0) \cap S^3$ is the desired link. For example we have that $p_{\lambda a,\lambda b}(u, e^{it}) = f_{\lambda a,\lambda b}(u, e^{it}) = g_{\lambda a,\lambda b}(u,t)$. Which part of the proof in Section 5.2 is it then that does not work in this setting?

The key observation is that $\widetilde{f}_{\lambda a,\lambda b}(u,0)$ is simply a constant (not depending on u). This means that $|u_{j,1,t}(r)|$ goes to infinity as r goes to zero from above. Thus the third problem above can not be resolved by choosing λ small enough. In fact, for small enough λ and every t and j the curve $u_{j,\lambda,t}(r)$ intersects S^3 in exactly two points, one very close to $r = 1$ and one close to $r = 0$ (cf. Figure 5.5). Thus the link $\widetilde{f}^{-1}_{\lambda a,\lambda b}(0) \cap S^3$ is the union of two links L_1 (the intersection points near $r = 1$) and L_0 (the intersection points near $r = 0$).

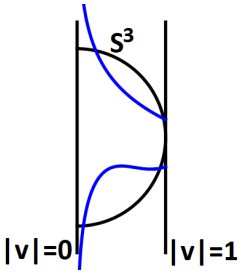

Figure 5.5: The u-coordinates of the roots of $\widetilde{f}_{a,b}(u, re^{it})$ go to infinity as r goes to zero.

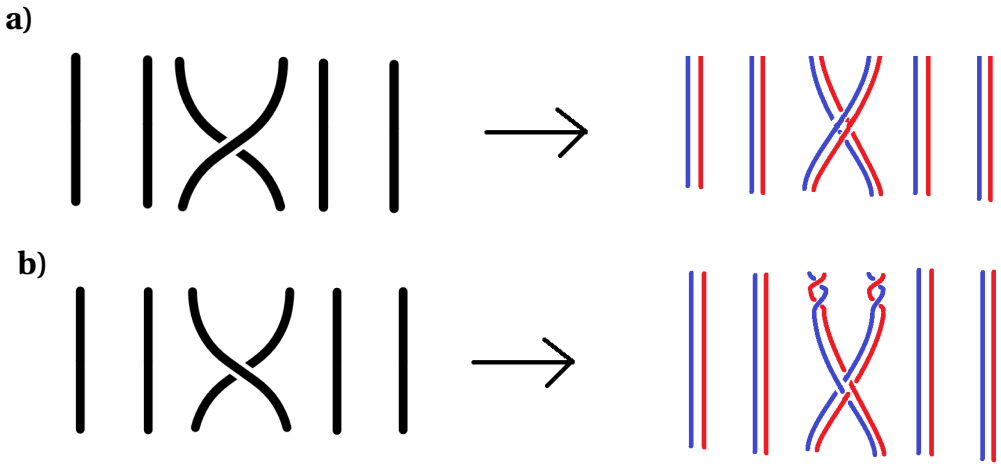

Figure 5.6: Construction of a quasipositive braid whose closure contains the closure of a given braid B as a sublink. a) The generator σ_i is sent to the quasipositive word $\sigma_{2i}\sigma_{2i-1}\sigma_{2i+1}\sigma_{2i}$. b) The generator σ_i^{-1} is sent to the quasipositive word $\sigma_{2i}\sigma_{2i-1}^{-1}\sigma_{2i+1}^{-1}\sigma_{2i}\sigma_{2i+1}\sigma_{2i-1}\sigma_{2i+1}\sigma_{2i-1}$.

Everything else in the proof in Section 5.2 still holds, which means that L_1 is the desired link, the closure of the braid whose parametrisation we started with. We have thus shown the following results.

Theorem 5.15. *For every link L there exists a complex plane curve $\widetilde{f} : \mathbb{C}^2 \to \mathbb{C}$ such that L is a sublink of the link formed by the transverse intersection of $\widetilde{f}^{-1}(0)$ and the unit three-sphere S^3.*

Corollary 5.16. *For every link L there exists a quasipositive link $\widetilde{L}$ such that L is a sublink of $\widetilde{L}$.*

This corollary follows from Theorem 5.15, since by Boileau and Orevkov [25] $f^{-1}(0) \cap S^3$ is a quasipositive link for every complex plane curve f (Theorem 2.22).

From discussions with Peter Feller [51] it has become clear that Corollary 5.16 is known to some mathematicians from the following considerations. Starting with a braid that closes to the desired link L, we can define a new braid on twice the number of strands by sending σ_i to $\sigma_{2i}\sigma_{2i+1}\sigma_{2i-1}\sigma_{2i}$ and sending σ_i^{-1} to $\sigma_{2i}\sigma_{2i-1}^{-1}\sigma_{2i+1}^{-1}\sigma_{2i}\sigma_{2i+1}\sigma_{2i-1}\sigma_{2i+1}\sigma_{2i-1}$.

Figure 5.6 depicts the new braid that is obtained from the old by drawing a parallel copy next to each strand, changing some signs of crossings that involve one strand from the original braid and one from the parallel copy and introducing some twists between the two copies. Note that both $\sigma_{2i}\sigma_{2i+1}\sigma_{2i-1}\sigma_{2i}$ and $\sigma_{2i}\sigma_{2i-1}^{-1}\sigma_{2i+1}^{-1}\sigma_{2i}\sigma_{2i+1}\sigma_{2i-1}\sigma_{2i+1}\sigma_{2i-1}$ are quasipositive, so the new braid is quasipositive. Furthermore, the closure of the new link has twice as many components as L and since the crossings that were changed are between the two copies, the new link consists of two copies of L that may be linked in some non-trivial way.

Theorem 5.15 and Corollary 5.16 give an explicit construction of the complex plane curve corresponding to the quasipositive link $\widetilde{L}$ containing L, but also offer a concrete description of how L is linked with the rest of $\widetilde{L}$ (or with the notation of above how L_1 links with L_0). For small λ the link L_1 lies in a tubular neighbourhood of $|v| = 1$ in S^3 and L_0 lies in a tubular neighbourhood of $|u| = 1$ in S^3. Therefore L_1 and L_0 each lie inside a solid torus and these two tori form a Hopf link.

Note that this is very different from Feller's illustration. In our construction, we know exactly how L_1 links with L_0, but we do not know a priori what link type L_0 has. On the other hand, in Feller's construction $\widetilde{L}$ consists of two copies of L, but how these two copies are linked is more complicated and depends on the original braid representative.

Corollary 5.11 gives a bound on the degree of the semiholomorphic polynomial f in terms of the number of strands s and the number of crossings ℓ of the parametrised braid. Since the relevant steps of the construction of $\widetilde{f}$ are identical to those in the construction of f, these imply the following result.

Theorem 5.17. *Let B be a braid on s strands with ℓ crossings and let L be its closure. Then there exists a complex plane curve $\widetilde{f} : \mathbb{C}^2 \to \mathbb{C}$ such that L is a sublink of the link formed by the transverse intersection of $f^{-1}(0)$ and the unit three-sphere S^3, $\deg_u \widetilde{f} = s$,*

$$\deg_v \widetilde{f} \leq \sum_{C \in \mathscr{C}} \left\lfloor \frac{(s_C + 1)(\ell s_C - 1) + \ell s_C (s - s_C)}{2} \right\rfloor, \tag{5.55}$$

and

$$\deg \widetilde{f} \leq \sum_{C\in\mathscr{C}} \max\left\{\left\lfloor \frac{(s_C+1)(\ell s_C-1)+\ell s_C(s-s_C)}{2}\right\rfloor, s_C\right\} \tag{5.56}$$

where as usual $\mathscr{C}$ denotes the set of components of L and for every $C\in\mathscr{C}$ the number of strands that C consists of is denoted by s_C.

Example: Consider the figure-eight knot, the closure of the braid $\sigma_1\sigma_2^{-1}\sigma_1\sigma_2^{-1}$ parametrised by

$$\bigcup_{j=1}^{3}\left(\cos\left(\frac{2t+2\pi j}{3}\right), \sin\left(\frac{2(2t+2\pi j)}{3}\right), t\right), \qquad t\in[0,2\pi]. \tag{5.57}$$

Note that the figure-eight knot is not quasipositive [119]. The corresponding braid polynomial is as in Chapter 4

$$\begin{aligned} g_{a,b}(u,t) &= \prod_{j=1}^{3}\left(u - a\cos\left(\frac{2t+2\pi j}{3}\right) - \mathrm{i}b\sin\left(\frac{2(2t+2\pi j)}{3}\right)\right)\\ &= u^3 + \frac{1}{4}u(-3a^2+3b^2-3ab(\mathrm{e}^{2\mathrm{i}t}-\mathrm{e}^{-2\mathrm{i}t}))\\ &+ \frac{1}{8}((-a^3-3ab^2)(\mathrm{e}^{2\mathrm{i}t}+\mathrm{e}^{-2\mathrm{i}t}) - b^3(\mathrm{e}^{4\mathrm{i}t}-\mathrm{e}^{-4\mathrm{i}t})). \end{aligned} \tag{5.58}$$

Replacing each $\mathrm{e}^{\mathrm{i}t}$ by v and every $\mathrm{e}^{-\mathrm{i}t}$ by $\frac{1}{v}$ we obtain

$$\begin{aligned} p_{a,b}(u,v) &= u^3 + \frac{1}{4}u(-3a^2+3b^2-3ab(v^2-\frac{1}{v^2})) + \frac{1}{8}((-a^3-3ab^2)(v^2+\frac{1}{v^2})\\ &- b^3(v^4-\frac{1}{v^4})\\ &= \frac{1}{8v^4}\left(8u^3v^4 + 2u((-3a^2+3b^2)v^4 - 3ab(v^6-v^2))\right.\\ &\left.+ (-a^3-3ab^2)(v^6+v^2) - b^3(v^8-1)\right). \end{aligned} \tag{5.59}$$

Therefore

$$\widetilde{f_{a,b}}(u,v) = (8u^3v^4+2u((-3a^2+3b^2)v^4-3ab(v^6-v^2))+(-a^3-3ab^2)(v^6+v^2)-b^3(v^8-1). \tag{5.60}$$

Figure 5.7 shows the zero level set of $\widetilde{f_{1/4,1/4}}$ on the unit three-sphere after projecting it into $\mathbb{R}^3$. One component is the figure-eight knot. The other components lie close to the z-axis and close near the point at infinity. Note that the number of strands of the components that are not the figure-eight knot (in this case 4) could be larger than the number of strands of the constructed knot (in this case 3).

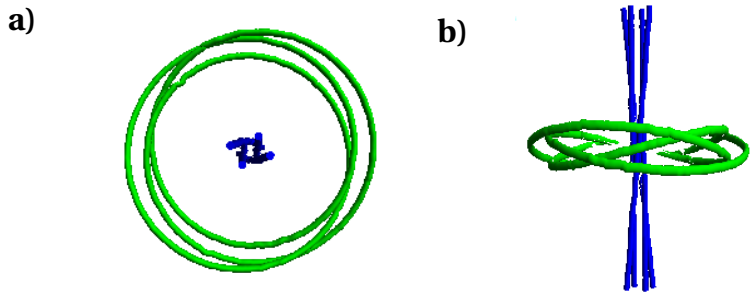

Figure 5.7: The zero level set of the complex plane curve $\widetilde{f}_{1/4,1/4}$ on the unit three-sphere projected into $\mathbb{R}^3$. The figure-eight knot (in green) lies in a solid torus around the unit circle in the $z = 0$-plane. The other components (in blue) lie close to the z-axis. a) Downwards view along the z-axis. b) View along the y-axis.

On the level of braid words we can easily see that while $\sigma_1\sigma_2^{-1}\sigma_1\sigma_2^{-1}$ is not quasipositive, the braid word

$$\sigma_5\sigma_6^{-1}\sigma_5\sigma_6^{-1}\prod_{j=4}^{6}\sigma_j\prod_{j=3}^{5}\sigma_j\prod_{j=2}^{4}\sigma_j\prod_{j=1}^{3}\sigma_j\sigma_6 \tag{5.61}$$

closes to a quasipositive link, one of whose components is the figure-eight knot, the closure of $\sigma_1\sigma_2^{-1}\sigma_1\sigma_2^{-1}$.

Recall from Section 3.1 that there is an electromagnetic field satisfying Maxwell's equation with a stable optical vortex link L for every transverse $\mathbb{C}$-link L. Theorem 5.15 therefore shows that every link can be realised as the sublink of a stable optical vortex link. Furthermore, we have an explicit construction of the complex plane curve $\widetilde{f}$ and therefore of the electromagnetic field as in Section 3.1.

We should however stress that the electromagnetic fields that we construct in this way should not be expected to be monochromatic, a shortcoming that they share with the fields of de Klerck et al [39]. Hence an experimental realisation of these fields with laser light as in [41] is not possible.

5.6 Discussion

We have shown that every link can be constructed as the transverse intersection of the vanishing set of a semiholomorphic polynomial $f : \mathbb{C}^2 \to \mathbb{C}$ and the unit three-sphere S^3. This polynomial can be found algorithmically using a braid

word of the desired link as an input and finding a trigonometric parametrisation for that braid by trigonometric interpolation.

This means that the degree of the resulting polynomials can be bounded by the number of data points used in this interpolation, which is in turn related to numbers associated with the braid word, such as the number of crossings or the number of strands.

The algorithmic construction allows us to create knotted initial conditions for the wide range of physical systems discussed in Chapter 3. It is an interesting question how our algorithm compares to the numerical Biot-Savart approach.

The data points that are needed for the trigonometric interpolation for F_C can be obtained in a number of steps that grows linearly with the length of the braid word and the number of strands. The complexity of trigonometric interpolation itself is also linear. The data points for G_C correspond to crossings of the strands parametrised by F_C, which are solutions to certain trigonometric equations. Note that the Biot-Savart integral requires a knotted parametric curve as an input, so we could use the interpolation of Section 5.3.

Once we have found the parametrisation it seems like our polynomial approach is much simpler than the Biot-Savart integral. It is important to note though that the step from g to f, expansion of the product and cancellation of terms of the form $\mathrm{e}^{\mathrm{i}t}\,\mathrm{e}^{-\mathrm{i}t}$, while on a mathematical level straightforward, requires a certain amount of computing, since the number of factors is n^s, where n is the sum of the number of terms in F_C and the number of terms in G_C plus 1. Therefore the bounds on the degrees of F_C and G_C are also important to guarantee that this step in the algorithm does not take too long. It also illustrates that finding parametrisations that have few trigonometric terms is desirable for computational purposes.

For any r-periodic braid B^r we can find a parametrisation of B as in Section 5.3 and then multiply each occurrence of t by r to obtain a parametrisation of B^r. Since this typically results in fewer trigonometric terms than extracting data points from B^r directly, it becomes desirable to use braid words as an input that are powers of very short and ideally symmetric braid words.

In general, finding braid representatives that lead to optimal parametrisations is still an open problem.

Apart from numerical complexity, our method has two decisive advantages when compared with the Biot-Savart integral. Firstly, we have a way to control the Hopf charge of the constructed fields in the Skyrme-Faddeev model

and similarly the helicity of constructed vector fields. Secondly, our method can be extended to holomorphic functions, which is a necessary condition in the construction of vortex knots in electromagnetic fields satisfying Maxwell's equations.

This holomorphicity comes at the price of additional components in the intersection of the vanishing set with S^3. More concretely, we have a way to construct every link as the sublink of the transverse intersection of a complex plane curve with S^3 and similar bounds on the degree as in the semiholomorphic case hold.

6 Fibrations of knot complements

From the previous chapter we have for every link L a semiholomorphic polynomial $f : \mathbb{C}^2 \to \mathbb{C}$ such that $f^{-1}(0) \cap S^3 = L$. Thus restricting f to $S^3 \backslash L$ and taking its argument $\arg f$ gives a smooth map from $S^3 \backslash L$ to S^1.

It is now a natural question whether this map is a fibration. Recall that by the Ehresmann fibration theorem this corresponds to $\arg f$ having no critical points. By definition this can only happen if L is a fibred link.

In this chapter we first show in Section 6.1 how properties of the braid are related to the number of critical points one encounters when applying the construction from the previous section to certain braid parametrisations. In particular, we show that if L is the closure of a homogeneous braid B, then there is a braid that closes to L and can be parametrised in such a way that the argument $\arg g$ of the corresponding braid polynomial g does not have any critical points.

We then show in Section 6.2 that for low values of the scaling parameter λ the argument $\arg f_{\lambda a, \lambda a}|_{S^3 \backslash L}$ has the same number of critical points as $\arg g_{\lambda a, \lambda b}$, yielding a fibration $\arg f_{\lambda a, \lambda b} : S^3 \backslash L \to S^1$ for closures of homogeneous braids. The results from Sections 6.1 and 6.2 were originally shown in [23] and [22].

In Section 6.3 we illustrate in more detail what happens if $\arg f$ has critical points by studying the example of the three-twist knot 5_2, the simplest unfibred knot, following [40].

The process of finding trigonometric braid parametrisations that result in fibrations can be also be used to define braid invariants that generalise the permutation representation of the braid group, which could lead to a new topological approach to the word and conjugacy problem in braid groups. This is discussed in Section 6.4

6.1 Lifted braid parametrisations

In Chapters 4 and 5 we encountered two methods of finding trigonometric braid parametrisations. The first one is driven by geometric investigation and intuition, is not algorithmic and therefore often very tedious. It does however typically result in very few trigonometric terms with low orders.

The construction presented in Section 5.3 is algorithmic and easily implementable. While the degree is bounded in terms of the number of strands and crossings of the braid, the resulting parametrisations are typically more complicated than the ones found from the first method. With a view towards applications both methods are in some way aiming to give a parametrisation that is as simple as possible in terms of the number of trigonometric terms.

In this section we show another way to find trigonometric braid parametrisations that is not very practical, but we can use this procedure to show that braid parametrisations with certain properties exist. The aim of this method is to minimize the number of critical points of the argument $\arg g$ of the braid polynomial g corresponding to the constructed parametrisation. The number of terms however can get arbitrarily large.

Recall from Chapter 2 the definition of a homogeneous braid, a braid on s strands where every generator $\sigma_1, \ldots, \sigma_{s-1}$ appears at least once in its braid word, either with a positive or a negative sign and whenever it appears it carries the same sign.

Lemma 6.1. *Let B be a homogeneous braid. Then there exists a braid B' closing to the same link as B and a trigonometric parametrisation of B' as in Equation (5.3) such that the corresponding g does not have any phase-critical points.*

Before we begin with the proof of the lemma, we need some background on the critical values of polynomials. There is a one-to-one correspondence between unordered s-tuples of distinct complex numbers and monic complex polynomials in $\mathbb{C}[u]$ with simple roots that sends $(z_1, z_2, \ldots, z_s)$ to $\prod_{j=1}^{s}(u-z_j)$. This turns the s distinct complex numbers into the s distinct roots of the resulting polynomial. This is of course the underlying idea of the construction of the braid polynomial g, where to a cyclic 1-parameter family of s-tuples of complex numbers $X_j(t) + \mathrm{i}Y_j(t)$ we associate a family of complex polynomials $g(u,t)$ with roots given by the parametric curves.

In this chapter we are interested in critical points of the argument $\arg g$, which makes it necessary to think of different ways to interpret relations between braids and complex polynomials.

Suppose $\arg g_{a,b}(u,t)$ has a critical point at (u_*,t_*), i.e.

$$\left(\frac{\partial \arg g_{a,b}}{\partial \mathrm{Re}(u)}(u_*,t_*), \frac{\partial \arg g_{a,b}}{\partial \mathrm{Im}(u)}(u_*,t_*), \frac{\partial \arg g_{a,b}}{\partial t}(u_*,t_*)\right) = (0,0,0). \tag{6.1}$$

We find that

$$\begin{aligned}\frac{\partial \arg g_{a,b}}{\partial \mathrm{Re}(u)} &= \mathrm{Im}\frac{\partial}{\partial \mathrm{Re}(u)}\mathrm{Log}\, g_{a,b} = \mathrm{Im}\frac{1}{g_{a,b}}\frac{\partial g_{a,b}}{\partial \mathrm{Re}(u)} \\ &= \mathrm{Im}\frac{1}{|g_{a,b}|^2}\frac{\overline{g_{a,b}}\partial g_{a,b}}{\partial \mathrm{Re}(u)} = \frac{1}{|g_{a,b}|^2}\left(\mathrm{Re}(g_{a,b})\frac{\partial \mathrm{Im}\, g_{a,b}}{\partial \mathrm{Re}(u)} - \mathrm{Im}\,(g_{a,b})\frac{\partial \mathrm{Re}\, g_{a,b}}{\partial \mathrm{Re}(u)}\right).\end{aligned} \tag{6.2}$$

Note that this is well-defined since $g_{a,b}(u_*,t_*) \neq 0$. Similarly for $\frac{\partial \arg g_{a,b}}{\partial \mathrm{Im}(u)}$ we get $\frac{1}{|g_{a,b}|^2}\left(\mathrm{Re}(g_{a,b})\frac{\partial \mathrm{Im}\, g_{a,b}}{\partial \mathrm{Im}(u)} - \mathrm{Im}(g_{a,b})\frac{\partial \mathrm{Re}\, g_{a,b}}{\partial \mathrm{Im}(u)}\right)$. Since $g_{a,b}(u_*,t_*) \neq 0$, we can assume that $\mathrm{Re}(g_{a,b}(u_*,t_*)) \neq 0$ or $\mathrm{Im}(g_{a,b}(u_*,t_*)) \neq 0$. In either case, Equation (6.1) implies a linear relation between $\frac{\partial g_{a,b}(u_*,t_*)}{\partial \mathrm{Re}(u)}$ and $\frac{\partial g_{a,b}(u_*,t_*)}{\partial \mathrm{Im}(u)}$, but since $g_{a,b}$ is a complex polynomial in u, the Cauchy-Riemann equations imply that $\frac{\partial g_{a,b}}{\partial u}(u_*,t_*) = 0$.

If we denote by $c_j(t)$, $j = 1,2,\ldots,s-1$ the complex roots of $\frac{\partial g_{a,b}(u,t)}{\partial u}$, then (u_*,t_*) is a critical point of $\arg g_{a,b}$ if and only if there is a $j \in \{1,2,\ldots,s-1\}$ such that $u_* = c_j(t_*)$ and

$$\frac{\mathrm{d}\ \arg g_{a,b}(c_j(t))}{\mathrm{d}t} = 0. \tag{6.3}$$

The geometric interpretation of this equation is as follows. The roots $c_j(t)$ of $\frac{\partial g_{a,b}}{\partial u}$ form $s-1$ curves in $\mathbb{C}\times[0,2\pi]$. Evaluating $g_{a,b}$ on these curves $c_j(t)$ gives $s-1$ parametric curves $g_{a,b}(c_j(t),t)$ in $\mathbb{C}\times[0,2\pi]$. Note that since $g_{a,b}(u,t)$ only has simple roots for each t, we have $g_{a,b}(c_j(t),t) \neq 0$ for all $t \in [0,2\pi]$ and $j \in \{1,2,\ldots,s-1\}$. Thus as t increases from 0 to 2π, the points $c_j(t)$ move in the complex plane, always avoiding zero. Equation (6.3) picks out the points at which one of these curves changes its orientation at which it twists around zero. For each t the points $g_{a,b}(c_j(t),t)$ are called the *critical values* of $g_{a,b}(\bullet,t)$.

Note that if we require $g_{a,b}(\bullet,t)$ to have $s-1$ distinct critical values, then the union of the $s-1$ curves $g_{a,b}(c_j(t),t)$ and $(0,t)$ form a braid in $\mathbb{C}\times[0,2\pi]$. It turns out that there is a topological connection between the braid type of this braid of critical values with the zero line and the braid that is formed by the roots of $g_{a,b}$.

We define

$$\begin{aligned}\tilde{V}_s = \{p \in \mathbb{C}[u] : &p \text{ is monic, of degree } s,\ p(0) = 0 \text{ and has } s-1 \text{ distinct critical} \\ &\text{values, all of which are not equal to zero}\}\end{aligned} \tag{6.4}$$

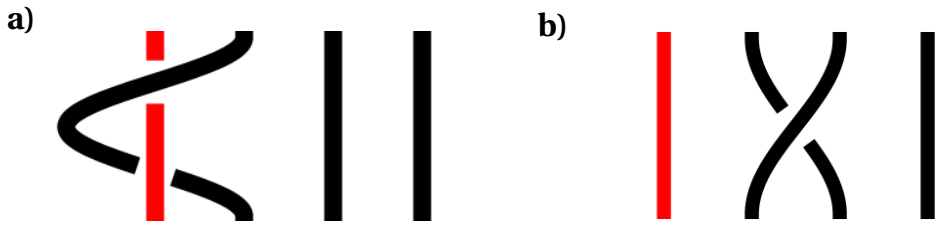

Figure 6.1: The generators of the affine braid group. a) The generator $A = \sigma_1^2$. b) One of the standard braid group generators σ_2.

and

$$W_s = \{(v_1, v_2, \ldots, v_{s-1}) \in (\mathbb{C}\backslash\{0\})^{s-1} : v_i \neq v_j \text{ for all } i \neq j\}/S_{s-1}, \tag{6.5}$$

where S_{s-1} is the symmetric group on $s-1$ elements.

The following theorem is due to Beardon, Carne and Ng [11].

Theorem 6.2. *[11] The map $\tilde{\phi} : \tilde{V}_s \to W_s$ that sends a polynomial $p \in \tilde{V}_s$ to its set of critical values is a covering map of degree s^{s-1}.*

The space $\tilde{V}_s$ is a bit too small for our purposes. We work instead with

$$\begin{aligned} V_s = \{p \in \mathbb{C}[u] : & p \text{ is monic, of degree } s \text{ and has } s-1 \text{ distinct critical values} \\ & \text{none of which are equal to zero or the constant term of } p\}. \end{aligned} \tag{6.6}$$

Theorem 6.3. *The map $\phi : V_s \to W_s$ that sends a polynomial $p \in V_s$ to its set of critical values is a fibration.*

Proof. This theorem is a straightforward extension of Theorem 6.2. We only have to note that for a given set of critical values $(v_1, v_2, \ldots, v_{s-1}) \in W_s$ the polynomials with constant term $c \neq v_i$ for all i that have $(v_1, v_2, \ldots, v_{s-1})$ as critical values are given by the s^{s-1} polynomials $p_j + c$, where p_j, $j = 1, 2, \ldots, s^{s-1}$, are the polynomials in $\tilde{V}_s$ with $\tilde{\phi}(p_j) = (v_1 - c, v_2 - c, \ldots, v_{s-1} - c)$. □

It follows that the fibre over each point in W_s is $s^{s-1} \times \{\mathbb{C}\backslash\{s-1 \text{ points}\}\}$.

Note that the fundamental group of W_s is the affine braid group AB_s [107], which is a subgroup of the braid group B_s and consists precisely of those braids, that can be parametrised in such a way that the first strand is stationary (say at 0). The group AB_s is generated by the standard Artin generators σ_i for $i > 2$ and

$A = \sigma_1^2$, shown in Figure 6.1, instead of σ_1 modulo the relations

$$\begin{aligned} \sigma_i\sigma_j &= \sigma_j\sigma_i && \text{if } |i-j|>1, \\ \sigma_i\sigma_{i+1}\sigma_i &= \sigma_{i+1}\sigma_i\sigma_{i+1} && \text{for all } 1<i<s-1, \\ \sigma_i A &= A\sigma_i && \text{if } i>2, \\ \sigma_2 A\sigma_2 A &= A\sigma_2 A\sigma_2. \end{aligned} \tag{6.7}$$

Therefore a loop γ in W_s is a closed braid on s strands, one of which is given by $(0,0,t)$, $t \in [0,2\pi]$. By Theorem 6.2 there are paths $\tilde{\gamma}$ in V_s whose image under ϕ is the loop γ. If a path $\tilde{\gamma}$ is actually a loop in $\tilde{V}_s$, we can interpret $\tilde{\gamma}$ as a closed braid on s strands by considering the complex roots of the cyclic 1-parameter family of polynomials $\tilde{\gamma}(t)$. We will see that there is a certain topological relation between the braid corresponding to γ and the braid that corresponds to one of its lifts $\tilde{\gamma}$.

Consider a monic complex polynomial $g \in \mathbb{C}[u]$, $g(u) = \prod_{j=1}^{s}(u-u_j)$ with simple real roots $u_j \in \mathbb{R}$. Then the roots c_j of $\frac{\partial g}{\partial u}$, the critical points of g, are all real too and there is exactly one critical point between each pair of neighbouring roots as in Figure 6.2a). We label the roots u_j and the critical points c_j from small to large values, so that the critical point c_j lies between u_j and u_{j+1}. Since all roots are real, the image of the real line under g is again real (half the real line if the polynomial degree s is odd and all of it if s is even) and in particular the critical values $v_j = g(c_j)$ of g are real. Figure 6.2a) shows the roots u_j of g, its critical points c_j and its critical values v_j. We also highlighted the other $s-2$ points that g maps to v_j. We will think of this picture as the situation at an initial time $t = 0$.

Consider a loop $\gamma_j : S^1 \to \mathbb{C}\backslash\{v_1, v_2, \ldots, v_{s-1}\}$ as in the bottom half of Figure 6.2b) that starts at 0, then follows the real line avoiding all critical values by tracing out a small half circle around the critical value until it reaches the critical value v_j. It encircles v_j with a small radius and then travels back exactly the way it came.

Since every polynomial g is itself a branched covering map from $\mathbb{C}$ to $\mathbb{C}$, where the branching set is the set of critical values, there are s paths in the complex plane that g maps to γ_j, all of which start at a root u_i and end at a (potentially different) root $u_{i'}$. Since all the points on γ_j apart from those in a neighbourhood of a critical value are real, it is not too hard to figure out what the lifts of γ_j should be.

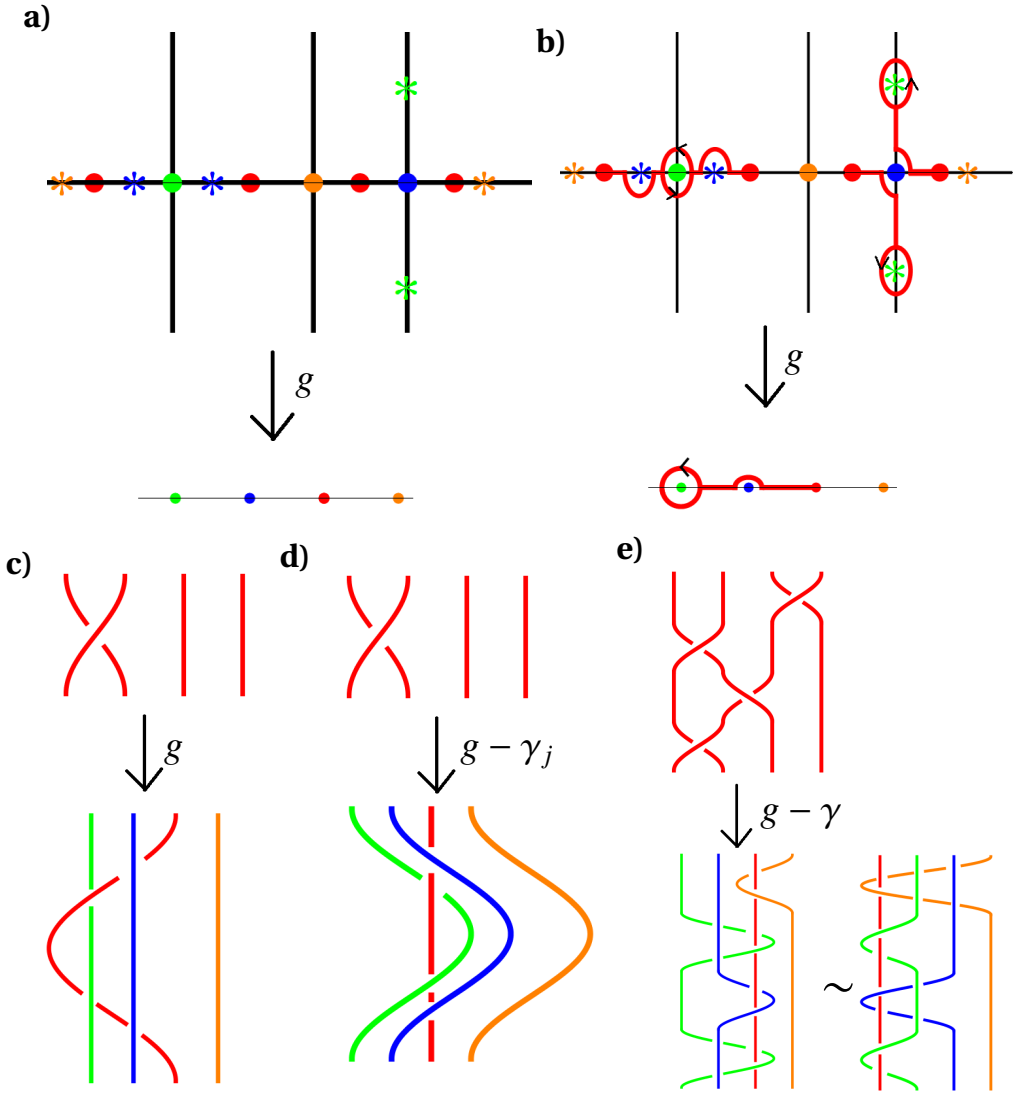

Figure 6.2: The lifting of a loop in W_s to a braid. a) The roots (red), critical points (points that are not red) and other preimage points of critical values (stars in the colour of the critical point that has the same image) of a polynomial g mapped by the polynomial to 0 and the set of critical values. b) The loop γ_j with basepoint 0, lifts to several paths that start and end at roots. c) The loop γ_j lifts to paths that form the braid σ_j. d) The loop γ_j can be interpreted as the braid formed of the critical values of $g - \gamma_j$ and the zero strand. e) The loop downstairs lifts to a braid $B = \prod_{i=1}^{n} \sigma_{j_i}^{\epsilon_i}$ and is conjugate to $\prod_{i=1}^{n} X_{j_i}^{\epsilon_i}$.

Consider first the lifted path $\tilde{\gamma}_j$ that starts at a root u_i with $i \notin \{j, j+1\}$. Recall that j is defined by the critical value v_j that γ_j encircles. The lifted path $\tilde{\gamma}_j$ has to follow the real line until it reaches a preimage point x of a critical value (which is not necessarily a critical point). Since γ_j is avoiding all critical values, its lifts must avoid every one of their preimage points x by going around them in a small half-circle if x is not a critical point and in a small circle-arc if x is a critical point. In the latter case $\tilde{\gamma}_j$ does not continue on the real line, but on one of the other lines that form the preimage of the real line under g.

The lift $\tilde{\gamma}_j$ continues like this avoiding all preimage points of critical values until it reaches a preimage point x of v_j, the critical value that γ_j encircles. Note that x is not the critical point c_j and hence no critical point at all, but $g(c_j) = g(x)$. The lift $\tilde{\gamma}_j$ must encircle x and then, like γ_j, travel back exactly the way that it came. This is the lifted path starting at a root that is not u_j or u_{j+1}.

Now we study what the lifted paths look like that start at u_j or u_{j+1}. Again the paths have to follow the real line, both moving towards the critical point c_j and avoiding other preimage points of critical values. Then they both reach c_j. Since it is one of the branch points, the circle that γ_j forms around v_j lifts only to a half circle, so that both lifted paths return to the real line at the point where the other lifted path left it. After encircling v_j the path γ_j travels back the way it came, so now each of the two lifted paths travels back the way the other lifted path came, so that the lifted path that started at u_j ends at u_{j+1} and vice versa.

Note that the union of the lifted paths form a braid B on s strands and it is easy to see that it is σ_j or σ_j^{-1}, where the sign depends on the clockwise or anti-clockwise direction in which γ_j encircles v_j. If $\gamma : S^1 \to \mathbb{C}$ is now a loop that is the concatenation of n γ_{j_i}s and $\gamma_{j_i}^{-1}$s, i.e. $\gamma(\frac{t+2\pi i}{n}) = \gamma_{j_i}^{\epsilon_i}(t)$ for all $i \in \{0, 1, \ldots, n-1\}$ and some $\epsilon_i \in \{\pm 1\}$, then the corresponding lift forms the braid $B = \prod_{i=1}^{n} \sigma_{j_i}^{\epsilon_i}$.

Since the braid B gets mapped to γ by g, it is the vanishing set of $g - \gamma(t)$. The critical values of the cyclic family of polynomials $g - \gamma(t)$ are $v_i - \gamma(t)$. These curves together with the zero strand $(0, t)$ form another braid on s strands. It can be seen as a loop in W_s. Earlier we only stated that each γ_j should avoid all critical values that it encounters on its way to v_j by going in a small half-circle around each of them. For each v_i and γ_j we can choose whether this half-circle lies in the upper or lower half-plane. We can make these choices such that deforming the closed loop as in Figure 6.2c)-e), corresponding to a homotopy (from c) to d)) and a conjugation (in AB_s) of the loop (cf. e)), gives the braid word B' that can be found from $B = \prod_{i=1}^{n} \sigma_{j_i}^{\epsilon_i}$ as follows.

Let

$$\begin{aligned} A_{1,1} &= A = \sigma_1^2 \\ A_{j,1} &= (\sigma_{j-1}\sigma_{j-2}\dots\sigma_2)\sigma_1^2(\sigma_{j-1}\sigma_{j-2}\dots\sigma_2)^{-1}, \qquad \text{if } j>1 \end{aligned} \tag{6.8}$$

which corresponds to the jth strand passing behind the strands $j-1$, $j-2$ and so on, encircling the first strand and going back the way that it came. Furthermore let

$$X_j = \begin{cases} A_{\frac{j+1}{2},1} & \text{if } j \text{ is odd} \\ A_{\frac{j}{2}+\lfloor\frac{s}{2}\rfloor,1} & \text{if } j \text{ is even.} \end{cases} \tag{6.9}$$

Then the braid that is formed by the critical values of $g-\gamma(t)$ and the zero-axis can be arranged to be isotopic to a conjugate of $\prod_{i=1}^n X_{j_i}^{\epsilon_i}$. Note that the roots of $g-\gamma$ form the braid $B=\prod_{i=1}^n \sigma_{j_i}^{\epsilon_i}$, so there is indeed a very easy relation between the braid of critical values and the braid of roots of the same cyclic family of polynomials.

This is inspired by works of Rudolph [117] and nicely illustrated for positive braids in [120], where he claims that instead of $\prod_{i=1}^n X_{j_i}^{\epsilon_i}$, we could have used $\prod_{i=1}^n A_{j_i,1}^{\epsilon_i}$.

Theorem 6.3 is important because it means that we can use the Homotopy Lifting Property. It says that any homotopy of a loop in W_s lifts to a homotopy for any of its preimages under ϕ. Furthermore, conjugate loops in W_s lift to conjugate paths. Note that a homotopy of $(v_1-\gamma(t),\dots,v_{s-1}-\gamma(t))$ is a braid isotopy of the braid formed by the union of $\cup_{i=1}^{s-1}(v_i-\gamma(t),t)\subset\mathbb{C}\times[0,2\pi]$ and the zero strand $(0,t)\subset\mathbb{C}\times[0,2\pi]$ that does not move the zero strand.

Conjugating the loop $v_i-\gamma(t)$ and applying the homotopy that sends it to $\prod_{i=1}^n X_{j_i}^{\epsilon_i}$ therefore lifts to a homotopy of a conjugate of $g-\gamma(t)$. This lifted homotopy is a homotopy of a conjugate of the loop $g-\gamma(t)$ in V_s and therefore a conjugate of an isotopy of the closed braid that is formed by the roots of $g-\gamma(t)$. In particular, the resulting braid closes to the same link. In other words, the link type of the closure of the lifted braid does not depend on the actual parametrisation $(v_1-\gamma(t),v_2-\gamma(t),\dots,v_{s-1}-\gamma(t))$, but only on the braid type $\prod_{i=1}^n X_{j_i}^{\epsilon_i}$. We have shown that every conjugate of $\prod_{i=1}^n X_{j_i}^{\epsilon_i}$ as a loop in W_s lifts to a loop in V_s, whose roots form the braid that closes to the same link as $B=\prod_{i=1}^n \sigma_{j_i}^{\epsilon_i}$.

Recall that our goal is to find a trigonometric parametrisation of the braid B such that the argument of the corresponding braid polynomial $\arg g$ has as few critical points as possible. In order to prove Lemma 6.1 we need to find a

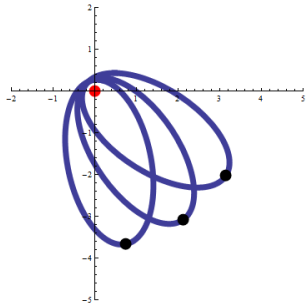

Figure 6.3: The strands of $\prod_{i=1}^{n} X_{j_i}^{\epsilon_i}$ can be parametrised in such a way that they move on ellipses around zero.

parametrisation $(v_1(t), v_2(t), \ldots, v_{s-1}(t))$ of the braid $\prod_{i=1}^{n} X_{j_i}^{\epsilon_i}$ such that $\frac{\partial \arg v_i(t)}{\partial t} \neq 0$ for all $i \in \{1, 2, \ldots, s-1\}$ and all $t \in [0, 2\pi]$.

Proof of Lemma 6.1. Let $B = \prod_{i=1}^{n} \sigma_{j_i}^{\epsilon_{j_i}}$ be a homogeneous braid. Any parametrisation $(v_1(t), v_2(t), \ldots, v_{s-1}(t))$ of a conjugate of $\prod_{i=1}^{n} X_{j_i}^{\epsilon_i}$ lifts to paths in V_s, each of which corresponds to a 1-parameter family of complex polynomials whose critical values are $(v_1(t), v_2(t), \ldots, v_{s-1}(t))$. One of these paths is actually a loop and the roots of the corresponding family of polynomials form a braid that closes to the same link as B. It is therefore sufficient to find a parametrisation $(v_1(t), v_2(t), \ldots, v_{s-1}(t))$ of a conjugate $\prod_{i=1}^{n} X_{j_i}^{\epsilon_i}$ where $\frac{\partial \arg v_j}{\partial t}$ never vanishes.

As in Figure 6.2e) we can find a parametrisation for $X_{j_i}^{\epsilon_i}$ by only moving the critical value v_{j_i} and leaving all other strands fixed. If we let v_{j_i} move on an ellipse with one of the focal points equal to 0 as in Figure 6.3, then $\frac{\partial \arg v_{j_i}(t)}{\partial t} \neq 0$. The parametrisation of $\prod_{i=1}^{n} X_{j_i}^{\epsilon_i}$ is then the concatenation of the parametrisations of the X_{j_i}. At any given time in this parametrisation only one v_{j_i} is moving on an ellipse around 0 and all other critical values are stationary. We can arrange the $s-1$ ellipses as in Figure 6.3 such that if the strands move on the ellipses, they form the braid $\prod_{i=1}^{n} X_{j_i}^{\epsilon_i}$.

We only have to adjust this parametrisation very slightly to get rid of all points with $\frac{\partial \arg v_j(t)}{\partial t} = 0$. Since B is homogeneous, every critical value $v_j(t)$ moves on its ellipse and never changes direction. Before, only one of the critical values was moving at any given time, while the others remained in their positions. We now reparametrise $v_j(t)$ such that all of them are always in motion. In the same time that one of them moves across almost its entire ellipse, the others only move a small $\epsilon > 0$ on theirs. This is clearly sufficient to guarantee that $\frac{\partial \arg v_j(t)}{\partial t} \neq 0$ for all j and t and by the reasoning from before there is a cyclic

1-parameter family of complex polynomials $g(u,t)$ whose critical values are $v_j(t)$ and whose roots form a braid that closes to the same link as B.

Let $u_i(t)$, $i = 1,2,\dots,s$ be the roots of $g(\bullet,t)$. Note that since the parametrisation of $v_j(t)$ is smooth for every j, so are the functions $u_j(t)$. For each link component C of the closure of B this gives two smooth real functions $F_C : [0,2\pi] \to \mathbb{R}$, $F_C\left(\frac{t+2\pi j}{s_C}\right) = \mathrm{Re}(u_j(t))$, $G_C : [0,2\pi] \to \mathbb{R}$ and $G_C\left(\frac{t+2\pi j}{s_C}\right) = \mathrm{Im}(u_j(t))$ with $F_C(0) = F_C(2\pi)$ and $G_C(0) = G_C(2\pi)$.

We cannot expect these functions to be trigonometric polynomials, but since trigonometric polynomials are dense in the set of 2π-periodic C^1-functions with respect to the C^1-metric, we can approximate F_C and G_C by trigonometric polynomials $\tilde{F}_C$ and $\tilde{G}_C$ such that for all $\epsilon > 0$ we have $\max\{|F_C(t) - \tilde{F}_C(t)|, |F'_C(t) - \tilde{F}'_C(t)|\} < \epsilon$, where $F'_C(t) = \frac{\partial F_C(t)}{\partial t}$ and similarly for G_C.

This implies that $X_{C,j}(t) + \mathrm{i}Y_{C,j}(t)$ given by $X_{C,j}(t) = \tilde{F}_C\left(\frac{t+2\pi j}{s_C}\right)$ and $Y_{C,j}(t) = \tilde{G}_C\left(\frac{t+2\pi j}{s_C}\right)$ are the roots of cyclic 1-parameter family of complex polynomials $g(u,t) = \prod_{j=1}^{s}\left(u - X_{C,j}(t) - \mathrm{i}Y_{C,j}(t)\right)$ with critical values $\tilde{v}_j(t)$ such that $\max\{|v_j(t) - \tilde{v}_j(t)|, |v'_j(t) - \tilde{v}'_j(t)|\} < \tilde{\epsilon}$ for some $\tilde{\epsilon} > 0$ that can be made arbitrarily small by choosing ϵ in the trigonometric approximation arbitrarily small.

It follows that the roots of the corresponding polynomials $g(u,t)$ form a braid that closes to the same link as B and $\frac{\partial \arg v_j(t)}{\partial t} \neq 0$ for all j and t. Therefore $\arg g$ does not have any critical points. □

Lemma 6.1 is in fact the special case of a more general result. Let $B = \sigma_{i_1}^{\varepsilon_{i_1}}\sigma_{i_2}^{\varepsilon_{i_2}}\dots\sigma_{i_\ell}^{\varepsilon_{i_\ell}}$ and let $\beta(B)$ denote

$$\begin{aligned}\beta(B) = \sum_{i=1}^{s-1} \Big|\{j \in \{1,2,\dots,\ell-1\} : \exists\, k \in \{0,1,\dots,\ell-2\} \text{ s.t. } i_j = i_{1+(j+k) \bmod \ell},\\ i_{1+(j+m) \bmod \ell} \neq i_j \text{ for all } m < k \text{ and } \varepsilon_{i_j}\varepsilon_{i_{1+(j+k) \bmod \ell}} = -1\}\Big|\\ + 2\Big|\{j \in \{1,2,\dots,s-1\} : \text{ There is no } k \text{ s.t. } i_k = j\}\Big|. \qquad (6.10)\end{aligned}$$

If for each $i = 1,2,\dots,s-1$ we list the σ_is and σ_i^{-1}s as they appear in the braid word of B, then the first term of $\beta(B)$ counts the number of times that a change of sign occurs, i.e. the number of times that a σ_i is followed by σ_i^{-1} or vice versa. This sum is considering the closed braid, so if the last appearance of $\sigma_i^{\pm 1}$ has a different sign from its first appearance in the braid word, this is counted as well.

The second term in the definition of $\beta(B)$ counts the number of generators that do not appear in the braid word, neither with a positive nor with a negative sign.

Take for example $B = \sigma_1\sigma_3\sigma_1\sigma_3^{-1}$. All σ_1s appear with the same sign, so they do not contribute to the first term in $\beta(B)$. The generator σ_3 appears with a positive sign as the second letter and after that with a negative sign in fourth position. We thus have to change the sign. Considering B as a closed braid, we see that the next time that $\sigma_3^{\pm 1}$ appears after the fourth letter is σ_3 as the second letter in the word, which means that we have to change the sign again. Therefore the first term of $\beta(B)$ is 2. Since σ_2 does not appear in the braid word, it contributed to the second term in $\beta(B)$. If we consider B as a braid on 4 strands, it is the only generator that does not appear with either sign and so $\beta(B) = 2 + 2 = 4$.

Note that for any homogeneous braid B, it is $\beta(B) = 0$. The β-value measures in some sense how far a braid is from being homogeneous.

Lemma 6.4. *Let B be a braid. Then there exists a trigonometric parametrisation as in Equation (5.3) such that the corresponding g has exactly $\beta(B)$ phase-critical points.*

The proof of Lemma 6.4 is identical to the proof of Lemma 6.1. Similarly to Lemma 6.1 we can find a parametrisation of the critical values, such that all of them move on ellipses. The turning points of $\arg v_i(t)$ then correspond to an occurrence of σ_i^{-1} in the braid word after σ_i or the other way around. For generators σ_i that do not appear at all in the braid we have to parametrise v_i such that they move only an $\epsilon > 0$ in one direction on their ellipse and then move back to their original position. This leads to two turning points.

Having chosen the parametrisation of the braid formed by the critical values such that the second derivatives of the parametric curves do not vanish at the $\beta(B)$ many turning points guarantees that the trigonometric approximation results in a trigonometric parametrisation of B that leads to a map g with exactly $\beta(B)$ phase-critical points.

We would like to emphasize again that the number of critical points of $g_{\lambda a,\lambda b}$ does not depend on $\lambda > 0$. Hence Lemma 6.4 really states the existence of a whole family of braid polynomials $g_{\lambda,\lambda}$ with $\beta(B)$ phase-critical points.

6.2 Existence of fibrations

In this section we show that for small λ the function $\arg f_{\lambda a,\lambda b} : S^3\backslash L \to S^1$ behaves in many ways like the function $\arg g_{a,b} : (\mathbb{C}\times S^1)\backslash B \to S^1$. In particular,

they have the same number of critical points. The philosophy behind this is similar to the proof of Theorem 5.1. For small λ the 'interesting' parts of the function $\arg f_{\lambda a,\lambda b}$ lie close to the set $\{0\}\times S^1 \subset \mathbb{C}^2$. This region however is close to $\mathbb{C}\times S^1$, where $f_{\lambda a,\lambda b}(u,\mathrm{e}^{\mathrm{i}t})$ is equal to $g_{\lambda a,\lambda b}(u,t)$ and therefore shares a lot of its properties due to continuity.

Lemma 6.5. *Suppose that* $\arg g_{a,b}$ *has* n *critical points on* $(\mathbb{C}\times[0,2\pi])\backslash B$*, all of which have multiplicity one. Then there is an* $\epsilon>0$ *such that for all* $0<\lambda<\epsilon$ *the number of critical points of* $\arg f_{\lambda a,\lambda b}$ *on* $S^3\backslash f^{-1}_{\lambda a,\lambda b}(0)$ *is* n *and they all have multiplicity one.*

Proof. We can assume that λ is small enough such that $f^{-1}_{a,b}(0)\cap S^3$ is the closure of B. It is important to note that the number of argument-critical points of $g_{\lambda a,\lambda b}$ does not depend on λ, so $\arg g_{\lambda a,\lambda b}$ has n critical points for all values of $\lambda=0$.

First assume that $n=0$.

Note that the derivative $\partial\arg(f_{a,b})/\partial\arg(u)$ converges uniformly to s on $\{(u,v)\in\mathbb{C}^2 : |u|=R, |v|\le 1\}$ as $R\to\infty$. In particular, for some $R>0$,

$$\partial\arg(f_{a,b})/\partial\arg(u)>0 \tag{6.11}$$

when evaluated at all $(u,\ v)\in\mathbb{C}^2$ with $|v|\le 1$ and $|u|>R$. This means that for $f_{\lambda a,\lambda b}$ with $\lambda>0$ the same statement holds for all $|u|>\lambda R$.

Let (λ_1,λ_2) be a unit-vector in $\mathbb{R}^2$. We know that if $v=\mathrm{e}^{\mathrm{i}t}$, then

$$\frac{\partial\arg f_{a,b}(u,\mathrm{e}^{\mathrm{i}t})}{\partial t}=\frac{\partial\arg g_{a,b}(u,t)}{\partial t}=0 \tag{6.12}$$

and the vanishing of the derivative in the direction $w=\lambda_1\mathrm{Re}(u)+\lambda_2\mathrm{Im}(u)$,

$$\begin{aligned}\nabla_w\arg f_{a,b}(u,\mathrm{e}^{\mathrm{i}t}) &= \lambda_1\frac{\partial\arg f_{a,b}(u,\mathrm{e}^{\mathrm{i}t})}{\partial\mathrm{Re}(u)}+\lambda_2\frac{\partial\arg f_{a,b}(u,\mathrm{e}^{\mathrm{i}t})}{\partial\mathrm{Im}(u)}\\ &= \lambda_1\frac{\partial\arg g_{a,b}(u,t)}{\partial\mathrm{Re}(u)}+\lambda_2\frac{\partial\arg g_{a,b}(u,t)}{\partial\mathrm{Im}(u)}=0,\end{aligned} \tag{6.13}$$

imply that the derivative in the direction $w'=\lambda_2\mathrm{Re}(u)-\lambda_1\mathrm{Im}(u)$ does not vanish:

$$\begin{aligned}\nabla_{w'}\arg f_{a,b}(u,\mathrm{e}^{\mathrm{i}t}) &= \lambda_2\frac{\partial\arg f_{a,b}(u,\mathrm{e}^{\mathrm{i}t})}{\partial\mathrm{Re}(u)}-\lambda_1\frac{\partial\arg f_{a,b}(u,\mathrm{e}^{\mathrm{i}t})}{\partial\mathrm{Im}(u)}\\ &= \lambda_2\frac{\partial\arg g_{a,b}(u,\mathrm{e}^{\mathrm{i}t})}{\partial\mathrm{Re}(u)}-\lambda_1\frac{\partial\arg g_{a,b}(u,\mathrm{e}^{\mathrm{i}t})}{\partial\mathrm{Im}(u)}\neq 0.\end{aligned} \tag{6.14}$$

The vector $w'=\lambda_2\mathrm{Re}(u)-\lambda_1\mathrm{Im}(u)$ is orthogonal to w in the complex plane.

It follows from continuity of $\arg f_{a,b}$ and compactness of $\{(u, e^{it}) : u \in \mathbb{C}, |u| \leq R, t \in [0, 2\pi]\}$ and S^1 that there are $\epsilon_1 > 0$ and $\epsilon_2 > 0$ (independent of (λ_1, λ_2)) such that if

$$\frac{\partial \arg f_{a,b}(u,v)}{\partial t} = 0 \tag{6.15}$$

and

$$\nabla_w \arg f_{a,b}(u,v) = 0, \tag{6.16}$$

then

$$\nabla_{\tilde{w}} \arg f_{a,b}(u,v) \neq 0, \tag{6.17}$$

for all (u, v) with $|u| \leq R$, $0 < 1 - |v| < \epsilon_1$ and all $|w' - \tilde{w}| < \epsilon_2$. This last inequality should be interpreted as the Euclidean distance between two vectors in $\mathbb{R}^4$. Using $(\mathrm{Re}(u), \mathrm{Im}(u), \mathrm{Re}(v), \mathrm{Im}(v))$ as a basis for $\mathbb{R}^4$ the vector w' has a third and fourth component equal to zero. As above $\nabla_{\tilde{w}}$ denotes the derivative in direction $\tilde{w}$.

Similarly, if

$$\frac{\partial \arg f_{\lambda a,\lambda b}(u,v)}{\partial t} = 0 \tag{6.18}$$

and

$$\nabla_w \arg f_{\lambda a,\lambda b}(u,v) = 0, \tag{6.19}$$

then

$$\nabla_{\tilde{w}} \arg f_{\lambda a,\lambda b}(u,v) \neq 0, \tag{6.20}$$

for all $0 < \lambda \leq 1$, (u, v) with $|u| \leq \lambda R$, $0 < 1 - |v| < \epsilon_1$ and all $|w' - \tilde{w}| < \epsilon_2$. Note in particular that ϵ_1 and ϵ_2 do not depend on λ.

Furthermore, there is an $\epsilon_3 > 0$ such that at every point $(u, v) \in \{(u, v) \in S^3 : |v| \geq 1 - \epsilon_3\}$ on the unit three-sphere the tangent space of S^3 at (u, v), $v \neq 0$ is spanned by $\frac{\partial}{\partial \arg u}$, $\frac{\partial}{\partial \arg v}$ and a third vector $\frac{\partial}{\partial \tilde{w}}$ with $|w' - \tilde{w}| < \epsilon_2$, where $w' = (\mathrm{Re}(u), \mathrm{Im}(u), 0, 0) \in \mathbb{R}^4$ is orthogonal to $\arg u$ in the complex plane. The value of ϵ_3 clearly does not depend on λ either.

This means that for all $\lambda \in (0, 1]$ the map $\arg f_{\lambda a,\lambda b}$ does not have any critical points on $S^3 \cap \{(u, v) \in \mathbb{C}^2 : 0 < 1 - |v| < \min\{\epsilon_1, \epsilon_3\}\}$, either by Equation (6.11) if $|u| > \lambda R$ or by Equation (6.20) if $|u| \leq \lambda R$.

Note that since λ is only a scaling in the u-coordinate as in the proof of Theorem 5.1 we can choose λ small enough such that if (u, v) is a point on the unit three-sphere and $|v| < 1 - \min\{\epsilon_1, \epsilon_3\}$, we have $|u| > \lambda R$. This is achieved as long as $\lambda^2 R^2 + (1 - \min\{\epsilon_1, \epsilon_3\}) < 1$. Thus if λ is small enough, then $\nabla_{S^3} \arg f_{\lambda a,\lambda b}(u, v) \neq (0, 0, 0)$ for all $(u, v) \in S^3$ with $|v| \leq 1 - \min\{\epsilon_1, \epsilon_3\}$.

Therefore $\arg f_{\lambda a,\lambda b}$ does not have any critical points on the unit three-sphere and is hence a fibration of the link complement $S^3 \setminus f^{-1}_{\lambda a,\lambda b}(0)$ if λ is chosen sufficiently small.

Now we turn to the more general case where $\arg g_{a,b}$ has $n > 0$ critical points. Without loss of generality we can assume that none of the critical points has a u-coordinate equal to zero. Otherwise we can work with $g_{a,b}(u - c, t)$ with some $c \in \mathbb{C}$ of small modulus such that $(u, t) \mapsto \arg g_{a,b}(u - c, t)$ has exactly n critical points and none of them has a u-coordinate equal to zero. The fact that they all have multiplicity one means that the matrix of second derivatives is invertible.

Thus we can apply the Implicit Function Theorem to $F : \mathbb{R}_{>0} \times [0, 2\pi] \times [0, 2\pi] \times \mathbb{R}_{>0} \times \mathbb{R} \to \mathbb{R}^3$ given by

$$F(|u|, \arg u, t, r, \mu) := \left(\frac{\partial \arg f_{a,b}}{\partial \arg u}(u, r\,\mathrm{e}^{\mathrm{i}t}), r\frac{\partial \arg f_{a,b}}{\partial |u|}(u, r\,\mathrm{e}^{\mathrm{i}t}) - \mu\frac{\partial \arg f_{a,b}}{\partial r}, \frac{\partial \arg f_{a,b}}{\partial r}(u, r\,\mathrm{e}^{\mathrm{i}t}) \right) \tag{6.21}$$

as a function of $|u|$, $\arg u$, t, r and μ.

Thus there is an $\epsilon_1 > 0$ and an open set $V \subset \mathbb{C} \times S^1$ containing the u- and t-coordinates of the critical points of $\arg g_{a,b}$ such that the u- and t-coordinates of the zeros of $F(\bullet, \bullet, \bullet, r, \mu)$ are unique for every r and μ as long as $0 < 1 - r < \epsilon_1$ and $0 < \mu < \epsilon_1$ and are continuously differentiable functions of r and μ as long as $0 < 1 - r < \epsilon_1$ and $0 < \mu < \epsilon_1$.

Consider now the function

$$\tilde{F}(|u|, \arg u, t, r) := \left(\frac{\partial \arg f_{a,b}}{\partial \arg u}(u, r\,\mathrm{e}^{\mathrm{i}t}), r\frac{\partial \arg f_{a,b}}{\partial |u|}(u, r\,\mathrm{e}^{\mathrm{i}t}) - \sqrt{1 - r^2}\frac{\partial \arg f_{a,b}}{\partial r}, \frac{\partial \arg f_{a,b}}{\partial r}(u, r\,\mathrm{e}^{\mathrm{i}t}) \right). \tag{6.22}$$

Then the u- and t-coordinates of the zeros of this function are unique for every choice of r and are continuous functions of r on $[1-\epsilon_1, 1]$ and continuously differentiable on $[1 - \epsilon_1, 1)$.

Again we can introduce λ as a scaling parameter in the u-coordinate and analogously to the proof of Theorem 5.1 we can show that for small enough λ each of these n continuously differentiable curves in $V \times [1-\epsilon_1, 1) \subset \mathbb{C}^2$ intersects the unit three-sphere $S^3 \subset \mathbb{C}^2$ in a unique point. Note that if $(\lambda u, v) \in S^3$, then $\tilde{F}(|u|/\lambda, \arg u, t, r) = (0, 0, 0)$ if and only if $\nabla_{S^3} \arg f_{\lambda a,\lambda b}(u, r\,\mathrm{e}^{\mathrm{i}t}) = (0, 0, 0)$. Thus on $V \times [1 - \epsilon_1, 1]$ there are exactly n zeros of $\nabla_{S^3} \arg f_{\lambda a,\lambda b}$.

On $\mathbb{C}^2 \setminus (V \times [1 - \epsilon_1, 1])$ the same arguments as in the $n = 0$-case show that $\arg f_{\lambda a,\lambda b}$ does not have any critical points on the intersection of S^3 with this

set if λ is small enough. Thus the total number of critical points (with respect to S^3) of $\arg f$ on S^3 is n and by the Constant Rank Theorem they all still have multiplicity one. □

The special case of $n = 0$ gives the following Corollary.

Corollary 6.6. *If $g_{a,b}$ is such that $\arg g_{a,b} : (\mathbb{C} \times [0, 2\pi])\backslash B \to S^1$ is a fibration, then $\arg f_{\lambda a,\lambda b} : S^3\backslash L \to S^1$ is a fibration as long as $\lambda > 0$ is small enough.*

Combining the lemmas from this and the previous section implies the following result.

Theorem 6.7. *Let B be a braid on s strands and L be its closure. Then there exists a semiholomorphic polynomial $f : \mathbb{C}^2 \to \mathbb{C}$ s.t. $\deg_u f = s$, $f^{-1}(0) \cap S^3 = L$ and $\arg(f)|_{S^3}$ has $\beta(B)$ many critical points of multiplicity one.*

Proof. By Lemma 6.5 there exists a trigonometric parametrisation of B such that the corresponding $\arg g$ has $\beta(B)$ many critical points of multiplicity one. Then Lemma 6.5 shows that there exists a semiholomorphic polynomial $f = f_{\lambda,\lambda}$ for small enough $\lambda > 0$ with the desired properties. □

The $n = 0$-case directly implies the following.

Corollary 6.8. *Let B be a homogeneous braid on s strands and L be its closure. Then L is fibred and there exists a semiholomorphic polynomial $f : \mathbb{C}^2 \to \mathbb{C}$ s.t. $\deg_u f = s$, $f^{-1}(0) \cap S^3 = L$ and $\arg(f) : S^3\backslash L \to S^1$ is a fibration.*

Stallings [128] already showed that closures of homogeneous braids are fibred. Corollary 6.8 specifies this by providing a certain form of the fibration map, namely the argument of a semiholomorphic polynomial.

Let f be as in Theorem 6.7. Then it can be arranged that $\arg(f)$ is a smooth circle-valued Morse function on $S^3\backslash L$. Such a function is called *regular* if there is a diffeomorphism φ of the union of $|\mathscr{C}|$ solid tori, such that the composition of φ and $\arg(f)$ applied to a tubular neighbourhood of the link is just the projection map $L \times (\mathring{D}\backslash\{0\}) \to S^1 : (x, y) \mapsto y/|y|$. Since $\arg(f)$ is the argument of a semiholomorphic polynomial, it is regular.

The Morse-Novikov number $\mathcal{MN}(L)$ of a link L is the minimal number of critical points of all smooth, regular circle-valued Morse functions [110]. Thus $\mathcal{MN}(L) = 0$ if and only if L is fibred and we can think of $\mathcal{MN}(L)$ as a measure of how far L is from being fibred.

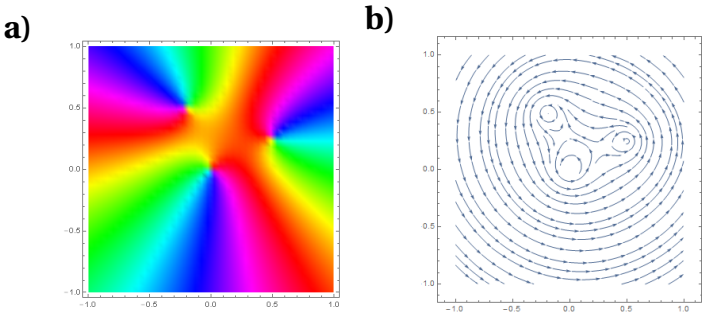

Figure 6.4: The magnetic field induced by electric currents through vertical wires is the gradient of the argument of a complex polynomial. a) The argument of a complex polynomial with three distinct roots. b) The corresponding gradient field with vortices in the position of the roots.

The discussion above and Theorem 6.7 then implies the next corollary.

Corollary 6.9. *Let B be a braid that closes to a link L. Then*

$$\mathcal{MN}(L) \leq \beta(B). \tag{6.23}$$

We should point out that this bound is a strict inequality for some knots. For example the knot 8_{20} is known to be fibred and has thus $\mathcal{MN}(L)$ equal to zero. However, it is not the closure of a homogeneous braid and hence $\beta(B) > 0$ for all braids B that close to 8_{20} [12].

We now briefly return to the question brought up in Chapter 3, namely whether for any fibred knot K there exists a parametrisation of K such that the magnetic field that is induced by a constant electric current through K vanishes nowhere. We do not have a formal proof for this, but the following should be considered as a small indication that at least for closures of homogeneous braids this could be the case.

For s parallel wires, say $(\mathrm{Re}(u_i), \mathrm{Im}(u_i), z)$, $i = 1, 2, \ldots, s$, the magnetic field induced by a constant current in the plane of constant z is for each z exactly the gradient field of $\arg(\prod_i u - u_i)$ (cf. Figure 6.4). The z-component of the magnetic field is zero everywhere. We know from Lemma 6.1 that for homogeneous braids, we can parametrise the s strands $u_i(t)$ in such a way that $\arg(\prod_i u - u_i(t))$ is a fibration.

Embedding the closed braid in $\mathbb{R}^3$ as $(R + \mathrm{Re}(u_i(t)), t, \mathrm{Im}(u_i(t)))$, $i = 1, 2, \ldots, s$ in cylindrical coordinates (r, ϕ, z) with large $R \in \mathbb{R}$ results in an embedding of K that induces a magnetic field that in some solid torus is a good approximation of the embedding of the vector field $\nabla \arg \prod_{i=1}^{s}(u - u_i(t))$. One of the radii of the torus is R and the other is determined by $\max_{t\in[0,2\pi],i}\{|u_i(t)|\}$.

Since the vector field $\nabla \arg \prod_{i=1}^{s}(u-u_i(t))$ does not vanish, the magnetic field does not vanish inside the solid torus either. Similarly, there is a solid torus around the z-axis, on which the induced magnetic field vanishes only at infinity. If these two solid tori cover S^3, this parametrisation of the knot indeed results in a magnetic field that is the gradient field of a fibration. However, proving that this condition is met in general remains challenging.

6.3 The three-twist knot 5_2

In this section we use the simplest non-fibred knot, the three-twist knot 5_2, as an example of the construction of an unfibred knot. As such the function $\arg f_{\lambda a,\lambda b}$ must have critical points. We investigate where these occur and how the topology of the Seifert surfaces changes at these points.

The knot 5_2 is the closure of the braid $w=\sigma_2^{-1}\sigma_1\sigma_2^3\sigma_1$. In Section 4.2 we used trigonometric interpolation to find a Fourier parametrisation of degree 8 for the braid $\sigma_1\sigma_2^{-1}\sigma_1\sigma_2^3$, which obviously closes to the same knot. It turns out that there is a simpler parametrisation [40], given by

$$\begin{aligned}(X_j(t),Y_j(t),t)=\Big(&-\cos\Big(\frac{2(t+2\pi j)}{3}\Big)-\frac{3}{4}\cos\Big(\frac{5(t+2\pi j)}{3}\Big),\\ &-\frac{1}{2}\sin\Big(\frac{t+2\pi j}{3}\Big)-\sin\Big(\frac{4(t+2\pi j)}{3}\Big),t\Big).\end{aligned}\tag{6.24}$$

Applying the later steps of the algorithm to this parametrisation results in the following polynomials for the knot 5_2

$$\begin{aligned}g_{a,a}(u,t)=&\frac{1}{256}\{256u^3-12a^2u\{5+8\cos(t)+4\mathrm{i}[4\sin(t)+11\sin(2t)+6\sin(3t)]\}\\ &+a^3\{192+372\cos(t)+256\cos(2t)+144\cos(3t)+108\cos(4t)+27\cos(5t)\\ &2\mathrm{i}[188\sin(t)+102\sin(2t)-21\sin(3t)-32\sin(4t)]\}\},\\ f_{a,a}(u,v)=&\frac{1}{256}[256u^3+12a^2u(12v^3-12\overline{v}^3+22v^2-22\overline{v}^2+4v12\overline{v}-5)\\ &+\frac{1}{2}a^3(384+27v^5+27\overline{v}^5+44v^4+172\overline{v}^4+102v^3+186\overline{v}^3\\ &+460v^2+52\overline{v}^2+748v-4\overline{v})].\end{aligned}\tag{6.25}$$

For $a=1$ the nodal set of $f_{a,a}$ on the unit three-sphere is a 3-component unlink, but as the value of a decreases the nodal set undergoes several reconnections and for $a=0.4$ we obtain the desired knot 5_2.

Since 5_2 is not fibred, the map $\arg f : S^3\backslash 5_2 \to S^1$ must have critical points. We are now going to investigate what exactly happens at these critical points.

For every regular value $\chi \in S^1$ of $\arg f$ the preimage $(\arg f)^{-1}(\chi)$ is an orientable 2-manifold whose boundary is the knot 5_2 and hence by definition a Seifert surface of a certain genus g. Varying χ continuously does not change g and hence does not change the homeomorphism type of the Seifert surface unless we pass through a critical value.

For a critical value its preimage is not necessarily a manifold, since it contains a critical point. By the arguments of Lemma 6.5 the positions of the critical points of $\arg g : (\mathbb{C} \times S^1) \backslash B_{5_2} \to S^1$ can help us to find good approximations of the positions of the critical points of $\arg f$.

We first find the solutions to $\frac{\partial g_{1/4,1/4}}{\partial u} = 0$. Since g is a polynomial of degree 3 in u, we obtain two solutions $c_{1,2}(t)$ parametrised by $0 \leq t \leq 2\pi$. The argument of $g_{1/4,1/4}$ evaluated on these curves is shown in Figure 6.5. We see that there are six minima or maxima at $t = t_i$, $i = 1, 2, \ldots, 6$.

This means that for small λ we have 6 critical points of $\arg f_\lambda$ located approximately at $(\frac{\lambda}{4} c_{1,2}(t_i), \sqrt{1 - \frac{\lambda^2}{16}|u_\pm(t_i)|^2})\, \mathrm{e}^{\mathrm{i}t_i}) \in S^3$. Note that the Morse-Novikov number of 5_2 is 2, so while the parametrisation has only very few terms and low degree, it is not optimal with respect to the number of its argument-critical points.

Recall from Chapter 3 that if we use f_λ to construct knotted fields, the critical points of $\arg f_\lambda$ have physical meaning, for example as stagnation points of superfluids or as point defects in liquid crystals in the smectic A phase. Finding the extrema of $\arg g_\lambda(c_j(t), t)$ and hence the approximate positions of the critical points of $\arg f_\lambda$ can help us to locate the stagnation points or point defects in the constructed knotted fields.

Plots of the preimages of the critical value at χ_{crit} and of two close regular values are shown in Figure 6.5b)-e). We can see that for values slightly below χ_{crit} the preimages are Seifert surfaces. Two parts of the surface approach the critical point as we increase χ towards χ_{crit}. At $\chi = \chi_{\text{crit}}$ the two parts meet at the critical point resulting in a double-cone around the critical point. Increasing χ further makes the double cone split into two parts that move away from the critical point in a direction almost orthogonal to the direction in which the two parts were approaching the critical point earlier. Since the rest of the surface remains unchanged (unless there are other critical points), this process changes the genus of the surface.

Since g is a polynomial in u, there is another interpretation of the critical points of $\arg g$. We have discussed the critical braid earlier, the braid that is

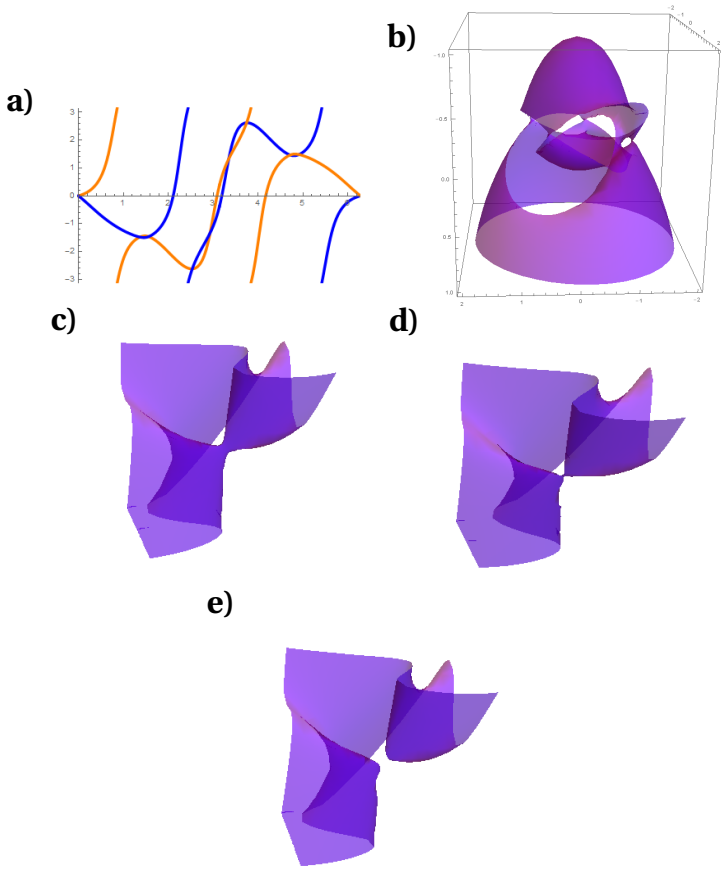

Figure 6.5: The knot 5_2 has critical points. a) A plot of $\arg g_{1/4,1/4}(c_{1,2}(t),t)$. b) The level set $\arg g^{-1}_{1/4,1/4}(1.4985)$. The value 1.4985 is approximate. c) A neighbourhood of the critical point and the level set for $\arg g_{1/4,1/4} = 1.498$. d) A neighbourhood of the critical point and the level set for $\arg g_{1/4,1/4} = 1.4985$. e) A neighbourhood of the critical point and the level set for $\arg g_{1/4,1/4} = 1.499$. Note that the topology of the surface has changed in the process of passing through the critical point.

formed by the roots of $\frac{\partial g}{\partial u}$. This critical braid can be interpreted as the collection of all saddle points of the phase surfaces, the level sets of $\arg g$. Let $\chi \in S^1$ be a regular value. Then the corresponding surface $(\arg g)^{-1}(\chi)$ intersects the critical braid in a certain number of points. As χ increases the intersection points move along the critical braid, but their number does not change as long as χ is still regular.

When χ is a critical value, intersection points of $(\arg g)^{-1}(\chi)$ and the critical braid collide and annihilate, so that when χ increases further, the number of intersection points is reduced. Obviously, the inverse process is also possible: Two parts of a surface can approach a strand of the critical braid, then touch it

(with multiplicity > 1) at a critical point and then intersect the critical braid in more points than before.

The example of the unfibred knot 5_2 and the discussion of critical points is important because there used to be some misunderstanding about the possibility of constructing unfibred knots in physical systems. The idea here was that taking the argument of a complex-valued polynomial that vanishes on 5_2 would result in a fibration of the knot complement [79], which can not exist, since 5_2 is unfibred. This contradiction led to the conclusion that there are no complex-valued polynomials vanishing exactly on 5_2.

The problem with this argument is of course that the argument of a complex-valued polynomial is not necessarily a fibration. It could have critical points. Our construction (and the proof in Chapter 5) shows that fibredness is not necessary for the construction of semiholomorphic polynomials to work. There might however be reasons why certain physical systems favour fibred knots over unfibred knots as mentioned in Chapter 3.

6.4 Lifted permutation invariants

The key to the existence of polynomial fibrations is Theorem 6.2 and its generalisation Theorem 6.3. This makes it possible to lift parametrisations of the critical values of a family of polynomials to a parametrisations of its roots due to the Homotopy Lifting Property.

We can use the same principle to define new braid invariants from old ones. Recall from Chapter 2 the homomorphism h from the braid group on s strands B_s to the symmetric group s elements S_s that sends the Artin generator σ_i to the transposition τ_i, in cycle notation $(i,\ i+1)$. Then $h(B)$ is obviously a braid invariant, albeit not a very good one.

For the braid group B_2 for example, there are only two possible permutations id and τ_1, while $B_2 = \mathbb{Z}$. The only information that we can obtain from the permutation representation is whether the two strands twist an odd or even number of times.

The case of B_2 is of course in some sense too simple, since the exponent of σ_1 in any braid word is a perfect braid invariant in B_2, but it makes it clear that the permutation representation is not very good at distinguishing braids.

In this section we discuss how the results from the previous sections could lead to a new approach to the word problem and the conjugacy problem in braid

groups. Both are solved [8, 18, 45, 48, 52, 54], but a new topological approach could result in more efficient algorithms or a better way to extract link invariants from the solution.

In B_2 we solve the word problem in $O(\ell \log \ell)$ steps, where ℓ is the sum of the lengths of the two braid words in question. This is obviously less efficient than simply taking the exponent of σ_1, but the method has a lot of potential to generalise to an efficient solution of the word problem and the conjugacy problem for every braid group.

Let A and B be two braid words in B_2. Then in order to decide whether $A = B$, we check whether $AB^{-1} = e$. The first thing that we can do is apply the permutation representation and see if $h(AB^{-1})$ is even or odd. If it is odd, then it is obviously $AB^{-1} \neq e$. If it is even, then AB^{-1} is by definition a pure braid. Therefore there will be a parametrisation of AB^{-1} where one strand is given by $(0, 0, t)$, $t \in [0, 2\pi]$ and the other by say $\left(\cos\left(\frac{k}{2}t\right), \sin\left(\frac{k}{2}t\right), t\right)$, $t \in [0, 2\pi]$, where k is the the exponent of σ_1 in the braid word AB^{-1}. In order to decide whether $AB^{-1} = e$, we need to know whether $k = 0$. This makes the choice of parametrisation seem odd because it makes it look like we already know the value of k. But in fact the exact parametrisation does not really matter. The important point is that one of the strands never moves away from its position as the zero strand and the other one twists around it a certain number of times that can be extracted from the braid word. As an alternative to the given parametrisation we could write down a parametrisation for σ_1 (which also gives a parametrisation for σ_1^{-1}) and build a parametrisation of AB^{-1} by concatenating the individual parametrisations for each letter in the braid word of AB^{-1}.

We think of the given parametrisation as the parametrisation of a braid that is formed by one critical value $v(t)$ and the zero strand. By Theorem 6.2 there are $s^{s-1} = 2$ cyclic 1-parameter families of monic complex polynomials $g^{(i)}(u, t)$, $i = 1, 2$, of degree 2 in $\tilde{V}_2$ such that $v(t)$ is the complex critical value of both $g^{(1)}(u, t)$ and $g^{(2)}(u, t)$.

Given $v(t)$ by the parametrisation above, we have to solve

$$\begin{aligned} c(t)^2 + a(t)c(t) &= v(t), \\ 2c(t) + a(t) &= 0 \end{aligned} \tag{6.26}$$

and find the two solutions for the coefficient $a(t)$

$$\begin{aligned} a_1(t) &= -2\mathrm{i}\,\mathrm{e}^{\mathrm{i}kt/4}, \\ a_2(t) &= 2\mathrm{i}\,\mathrm{e}^{\mathrm{i}kt/4}\,. \end{aligned} \tag{6.27}$$

The family of polynomials $g^{(1)}(u,t) = u^2 - a_1(t)u$ has the roots

$$\begin{aligned} u_1(t) &= 0, \\ u_2(t) &= -2\mathrm{i}\,\mathrm{e}^{\mathrm{i}kt/4}, \end{aligned} \tag{6.28}$$

while $g^{(2)}(u,t) = u^2 - a_2(t)u$ has the roots

$$\begin{aligned} u_1(t) &= 0, \\ u_2(t) &= 2\mathrm{i}\,\mathrm{e}^{\mathrm{i}kt/4}\,. \end{aligned} \tag{6.29}$$

Thus in both cases the roots form a braid on two strands with braid word $\sigma_1^{k/2}$. We can now again apply the permutation representation to this braid. The resulting even or odd permutation tells us whether $k/2$ is even or odd. As before an odd permutation implies that k can not be zero, while an even result means that $\sigma_1^{k/2}$ is a pure braid. Therefore, we can find a parametrisation for the braid where one of the strand is always zero and the other one twists around it. Interpreting this as the parametrisation of one critical value $v(t)$ twisting around the zero axis again lifts the parametrisation to 2 cyclic 1-parameter families of monic complex polynomials whose critical value is $v(t)$.

This process can go on infinitely in theory. At every stage one obtains a 2-strand braid where one strand twists around the other half the number of times as in the previous case. If the initial braid word AB^{-1} was trivial, then all of these lifted braids are trivial as well and applying the permutation representation to each of them must result in an even permutation. However, if $AB^{-1} \neq e$, then $k \neq 0$ and after $n = \lfloor \log_2 k \rfloor \leq \lfloor \log_2 \ell \rfloor$ iterations the lift of the critical value parametrisation to polynomials results in a braid that is an odd permutation of the two strands. This method thus solves the word problem in B_2. It does this obviously a lot less efficiently than simply adding all exponents of σ_1 in the braid word AB^{-1}.

We need to apply h to AB^{-1} and decide whether $h(AB^{-1})$ is the identity permutation which takes $O(\ell)$ operations, where ℓ is the length of the braid word AB^{-1}. Then we need to find a parametrisation of AB^{-1}, where one strand is constantly zero. This can be prepared before the actual calculation, meaning that if we

have parametrisations for σ_1 and σ_1^{-1} for each of the two cases, where the zero strand is in the first or in the second position, then we can build a parametrisation for any braid word in B_2 by simply concatenating these parametrisations according to the braid word in question.

Then we need to lift this parametrisation to find polynomials whose critical values are given by precisely this parametrisation. This corresponds to solving one quadratic and one linear equation, but in fact with a possible extension to braids with more strands in mind it is more convenient to have this calculation already prepared, again in the sense that we have already found the lifts for the parametrisations of σ_1 and σ_1^{-1} for both relevant cases. Then finding the lift of AB^{-1} is again just a matter of concatenation and thus of the order $O(\ell)$.

Since for the $s = 2$ case all of the braids that consist of the roots of the polynomials that were obtained by lifting the critical value parametrisations are isotopic (they were both $\sigma_1^{k/2}$), we can pick any one of them and repeat the whole process. Thus every repeat needs $O(\ell)$ steps and by the earlier remark we can decide after at most $\lfloor \log_2 \ell \rfloor$ iterations whether $AB^{-1} = e$ or not.

Let us now consider the general case of braids with more than two strands A and B in B_s. Again we first apply the h to AB^{-1} and if it is not the trivial permutation in S_s, then we know that $A \neq B$. If it is the trivial permutation, then AB^{-1} is a pure braid and for each of the s strands $j \in \{1, 2, \ldots, s\}$ of AB^{-1} there is a parametrisation of AB^{-1} where the jth strand is constantly zero.

Each of these parametrisations can be seen as the parametrisation of $s-1$ critical values $(v_1(t), v_2(t), \ldots, v_{s-1}(t))$ twisting around the zero line. Lifting this loop in W_s to paths in the space of polynomials $\tilde{V}_s$ results in s^{s-1} families of monic complex polynomials $g^i(u,t)$ with $g^i(0,t) = 0$ and $(v_1(t), v_2(t), \ldots, v_{s-1}(t))$ as the critical values of $g^i(u,t)$ for all $t \in [0, 2\pi]$ and all $i \in \{1, 2, \ldots, s^{s-1}\}$.

Note that since the lifts are not necessarily loops in the space of polynomials, it is not true in general that $g^i(u,0) = g^i(u,2\pi)$, but rather $g^i(u,0) = g^j(u,2\pi)$ for some $j \in \{1, 2, \ldots, s^{s-1}\}$.

The group $\pi_1(W_s, (v_1(0), v_2(0), \ldots, v_{s-1}(0)))$ is acting on the s^{s-1} preimage points of $(v_1(0), v_2(0), \ldots, v_{s-1}(0))$ in the usual way. Thus we associate an element π of the permutation group $S_{s^{s-1}}$ to each element of $\pi_1(W_s, (v_1(0), v_2(0), \ldots, v_{s-1}(0)))$. This permutation can also be used as a braid invariant for the word problem, since again the trivial braid is associated with a trivial permutation.

If the induced permutation in $S_{s^{s-1}}$ is trivial, then all the lifts are indeed loops and not just paths in the space of polynomials. Therefore each of them

corresponds to a (closed) braid on s strands by considering the complex roots of the given polynomials. We thus have obtained s^{s-1} new braids that we can apply the permutation representation h to. If $A = B$, then all of the resulting s^{s-1} permutations in S_s must be trivial.

If that is the case, then we can again consider all of these s^{s-1} closed braids as loops in W_s, lift them, check the corresponding permutation in $S_{s^{s-1}}$ and apply h to the resulting s^{s-1} loops in the space of polynomials and so on.

The main difference to the case of $s = 2$ is that it is not the case that all of the s^{s-1} braids, the lifts in $\tilde{V}_s$, form isotopic braids. In the case of $s = 2$ we could pick any of the loops and repeat the procedure of lifting and applying permutation representation to any one of them. For $s > 2$ it seems like we either have to make a choice or have to go through the process for every single one of the s^{s-1} many braids, which obviously is not very efficient.

On the other hand, choosing only one (or in general a low number) of them seems a bit unnatural, as there is not one lift that is clearly preferable to the others, and also ignores all the information that comes from the ones that were not chosen.

This problem is connected to the main question here. In principle the procedure of lifting and checking permutations can be repeated ad infinitum, but in the case of $s = 2$ only finitely many ($\log_2 \ell$) iterations were needed to solve the word problem. Can we choose the loop that we lift in the next iteration in such a way that the algorithm terminates after finitely many (and ideally a comparatively low number of) steps?

While this question remains open, it is true that we can use the (in principle infinitely many) permutations as braid invariants. Instead of comparing the permutations that we obtain for AB^{-1} with the trivial one that we obtain for the trivial braid e, we directly compare the ones of A and B.

Again the first step is simply the application of the permutation representation h to both A and B. If $A = B$, then they must induce the same permutation in S_s. Previously, we were dealing with pure braids because they are the only ones that give the same trivial permutation as e. For pure braids there is a parametrisation such that one strand does not move at all, which we need in order to view this strand as the zero strand around which critical values twist. If A and B are not pure braids, such a parametrisation might not exist. However, it does exist if A and B are isotopic to an affine braid.

In order to obtain a valid parametrisation for all braids and not just the affine

ones, we do the following. We apply the standard embedding i of the B_s in AB_{s+1} that sends σ_i to σ_{i+1} and study the $(s+1)^s$ lifts of $i(A)$ and $i(B)$ to $\tilde{V}_{s+1}$. Loops in $\tilde{V}_{s+1}$ then again form affine braids, so we only have to apply i to A and B, not to the braids that are formed by concatenations of their lifts.

The action of the loop in W_{s+1} on the fibre $(s+1)^s$ gives a permutation in $S_{(s+1)^s}$. If $A = B$, then both yield the same permutation $\rho(A) = \rho(B)$. The cycles of the permutations correspond to loops in $\tilde{V}_{s+1}$ and the length of each cycle reflects the number of lifts/paths that the corresponding loop is made of. Thus if $A = B$, we obtain the same number of loops, each of which corresponds to a (closed) braid on $s+1$ strands. Each of these braids induces a permutation in S_{s+1}, which means that if $A = B$, then there should be a bijection b_n between the cycles of $\rho(A)$ of length n and the cycles of $\rho(B)$ of length n such that the induced permutations in S_{s+1} of $b_n(C)$ and C are identical for all n and all cycles C of $\rho(A)$ of length n.

Note that all loops in $\tilde{V}_s$ form affine braids for all s, since every polynomial in $\tilde{V}_s$ has zero as a root. We can regard the lifted loops in $\tilde{V}_{s+1}$ as loops in W_{s+1}, where $(v_1(t), \ldots, v_s(t))$ is given by the non-zero roots of the polynomials. As loops in W_{s+1} they come with a permutation in $S_{(s+1)^s}$ and lifts in $\tilde{V}_s$, all of which are invariants of the original braids A and B. This process can be repeated infinitely.

We have discussed that we can apply the permutation representation h not only to the braids A and B, but to each of their infinitely many lifts. This infinite sequence of permutations is now a much stronger invariant than the original permutations $h(A)$ and $h(B)$. For $s = 2$ for example, h only carries information about the parity of the exponent of σ_1, but the sequence (in fact the first $\log_2 k$ elements) is strong enough to solve the word problem in B_2. There is no reason why one should only do this for the permutation representation h. We can take our favourite braid invariant and apply it to each of the braids that one obtains from infinitely lifting A and B. We thus obtain an infinite sequence of braid invariants and if $A = B$, then there must be some bijection between the invariants that one obtains at each level. For example the braids A_C that are formed by the cycles C of the lifts of A must give the same invariants as the braids B_C that are formed by the cycles $b(C)$ of the lifts of B. For each of the braids A_C its lifts must give rise to the same invariants as the braids that one obtains from lifting the corresponding B_C.

Similar considerations apply to invariants of conjugacy classes of braids. Note that conjugate affine braids lift to conjugate paths in $\tilde{V}_s$. Furthermore,

$i(A)$ and $i(B)$ are conjugate in AB_{s+1} if and only if A and B are conjugate in B_s. Therefore, we can take our favourite invariant of conjugacy classes of braids and the lifting procedure will provide us with an infinite sequence of conjugacy invariants, which as a whole we expect to be more powerful than the original invariant.

It is an ongoing research project, how lifted braids and their invariants behave under Markov stabilization and destabilization moves. If one could find some information in the sequence of lifted invariants that is invariant under these moves, then the sequence would by Markov's theorem turn out to be a (potentially very powerful) link invariant.

6.5 Discussion

We have shown that if we do not use trigonometric interpolation as in Section 5.3, but a lifting procedure to find trigonometric braid parametrisations, we can construct for any braid B a semiholomorphic polynomial f whose vanishing set on S^3 is the closure of B and whose argument $\arg f$ on S^3 has $\beta(B)$ many critical points, where $\beta(B)$ is a measure of how far B is from being homogeneous.

In particular, we can construct explicit fibrations for complements of closures of homogeneous braids. These fibrations are then simply the arguments of the constructed polynomials, which adds some constructive detail to a theorem by Stallings.

When we use the constructed functions as initial configurations of physical systems, the critical points often carry physical importance. They are for example the stagnation points of a superfluid or the point defects of a smectic liquid crystal. Depending on how such points affect the energy of the configuration in the relevant system, a construction that results in as few critical points as possible could be desirable as it could lead to a knotted initial configuration that has low energy and therefore is more likely to be stable.

The lifting procedure that is applied to show the existence of the desired trigonometric parametrisations can also be used (repeatedly) to associate a sequence of braids to each braid. This offers the possibility of making braid invariants and invariants of conjugacy classes of braids a lot stronger. Instead of comparing the invariants of two braids A and B, we can now compare the invariants of the braids in the sequences associated to A and B, which is expected to be a lot better at distinguishing braids. How efficient and effective these new

invariants can be is a current research topic.

7 Real algebraic links

The most common context in which knots and algebraic varieties are studied together is that of links of singularities. We want to investigate if there is any connection between the polynomials constructed in the previous chapters and the polynomials for algebraic, weakly real algebraic and real algebraic links that were discussed in Chapter 2.

The semiholomorphic polynomials whose construction was described in the previous chapters have the desired link as their zero level set on the unit three-sphere. However, the construction does not provide any information about three-spheres of different radii and it is straightforward to see that the constructed polynomials typically do not have a (weakly) isolated singular point at the origin and the required link around it [40].

In this chapter we introduce conditions under which we can manipulate the polynomials constructed in [22] to obtain a polynomial that satisfies all of Akbulut and King's properties [5], i.e. a real polynomial $\mathbb{R}^4 \to \mathbb{R}^2$ with a weakly isolated singularity at the origin and a given link around it. Furthermore, if additional conditions are met, the singular point at the origin is shown to be not only weakly isolated, but isolated. This explicit construction allows us to show the real algebraicity of an infinite family of links. The main result of this chapter is the following theorem.

Theorem 7.1. *Let B be a braid on s strands such that $B = w^2$ for some homogeneous braid w. Then there exists a function $f : \mathbb{C}^2 \to \mathbb{C}$ such that*

- *f is a polynomial in u, v and $\bar{v}$;*
- *as a map from $\mathbb{R}^4$ to $\mathbb{R}^2$ the map f has an isolated singularity at the origin;*
- *$f^{-1}(0) \cap S^3_\rho$ is ambient isotopic to the closure of B for all positive $\rho \leq 1$;*
- *$\deg_u f = s$.*

Hence the closure of B is real algebraic.

Hopefully the proof might be extended to more links and some of the desirable properties of algebraic links can be found for links of real singularities as well.

The structure of this chapter is as follows. Section 7.1 discusses ways of manipulating the polynomials from Chapters 5 and 6 to obtain maps with weakly isolated singularities and Section 7.2 states when the resulting maps can be taken to be polynomials. The proof of Theorem 7.1 can be found in Section 7.3. In Section 7.4 we give indications that some links not covered by Theorem 7.1 can be proven to be real algebraic in a similar fashion. In Section 7.5 we show that the argument of the constructed polynomial f is a fibration of $S^3_\epsilon \backslash f^{-1}(0)$ over S^1.

The results of this chapter have first appeared in [20].

7.1 Weakly isolated singularities

Recall from Chapter 4 that for every braid B on s strands there is a trigonometric parametrisation as in Equation (5.3). We can then define the family of functions

$$\begin{aligned} g_{a,b}(u,t) &= \prod_{j=1}^{s}(u - aX_j(t) - \mathrm{i}bY_j(t)) \\ &= \prod_{C\in\mathscr{C}}\prod_{j=1}^{s_C}\left(u - aF_C\left(\frac{t+2\pi j}{s_C}\right) - \mathrm{i}bG_C\left(\frac{t+2\pi j}{s_C}\right)\right), \end{aligned} \tag{7.1}$$

which is a polynomial in the complex variable u, $\mathrm{e}^{\mathrm{i}t}$ and $\mathrm{e}^{-\mathrm{i}t}$ and as a map $\mathbb{C}\times[0,2\pi]$ has a nodal set that is exactly the parametrised braid B.

We know from Chapter 6 that if B is homogeneous, then there exists a trigonometric parametrisation that guarantees that $\arg g_{1,1} : (\mathbb{C}\times[0,2\pi])\backslash B \to S^1$ does not have any critical points.

Replacing every instance of $\mathrm{e}^{\mathrm{i}t}$ and $\mathrm{e}^{-\mathrm{i}t}$ in the polynomial expression of $g_{a,b}$ by a complex variable v and its complex conjugate $\overline{v}$ respectively yields a family of semiholomorphic polynomials $f_{a,b}$. We know from Theorem 5.1 that for every choice of a and b, there is an ε such that the nodal set of $f_{\lambda a,\lambda b}$ on the unit three-sphere is the closure of B if $\lambda<\varepsilon$.

In order to prove Theorem 7.1 we need to make certain alterations to this construction. While $f^{-1}_{\lambda a,\lambda b}(0)\cap S^3$ is the closure of B if $\lambda>0$ is small enough, it does not necessarily have a weakly isolated singularity and the zero level set on three-spheres of small radii is typically different from the closure of B.

In some cases however, the function $f_{a,b}$ can be manipulated in such a way that it has a weakly isolated singular point at the origin with the desired link around it.

Lemma 7.2. *Let $q_1, q_2 \in \mathbb{R}_{\geq 0}$ and $g_{a,b}$ be constructed as in Equation (7.1) from a braid parametrisation (5.3) of the braid B on s strands. Let $f_{a,b}$ be constructed from this parametrisation as in Chapter 5 and $k \geq \deg f_{a,b}/2s$. We define*

$$P_{a,b,k} : \mathbb{C} \times [0,1] \times S^1 \to \mathbb{C}, \quad P_{a,b,k}(u,r,t) = r^{2sk} g_{r^{q_1}a, r^{q_2}b}\left(\frac{u}{r^{2k}}, t\right). \tag{7.2}$$

Then, since $P_{a,b,k}(u,0,t) = u^s$ for all $t \in [0,2\pi]$, we can define $p_{a,b,k} : \mathbb{C}^2 \to \mathbb{C}$, $p_{a,b,k}(u, r\,\mathrm{e}^{\mathrm{i}t}) = P_{a,b,k}(u,r,t)$. For small enough $a, b > 0$ the map $p_{a,b,k} : \mathbb{R}^4 \to \mathbb{R}^2$ has a weakly isolated singular point at the origin and $p^{-1}_{a,b,k}(0) \cap S^3_\rho$ is the closure of B for all $\rho \in (0,1]$.

Proof. First of all, by definition $P_{a,b,k}$ and $p_{a,b,k}$ are polynomials in u for every fixed r and t. A straightforward calculation shows that $p_{a,b,k}(0,0) = 0$ and $(0,0,0,0)$ is a singular point when $p_{a,b,k}$ is viewed as a map $\mathbb{R}^4 \to \mathbb{R}^2$.

Next we need to show that the singular point at the origin is weakly isolated. Note that $p_{a,b,k}(u,0) = u^s$, so the origin is the only point with $p_{a,b,k}(u,v) = 0$ and $v = 0$. Now let $(u,v) = (u, r\,\mathrm{e}^{\mathrm{i}t}) \in \mathbb{C} \times \mathbb{C}\backslash\{0\}$ be in the zero level set. We find that $p_{a,b,k}(u, r\,\mathrm{e}^{\mathrm{i}t}) = r^{2sk} g_{r^{q_1}a, r^{q_2}b}(u/r^{2k}, r, t)$ and since for every $r \in (0,1]$ and $t \in [0,2\pi]$ the polynomials $g_{a,b}(\bullet, t)$ for all a, b only has simple roots, we get

$$\frac{\partial p_{a,b,k}}{\partial u}(u, r\,\mathrm{e}^{\mathrm{i}t}) = r^{2k(s-1)} \frac{\partial g_{r^{q_1}a, r^{q_2}b}}{\partial u}\left(\frac{u}{r^{2k}}, r, t\right) \neq 0. \tag{7.3}$$

It follows from the Cauchy-Riemann equations that the Jacobian of $p_{a,b,k}$, again viewed as a map $\mathbb{R}^4 \to \mathbb{R}^2$, has full rank at (u,v) and hence the singular point at the origin is weakly isolated.

Since $p_{a,b,k}(u,1,t) = g_{a,b}(u,t)$ the same arguments as in the construction of $f_{a,b}$ apply to $p_{a,b,k}$ (cf. Section 5.2), meaning that as long as $\lambda > 0$ is chosen small enough the zero level set of $p_{\lambda a, \lambda b, k}$ on the unit three-sphere is the closure of B. Furthermore, if λ is small enough, the intersection of the zero level set of $p_{\lambda a, \lambda b, k}$ and the unit three-sphere is transverse (cf. Corollary 5.7).

In order to guarantee that the zero level set of $p_{\lambda a, \lambda b, k}$ on the three-sphere of any radius is the closure of B and not just on the unit three-sphere, it suffices to show that for all $\rho \in (0,1]$ and all $x \in p^{-1}_{\lambda a, \lambda b, k}(0) \cap S^3_\rho$ the Jacobian on the three-sphere $\nabla_{S^3_\rho} p_{a,b,k}(x)$ has full rank. Since for every $v \in \mathbb{C}\backslash\{0\}$ the roots of the complex polynomial $p_{\lambda a, \lambda b, k}(\bullet, v)$ are simple, it is sufficient to show that for all

$\rho \in (0,1]$ the intersection of S^3_ρ with $p^{-1}_{\lambda a,\lambda b,k}(0)$ is transverse. Note that for every $t \in [0,2\pi]$ the roots of $p_{\lambda a,\lambda b,k}(\bullet, r\,\mathrm{e}^{\mathrm{i}t})$ are given by $r^{2k+q_1}\lambda a\mathrm{Re}(u_j(t)) + \mathrm{i}r^{2k+q_2}\lambda b\mathrm{Im}(u_j(t))$, $j = 1,2,\ldots,s$, where $u_j(t)$ is the jth root of $g_{1,1}(\bullet, t)$.

Let (u,v) be a point on $p^{-1}_{\lambda a,\lambda b,k}(0)$ that is not the origin, then $v = r\,\mathrm{e}^{\mathrm{i}t} \neq 0$. If $u = 0$, then there is a $j \in \{1,2,\ldots,s\}$ such that $u_j(t) = 0$ and then $r^{2k+q_1}\lambda a\mathrm{Re}(u_j(t)) + \mathrm{i}r^{2k+q_2}\lambda b\mathrm{Im}(u_j(t)) = 0$ for all r. Thus in the basis $(\mathrm{Re}(u), \mathrm{Im}(u), r, t)$ the vector $(0,0,1,0)$ is tangent to $p^{-1}_{\lambda a,\lambda b,k}(0)$ at (u,v) and the intersection of $p^{-1}_{\lambda a,\lambda b,k}(0)$ with $S^3_{|(u,v)|}$ is transverse at (u,v).

If $u \neq 0$, then one tangent vector of $p^{-1}_{\lambda a,\lambda b,k}(0)$ at (u,v) in the basis $(|u|, \arg(u), r, t)$ is

$$(2kr^{2k-1}\lambda|U| + r^{2k}\lambda^2(q_1 r^{2q_1-1}a^2\mathrm{Re}(u_j(t))^2 + q_2 r^{2q_2-1}b^2\mathrm{Im}(u_j(t))^2)/(\lambda|U|), 0, 1, 0), \quad (7.4)$$

where $|U| = \sqrt{r^{2q_1}a^2\mathrm{Re}(u_j(t))^2 + r^{2q_2}b^2\mathrm{Im}(u_j(t))^2}$. The vector in Equation (7.4) is for small enough λ not in the tangent space of $S^3_{|(u,v)|}$ (which is for example spanned by $(0,1,0,0)$, $(0,0,0,1)$ and $(-r/|u|, 0, 1, 0)$). Hence the intersection of $p^{-1}_{a,b,k}(0)$ and $S^3_{|(u,v)|}$ is transverse at (u,v).

Therefore all intersections of $p^{-1}_{\lambda a,\lambda b,k}(0)$ with S^3_ρ are transverse for all $\rho \in (0,1]$.

We have thus shown that as the radius ρ of the three-sphere S^3_ρ varies between zero and one the link type of $p^{-1}_{\lambda a,\lambda b,k}(0) \cap S^3_\rho$ does not change if λ is small enough. Hence for sufficient choices of a, b and k the zero level set of $p_{a,b,k}$ on the three-sphere of any radius at most one is the closure of B, which finishes the proof. □

If we set $q_1 = q_2 = 0$, the resulting function

$$p_{a,b,k}(u, r\,\mathrm{e}^{\mathrm{i}t}) = r^{2sk} g_{a,b}\left(\frac{u}{r^{2k}}, t\right) = r^{2sk} f_{a,b}\left(\frac{u}{r^{2k}}, \mathrm{e}^{\mathrm{i}t}\right) \quad (7.5)$$

only depends on r by the scaling in the u-coordinate and the overall factor r^{2sk}. Hence the next lemma follows from Lemma 7.2 with $q_1 = q_2 = 0$.

Lemma 7.3. *For large enough k and small enough $a, b > 0$*

$$p_{a,b,k}(u,v) := (v\bar{v})^{sk} f_{a,b}\left(\frac{u}{(v\bar{v})^k}, \frac{v}{\sqrt{v\bar{v}}}\right), \quad (7.6)$$

has a weakly isolated singular point at the origin and $p^{-1}_{a,b,k}(0) \cap S^3_\rho$ is the closure of B for all $\rho \in (0,1]$.

Lemma 7.2 and 7.3 are in general not constructing functions of the form discussed by Akbulut and King [5]. The newly defined function $p_{a,b,k}$ is a polynomial in u, but it might not be possible to write it as a polynomial in v and $\overline{v}$.

As an example we consider the $(4,2,3)$-lemniscate braid parametrised by

$$\left(a\cos\left(\frac{2t+2\pi j}{4}\right), b\sin\left(\frac{3(2t+2\pi j)}{4}\right), t\right) \qquad t\in[0,2\pi],\ j=1,2,3,4 \tag{7.7}$$

with $a,b>0$. Its closure is the 2-component link L_{6a1} [23]. Defining $g_{a,b}$ as in Equation (7.1) and expanding the product yields

$$\begin{aligned} g_{a,b}(u,t) =& u^4 + u^2(b^2-a^2-2\mathrm{i}ab\sin(2t)) + \frac{1}{8}(a^4 - 2a^2b^2 + b^4 \\ &- a^2(a^2+6b^2)\cos(2t) + 2a^2b^2\cos(4t) - b^4\cos(6t) + 4\mathrm{i}a^3b\sin(2t) \\ &- 4\mathrm{i}ab^3(\sin(2t)+\sin(4t))). \end{aligned} \tag{7.8}$$

Then using the de Moivre's identities $\sin(nt) = 1/(2i)(\mathrm{e}^{\mathrm{i}nt} - \mathrm{e}^{-\mathrm{i}nt})$ and $\cos(nt) = 1/2(\mathrm{e}^{\mathrm{i}nt} + \mathrm{e}^{-\mathrm{i}nt})$ we get with $k = 1 \geq 2/3 = \deg f_{a,b}/2s$,

$$\begin{aligned} P_{a,b,1}(u,r,t) =& r^8 g_{r^{q_1}a,r^{q_2}b}\left(\frac{u}{r^2},t\right) \\ =& u^4 + u^2r^4(r^{2q_2}b^2 - r^{2q_1}a^2 - ab(\mathrm{e}^{2\mathrm{i}t} - \mathrm{e}^{-2\mathrm{i}t})) \\ &+ \frac{r^8}{16}(2a^4r^{4q_1} - 4a^2b^2r^{2q_1+2q_2} + 2b^4r^{4q_2} \\ &- a^2r^{2q_1}(a^2r^{2q_1} + 6b^2r^{2q_2})(\mathrm{e}^{2\mathrm{i}t} + \mathrm{e}^{-2\mathrm{i}t}) \\ &+ 2a^2b^2r^{2q_1+2q_2}(\mathrm{e}^{4\mathrm{i}t} + e^{-4\mathrm{i}t}) - b^4r^{4q_2}(\mathrm{e}^{6\mathrm{i}t} + \mathrm{e}^{-6\mathrm{i}t}) \\ &+ 4a^3br^{3q_1+q_2}(\mathrm{e}^{2\mathrm{i}t} - \mathrm{e}^{-2\mathrm{i}t}) \\ &- 4ab^3r^{q_1+3q_2}(\mathrm{e}^{2\mathrm{i}t} - \mathrm{e}^{-2\mathrm{i}t} + \mathrm{e}^{4\mathrm{i}t} - \mathrm{e}^{-4\mathrm{i}t})). \end{aligned} \tag{7.9}$$

We set $r = \sqrt{v\overline{v}}$, $\mathrm{e}^{\mathrm{i}t} = v/\sqrt{v\overline{v}}$, $\mathrm{e}^{-\mathrm{i}t} = \overline{v}/\sqrt{v\overline{v}}$ and $q_1 = q_2 = 0$ and obtain

$$\begin{aligned} p_{a,b,1}(u,v) =& u^4 + u^2((v\overline{v})^2(b^2-a^2) - abv\overline{v}(v^2-\overline{v}^2)) \\ &+ \frac{(v\overline{v})^4}{16}(2a^4 - 4a^2b^2 + 2b^4) + \frac{1}{16}((-a^4 - 6a^2b^2)(v\overline{v})^3(v^2+\overline{v}^2) \\ &+ 2a^2b^2(v\overline{v})^2(v^4+\overline{v}^4) - b^4v\overline{v}(v^6+\overline{v}^6) + 4a^3b(v\overline{v})^3(v^2-\overline{v}^2) \\ &- 4ab^3((v\overline{v})^3(v^2-\overline{v}^2) + (v\overline{v})^2(v^4-\overline{v}^4))). \end{aligned} \tag{7.10}$$

This function is easily checked to have a weakly isolated singularity at the origin. By the previous lemmas the link of the singularity is the closure of the braid parametrised by Equation (7.7) if a and b are small enough.

Note that in this example we obtain a polynomial in u, v and $\bar{v}$. The next section discusses for which braid parametrisations this happens.

7.2 Braid parametrisations leading to polynomial maps

The construction described in Section 7.1 clearly works for any given braid and the resulting function $p_{a,b,k}$ is a polynomial in u, v, $\bar{v}$ and $\sqrt{v\bar{v}}$. It is in general not a polynomial map $\mathbb{R}^4 \to \mathbb{R}^2$. In the following we investigate braid parametrisations that guarantee that $p_{a,b,k}$ is a polynomial in u, v and $\bar{v}$ and thus of the form discussed by Akbulut and King [5].

Let $B = w^2$ be the square of some braid word $w \in B_s$. Then we can find a finite Fourier parametrisation of w and define the corresponding braid polynomial $g_{a,b}(u,t)$ that has w as its zero level set. Making a simple change of variable results in the function $\tilde{g}_{a,b}(u,t) = g_{a,b}(u,2t)$ whose zero level set is $B = w^2$. Moreover, since $g_{a,b}$ is a polynomial in u, e^{it} and e^{-it}, $\tilde{g}_{a,b}$ is a polynomial in u, e^{i2t} and e^{-i2t}. Let $\tilde{f}_{a,b}$ be the semiholomorphic polynomial that results from $\tilde{g}_{a,b}$ by replacing every instance of e^{it} by v and every instance of e^{-it} by $\bar{v}$. Then all exponents of v and $\bar{v}$ in $\tilde{f}_{a,b}$ are even. We define $p_{a,b,k}$ as in Lemma 7.3 using $\tilde{f}_{a,b}$. It is by construction a polynomial in u, v, $\bar{v}$ and $\sqrt{v\bar{v}}$. Since all exponents of v and $\bar{v}$ of $\tilde{f}_{a,b}$ are even, so are all exponents of $\sqrt{v\bar{v}}$ and hence $p_{a,b,k}$ is a polynomial in u, v and $\bar{v}$. In combination with Lemma 7.3 this proves the following lemma.

Lemma 7.4. *Let $B = w^2$ be the square of some braid word $w \in B_s$. Then there exists a function $F : \mathbb{R}^4 \to \mathbb{R}^2$ such that*

- *F is a polynomial in u, v and $\bar{v}$;*
- *F has a weakly isolated singular point at the origin;*
- *$F^{-1}(0) \cap S^3_\rho$ is the closure of B for all $\rho \in (0,1]$;*
- *$\deg_u F = s$.*

Proof. Take F to be $p_{a,b,k}$ for small enough a and b. Then the first three properties are shown above or follow directly from Lemma 7.3. The fourth property follows directly from the construction and $\deg_u F = \deg_u \tilde{f}_{a,b} = \deg_u \tilde{g}_{a,b} = \deg_u g_{a,b} = s$. □

More generally, $p_{a,b,k}$ is a polynomial in u, v and $\bar{v}$ if all exponents of v and $\bar{v}$ in the corresponding polynomial $f_{a,b}$ are even or equivalently if the corresponding braid polynomial $g_{a,b}$ is a polynomial in u, e^{2it} and e^{-2it}. In order to construct

polynomial maps $\mathbb{R}^4 \to \mathbb{R}^2$ with a weakly isolated singular point it is hence sufficient to find braid parametrisations as in Equation (5.3) that lead to a function $g_{a,b}$ of this form.

Lemma 7.4 covers an obvious case of braids that lead to a polynomial $f_{a,b}$ where all exponents of v and $\overline{v}$ are even, so that $p_{a,b,k}$ is a polynomial in u, v and $\overline{v}$. It is not the only way to achieve this though.

Lemma 7.5. *Let B be a braid such that every link component C of the closure of B consists of the same number of strands s_C. Furthermore, let 2^m be the highest power of two dividing s_C. Let B be parametrised as in Equations (5.3) and (5.2) satisfying*

- *all $j \in \{0, 1, \ldots, N_C\}$ with non-vanishing $a_{C,j}$ for some link component $C \in \mathcal{C}$ lie in the same residue class mod 2^{m+1}, say $x \bmod 2^{m+1}$, and*
- *all $j \in \{0, 1, \ldots, M_C\}$ with non-vanishing $b_{C,j}$ for some link component $C \in \mathcal{C}$ lie in the same residue class mod 2^{m+1}, say $y \bmod 2^{m+1}$.*

Then $p_{a,b,k}$ with $q_1 = x/2^m$ and $q_2 = y/2^m$ as in Lemma 7.3 is a polynomial in u, v and $\overline{v}$.

Proof. We can write the polynomial $g_{a,b}$ as

$$g_{a,b}(u,t) = \sum_{i=0}^{s} u^i \sum_{j+n=s-i} a^j b^n \sum_{}^{'} c_{i,j,n,\text{pair}}\, \mathrm{e}^{\mathrm{i}t\sum''(j'+n')/s_C}, \tag{7.11}$$

where $\sum'$ is the sum over pairs of tuples, one j-tuple of $j' \in \{0, 1, \ldots, N_C\}$ with non-vanishing $a_{C,j'}$ for some $C \in \mathcal{C}$ and one n-tuple of $n' \in \{0, 1, \ldots, M_C\}$ with non-vanishing $b_{C,n'}$ for some $C \in \mathcal{C}$ and for each such pair of such tuples $\sum''$ is taken to be the sum over all entries j' of the j-tuple plus the sum over all entries n' of the n-tuple. The coefficients $c_{i,j,n,\text{pair}}$ are complex numbers depending on the values of i, j, n and the pair of tuples.

The two conditions listed in Lemma 7.5 imply that Equation (7.11) results in

$$g_{a,b}(u,t) = \sum_{i=0}^{s} u^i \sum_{j+n=s-i} a^j b^n \sum_{}^{'} c_{i,j,n,\text{pair}}\, \mathrm{e}^{\mathrm{i}t(jx+ny+2^{r+1}m_{\text{pair}})/s_C}, \tag{7.12}$$

where m_{pair} is an integer depending on the pair of tuples.

With this equality and $q_1 = x/2^m$, $q_2 = y/2^m$ the map $p_{a,b,k}$ becomes

$$\begin{aligned} p_{a,b,k}(u,v) &= (v\overline{v})^{sk} g_{r^{x/2^m} a, r^{y/2^m} b}\left(\frac{u}{(v\overline{v})^k}, t\right) \\ &= (v\overline{v})^{sk} \sum_{i=0}^{s} \left(\frac{u}{(v\overline{v})^k}\right)^i \sum_{j+n=s-i} \sqrt{v\overline{v}}^{\frac{xj+ny}{2^m}} a^j b^n \sum_{}^{'} c_{i,j,n,\text{pair}} \left(\frac{v}{\sqrt{v\overline{v}}}\right)^{\frac{jx+ny+2^{m+1}m_{\text{pair}}}{s_C}}. \end{aligned} \tag{7.13}$$

What we need to show is that for every i, j, n and m_{pair} that can appear in this expression with a non-zero coefficient the exponent of $\sqrt{v\bar{v}}$ is even, so that one obtains a polynomial in u, v and $\bar{v}$. We know that $g_{a,b}$ is a polynomial in u, e^{it} and e^{-it}, so for all terms that have a non-vanishing coefficient $c_{i,j,n,\text{pair}}$, the exponent of e^{it} given by $(jx + ny + 2^{m+1}m_{\text{pair}})/s_C$ is an integer. This means that $(jx + ny + 2^{m+1}m_{\text{pair}})$ is a multiple of s_C and hence divisible by 2^m, which is by definition a divisor of s_C. It follows that $jx + ny$ is a multiple of 2^m.

Now consider a monomial of $p_{a,b,k}$. The exponent of $\sqrt{v\bar{v}}$ in a monomial is given by $(jx + ny)/2^m - (jx + ny + 2^{m+1}m_{\text{pair}})/s_C$. By the remark above this is an integer and hence $(jx + ny)s_C/2^m - (jx + ny + 2^{m+1}m_{\text{pair}})$ is a multiple of s_C. We find that

$$\begin{aligned}(jx + ny)\frac{s_C}{2^m} - (jx + ny + 2^{m+1}m_{\text{pair}}) &= -2^{m+1}m_{\text{pair}} - (jx + ny)(\frac{s_C}{2^m} - 1)\\ &\equiv 0 \bmod 2^{m+1}, \end{aligned} \tag{7.14}$$

since $jx + ny$ is a multiple of 2^m and 2^m is the highest power of two dividing s_C. Thus $s_C/2^m$ is odd and hence $(s_C/2^m - 1)$ is even and $(jx + ny)(s_C/2^m - 1)$ is divisible by 2^{m+1}.

It follows that $(jx + ny)s_C/2^m - (jx + ny + 2^{m+1}m_{\text{pair}})$ is a multiple of $2s_C$ and hence the exponent of $\sqrt{v\bar{v}}$, which is $(jx + ny)/2^m - (jx + ny + 2^{m+1}m_{\text{pair}})/s_C$ is even. □

Note that by Lemma 7.2 $p_{a,b,k}$ has a weakly isolated singularity at the origin with the closure of B as the link of the singularity. Hence Lemma 7.2 and Lemma 7.5 provide a way of constructing the maps that were shown to exist by Akbulut and King for closures of braids that allow certain parametrisations.

It follows from Lemma 7.2 and Lemma 7.5 that all lemniscate links, which are defined and discussed in more detail in Chapter 4, can be constructed as links of weakly isolated singularities of semiholomorphic polynomials $p_{a,b,k} : \mathbb{R}^4 \to \mathbb{R}^2$.

We are not aware of a general procedure that decides if a given link is the closure of a braid that admits a parametrisation as in Lemma 7.4 or as in Lemma 7.5. An obvious obstruction is that the the links from Lemma 7.4 are 2-periodic.

The braids of the form in Lemma 7.5 must in particular satisfy that all Fourier frequencies with non-zero coefficient in the parametrisation of the x-coordinate are in the same residue class $\bmod 2$ and all frequencies with non-zero coefficient in the parametrisation of the y-coordinate are in the same residue class $\bmod 2$. This makes each F_C and G_C into a periodic or anti-periodic function, i.e. $F_C(t +$

$\pi) = F_C(t)$ if x is even and $F_C(t+\pi) = -F_C(t)$ if x is odd. These symmetries in the braid parametrisation are reflected in symmetries of the corresponding braid words. These are easier to describe if we assume in the following that s_C, the number of strands in each link component, is odd.

If both x and y are even, then it is a parametrisation as in Lemma 7.4 and the closure must be 2-periodic.

If the trigonometric polynomials F_C parametrising the x-coordinate have only odd frequencies and all G_C only even ones (or similarly the other way around), then for every crossing, say $F_C(t) = F_{C'}(t')$ with $ts_C = t's_{C'} = t's_C \bmod 2\pi$, there is another crossing with $F_C(t+\pi) = -F_C(t) = -F_{C'}(t') = F_{C'}(t+\pi)$ and $(t+\pi)s_C = (t'+\pi)s_{C'} = (t'+\pi)s_C \bmod 2\pi$. For example if $F_C\left(\frac{t+2\pi j}{s_C}\right) = F_{C'}\left(\frac{t+2\pi k}{s_C}\right)$, then $F_C\left(\frac{t+\pi+2\pi(j+(s_C-1)/2)}{s_C}\right) = F_{C'}\left(\frac{t+\pi+2\pi(k+(s_C-1)/2)}{s_C}\right)$.

This means that any braid B that can be parametrised this way is of the form

$$B = \sigma_{j_1}^{\epsilon_1}\sigma_{j_2}^{\epsilon_2}\dots\sigma_{j_l}^{\epsilon_l}\ \sigma_{s-j_1}^{-\epsilon_1}\sigma_{s-j_2}^{-\epsilon_2}\dots\sigma_{s-j_l}^{-\epsilon_l}, \tag{7.15}$$

i.e. the second half of the braid word is identical to the first, but with mirrored indices and signs. If we write

$$\Delta_s = (\sigma_1)(\sigma_2\sigma_1)(\sigma_3\sigma_2\sigma_1)\dots(\sigma_{s-1}\dots\sigma_1) \tag{7.16}$$

for the Garside element, the half twist of all strands, and $\overline{w}$ for the mirrored word $\prod_{i=1}^{l}\sigma_{j_i}^{-\epsilon_i}$ of the word $w = \prod_{i=1}^{l}\sigma_{j_i}^{\epsilon_i}$, then braids of this form can be written as

$$B = w\Delta_s\overline{w}\Delta_s^{-1}. \tag{7.17}$$

Note that the braids that can be parametrised so that all F_C's have only odd frequencies and all G_C's have only even frequencies can be rotated by $\pi/2$ to give a braid in with a parametrisation where all F_C's have only even frequencies and all G_C's have only odd frequencies. This rotation is a braid conjugation, so the two classes of symmetries actually give rise to the same links.

If both x and y are odd and s_C is odd too, then the link is the closure of a braid B of the form $B = w\Delta_s w\Delta_s^{-1}$ for some braid word w, i.e. the second half of B is the same as the first, but with mirrored indices,

$$B = \sigma_{j_1}^{\epsilon_1}\sigma_{j_2}^{\epsilon_2}\dots\sigma_{j_l}^{\epsilon_l}\ \sigma_{s-j_1}^{\epsilon_1}\sigma_{s-j_2}^{\epsilon_2}\dots\sigma_{s-j_l}^{\epsilon_l}, \tag{7.18}$$

If s_C is even, the symmetry in the braid word is more complicated and so far we have not found a precise description. The difficulty arises because the symmetry of the parametrisation implies that a crossing at a given value of t

and $F_C(\frac{t+2\pi j}{s_C})$ leads to another crossing at t and $-F_C(\frac{t+2\pi j}{s_C})$ (rather than $t+\pi$ as in the previous case). There is now a multitude of different cases, depending on for which values of t there are strands that cross at $F_C\left(\frac{t+2\pi j}{s_C}\right) = 0$ (and thus do not necessarily induce an extra crossing) and how many of these strands there are. Note that several crossings could occur simultaneously at a given value of t at $F_C\left(\frac{t+2\pi j}{s_C}\right) = 0$. This makes a description of the symmetry in terms of braid words harder than in the previous cases.

Although we are not aware of any concrete examples, we expect that not every braid with a braid word of one of the forms above satisfies the conditions in Lemma 7.5. Again we are not aware of an algorithm that determines whether a given link satisfies one of these properties.

Lemmas 7.4 and 7.5 allow us to construct polynomial maps $\mathbb{R}^4 \to \mathbb{R}^2$ whose vanishing set on the three-sphere of any radius is a certain link. As mentioned in the Chapter 3 the initial motivation for us to construct knotted vanishing sets of polynomials came from physics. A polynomial whose nodal set on a three-sphere is a given link can be used as an initial configuration in a variety of physical systems. We would like to point out that the polynomials constructed in this section can be used in this way when they are restricted to a three-sphere of radius ρ. However, since they are related to the polynomials from Chapter 5 simply by a rescaling of u, we do not really expect new insight into the physics of knotted fields from them.

The constructed polynomials have a weakly isolated singular point at the origin. In both Lemmas 7.4 and 7.5 the resulting polynomials are semiholomorphic and their degree with respect to the complex variable u is equal to the number of strands s used in the construction.

In the following we investigate if some of the constructed polynomials have in fact an isolated singular point rather than only a weakly isolated one.

7.3 Real algebraic links

Sections 7.1 and Section 7.2 describe an explicit construction of real polynomial maps with weakly isolated singularities, namely $p_{a,b,k}$. It is a natural question if in some cases the functions constructed in this manner have in fact an isolated singularity rather than only a weakly isolated singularity. A link L for which this is the case is then by definition real algebraic.

7.3.1 The proof of Theorem 7.1

Since the real algebraic links are a (conjecturally not proper [13]) subset of the fibred links [99], it is clear that in general the singular point of $p_{a,b,k}$ is not isolated. One natural family of links to consider consists of the links which are closures of braids that come with a natural fibration. Consider a braid parametrised as in Equation (5.3) and such that $g_{a,b}$ does not have any argument-critical points, i.e. for all $t \in [0, 2\pi]$ and $u \in \mathbb{C}$ we have $\nabla_{\mathbb{R}^2\times[0,2\pi]} \arg(g_{a,b}) \neq (0,0,0)$. Then $\arg(g_{a,b})$ extends to a fibration map from $S^3\backslash L$ to S^1, where L is the closure of B. Hence L is fibred. It turns out that a parametrisation of this form is almost sufficient to allow a construction of L as the link of an isolated real singularity.

Recall from Lemma 6.4 that if a braid w is homogeneous, then there is a braid parametrisation as in Equation (5.3) of a conjugate of w such that the resulting $g_{a,a}$ does not have any argument-critical points for any $a > 0$.

Suppose now that B is the square of another braid word, say $B = w^2$. Let

$$\bigcup_{C\in\mathcal{C}}\bigcup_{j=1}^{s_C}\left(F_C\left(\frac{t+2\pi j}{s_C}\right), G_C\left(\frac{t+2\pi j}{s_C}\right), t\right), \quad t \in [0, 2\pi], \tag{7.19}$$

be a finite Fourier parametrisation of the braid w. Then

$$\bigcup_{C\in\mathcal{C}}\bigcup_{j=1}^{s_C}\left(F_C\left(\frac{2t+2\pi j}{s_C}\right), G_C\left(\frac{2t+2\pi j}{s_C}\right), t\right), \quad t \in [0, 2\pi], \tag{7.20}$$

is a finite Fourier parametrisation of the braid B. Furthermore, if we use the parametrisation given in Equation (7.20) to define $g_{a,a}$ and $p_{a,a,k}$ as in Lemma 7.3 we find that all exponents of $\sqrt{v\bar{v}}$ in $p_{a,a,k}$ are even. Thus working with this parametrisation ensures that $p_{a,a,k}$ is a polynomial in u, v and $\bar{v}$ as shown in Lemma 7.4.

By Lemma 7.3 the function $p_{a,a,k}$ has a weakly isolated singularity at the origin.

Note that if w has a parametrisation as in Equation (7.19) such that the corresponding $g_{a,a}$ does not have any argument-critical points, then Equation (7.20) is a parametrisation of $B = w^2$ such that the function $g_{a,a}$ corresponding to this parametrisation does not have any argument-critical points either. Thus all squares $B = w^2$ of homogeneous braids w are conjugates of braids that have a parametrisation as in Equation (7.20) such that the corresponding $g_{a,a}$ does not have any argument-critical points and the corresponding $p_{a,a,k}$ with $q_1 = q_2 = 0$ is a polynomial in u, v and $\bar{v}$ with a weakly isolated singular point at the origin.

We now use Lemma 6.4 to show the following lemma.

Lemma 7.6. *Let $B = w^2$, where w is a homogeneous braid. Then there exists a finite Fourier parametrisation of a conjugate of B as in Equation (5.3) such that the resulting $p_{a,a,k}$ with $q_1 = q_2 = 0$ has an isolated singularity at the origin if a is small enough.*

Proof. As discussed above, there is a conjugate of B that has a finite Fourier parametrisation such that the corresponding $g_{a,a}$ does not have any argument-critical points and the corresponding $p_{a,a,k}$ is a polynomial in u, v and $\overline{v}$.

Assume (u, v) is a critical point of $p_{a,a,k}$ that is not the origin. Then since $p_{a,a,k}$ is a polynomial in u, it must be $\frac{\partial p_{a,a,k}}{\partial u}(u, v) = 0$. Otherwise the Cauchy-Riemann equations would guarantee that the Jacobian of $p_{a,a,k}$ at (u, v) has full rank. Since for $v = 0$ we have that $p_{a,a,k}(u, 0) = u^s$, a critical point which is not the origin must have non-zero v.

It follows from $p_{a,a,k}(u, r\,\mathrm{e}^{\mathrm{i}t}) = r^{2sk} g_{a,a}(u/r^{2k}, t)$ that for every $u \in \mathbb{C}$, $v = r\,\mathrm{e}^{\mathrm{i}t} \in \mathbb{C}\backslash\{0\}$ with $\frac{\partial p_{a,a,k}}{\partial u}(u, v) = 0$ we have

$$\frac{\partial \arg p_{a,a,k}}{\partial t}(u, r\,\mathrm{e}^{\mathrm{i}t}) = \frac{\partial \arg g_{a,a}}{\partial t}(u/r^{2k}, t) \neq 0, \tag{7.21}$$

since $g_{a,a}$ does not have any argument-critical points.

Consider now the Jacobian of $p_{a,a,k}$ at a point $(u, v) \in \mathbb{C}\times(\mathbb{C}\backslash\{0\})$ with $\frac{\partial p_{a,a,k}}{\partial u}(u, v) = 0$ using $(\mathrm{Re}(u), \mathrm{Im}(u), |v|, \arg(v))$ as a basis for $\mathbb{R}^4$. Whether the Jacobian has full rank or not does not depend on the choice of basis. We already know that in this basis the Jacobian has the form

$$\nabla p_{a,a,k}(u, v) = \begin{pmatrix} 0 & 0 & \alpha & \beta \\ 0 & 0 & \gamma & \delta \end{pmatrix}, \tag{7.22}$$

where $\alpha = \partial\mathrm{Re}(p_{a,a,k})/\partial r$, $\beta = \partial\mathrm{Re}(p_{a,a,k})/\partial \arg(v)$, $\gamma = \partial\mathrm{Im}(p_{a,a,k})/\partial r$ and $\delta = \partial\mathrm{Im}(p_{a,a,k})/\partial \arg(v)$. As in Equation (6.2) we find that Equation (7.21) is then equivalent to

$$\mathrm{Im}(p_{a,a,k})\beta - \mathrm{Re}(p_{a,a,k})\delta \neq 0. \tag{7.23}$$

We calculate

$$\begin{aligned} \frac{\partial p_{a,a,k}}{\partial r}(u, r\,\mathrm{e}^{\mathrm{i}t}) &= r^{2sk}\frac{\partial f_{a,a}}{\partial r}\left(\frac{u}{r^{2k}}, \mathrm{e}^{\mathrm{i}t}\right) + 2skr^{2sk-1} f_{a,a}\left(\frac{u}{r^{2k}}, \mathrm{e}^{\mathrm{i}t}\right) \\ &= -2kur^{2k(s-1)-1}\frac{\partial f_{a,a}}{\partial u} + 2skr^{2sk-1} f_{a,b}\left(\frac{u}{r^{2k}}, \mathrm{e}^{\mathrm{i}t}\right) \\ &= 2skr^{-1} p_{a,a,k}(u, r\,\mathrm{e}^{\mathrm{i}t}), \end{aligned} \tag{7.24}$$

where the last equality follows from $\frac{\partial f_{a,a}}{\partial u}\left(\frac{u}{r^{2k}}, \mathrm{e}^{\mathrm{i}t}\right) = r^{2k(1-s)}\frac{\partial p_{a,a,k}}{\partial u}(u, r\,\mathrm{e}^{\mathrm{i}t}) = 0$.

But this means that by Equation (7.23)

$$\begin{aligned}\beta\gamma - \alpha\delta &= 2skr^{2sk-1}\frac{\partial \mathrm{Im}(p_{a,a,k})}{\partial r}(u, vr\,\mathrm{e}^{\mathrm{i}t})\beta - 2skr^{2sk-1}\frac{\partial \mathrm{Re}(p_{a,a,k})}{\partial r}(u,v)\delta \\ &= 2skr^{-1}(\mathrm{Im}(p_{a,a,k}(u,v))\beta - \mathrm{Re}(p_{a,a,k}(u,v))\delta) \neq 0. \end{aligned} \tag{7.25}$$

Hence $\left(\begin{smallmatrix}\alpha & \beta\\ \gamma & \delta\end{smallmatrix}\right)$ has rank 2 and (u,v) is a regular point. Thus the origin is the only critical point of $p_{a,a,k}$ and therefore isolated. □

Since conjugate braids close to the same link, Lemma 7.6 concludes the proof of Theorem 7.1. We have shown that closures of even powers of homogeneous braids are real algebraic.

7.3.2 More constructions of real algebraic links

In Section 7.2 we introduced two classes of braid parametrisations that lead to $p_{a,b,k}$ being a polynomial map if q_1 and q_2 are chosen appropriately. The first of these classes is the set of squares of braids (cf. Lemma 7.4) and the second class consists of the braids whose parametrisations satisfy certain arithmetic conditions (cf. Lemma 7.5). For the first class we showed in the proof of Lemma 7.6 that one extra condition, namely the absence of argument-critical points, is sufficient to guarantee that $p_{a,b,k}$ has an isolated singular point. In this section we investigate the effects of such a parametrisation of braids that belong to the second class.

In the proof of Lemma 7.6 the stretching parameters a and b are constants (and in fact equal). In the following they depend on $r = |v|$, since for the relevant polynomial $p_{a,b,k}$ for braid parametrisations of the second class q_1 and q_2 are not both zero. While large parts of the proof of Lemma 7.6 remain unchanged, this fact implies that the derivatives with respect to r differ.

Recall that the arithmetic condition in Lemma 7.5 requires a finite Fourier parametrisation of the braid where for both the x-coordinate and the y-coordinate all frequencies with non-zero coefficients are in the same residue class $\bmod 2^{m+1}$, where 2^m is the largest power of 2 dividing s_C, the number of strands in each link component.

This way every parametrisation of this form specifies two residue classes mod 2^{m+1}, one for the x-coordinate and for the y-coordinate. While in general these two classes are not identical, we begin by studying the special case where they are.

Lemma 7.7. *Let B be a braid with a parametrisation as in Lemma 7.5 such that all $j \in \{0, 1, \dots, \max\{N_C, M_C\}\}$ with non-vanishing $a_{C,j}$ or $b_{C,j}$ are in the same residue class* $\bmod 2^{m+1}$*, i.e. $x = y$, and such that the function $g_{a,b}$ corresponding to this parametrisation does not have any argument-critical points for some $a, b > 0$. Then $p_{a,b,k}$ with $q_1 = q_2 = x/2^m$ has an isolated singular point at the origin and the vanishing set of $p_{a,b,k}$ on S^3_ρ is the closure of B for all positive $\rho \leq 1$.*

Proof. By Lemma 7.5 $p_{a,b,k}$ is a polynomial in u, v and $\bar{v}$. Note that if $x = y$, then

$$p_{a,b,k}(u, v) = (v\bar{v})^{s(k+x/2^m)} f_{a,b}\left(\frac{u}{(v\bar{v})^{k+x/2^m}}, \frac{v}{\sqrt{v\bar{v}}}\right) \tag{7.26}$$

and hence

$$p_{a,b,k}(u, r\,\mathrm{e}^{\mathrm{i}t}) = g_{r^{2(k+x/2^m)}a, r^{2(k+x/2^m)}b}(u, t) = r^{2s(k+x/2^m)} g_{a,b}\left(\frac{u}{r^{2(k+x/2^m)}}, \mathrm{e}^{\mathrm{i}t}\right) \tag{7.27}$$

and $p_{a,b,k}(u, 0) = u^s$.

It is easy to see that the origin is a singular point of $p_{a,b,k}$. As shown in Lemma 7.2 the vanishing set of $p_{a,b,k}$ on S^3_ρ is the closure of B for all positive $\rho \leq 1$.

What is left to show is that the singular point at the origin is isolated. This is similar to the proof of Lemma 7.6. Again every critical point of $p_{a,b,k}$ that is not the origin must satisfy $v \neq 0$ and $\partial p_{a,b,k}/\partial u = 0$. Since $g_{a,b}$ does not have any argument-critical points, $g_{\lambda a,\lambda b}$ does not have any argument-critical points either for any $\lambda > 0$. Hence the Jacobian $\nabla p_{a,b,k}$ is of the form of Equation (7.22) with $\mathrm{Im}(p_{a,b,k})\beta - \mathrm{Re}(p_{a,b,k})\delta \neq 0$.

The argument that the singular point at the origin is isolated is now seen to be exactly the same as in the proof of Lemma 7.6. □

In Lemma 7.7 the values of the scaling parameters a and b are not constant anymore, but depend on $r = |v|$. This dependence however, is exactly the same for a and b, namely $r^{x/2^m}$ times a constant. This makes the same arguments as in Lemma 7.6 work in this case, too.

If $x \neq y$ on the other hand, the derivatives with respect to $r = |v|$ now change in a non-trivial way compared to the derivatives in the proofs of Lemma 7.7 and Lemma 7.6. Furthermore, one essential tool in the proof of Lemma 7.7, that $g_{\lambda a,\lambda b}$ has argument-critical points if and only if $g_{a,b}$ has, can now not be employed, since a and b scale differently with r. Therefore, the described method of constructing isolated singularities does not necessarily work for these links.

Note that as in Theorem 7.1 the polynomial maps constructed in Lemma 7.7 are semiholomorphic in u and their degree with respect to u is equal to

the number of strands s used in the construction. In contrast to the construction of semiholomorphic polynomials with knotted vanishing sets on the unit three-sphere we cannot give a bound on the degree with respect to v and $\overline{v}$. This is due to the fact that because of the several conditions that the braid parametrisations have to satisfy we cannot use trigonometric interpolation to find a parametrisation of the desired form.

It is not clear how Lemma 7.7 could be used to decide whether a given link L is real algebraic. At least we are not aware of any algorithm that determines if L is the closure of a braid of the desired form.

However, Lemma 7.7 offers a way of constructing real algebraic links that are not necessarily of the form of Lemma 7.6. For each Fourier parametrisation that satisfies the arithmetic condition, we can try to find values of $a, b > 0$ such that $\arg g_{a,b}$ does not have any critical points. This might not always be possible, but if we can do this, then the closure of the braid parametrised in this way is real algebraic. The next section is devoted to following this procedure for particularly simple Fourier parametrisations.

7.4 Real algebraic lemniscate knots

We discussed lemniscate knots in Chapter 4 as a family of links that have a parametrisation as in Equation (5.3) of a particularly simple form. The (s, r, ℓ)-lemniscate link is the closure of the braid given by

$$\bigcup_{j=0}^{s-1}\left(\cos\left(\frac{rt+2\pi j}{s}\right), \sin\left(\frac{\ell(rt+2\pi j)}{s}\right), t\right) \qquad t \in [0, 2\pi]. \tag{7.28}$$

Several properties of this family of links can be found in Chapter 4, among others that a braid parametrised by Equation (7.28) has a braid word of the form $(\sigma_1^{\varepsilon_1}\sigma_3^{\varepsilon_3}\ldots\sigma_2^{\varepsilon_2}\sigma_4^{\varepsilon_4}\ldots)^r$, where $\varepsilon_j \in \{\pm 1\}$ depends on ℓ and s. In particular, this braid word is homogeneous and hence there exists a Fourier parametrisation of this braid whose corresponding function $g_{a,b}$ does not have any phase-critical points for some $a, b > 0$. However, this parametrisation might be different from the one given in Equation (7.28).

Lemma 7.2 and Lemma 7.5 give us a way of explicitly constructing any lemniscate link as the link of a weakly isolated singularity, since the defining parametrisation obviously satisfies the conditions of Lemma 7.5.

The lemniscate links for which Lemma 7.7 implies the stronger notion of isolation of the singular point must satisfy

$$r\ell \equiv r \bmod 2^{m+1}, \tag{7.29}$$

where 2^m is the largest power of 2 dividing $s_C = s/\gcd(s,r)$. Since all lemniscate links are closures of homogeneous braids, all lemniscate links with even r are real algebraic and can be constructed as links of isolated real singularities as described in Section 7.1. We can hence assume that r is odd and thus 2^m is the largest power dividing s.

If r is odd, then it is coprime to 2^{m+1} and hence Equation (7.29) implies $\ell \equiv 1 \bmod 2^{m+1}$. These are all lemniscate links that Lemma 7.7 can potentially be applied to and that are not already covered by Section 7.1.

We encounter one typical intricacy in the application of Lemma 7.7. As we have seen, a lemniscate link with $\ell \equiv 1 \bmod 2^{m+1}$ has a Fourier parametrisation that satisfies the desired arithmetic properties. That same braid is homogeneous and hence also has a parametrisation that satisfies the condition that the corresponding $g_{a,b}$ does not have any argument-critical points. In order to use Lemma 7.7 we need to find a parametrisation that satisfies both conditions simultaneously.

Note that by Lemma 7.7 finding a value for b such that $g_{1,b}$, constructed as in Equation (7.1) from Equation (7.28), does not have any argument-critical points is sufficient to show that the closure of the braid is real algebraic. Finding such a b for the $(s,1,\ell)$-lemniscate link shows that every (s,r,ℓ)-lemniscate link is real algebraic.

We denote by $c_k(t)$, $k = 1,2,\dots,s-1$ the $s-1$ solutions of $\frac{\partial g_{1,b}}{\partial u}(u,t) = 0$ for a given $t \in [0,2\pi]$ and need to check that

$$\frac{\partial \arg g_{1,b}(c_k(t),t)}{\partial t} = \operatorname{Im} \sum_{j=1}^{s} \frac{\frac{1}{s}\sin\left(\frac{t+2\pi j}{s}\right) - \frac{ib\ell}{s}\cos\left(\frac{\ell(t+2\pi j)}{s}\right)}{u_k(t) - \cos\left(\frac{t+2\pi j}{s}\right) - ib\sin\left(\frac{\ell(t+2\pi j)}{s}\right)} \neq 0 \tag{7.30}$$

for all $k = 1,2,\dots,s-1$ and all $t \in [0,2\pi]$.

In the case of $\ell = 3$ and $s = 5$, which are the lowest numbers satisfying $\ell \equiv 1 \bmod 2^{m+1}$ that do not lead to torus links, we find numerically that it is sufficient to let b equal $1/4$. Thus the $(s=5,r,\ell=3)$-lemniscate link is real algebraic for every r.

This includes several examples of real algebraic links that are not covered by Theorem 7.1.

Preliminary numerical investigation indicates that for other lemniscate links small enough choices of b again lead to braid polynomials $g_{1,b}$ without any argument-critical points. We may thus conjecture that all lemniscate links with $\ell \equiv 1 \bmod 2^{m+1}$ are real algebraic, but at the moment this remains an open problem.

An analytic proof of this would be desirable, but note that for $b = 0$ the function $\frac{\partial \arg g_{1,0}}{\partial t}(c_k(t), t)$ is piecewise constant where it is defined. This means that using limit arguments becomes challenging.

It becomes increasingly harder to determine sufficient values of b numerically as ℓ and s increase, since it involves finding the roots of a continuous family of polynomials of degree $s-1$.

7.5 The strong Milnor condition

For a complex plane curve $f : \mathbb{C}^2 \to \mathbb{C}$ with an isolated singularity at the origin $f/|f|$ automatically is a fibration of $S^3_\epsilon \backslash f^{-1}(0)$ over S^1 for small enough $\epsilon > 0$. Even though real algebraic links are fibred, it is not always the case that $f/|f|$ is a fibration of $S^3_\epsilon \backslash f^{-1}(0)$ when $f : \mathbb{R}^4 \to \mathbb{R}^2$ is a polynomial with an isolated singularity.

The following definitions and Theorem 7.11 can be found in [33] and [34].

Definition 7.8. *Let $f : \mathbb{R}^4 \to \mathbb{R}^2$ be a polynomial map with isolated singular point at the origin. Then f satisfies the **strong Milnor condition** if there exists an $\epsilon > 0$ such that*

$$f/|f| : S^3_\rho \backslash f^{-1}(0) \to S^1 \tag{7.31}$$

is a fibration for all $0 < \rho < \epsilon$.

In this section we show that the maps $p_{a,b,k}$ as in Lemma 7.6 and Lemma 7.7 satisfy the strong Milnor condition. Milnor himself remarks in his book [99] that the condition is so strong that it is very difficult to find non-trivial examples, i.e. examples that are not simply complex plane curves written as real polynomial maps. Until A'Campo gave the first example in [1], it was not even known if they exist.

We start with a definition.

Definition 7.9. *Let $f : \mathbb{R}^4 \to \mathbb{R}^2$ be a polynomial map with an isolated singularity at the origin and $\mathcal{L}_\ell \subset \mathbb{R}^2$ be the line through the origin corresponding to $\ell \in \mathbb{RP}^1$.*

Then we define $X_\ell = \{x \in \mathbb{R}^4 : f(x) \in \mathcal{L}_\ell\}$ *and call* $X = \{X_\ell : \ell \in \mathbb{RP}^1\}$ *the* ***canonical pencil****.*

Note that with this definition each X_ℓ is a 3-dimensional manifold and the different X_ℓ meet at $f^{-1}(0)$.

Definition 7.10. *We say a map* $f : \mathbb{R}^4 \to \mathbb{R}^2$ *is* **d-*regular*** *with respect to the standard metric on* $\mathbb{R}^4$ *if there exists an* $\epsilon > 0$ *such that every three-sphere* S^3_ρ *of radius* $\rho < \epsilon$ *intersects all* $X_\ell \backslash f^{-1}(0)$ *transversely (provided the intersection is non-empty).*

The property of d-regularity can be used to study if a given map satisfies the strong Milnor condition.

Theorem 7.11. *(cf. [33]) If a polynomial map* $f : \mathbb{R}^4 \to \mathbb{R}^2$ *with an isolated singularity at the origin is* d*-regular with respect to the standard metric, then it satisfies the strong Milnor condition.*

The concept of d-regularity can also be defined for metrics that are not the standard metric. In fact, d-regularity for some metric induced by a positive definite quadratic form is equivalent to the strong Milnor condition. In the case of the maps that we constructed in Section 7.3, it is sufficient to consider the standard metric.

Proposition 7.12. *Let* $p_{a,b,k}$ *be a polynomial constructed as in Lemma 7.6 or Lemma 7.7. Then* $p_{a,b,k}$ *is* d*-regular with respect to the standard metric.*

Proof. We need to show that for all small enough radii ρ and all $\ell \in \mathbb{RP}^1$ the intersection $S^3_\rho \cap X_\ell$ is either empty or transverse.

Let $(u, v) \in S^3_\rho \cap X_\ell$. There are three different cases to consider: one where $u = 0$, one where $v = 0$ and the remaining case where both are non-zero.

If $u = 0$, then either $p_{a,b,k}(0, r\,\mathrm{e}^{\mathrm{i}t})$ is for every fixed $t \in [0, 2\pi]$ constant zero (if $g_{a,b}(0, t) = 0$) or the argument $\arg(p_{a,b,k})(0, r\,\mathrm{e}^{\mathrm{i}t})$ is constant for all $r > 0$. Hence in the basis $(\mathrm{Re}(u), \mathrm{Im}(u), r, t)$ the vector $(0, 0, 1, 0)$ is tangent to X_ℓ at $(0, v)$. Thus the intersection with S^3_ρ is transverse.

If $v = 0$, then $p_{a,b,k}(u, 0) = u^s$. Hence in the basis $(|u|, \arg(u), \mathrm{Re}(v), \mathrm{Im}(v))$ the vector $(1, 0, 0, 0)$ is a tangent to X_ℓ at $(u, 0)$ and hence the intersection with S^3_ρ is transverse.

Now suppose both u and v are non-zero. Then we can use $(|u|, \arg(u), r, t)$ as a basis and by definition of $p_{a,b,k}$ the vector $(r^{2k+x/2^m}, 0, 1, 0)$ is tangent to

X_ℓ at (u,v). The tangent space of S^3_ρ at (u,v) is spanned by $(0,1,0,0)$, $(0,0,0,1)$ and $(-r/\sqrt{\rho^2-r^2},0,1,0)$. Thus the intersection is not transverse if and only if $r^{2k+x/2^m} = -r/\sqrt{\rho^2-r^2}$. Since $r > 0$, this equality is never satisfied, which completes the proof of d-regularity of $p_{a,b,k}$. □

The next corollary follows from Theorem 7.11 and Proposition 7.12.

Corollary 7.13. *The maps constructed in Lemma 7.6 and Lemma 7.7 satisfy the strong Milnor condition.*

We have thus shown that for small enough radii ρ

$$p_{a,b,k}/|p_{a,b,k}| : S^3_\rho \backslash p^{-1}_{a,b,k}(0) \to S^1 \tag{7.32}$$

is a fibration.

We hope that the explicit construction of polynomials and fibrations for the links that were shown to be real algebraic in Section 7.3 helps to investigate properties of real algebraic links and of their fibrations.

7.6 Discussion

We have shown that with slight modification to the construction from Chapters 5 and 6 we can construct polynomials with (weakly) isolated singularities and the desired link around them, as long as the link is the closure of a braid that can be parametrised in certain ways. It is not at all clear how to decide if a link is the closure of such a braid, but we have seen that closures of squares of homogeneous braids and some lemniscate links are in this family. In particular, this shows that these links are real algebraic, which constitutes the first proof of real algebraicity of an infinite family of links since Looijenga in 1971 [90].

Extending these results to a larger class of links (such as all closures of homogeneous braids) must involve new conditions on braid parametrisations to lead to desired polynomials, or a method to decide whether a braid can be parametrised as specified.

Furthermore, we find that the arguments of the constructed polynomials give fibrations of the link complement in small three-spheres around the singularity, a property that is usual called the strong Milnor condition.

In the case of algebraic links (the complex setting), there are striking connections between algebro-geometric quantities of the plane curves and link

invariants of the link of the singularity. Maulik [97] proved a conjecture by Oblomkov and Shende, that expresses the HOMFLY polynomial of the link in terms of the Euler characteristics of refined punctual Hilbert schemes [108]. A similar conjecture exists for the HOMFLY homology as well [106]. Similarly, the singularities of complex plane curves are related to the double affine Hecke algebra [32]. Another nice property that is true for algebraic links and that we can investigate for our constructed polynomials, is that the monodromy of the fibration map can be arranged to not have any fixed points [2]. Explicit constructions like the one outlined in this chapter could help in the investigation of potential real analogues of these results and conjectures.

The topology of analytic maps around isolated singularities is also a research topic in higher dimensions [98]. There is a straight-forward generalisation of our construction, which was suggested by Ishikawa [62]. We consider the map

$$(x_1, x_2, \ldots, x_n) \mapsto (\mathrm{Re}(p_{a,b,k}(x_1, x_2, x_3, x_4)), \mathrm{Im}(p_{a,b,k}(x_1, x_2, x_3, x_4)), x_5^2, x_6^2, \ldots, x_n^2). \tag{7.33}$$

This is a polynomial $\mathbb{R}^n \to \mathbb{R}^{n-2}$ that has an isolated singularity at the origin if $p_{a,b,k} : \mathbb{R}^4 \to \mathbb{R}^2$ does. A more general construction in higher dimensions would be desirable, but is still not found.

8 Crossing numbers of composite knots and embedded graphs

In this chapter we turn our attention away from the construction of polynomials and to one of the oldest open conjectures in knot theory, namely that the minimal crossing number is additive under the connected sum operation. That is, given two knots K_1 and K_2 of minimal crossing numbers $c(K_1)$ and $c(K_2)$ respectively, is it true that $c(K_1\#K_2) = c(K_1) + c(K_2)$? A positive answer to this question would not only help the understanding of this most fundamental knot invariant, but also contradict other conjectures, for example that the percentage of hyperbolic knots among all prime knots of minimal crossing number at most n approaches 100 as n goes to infinity [94].

By definition of the connected sum, we have $c(K_1\#K_2) \leq c(K_1) + c(K_2)$. Equality is established if both knots are torus knots [42, 59] or if both are alternating [102, 69, 131] (or more generally adequate [87]), but in general it is not even known if $c(K_1\#K_2) \geq c(K_1)$. The best lower bound that we are aware of, $c(K_1\#K_2) \geq \frac{1}{152}(c(K_1) + c(K_2))$, was shown by Lackenby [81]. In fact, he showed the stronger result that $c(K_1\#K_2\#\ldots\#K_n) \geq \frac{1}{152}\sum_{k=1}^{n} c(K_i)$ for all knots K_i and all $n \in \mathbb{Z}_{>0}$.

In this chapter we prove relations between the minimal crossing numbers of composite knots and certain spatial graphs, in particular theta-curves. We also formulate additional relations that, if satisfied, imply the additivity of crossing numbers or at least give a lower bound. Checking these conditions is very challenging, but we hope that this work inspires a general method to make progress in the crossing number conjecture.

A theta-curve is an embedding of the theta-graph θ (cf. Figure 8.2a)) in S^3, the planar graph consisting of two vertices with three edges between them. Theta-curves are studied up to equivalence under ambient isotopy. Therefore a large number of tools from knot theory applies to the theory of theta-curves

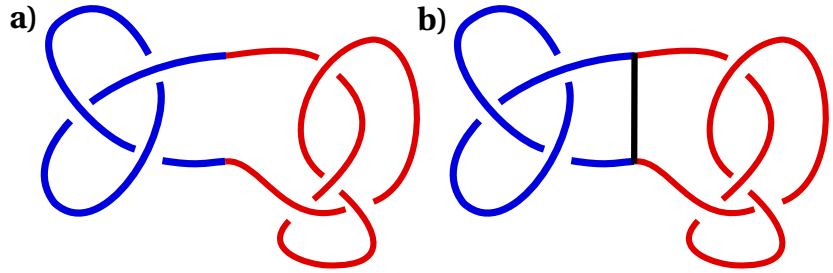

Figure 8.1: The definition of θ_{K_1,K_2}. a) A diagram of the connected sum $3_1\#4_1$. b) Adding an extra unknotted arc results in the theta-curve $\theta_{3_1,4_1}$.

as well. In particular, we can study theta-curves by considering their diagrams, projections in the plane with at most double points at which intersections are transverse.

Thus many diagrammatic invariants that were defined to distinguish knots and links, such as the minimal crossing number, extend to theta-curves. We label the edges of a theta-curve by x, y and z as in Figure 8.2a) and denote the numbers of crossings between two strands, by the concatenation of the two corresponding letters. Hence xy denotes the number of crossings between the x-strand and the y-strand, xx denotes the number of crossings of the x-strand with itself and so on. Theta-curves and their connections to knot theory have been studied before and especially their connections to knotoids has been stressed [70, 96, 134].

There is a very natural way to associate a theta-curve to a pair of knots K_1, K_2, or more precisely to their connected sum $K_1\#K_2$. Consider the diagram of $K_1\#K_2$ in Figure 8.1a) used to define the connected sum. Then adding an unknotted arc between the two points where K_1 and K_2 are glued together results in a theta-curve, denoted by θ_{K_1,K_2}. Among all theta-curves there is a unique planar embedding and we call the corresponding isotopy type the trivial theta-curve. Then θ_{K_1,K_2} is the theta-curve that results from tying K_1 into the x-arc of the trivial theta-curve and K_2 in its z-arc.

Deleting any of the three edges of a theta-curve leaves a knot, in the case of θ_{K_1,K_2} we have $x \cup y = K_1$, $y \cup z = K_2$ and $x \cup z = K_1\#K_2$. Note that theta-curves are not uniquely characterised by the knot types of these three knots, their constituent knots. For example for Kinoshita's theta-curve in Figure 8.2b), all pairs of edges form the unknot, but it is not the planar theta-curve shown in Figure 8.2a).

Since for any diagram of θ_{K_1,K_2} we have $x \cup z = K_1\#K_2$, it is clear that $c(\theta_{K_1,K_2}) \geq$

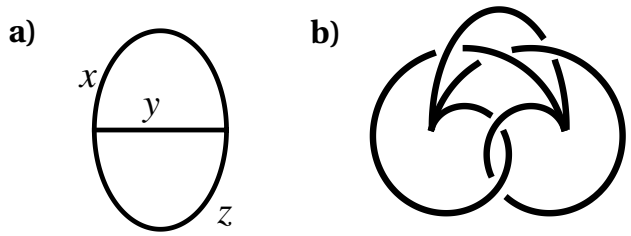

Figure 8.2: Two theta-curves with trivial constituent knots. a) The theta-graph in its planar embedding. b) Kinoshita's theta-curve. Both theta-curves have the same constituent knots, but are not ambient isotopic.

$c(K_1\#K_2)$ and from its construction we know that $c(\theta_{K_1,K_2}) \leq c(K_1) + c(K_2)$.

Although the definition of θ_{K_1,K_2} makes sense for all knots K_1 and K_2 and most statements remain true for composite knots, we require K_1 and K_2 to be prime in the following.

This chapter proceeds as follows. In Section 8.1 we relate $c(\theta_{K_1,K_2})$ to $c(K_1\#K_2)$.

In Section 8.2 we consider theta-curves of higher degree, that is, embeddings of planar graphs with two vertices and a number of edges between them. We are particularly interested in embeddings of the theta-curve with $2n$ edges, where n of the edges are tied into K_1 and the remaining n edges tied into K_2, similar to the case of θ_{K_1,K_2}. Here we show that for large enough n the minimal crossing number of these graphs is $n(c(K_1) + c(K_2))$.

Section 8.3 discusses a relation between $c(K_1\#K_2)$ and the minimal crossing numbers of the higher degree theta-curves $c(\Omega^n_{K_1,K_2})$ that are discussed in Section 8.2 resulting in the lower bound $c(K_1\#K_2) \geq \frac{1}{n^2}c(\Omega^n_{K_1,K_2})$. Thus finding values of n for which $c(\Omega^n_{K_1,K_2}) = n(c(K_1) + c(K_2))$ results in a lower bound of the form $c(K_1\#K_2) \geq \frac{1}{n}(c(K_1) + c(K_2))$.

In Section 8.4 we discuss further spatial graphs whose crossing numbers relate to the crossing numbers of composite knots.

The results from this chapter have originally appeared in [21].

8.1 The crossing numbers of theta-curves

Consider the theta-curve θ_{K_1,K_2}, which is shown in Figure 8.1b). Since deleting the y-arc in any diagram of θ_{K_1,K_2} results in a diagram of $K_1\#K_2$, we have the inequality

$$xx + xz + zz \geq c(K_1\#K_2) \tag{8.1}$$

for any diagram of θ_{K_1,K_2}, where we use the notation introduced above.

Similarly, $x \cup y = K_1$ and $y \cup z = K_2$ and we obtain

$$\begin{aligned} 2c(\theta_{K_1,K_2}) &= xx + xz + zz + xx + xy + yy + yy + yz + zz + xy + xz + yz \\ &\geq c(K_1\#K_2) + c(K_1) + c(K_2) + xy + xz + yz. \end{aligned} \tag{8.2}$$

Since xy, yz and xz are all non-negative, we obtain the inequality

$$2c(\theta_{K_1,K_2}) \geq c(K_1\#K_2) + c(K_1) + c(K_2). \tag{8.3}$$

Proposition 8.1. *The inequality in Equation (8.3) is an equality if and only if* $c(\theta_{K_1,K_2}) = c(K_1\#K_2) = c(K_1) + c(K_2)$.

In order to prove Proposition 8.1, we need the following lemma.

Lemma 8.2. *Let* κ_1, κ_2 *and* κ_3 *be knots and let* D *be a diagram of a theta-curve* θ *where* $x \cup z = \kappa_1$, $y \cup z = \kappa_2$ *and* $x \cup y = \kappa_3$ *and no pair of arcs cross each other, i.e.* $xy + yz + xz = 0$. *Then there are knots* K_1', K_2' *and* K_3' *such that* $\kappa_1 = K_1'\#K_3'$, $\kappa_2 = K_2'\#K_3'$ *and* $\kappa_3 = K_1'\#K_2'$. *Furthermore,* $xx \geq c(K_1')$, $yy \geq c(K_2')$, $zz \geq c(K_3')$ *and thus* $c(D) \geq c(K_1') + c(K_2') + c(K_3')$.

Proof. Consider the diagram D as a subset of the Euclidean plane with crossings as double points. Around each of the two nodes n_1, n_2 there is a neighbourhood $U(n_i)$ such that $(U(n_i)\backslash D) \cup \{n_i\}$ is path-connected. For small enough $\epsilon > 0$ the boundary of the ϵ-neighbourhood $U_\epsilon(D) = \{a \in \mathbb{R}^2\backslash(U(n_1) \cup U(n_2)) : \min_{b\in D} |a - b| < \epsilon\}$ of D is a collection of loops and divides $\mathbb{R}^2\backslash(U(n_1) \cup U(n_2))$ into a number of path-connected components.

We claim that the two nodes are in the same component of $P = (\mathbb{R}^2\backslash(\partial U_\epsilon(D) \cup (D \cap U(n_1) \cup (D \cap U(n_2)) \cup \{n_1\} \cup \{n_2\}$ shown in Figure 8.3d). Then there is a path $\gamma \subset P$ from n_1 to n_2. Since γ does not cross $\partial U_\epsilon(D)$, $D \cap U(n_1)$ or $D \cap U(n_2)$, it does not have any crossings with D and it can be be chosen to not cross itself. Call $K_1' := x \cup \gamma$, $K_2' := y \cup \gamma$ and $K_3' := z \cup \gamma$. Since γ does not have any crossings with D or with itself, we have $xx + x\gamma + \gamma\gamma = xx \geq c(K_1')$ and similarly $yy \geq K_2'$ and $zz \geq K_3'$. Note that it follows from the uniqueness of prime decomposition of knots that $xy = xz = yz = 0$ implies that $x \cup y = K_1'\#K_2'$, $y \cup z = K_2'\#K_3'$ and $x \cup z = K_1'\#K_3'$.

What is left to show is the claim that the two nodes are in the same path component of P. Assume they are not in the same path component. Then there is a loop $\ell \subset \partial(U_\epsilon(D)\backslash(U(n_1) \cup U(n_2))$ such that one of the nodes is in the bounded component of $\mathbb{R}^2\backslash\ell$ and the other one is in the unbounded component.

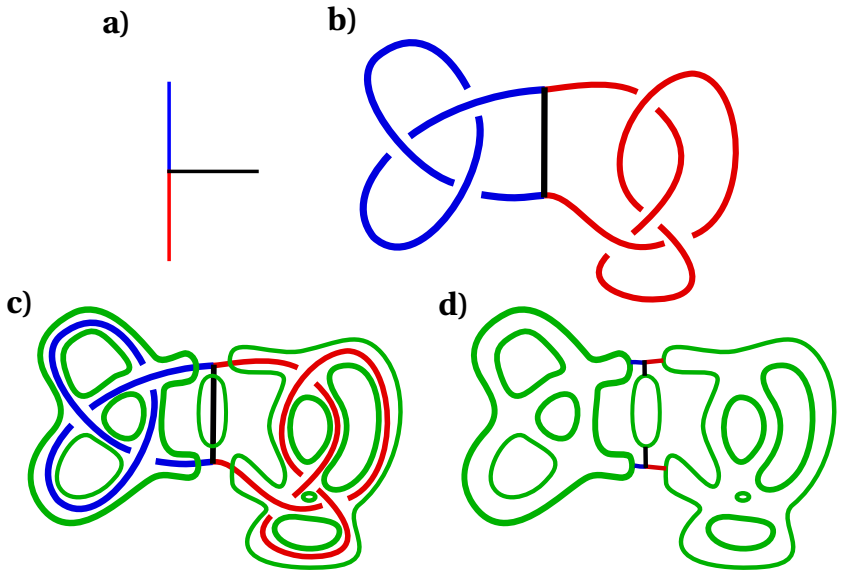

Figure 8.3: Illustration of the proof that the two nodes lie in the same path-connected component of P. a) The diagram D around a node n_i. b) A diagram of θ_{K_1,K_2}. c) The boundaries of the ϵ-neighbourhood of the diagram divide the plane into path-connected components. d) The two nodes are in the same path-connected component of P.

Since $xy = yz = xz = 0$, the loop ℓ is a boundary component of exactly one of $U_\epsilon(x) = \{p \in \mathbb{R}^2 \backslash (U(n_1) \cup U(n_2)) : \min_{q \in x} |p - q| < \epsilon\}$, $U_\epsilon(y)$ or $U_\epsilon(z)$ (defined analogously). But since x, y and z are paths from n_1 to n_2, all of them must cross ℓ. Then all of them must also cross the arc associated to ℓ (i.e. x if ℓ is a boundary component of $U_\epsilon(x)$ and so on) contradicting $xy = yz = xz = 0$. This proves the claim and finishes the proof of the lemma. □

Proof of Proposition 8.1. Note that in the case of $\theta = \theta_{K_1,K_2}$, we have $\kappa_1 = K_1 \# K_2$, $\kappa_2 = K_2$ and $\kappa_3 = K_1$.

We assume that $2c(\theta_{K_1,K_2}) = c(K_1) + c(K_2) + c(K_1 \# K_2)$. Then by Equation (8.2) we have $xy = yz = xz = 0$. Now we apply Lemma 8.2 to θ_{K_1,K_2}. We thus have knots K_1', K_2' and K_3' such that $K_1 \# K_2 = K_1' \# K_3'$, $K_2 = K_2' \# K_3'$ and $K_1 = K_1' \# K_2'$. Note that this implies $K_1' = K_1$, $K_2' = O$ and $K_3' = K_2$ and thus $c(\theta_{K_1,K_2}) \geq c(K_1) + c(K_2)$. Therefore $c(\theta_{K_1,K_2}) = c(K_1) + c(K_2)$ and since we assumed $c(K_1 \# K_2) = 2c(\theta_{K_1,K_2}) - c(K_1) - c(K_2)$, we have $c(K_1 \# K_2) = c(K_1) + c(K_2)$.

Now assume that $c(\theta_{K_1,K_2}) = c(K_1 \# K_2) = c(K_1) + c(K_2)$. Then the inequality Equation (8.2) is obviously an equality, which completes the proof of the proposition. □

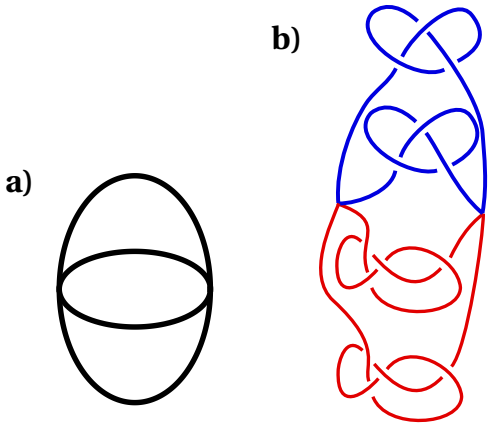

Figure 8.4: Definition of theta-curves of higher order. a) The planar embedding of the 4-theta-graph. b) A diagram for the ambient isotopy type $\theta^2_{K_1=3_1,K_2=4_1}$.

8.2 Higher degree theta-curves

In the previous section theta-curves are shown to be closely related to composite knots. A next plausible step is to add more arcs between the two nodes. In this section we consider graphs that have two nodes and $2n$ arcs between them, i.e. $2n$-theta-curves or theta-curves of degree $2n$. We sometimes refer to theta-curves with 3 edges and 2 vertices as *classical theta-curves* or *theta-curves of degree 3*.

Again there is a unique planar embedding of this graph, the trivial theta-curve of degree $2n$ as in Figure 8.4a). Tying knots into the different arcs is still a well-defined operation and we can thus study the minimal crossing number of the graph $\theta^n_{K_1,K_2}$ which is obtained from the trivial theta-curve of order $2n$ by tying K_1 into n arcs and K_2 into the remaining n arcs (cf. Figure 8.4b)). Note that $\theta^1_{K_1,K_2}$ is simply the connected sum $K_1\#K_2$.

We label the edges with a K_1 in it by $x_1,\dots,x_n$ and the edges with a K_2 in it by $z_1,\dots,z_n$. We thus obtain the following constituent knots: $x_i \cup z_j = K_1\#K_2$, $x_i \cup x_j = K_1\#K_1$ and $z_i \cup z_j = K_2\#K_2$ for all distinct $i,j \in \{1,\dots,n\}$.

We adopt the notation from the previous section, so x_ix_j denotes the number of times the edge x_i crosses the edge x_j. Analogous notations hold for the other edges.

The first thing that we should note is a direct corollary from Lemma 8.2.

Corollary 8.3. *For all knots K_1, K_2 and all $n \in \mathbb{N}$ we have that $c(\theta^n_{K_1,K_2}) \geq nc(K_1\#K_2)$. There is one $n > 1$ for which equality holds if and only if $c(K_1\#K_2) =$*

$c(K_1) + c(K_2)$.

Proof. The inequality follows directly from the definition of θ_{K_1,K_2}, in particular from the fact that $x_i \cup z_j = K_1 \# K_2$ for all i and j. In other words, for all $k \in \{0, 1, \dots, n-1\}$ we have

$$c(\theta^n_{K_1,K_2}) \geq \sum_{i=1}^{n} (x_i x_i + x_i z_{1+(i+k) \bmod n} + z_{1+(i+k) \bmod n} z_{1+(i+k) \bmod n}) + \sum_{\substack{i,j=1 \\ i>j}}^{n} (x_i x_j + z_i z_j) + \sum_{\substack{i,j=1 \\ j \neq (1+(i+k) \bmod n}}^{n} x_i z_j. \tag{8.4}$$

Summing over all k and using that $x_i \cup z_j = K_1 \# K_2$ for all i, j, we get

$$nc(\theta_{K_1,K_2}) \geq n^2 c(K_1 \# K_2) + (n-1) \sum_{i,j=1}^{n} x_i z_j + n \sum_{\substack{i,j=1 \\ i>j}}^{n} (x_i x_j + z_i z_j). \tag{8.5}$$

Thus $c(\theta_{K_1,K_2}) \geq nc(K_1 \# K_2)$ and if equality holds, then there are no crossings between different edges.

Hence in this case every edge is part of a classical theta-curve (as in Section 8.1), where none of the strands cross each other. It follows from Lemma 8.2 that each edge crosses itself at least $c(K_i)$, $i = 1, 2$ number of times, respectively, meaning $x_i x_i \geq c(K_1)$ and $z_i z_i \geq c(K_2)$ for all $i \in \{1, \dots, n\}$. Thus $c(\theta^n_{K_1,K_2}) = n(c(K_1) + c(K_2))$ and since $c(\theta^n_{K_1,K_2}) = nc(K_1 \# K_2)$ by assumption, we have $c(K_1 \# K_2) = c(K_1) + c(K_2)$.

If $c(K_1 \# K_2) = c(K_1) + c(K_2)$, then $c(\theta^n_{K_1,K_2}) \geq n(c(K_1) + c(K_2))$ for all $n \in \mathbb{N}$. Since on the other hand $c(\theta^n_{K_1,K_2}) \leq n(c(K_1) + c(K_2))$ for all $n \in \mathbb{N}$, we obtain $c(\theta^n_{K_1,K_2}) = n(c(K_1) + c(K_2)) = nc(K_1 \# K_2)$ for all $n \in \mathbb{N}$, which proves the corollary. □

We can also relate the crossing numbers of $\theta^n_{K_1,K_1}$ and the connected sum of n copies of $K_1 \# K_2$, denoted by $K_1^n \# K_2^n$.

Proposition 8.4. *For all knots K_1 and K_2, we have $c(\theta^n_{K_1,K_2}) \geq c(K_1^n \# K_2^n)$. There is one n for which equality holds if and only if $c(K_1 \# K_2) = c(K_1) + c(K_2)$.*

Proof. The key idea here is that we can take any diagram of $\theta^n_{K_1,K_2}$ and resolve the two nodes in a certain way (as in Figure 8.5) such that we obtain a diagram of $K_1^n \# K_2^n$. We do this as follows. We start at one of the nodes, say n_1 and pick any arc s_1. We follow it along the diagram until it reaches the other node n_2. We

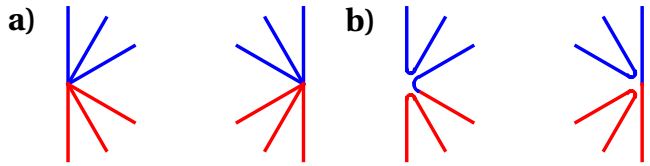

Figure 8.5: Resolution of nodes. a) Neighbourhoods of the nodes in a diagram of $\theta^n_{K_1,K_2}$. b) The nodes can be resolved to result in a diagram of $K_1^n \# K_2^n$.

then have to pick another arc s_2 to connect with s_1. We define s_2 to be the arc which enters n_2 next to s_1 in the clockwise direction.

We then follow s_2 along the diagram until it reaches n_1 and pick s_3 to be the arc which among all strands that we have not picked yet enters n_1 the closest to s_2 in the clockwise direction. In general, we connect the arc s_i to the arc s_{i+1}, where s_{i+1} is the arc that among all arcs that are not an element of $\{s_1, s_2, \dots, s_i\}$ enters the node $n_{(i \bmod 2)+1}$ closest to s_i in the clockwise direction.

With this rule, we obtain only one connected component, i.e. the diagram of a knot. It is clear, for example through induction on n, that the knot type of this diagram is $K_1^n \# K_2^n$.

Assume now that there is an n such that $c(\theta^n_{K_1,K_2}) = c(K_1^n \# K_2^n)$. Note that we have $c(K_1^n \# K_2^n) \leq nc(K_1 \# K_2) \leq c(\theta^n_{K_1,K_2})$. It then follows from Corollary 8.3 that $c(\theta^n_{K_1,K_2}) = c(K_1^n \# K_2^n) = nc(K_1 \# K_2)$ implies $c(K_1 \# K_2) = c(K_1 \# K_2)$.

If $c(K_1 \# K_2) = c(K_1) + c(K_2)$, then Equation (8.1) implies that $c(\theta_{K_1,K_2}) \geq c(K_1) + c(K_2)$. However, we know from the definition of θ_{K_1,K_2} that $c(\theta_{K_1,K_2}) \leq c(K_1) + c(K_2)$ and therefore $c(\theta_{K_1,K_2}) = c(K_1) + c(K_2) = c(K_1 \# K_2)$. Since $\theta_{K_1,K_2} = \theta^1_{K_1,K_2}$, this proves the proposition. □

The graph $\theta^n_{K_1,K_2}$ is an element of a special class of theta-curves of degree $2n$. We define $\Omega^n_{K_1,K_2}$ to be the set of theta-curves of degree $2n$ where we can colour n arcs blue and the remaining n arcs red, such that the union of any blue arc with any red arc is $K_1 \# K_2$ and the union of any two arcs of the same colour is neither the unknot nor $K_1 \# K_2 \# K_1 \# K_2$. Obviously $\theta_{K_1,K_2} \in \Omega^n_{K_1,K_2}$.

In order to keep notation consistent with that of the discussion of θ_{K_1,K_2}, we label the blue edges by $x_1, \dots, x_n$ and the n red edges by $z_1, \dots, z_n$.

We are now interested in $c(\Omega^n_{K_1,K_2}) = \min\{c(\theta) : \theta \in \Omega^n_{K_1,K_2}\}$. By the above we have $c(\Omega^n_{K_1,K_2}) \leq c(\theta^n_{K_1,K_2}) \leq n(c(K_1) + c(K_2))$. We want to show that for large enough n these inequalities are actually equalities. The idea here is that any

three arcs of a theta-curve of order $2n$ form a 'classical' theta-curve as in the previous section and we either have an intersection between a pair of arcs or the crossing number of the theta-curve is in some sense large. However, as n grows, the number of pairs of arcs grows more quickly than $n(c(K_1) + c(K_2))$.

We need several lemmas.

Lemma 8.5. *Let θ be a classical theta-curve with $x \cup z = K_1 \# K_2$ and $y \cup z = K_1 \# K_2$. If no pair of arcs cross each other and $x \cup y$ is neither the unknot nor $K_1 \# K_2 \# K_1 \# K_2$, then $xx \geq c(K_1)$, $zz \geq c(K_2)$ and $yy \geq c(K_1)$ or $xx \geq c(K_2)$, $zz \geq c(K_1)$ and $yy \geq c(K_2)$.*

Proof. By Lemma 8.2 there are knots K_1', K_2' and K_3' such that $K_1' \# K_3' = K_2' \# K_3' = K_1 \# K_2$ and $K_1' \# K_2'$ is neither the unknot nor $K_1 \# K_1 \# K_2 \# K_2$.

Since the prime decomposition of knots is unique and both K_1 and K_2 are prime, K_1' is either K_1, K_2, $K_1 \# K_2$ or the unknot. If it is the unknot, then $K_3' = K_1 \# K_2$. But then K_2' must also be the unknot and so $K_1' \# K_2'$ is the unknot, contradicting the assumption.

If $K_1' = K_1 \# K_2$, then K_3' is the unknot and hence $K_2' = K_1 \# K_2$. Thus $K_1' \# K_2' = K_1 \# K_2 \# K_1 \# K_2$, again contradicting the assumption.

If $K_1' = K_1$, then $K_3' = K_2$ and therefore $K_2' = K_1$ and so $xx \geq c(K_1)$, $yy \geq c(K_1)$ and $zz \geq c(K_2)$ by Lemma 8.2.

If $K_1' = K_2$, then $K_3' = K_1$ and hence $K_2' = K_2$. It follows that $xx \geq c(K_2)$, $yy \geq c(K_2)$ and $zz \geq c(K_1)$ by Lemma 8.2. □

This establishes the idea that if a theta-curve of degree 3 that is a subgraph of the diagram in question consists of three arcs that do not cross each other (only themselves), then its crossing number is comparatively large. We are thus interested in how many crossings between different edges are required to rule out the existence of any such subgraph.

We can associate a graph Γ, or $\Gamma(D)$, to any diagram D of a theta-curve $\theta \in \Omega^n_{K_1,K_2}$ that consists of $2n$ vertices, one for each edge of D, and an edge between two vertices if the corresponding edges in D do not cross each other. Hence there is an edge between the vertices corresponding to x_i and z_j if and only if $x_i z_j = 0$. Similarly, for x_i and x_j or z_i and z_j. We call a triangle in Γ *bicoloured* if its set of vertices consists of x's and z's, i.e. either (x_i, x_j, z_k) or (x_i, z_j, z_k).

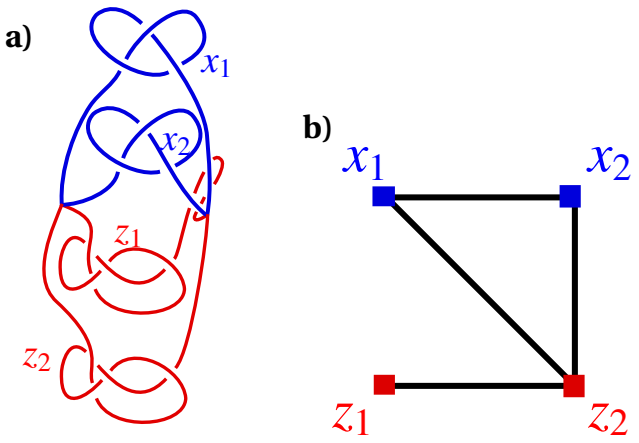

Figure 8.6: Definition of bicoloured triangles in the Γ-graph of a spatial graph. a) A diagram of $\theta^2_{K_1=3_1,K_2=4_1}$. b) The corresponding Γ-graph. x_1, x_2 and z_2 form a bicoloured triangle.

Note that three arcs (x_i, x_j, z_k) or (x_i, z_j, z_k) in the diagram D form a theta-curve as in Lemma 8.5 if and only if their corresponding vertices in $\Gamma(D)$ form a bicoloured triangle.

Lemma 8.6. *Let $n \geq 2$ and Γ be a graph with $2n$ vertices, labelled $x_1, \ldots, x_n, z_1, \ldots, z_n$, and m edges. If*

$$m > \frac{3}{2}n^2 - n, \tag{8.6}$$

then Γ contains a bicoloured triangle.

Proof. The proof is inspired by the standard proof of Mantel's Theorem that can be found in many graph theory lecture notes, for example Asaf Shapira's notes [125]. Let $d(v)$ denote the degree of the vertex v. Let $V(\Gamma)$ and $E(\Gamma)$ denote the set of vertices and edges of Γ respectively. Note that

$$\begin{aligned}\sum_{x\in V(\Gamma)} d^2(x) &= \sum_{(x,y)\in E(\Gamma)} (d(x)+d(y)) \\ &= \sum_{(x_i,x_j)\in E(\Gamma)} (d(x_i)+d(x_j)) + \sum_{(x_i,z_j)\in E(\Gamma)} (d(x_i)+d(z_j)) + \sum_{(z_i,z_j)\in E(\Gamma)} (d(z_i)+d(z_j)).\end{aligned} \tag{8.7}$$

Assume now that Γ does not contain a bicoloured triangle. Then if there is an edge between x_i and x_j every z_k is directly connected to at most one of them. Thus $d(x_i)+d(x_j) \leq 2(n-1)+n = 3n-2$. Similarly, $d(z_i)+d(z_j) \leq 3n-2$, whenever there is an edge between z_i and z_j.

If there is an edge between x_i and z_j every other vertex is directly connected to at most one of x_i and z_j. Thus $d(x_i) + d(z_j) \leq 2n$. We obtain if $n \geq 2$

$$\sum_{x \in V(\Gamma)} d^2(x) \leq m(3n-2). \tag{8.8}$$

Furthermore, since $\sum_{x \in V(\Gamma)} d(x) = 2m$, the Cauchy-Schwartz inequality implies that

$$\sum_{x \in V(\Gamma)} d^2(x) \geq \frac{\left(\sum_{x \in V(\Gamma)} d(x)\right)^2}{2n} = \frac{4m^2}{2n}. \tag{8.9}$$

Thus $\frac{2m^2}{n} \leq m(3n-2)$ and we obtain $m \leq \frac{3}{2}n^2 - n$. □

Lemma 8.7. *If $n > 2(c(K_1) + c(K_2) - c(K_1\#K_2)) + 1$, then for every diagram D of $\theta \in \Omega^n_{K_1,K_2}$ with $c(D) \leq n(c(K_1) + c(K_2))$ there is a bicoloured triangle in $\Gamma(D)$.*

Proof. Since $x_i \cup z_j = K_1\#K_2$ for all i, j, we have the inequality

$$nc(D) \geq n^2 c(K_1\#K_2) + (n-1)\sum_{i,j=1}^{n} x_i z_j + n\sum_{\substack{i,j=1 \\ i>j}}^{n} (x_i x_j + z_i z_j). \tag{8.10}$$

Assume there is no bicoloured triangle in $\Gamma(D)$. Then by Lemma 8.6 $\Gamma(D)$ has at most $\frac{3}{2}n^2 - n$ edges. Thus for at most $\frac{3}{2}n^2 - n$ pairs of arcs there is no crossing between them. Hence for at least $\frac{2n(2n-1)}{2} - \frac{3}{2}n^2 + n = \frac{n^2}{2}$ pairs there is a crossing between them. Note that since we only count crossings of x_i with x_j and z_j and crossings of z_i with x_j and z_j, we count every crossing only once.

Equation (8.10) then becomes

$$nc(D) \geq n^2 c(K_1\#K_2) + \frac{(n-1)n^2}{2}. \tag{8.11}$$

With the assumption that $c(D) \leq n(c(K_1) + c(K_2))$ we get

$$\begin{aligned} n^2(c(K_1) + c(K_2)) &\geq n^2 c(K_1\#K_2) + \frac{(n-1)n^2}{2} \\ \implies (c(K_1) + c(K_2) - c(K_1\#K_2)) &\geq \frac{n-1}{2}, \end{aligned} \tag{8.12}$$

which gives a contradiction if $n > 2(c(K_1) + c(K_2) - c(K_1\#K_2)) + 1$.

Thus $\Gamma(D)$ does contain a bicoloured triangle (x_i, x_j, z_k) or (x_i, z_j, z_k) if $n \geq 2(c(K_1) + c(K_2) - c(K_1\#K_2)) + 1$. □

Note that Lemma 8.7 directly implies the following result.

Lemma 8.8. *Let $n > 2\max\{(c(K_1) + c(K_2) - c(K_1\#K_2)), 1\}$ and D of $\theta \in \Omega^n_{K_1,K_2}$ with $c(D) \leq n(c(K_1) + c(K_2))$. Then D has at least $n - (c(K_1) + c(K_2) - c(K_1\#K_2))$ arcs x_i with $x_ix_i \geq c(K_1)$ and at least k arcs z_i with $z_iz_i \geq c(K_2)$. Each of these x_i and z_i is part of a classical theta-curve where no pair of arcs is crossing each other.*

Proof. By Lemma 8.7 $\Gamma(D)$ contains a bicoloured triangle. By Lemma 8.5 this means that the arcs (x_i, x_j, z_t) or (x_i, z_j, z_t) of D that correspond to the vertices of the bicoloured triangle satisfy $x_ix_i \geq c(K_1)$, $z_kz_k \geq c(K_2)$ and $x_jx_j \geq c(K_1)$ or $z_jz_j \geq c(K_2)$.

Deleting x_i and z_t results in a diagram D' of a theta-curve of degree $2n-2$ in $\Omega^{n-1}_{K_1,K_2}$ with $c(D') \leq (n-1)(c(K_1) + c(K_2))$. Repeatedly applying Lemma 8.7 and Lemma 8.5 results in the proof of the lemma. □

Proposition 8.9. *If $n \geq \max\{4(c(K_1) + c(K_2) - c(K_1\#K_2)) + 2, 2(c(K_1) + c(K_2) + 1)\}$, then $c(\Omega^n_{K_1,K_2}) = n(c(K_1) + c(K_2))$.*

Proof. Assume $c(\Omega^n_{K_1,K_2}) < n(c(K_1)+c(K_2))$ and let D be a diagram of a theta-curve of degree $2n$ that is in $\Omega^n_{K_1,K_2}$ such that $c(D) < n(c(K_1) + c(K_2))$.

Let l be the largest integer such that there are l arcs x_i and l arcs z_i with $x_ix_i \geq c(K_1)$ and $z_iz_i \geq c(K_2)$ whose corresponding vertices in $\Gamma(D)$ are not part of a bicoloured triangle. We label these arcs by x_i and z_i, $i = 1, \ldots, l$.

Let k be the largest integer such that there are k arcs x_i and k arcs z_i whose corresponding vertices in $\Gamma(D)$ are part of a bicoloured triangle in $\Gamma(D)$. Then by Lemma 8.2 these arcs each cross themselves at least $c(K_1)$ and $c(K_2)$ times, respectively, i.e. $x_ix_i \geq c(K_1)$ and $z_iz_i \geq c(K_2)$. We label these arcs x_i and z_i, $i = l+1, l+2, \ldots, l+k$.

Let $\widetilde{D}$ denote the diagram that results from deleting the arcs x_i and z_i, $i = 1, \ldots, l$. Note that $c(D) \geq c(\widetilde{D}) + l(c(K_1) + c(K_2))$.

We therefore have

$$\begin{aligned}(n-l)c(\widetilde{D}) =& (n-l)\left(\sum_{\substack{i,j=l+1\\ i\geq j}}^{l+k} x_ix_j + z_iz_j + \sum_{i,j=l+1}^{l+k} x_iz_j + \sum_{i=l+1}^{l+k}\sum_{j=l+k+1}^{n} x_ix_j + x_iz_j + z_ix_j + z_iz_j\right.\\ &\left. + \sum_{\substack{i,j=l+k+1\\ i\geq j}}^{n} x_ix_j + z_iz_j + \sum_{i,j=l+k+1}^{n} x_iz_j\right). \qquad (8.13)\end{aligned}$$

Rearranging the terms on the right hand side gives

$$\begin{aligned}
&\sum_{i,j=l+1}^{l+k}(x_ix_i+x_iz_j+z_jz_j)+\sum_{i=l+k+1}^{n}\sum_{j=l+1}^{l+k}(x_ix_i+x_iz_j+z_jz_j)\\
&+\sum_{i=l+k+1}^{n}\sum_{j=l+1}^{l+k}(x_jx_j+x_jz_i+z_iz_i)+\sum_{i,j=l+k+1}^{n}(x_ix_i+x_iz_j+z_jz_j)\\
&+(n-l-1)\sum_{i,j=l+1}^{n}x_iz_j+(n-l)\sum_{\substack{i,j=l+1\\ i>j}}^{n}(x_ix_j+z_iz_j).
\end{aligned}\tag{8.14}$$

Since $x_ix_i+x_iz_j+z_jz_j\geq c(K_1\#K_2)$ for all $i,j\in\{1,2,\dots,n\}$, and $x_ix_i\geq c(K_1)$ and $z_iz_i\geq c(K_2)$ for all $i\in\{l+1,l+2,\dots,l+k\}$, Equation (8.14) is at least

$$\begin{aligned}
&k^2(c(K_1)+c(K_2))+(n-l)k(c(K_1)+c(K_2))+(n-l-k)^2c(K_1\#K_2)\\
&+(n-l-1)\sum_{i,j=l+1}^{n}x_iz_j+(n-l)\sum_{\substack{i,j=l+1\\ i>j}}^{n}(x_ix_j+z_iz_j).
\end{aligned}\tag{8.15}$$

It follows from $k\geq 0$ and $c(D)<n(c(K_1)+c(K_2))$ and therefore $c(\widetilde{D})<(n-l)(c(K_1)+c(K_2))$ that

$$\begin{aligned}
(n-l)^2(c(K_1)+c(K_2))&>(n-l)k(c(K_1)+c(K_2))+(n-l-k)^2c(K_1\#K_2)\\
&\quad+(n-l-1)\sum_{i,j=l+1}^{n}x_iz_j+(n-l)\sum_{\substack{i,j=l+1\\ i>j}}^{n}(x_ix_j+z_iz_j)\\
\iff (n-l-k)(n-l)(c(K_1)+c(K_2))&>(n-l-k)^2c(K_1\#K_2)\\
&\quad+(n-l-1)\sum_{i,j=l+1}^{n}x_iz_j+(n-l)\sum_{\substack{i,j=l+1\\ i>j}}^{n}(x_ix_j+z_iz_j).
\end{aligned}\tag{8.16}$$

By construction there cannot be any bicoloured triangles in the Γ-graph associated to the theta-curve of order $2(n-l-k)$ that results from $\widetilde{D}$ by deleting the x_i and z_i with $i=l+1,l+2,\dots,l+k$. Thus there are at least $\frac{1}{2}(n-l-k)^2$ crossings between arcs with indices larger than $l+k$.

Furthermore, by definition of l and k for every $i>l+k$ either x_i or z_i must cross x_j or z_j for all $j=l+1,l+2,\dots,l+k$ at least once.

This gives

$$\begin{aligned}
(n-l-k)(n-l)(c(K_1)+c(K_2))&>(n-l-k)^2c(K_1\#K_2)\\
&\quad+(n-l-1)\left(\frac{1}{2}(n-l-k)^2+k(n-l-k)\right).
\end{aligned}\tag{8.17}$$

Assume that $k < n - l$. Then we can divide by $(n - l - k)$ and obtain

$$\begin{aligned}(n-l)(c(K_1)+c(K_2)) &> (n-l-k)c(K_1\#K_2) + (n-l-1)(\frac{1}{2}(n-l-k)+k)\\ &= (n-l-k)c(K_1\#K_2) + (n-l-1)\frac{n-l+k}{2}\\ \iff (n-l)(c(K_1)+c(K_2)-c(K_1\#K_2)) &+ kc(K_1\#K_2)\\ &> (n-l-1)\frac{n-l+k}{2}. \end{aligned} \tag{8.18}$$

If $c(K_1\#K_2) \leq \frac{1}{2}(c(K_1)+c(K_2))$, then

$$\begin{aligned}(n-l+k)(c(K_1)+c(K_2)-c(K_1\#K_2)) &> (n-l-1)\frac{n-l+k}{2}\\ \iff c(K_1)+c(K_2)-c(K_1\#K_2) &> \frac{n-l-1}{2}, \end{aligned} \tag{8.19}$$

which leads to a contradiction if $n - l \geq 2(c(K_1) + c(K_2) - c(K_1\#K_2)) + 1$. Note that by Lemma 8.8 we have $l \leq 2(c(K_1) + c(K_2) - c(K_1\#K_2)) + 1$. Therefore $k = n - l$ if $n \geq 4(c(K_1) + c(K_2) - c(K_1\#K_2)) + 2$, but this means that all arcs x_i and z_i whose corresponding vertices in $\Gamma(D)$ are not part of a bicloured triangle in $\Gamma(D)$ satisfy $x_i x_i \geq c(K_1)$ and $z_i z_i \geq c(K_2)$. Since the same is true for all arcs whose corresponding vertices in $\Gamma(D)$ are part of a bicoloured triangle, we have $c(D) \geq n(c(K_1) + c(K_2))$.

Similarly, if $c(K_1\#K_2) > \frac{1}{2}(c(K_1) + c(K_2))$, we obtain a contradiction if $n \geq 2(c(K_1) + c(K_2) + 1)$. Thus if $n \geq 2(c(K_1) + c(K_2) + 1)$, then $k = n - l$ and therefore $c(D) \geq n(c(K_1) + c(K_2))$. □

Since $\theta^n_{K_1,K_2} \in \Omega^n_{K_1,K_2}$, we immediately obtain the following result.

Corollary 8.10. *If* $n \geq \max\{4(c(K_1) + c(K_2) - c(K_1\#K_2)) + 2, 2(c(K_1) + c(K_2) + 1)\}$, *then* $c(\theta^n_{K_1,K_2}) = n(c(K_1) + c(K_2))$.

8.3 Composite knots and higher degree theta-curves

In this section we discuss relations between the $c(\Omega^n_{K_1,K_2})$ and $c(K_1\#K_2)$. In particular, we show that $c(K_1\#K_2) \geq \frac{1}{n^2}c(\Omega^n_{K_1,K_2})$. From the previous section we know that if n is sufficiently large, then $c(\Omega^n_{K_1,K_2}) = n(c(K_1) + c(K_2))$. Thus finding low values for n for which this equality holds is a way to obtain lower bounds of the form $c(K_1\#K_2) \geq \frac{1}{n}(c(K_1) + c(K_2))$.

Consider a minimal diagram of $K_1\#K_2$ and draw $n - 1$ parallel curves to the diagram in $\mathbb{R}^2$ that are at most ϵ away from D for some small $\epsilon > 0$. Obviously, we

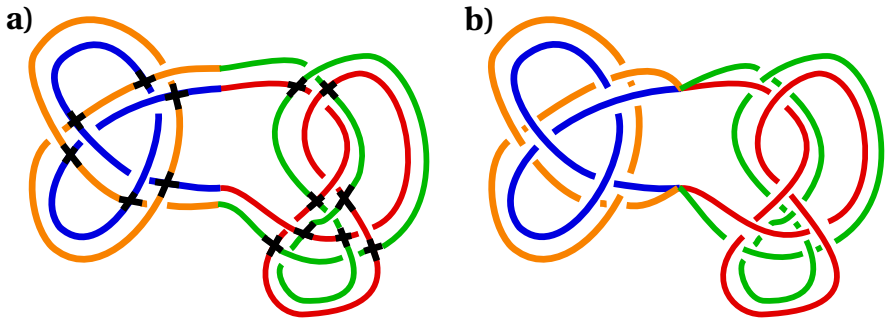

Figure 8.7: Constructing a diagram in $\Omega^n_{K_1,K_2}$ with $n^2c(K_1\#K_2)$ crossings. a) A minimal diagram of $3_1\#3_1$ with a parallel curve next to it. The black crossings indicate crossings with undetermined signs. b) A diagram of a theta-curve of degree 4 in $\Omega^2_{3_1,3_1}$, constructed by choosing signs for the black crossings and gluing the parallel curves together in two nodes.

typically do not know what the minimal diagram looks like, but the procedure is well-defined. We can think of these curves as a link diagram D_n, where many of the crossings, namely the ones between different parallel copies, have no determined signs yet (cf. Figure 8.7a)). We claim that we can choose the signs of these crossings and two points, where the parallel diagrams are glued together, such that we obtain a diagram of a theta-curve of degree $2n$ that is an element of $\Omega^n_{K_1,K_2}$. In Figure 8.7 this can be done by choosing the signs such that the one copy of the knot diagram lies completely below the other. We cannot assume that this is the case in general. Note that the diagram constructed in this way has $n^2c(K_1\#K_2)$ crossings and thus $n^2c(K_1\#K_2) \geq c(\Omega^n_{K_1,K_2})$.

We call the process of choosing two points n_1, n_2 on a knot diagram and thereby dividing the knot into two arcs α_1 and α_2 a *partition* of the knot diagram.

Lemma 8.11. *For all pairs of knots K_1, K_2, not both alternating, there is a partition $\alpha_1 \cup \alpha_2 = K_1\#K_2$ of any diagram of $K_1\#K_2$ such that for every $i \in \{1,2\}$ there is a crossing of α_i with itself.*

Proof. Let K_1 and K_2 be knots not both be alternating. Then $K_1\#K_2$ is not alternating [86]. We pick a point n_1 on a diagram D of $K_1\#K_2$ and consider the Gauss code starting at n_1 in an arbitrary direction.

Let $n_2 \neq n_1$ be a second point on the diagram and α_1 the arc from n_1 to n_2 in the direction of the Gauss code.

Assume that α_1 does not cross itself. This is equivalent to the position of n_2 on the knot diagram corresponding to a position in the Gauss code before an absolute value of a number appears for the second time in the Gauss code.

Similarly, α_2, the other arc in the diagram, does not cross itself if and only if between the positions in Gauss code corresponding to n_2 and n_1 (in the direction of the Gauss code), no absolute value appears twice.

Assume now that no matter where we place n_2 on the knot diagram, there is an $i = 1, 2$ such α_i does not cross itself. Then no matter where we split the Gauss code into two pieces, one piece will not contain any absolute value twice.

This means that every crossing must be visited once before the first instance of a crossing being visited for a second time, i.e. the first half of the Gauss code modulo signs reads $1, 2, \ldots, c(D)$. Now let $k \in \{1, 2, \ldots, c(D) - 1\}$ and assume that the crossing $k + 1$ is visited the second time before k is visited the second time. Then we could divide the Gauss code into two pieces, one of which contains both occurrences of the k and $-k$ and the other both occurrences of $k + 1$ and $-(k + 1)$. Hence we found a partition where both α_1 and α_2 cross themselves.

If for every k the crossing $k + 1$ is visited the second time after crossing k is visited the second time, then the sequence which is the absolute value of the Gauss code sequence is $1, 2, \ldots, c(D), 1, 2, \ldots, c(D)$. It is easy to see that a knot that allows a diagram with such a Gauss code must be alternating, contradicting the assumption that K_1 and K_2 are not both alternating. □

By Lemma 8.11 if K_1 and K_2 are not both alternating we can glue the link diagram D_n of n parallel copies of the diagram of $K_1\#K_2$ such that each of the edges of the resulting embedded graph crosses itself. Call the resulting diagram (with some undetermined crossing signs) $\widetilde{D}$. We claim that now we can choose the signs of the crossings that are not determined yet in such a way that the resulting theta-curve of order $2n$ is in $\Omega^n_{K_1,K_2}$, i.e. there are n blue arcs x_i and n red arcs z_i such that for all i and j the knot $x_i \cup z_j$ is $K_1\#K_2$ and none of $x_i \cup x_i$ and $z_i \cup z_i$ is the unknot or $K_1\#K_2\#K_1\#K_2$.

Lemma 8.12. *We can choose the signs of the crossings of $\widetilde{D}$ that are not determined yet in such a way that $\widetilde{D}$ is a diagram of a theta-curve of degree $2n$ in $\Omega^n_{K_1,K_2}$.*

Proof. Note that for every choice of $i, j \in \{1, 2, \ldots, n\}$ the union $x_i \cup z_j$ is the original diagram D of $K_1\#K_2$, where we deleted the information about the signs of the crossings. We can thus choose the signs of the crossings of x_i with z_j and the signs of crossings of x_i and z_j with themselves such that $x_i \cup z_j = K_1\#K_2$ for all i and j.

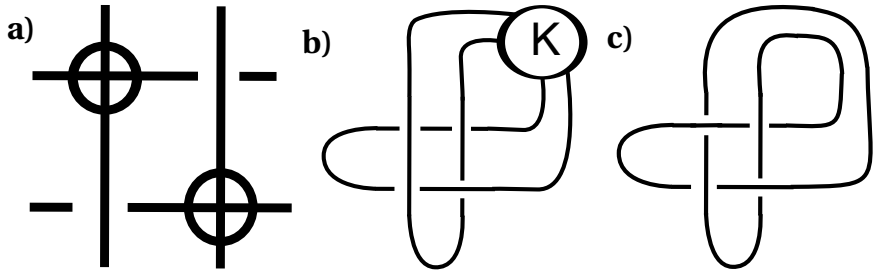

Figure 8.8: Choosing the signs of crossings appropriately. a) Doubling the strands turns every crossing into a 4-crossing, where two of the signs are given. Choosing the remaining signs results either in a diagram of a non-trivial Whitehead double of a knot K (b) or in a trefoil (c).

We now need to determine the signs of the crossings of x_i with x_j and z_i with z_j, $i \neq j$. Note that x_i and x_j are two parallel arcs. So for each crossing between them, there is a cluster of four crossings, one of x_i with itself, one of x_j with itself (both of whose crossings have been already determined to carry identical signs) and two crossings of x_i with x_j.

If for every such 4-crossing we choose to give the crossings of x_i and x_j the same sign as the corresponding crossings of x_i with itself and x_j with itself, then x_i and x_j are two parallel curves glued together at their ends and hence $x_i \cup x_j$ is the unknot. We can move the ends, where x_i and x_j are glued together, through the knot to untie it.

Instead we pick one such 4-crossing, which exists by Lemma 8.11 for each pair (x_i, x_j) and (z_i, z_j). For all the others we distribute signs exactly as above, but for the one we picked we give the two crossings between x_i and x_j different signs. Then as we slide the ends of the curves through the knot as in the previous case, we obtain a diagram as in Figure 8.8 b). It shows that the resulting knot is a Whitehead double of some knot K.

The only case where this Whitehead double is the unknot is if it is the untwisted Whitehead double of the unknot. In all other cases it is prime and therefore we have found a choice of signs for which $x_i \cup x_j$ is neither the unknot nor $K_1\#K_2\#K_1\#K_2$.

If K is the unknot and the Whitehead double is untwisted, we can change one of the crossings in the 4-crossing that we picked, so that now the two crossings between x_i and x_j both have different signs from the crossings of x_i and x_j with themselves. In this case the diagram that we obtain is the trefoil (Figure 8.8 c)).

Therefore, we can always choose the signs of the crossings in such a way that

$x_i \cup z_j = K_1\#K_2$ and $x_i \cup x_j$ and $z_i \cup z_j$ are neither the unknot nor $K_1\#K_2\#K_1\#K_2$ for all $i, j = 1, 2, \ldots, n$. □

Note that for alternating knots the additivity of the crossing number is known [69, 102, 103, 131, 132], so the next proposition follows from the previous lemmas and the opening remarks to this section.

Proposition 8.13. *For every $n \in \mathbb{Z}_{>0}$ we have $c(K_1\#K_2) \geq \frac{1}{n^2} c(\Omega^n_{K_1,K_2})$.*

As mentioned before, Proposition 8.13 opens up the possibility of finding lower bounds for $c(K_1\#K_2)$ by finding low n such that $c(\Omega^n_{K_1,K_2}) = n(c(K_1) + c(K_2))$, since then $c(K_1\#K_2) \geq \frac{1}{n}(c(K_1) + c(K_2))$.

Note that the Γ-graph associated to the constructed diagram $\widetilde{D}$ (after the signs have been assigned) does not contain a bicoloured triangle. The next corollary follows directly.

Corollary 8.14. *Let $n \in \mathbb{Z}_{\geq 2}$ such that every diagram D that has an associated graph $\Gamma(D)$ without any bicoloured triangles and represent a theta-curve $\theta \in \Omega^n_{K_1,K_2}$ satisfies $c(D) \geq n(c(K_1) + c(K_2))$. Then $c(K_1\#K_2) \geq \frac{1}{n}(c(K_1) + c(K_2))$.*

Lemma 8.7 shows that such values for n exist. However, the value that is stated in the Lemma only gives an obvious bound. However, if we could improve on the value of n, then we would obtain a new lower bound for $c(K_1\#K_2)$.

8.4 Other graphs

In this section we consider graphs with more than two nodes starting with the example graph $\oplus$ with four 3-valent vertices connected by edges in a circle and one 4-valent vertex that is connected to every other vertex by an edge. We want to think of this graph as two theta-graphs glued together in a neighbourhood of one of their vertices.

The set of theta-curves also comes with a notion of connected sum. We can orient the edges of a theta-curve such that one of its vertices is a source n_1 and the other is a sink n_2. Then the connected sum of two theta-curves, θ_1 and θ_2, is formed by deleting a neighbourhood of n_2 of θ_1 and a neighbourhood of n_1 of θ_2 and gluing the theta-curves together on the open ends of their arcs, joining arcs with the same labels x, y and z respectively. In order to make this a natural operation we should consider two embedded graphs to be equivalent

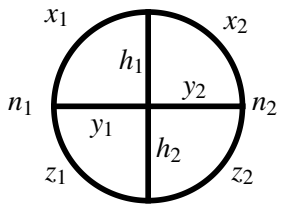

Figure 8.9: The planar embedding of the $\oplus$-graph with labelled edges.

if and only if they are related by an ambient isotopy that does not change the clockwise order in which the arcs meet the node.

Note that the connected sum commutes with tying knots into one of the arcs, in particular $\theta_{K_1,K_2}\#\theta_{K_3,K_4} = \theta_{K_1\#K_3,K_2\#K_4}$. This means that if the crossing number of theta-curves is additive under connected sum, then the crossing number of knots is also additive (simply take K_2 and K_4 to be the unknot).

A fundamental concept of Section 8.1 can now easily be generalised to $\oplus$ (and in fact beyond). The step from knots to theta-curves in Section 8.1 is adding an extra arc, which we will think of as adding the part of the knot (or in this case the theta-curve) that was deleted in the process of the connected sum. In the case of the connected sum of two theta-curves adding the deleted part back in results in $\oplus$.

We label the edges of this graph as follows: We fix one of the 3-valent vertices n_1 and denote the edges connected to n_1 by x_1, y_1 and z_1. The only 3-valent vertex that is not connected to n_1 is called n_2 and edges connecting to n_2 have labels x_2, y_2 and z_2 such that x_1 and x_2 (and similarly y_1 and y_2 as well as z_1 and z_2) meet at a vertex. The two edges that are left are called h_1 and h_2.

Consider now an embedding of $\oplus$ where a copy of K_1 is tied into x_1 and z_2 of the planar $\oplus$ and a copy of K_2 is tied into each of the edges z_1 and x_2, which we denote by $\oplus_{K_1,K_2}$. Then for each $i \in \{1,2\}$ deleting x_i, y_i and z_i results in a diagram of a theta-curve θ_{K_1,K_2}. In other words

$$c(\oplus_{K_1,K_2}) + h_1h_1 + h_2h_2 + h_1h_2 \geq 2c(\theta_{K_1,K_2}) + \sum_{(k,l)\in\{x,y,z\}^2} k_1l_2. \tag{8.20}$$

On the other hand, deleting the edges h_1 and h_2 results in the theta-curve $\theta_{K_1\#K_2,K_1\#K_2}$. It turns out that the analogues of Lemma 8.2 and Proposition 8.1 holds in this case too and we obtain

$$c(\oplus_{K_1,K_2}) \geq \frac{1}{2}(2c(\theta_{K_1,K_2}) + c(\theta_{K_1\#K_2,K_1\#K_2})), \tag{8.21}$$

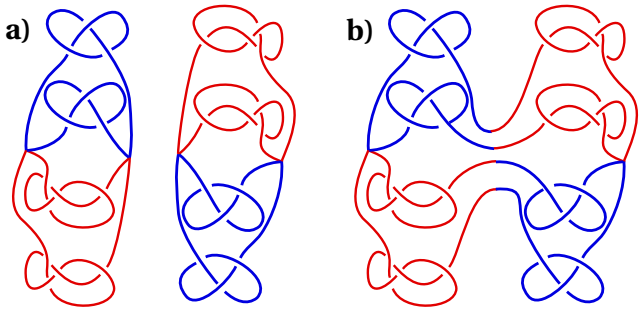

Figure 8.10: The connected sum operation for more general spatial graphs. a) Two 4-theta-curves. b) Their connected sum.

and equality is equivalent to $c(\theta_{K_1\#K_2,K_1\#K_2}) = 2c(\theta_{K_1,K_2})$. Since $c(\theta_{K_1\#K_2,K_1\#K_2}) \leq 2c(K_1\#K_2)$, this is then equivalent to $c(K_1\#K_2) = c(\theta_{K_1,K_2})$ and by Proposition 8.1 to the additivity of the crossing number.

Analogously, we can define the connected sum of two theta-curves of any degree (cf. Figure 8.10).

Let $\oplus^{n,k}$ denote the graph (as in Figure 8.11a)) with k vertical edges and $2n$ rows of horizontal edges. Let $\oplus^{n,k}_{K_1,K_2}$ denote the spatial graph that is obtained from the planar embedding of $\oplus^{n,k}$ by tying in each column n of the horizontal edges into K_1 and the remaining n horizontal edges into K_2, such that at every node an arc with a K_1 meets an arc with a K_2 (cf. Figure 8.11b)). We denote by $\mathrm{G}^{n,k,i}_{K_1,K_2}$ the graph (cf. Figure 8.11c)) that results from $\oplus^{n,k}_{K_1,K_2}$ by deleting the ith vertical edge. Note that $\oplus^{n,0}_{K_1\#K_2,K_1\#K_2} = \mathrm{G}^{n,1,1}_{K_1,K_2}$.

Lemma 8.15. *For all positive integers n, k and i we have*

$$c\left(\oplus^{n,i-1}_{K_1,K_2}\right) + c\left(\oplus^{n,k-i}_{K_1,K_2}\right) \geq c\left(\oplus^{n,k}_{K_1,K_2}\right) \geq c\left(\mathrm{G}^{n,k,i}_{K_1,K_2}\right). \tag{8.22}$$

Furthermore, if $c\left(\oplus^{n,k}_{K_1,K_2}\right) = c\left(\mathrm{G}^{n,k,i}_{K_1,K_2}\right)$, then

$$c\left(\oplus^{n,k}_{K_1,K_2}\right) = c\left(\oplus^{n,i-1}_{K_1,K_2}\right) + c\left(\oplus^{n,k-i}_{K_1,K_2}\right). \tag{8.23}$$

Proof. Equation (8.22) is almost immediate. We can form the connected sum of $\oplus^{n,i-1}_{K_1,K_2}$ and $\oplus^{n,k-i}_{K_1,K_2}$ using their minimal diagrams. Since this process involves deleting a small neighbourhood of two vertices, we can add an unknotted arc to form a diagram of $\oplus^{n,k}_{K_1,K_2}$ with $c\left(\oplus^{n,i-1}_{K_1,K_2}\right) + c\left(\oplus^{n,k-i}_{K_1,K_2}\right)$ many crossings. Deleting the ith vertical edge in the minimal diagram of $\oplus^{n,k}_{K_1,K_2}$ results in a diagram of $\mathrm{G}^{n,k,i}_{K_1,K_2}$, which proves the inequality on the right hand side of Equation (8.22)

If $c\left(\oplus^{n,k}_{K_1,K_2}\right) = c\left(\mathrm{G}^{n,k,i}_{K_1,K_2}\right)$, then the ith arc in the minimal diagram of $\oplus^{n,k}_{K_1,K_2}$ is not involved in any crossings, neither with itself nor with any other edge of

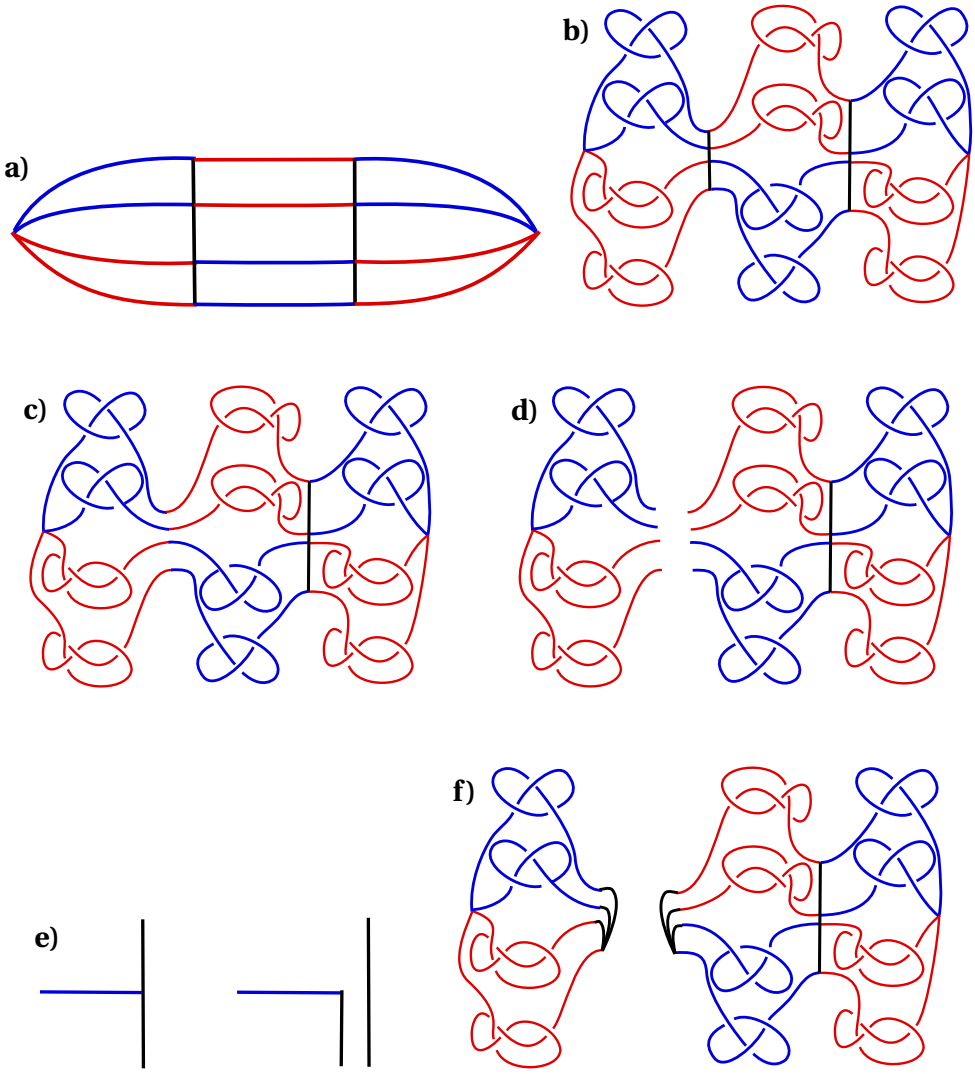

Figure 8.11: Definitions of several spatial graphs. a) $\oplus^{2,2}$. (b) A diagram of the embedding $\oplus^{2,2}_{K_1=3_1,K_2=4_1}$ of the graph $\oplus^{2,2}$. c) A diagram of $G^{2,2,2}_{3_1,4_1}$. d) Cutting a diagram of $\oplus^{2,2}_{3_1,4_1}$ along the first vertical edge. e) Resolution of the nodes in c) to close d) to a diagram of $\oplus^{2,0}_{3_1,4_1}$ and $\oplus^{2,1}_{3_1,4_1}$. f) The resulting diagram of $\oplus^{2,0}_{3_1,4_1}$ and $\oplus^{2,1}_{3_1,4_1}$.

the spatial graph. We can therefore cut $\oplus^{n,k}_{K_1,K_2}$ along the ith arc to obtain two spatial graphs (as in Figure 8.11d)), whose open ends can be joined in one vertex without introducing any crossings.

This can be seen as follows. The ith vertical edge in the minimal diagram of $\oplus^{n,k}_{K_1,K_2}$ has $2n$ vertices on it, 2 of valency 3 and $2(n-1)$ of valency 4. We cut the diagram along the ith vertical edge and now want to connect the open ends of the remaining diagram without introducing extra crossings. We start with

one of the endpoints of the deleted edge, i.e. one of the nodes that had valency 3 in $\oplus^{n,k}_{K_1,K_2}$. We follow the deleted ith vertical edge until we encounter the next node. We resolve this node as in Figure 11e) in a similar fashion to the proof of Proposition 8.4. Now we have two parallel curves that follow the deleted ith vertical edge until the next vertex, that also gets resolved accordingly. This process continues until all $2n-1$ parallel arcs are glued to the last remaining open end. It is clear that this results in a diagram of $\oplus^{n,i-1}_{K_1,K_2}$ and of $\oplus^{n,k-i}_{K_1,K_2}$ as in Figure 8.11f). Furthermore, this closing procedure does not lead to any new crossings, since all added arcs are parallel to the deleted ith vertical edge, which was not involved in any crossings.

This results in a diagram of $\oplus^{n,i-1}_{K_1,K_2}$ and of $\oplus^{n,k-i}_{K_1,K_2}$, which shows that $c\left(\oplus^{n,k}_{K_1,K_2}\right) \geq c\left(\oplus^{n,i-1}_{K_1,K_2}\right) + c\left(\oplus^{n,k-i}_{K_1,K_2}\right)$. Equation (8.23) then follows from Equation (8.22). □

Similar arguments apply to the spatial graph $\mathrm{G}^{n,k,i}_{K_1,K_2}$ as well.

Lemma 8.16. *For all positive integers n, k and $i \neq (k+1)/2$ we have*

$$c\left(\mathrm{G}^{n,k,i}_{K_1,K_2}\right) \leq c\left(\oplus^{n,\min\{i-1,k-i\}}_{K_1,K_2}\right) + c\left(\mathrm{G}^{n,k-1-\min\{i-1,k-i\},s}_{K_1,K_2}\right), \tag{8.24}$$

where

$$s = \begin{cases} i & \text{if } i-1 < k-i, \\ i-(k-i)-1 & \text{if } i-1 > k-i \end{cases}. \tag{8.25}$$

Proof. First note that the case of $i-1 = k-i$ cannot occur, since then $i = (k+1)/2$. Hence s is well-defined.

We can form the connected sum of $\oplus^{n,\min\{i-1,k-i\}}_{K_1,K_2}$ and $\mathrm{G}^{n,k-1-\min\{i-1,k-i\},s}_{K_1,K_2}$ using their minimal diagrams. Since the connected sum involves deleting neighbourhoods of two nodes, we can add an extra arc to obtain a diagram of $\mathrm{G}^{n,k,i}_{K_1,K_2}$ without adding any extra crossings. Therefore the minimal crossing number of $\mathrm{G}^{n,k,i}_{K_1,K_2}$ is at most

$$c\left(\oplus^{n,\min\{i-1,k-i\}}_{K_1,K_2}\right) + c\left(\mathrm{G}^{n,k-1-\min\{i-1,k-i\},s}_{K_1,K_2}\right). \tag{8.26}$$

□

Furthermore, Proposition 8.1 generalises to the following statement.

Proposition 8.17. *If there exist positive integers n, k and m such that $c\left(\oplus^{n,k}_{K_1,K_2}\right) = c\left(\mathrm{G}^{n,k,i}_{K_1,K_2}\right)$ holds for $i = k/m$ or $i = \frac{m-1}{m}k+1$, then $c(K_1\#K_2) = c(K_1) + c(K_2)$.*

Proof. We start with $m = 1$, so $i = 1$ or $i = k$. We assume that $i = 1$. The case of $i = k$ can be proven analogously. By Lemma 8.15 $c\left(\oplus^{n,k}_{K_1,K_2}\right) = c\left(\mathrm{G}^{n,k,1}_{K_1,K_2}\right)$ implies that

$$c(\oplus^{n,k}_{K_1,K_2}) = c(\oplus^{n,0}_{K_1,K_2}) + c(\oplus^{n,k-1}_{K_1,K_2}) = c(\mathrm{G}^{n,k,1}_{K_1,K_2}). \tag{8.27}$$

Using Equation (8.24) with $i = 1$,

$$c\left(\mathrm{G}^{n,k,1}_{K_1,K_2}\right) \leq c\left(\oplus^{n,0}_{K_1,K_2}\right) + c\left(\mathrm{G}^{n,k-1,1}_{K_1,K_2}\right), \tag{8.28}$$

we get

$$c\left(\oplus^{n,k-1}_{K_1,K_2}\right) \leq c\left(\mathrm{G}^{n,k-1,1}_{K_1,K_2}\right), \tag{8.29}$$

which by Lemma 8.15 implies

$$c\left(\oplus^{n,k-1}_{K_1,K_2}\right) = c\left(\mathrm{G}^{n,k-1,1}_{K_1,K_2}\right). \tag{8.30}$$

We have just shown that if $c\left(\oplus^{n,k}_{K_1,K_2}\right) = c\left(\mathrm{G}^{n,k,1}_{K_1,K_2}\right)$, then the same equality holds for $k-1$. Iterating this process shows that

$$c\left(\oplus^{n,1}_{K_1,K_2}\right) = c\left(\mathrm{G}^{n,1,1}_{K_1,K_2}\right) = 2c\left(\oplus^{n,0}_{K_1,K_2}\right). \tag{8.31}$$

Note that $\mathrm{G}^{n,1,1}_{K_1,K_2} = \theta^n_{K_1\#K_2,K_1\#K_2}$, so in particular

$$c\left(\mathrm{G}^{n,1,1}_{K_1,K_2}\right) \leq 2nc(K_1\#K_2). \tag{8.32}$$

Using Equation (8.31) we obtain

$$c\left(\oplus^{n,0}_{K_1,K_2}\right) \leq nc(K_1\#K_2). \tag{8.33}$$

Note that $\oplus^{n,0}_{K_1,K_2} = \theta^n_{K_1,K_2}$ and $c(\theta^n_{K_1,K_2}) \geq nc(K_1\#K_2)$ (by Corollary 8.3) and thus we have $c(\theta^n_{K_1,K_2}) = nc(K_1\#K_2)$, which by Corollary 8.3 implies that $c(K_1\#K_2) = c(K_1) + c(K_2)$.

Now we assume that we have $c\left(\oplus^{n,k}_{K_1,K_2}\right) = c\left(\mathrm{G}^{n,k,i}_{K_1,K_2}\right)$ with $i = k/m$ or $i = \frac{m-1}{m}k+1$ for some $m > 1$. In particular, $i \neq \frac{k+1}{2}$.

It follows again from Lemma 8.15 that

$$c\left(\oplus^{n,k}_{K_1,K_2}\right) = c\left(\oplus^{n,i-1}_{K_1,K_2}\right) + c\left(\oplus^{n,k-i}_{K_1,K_2}\right) = c\left(\mathrm{G}^{n,k,i}_{K_1,K_2}\right). \tag{8.34}$$

Combining Equation (8.34) and Equation (8.24) gives

$$\begin{aligned} c\left(\oplus^{n,\min\{i-1,k-i\}}_{K_1,K_2}\right) + c\left(\oplus^{n,\max\{i-1,k-i\}}_{K_1,K_2}\right) &= c\left(\oplus^{n,i-1}_{K_1,K_2}\right) + c\left(\oplus^{n,k-i}_{K_1,K_2}\right) \\ &\leq c\left(\oplus^{n,\min\{i-1,k-i\}}_{K_1,K_2}\right) + c\left(\mathrm{G}^{n,k-1-\min\{i-1,k-i\},s}_{K_1,K_2}\right), \end{aligned} \tag{8.35}$$

with s as in Equation (8.25).

Canceling $c\left(\oplus^{n,\min\{i-1,k-i\}}_{K_1,K_2}\right)$ leaves us with

$$c\left(\oplus^{n,\max\{i-1,k-i\}}_{K_1,K_2}\right) \leq c\left(\mathrm{G}^{n,k-1-\min\{i-1,k-i\},s}_{K_1,K_2}\right), \tag{8.36}$$

which implies

$$c\left(\oplus^{n,\max\{i-1,k-i\}}_{K_1,K_2}\right) = c\left(\oplus^{n,k-1-\min\{i-1,k-i\}}_{K_1,K_2}\right) = c\left(\mathrm{G}^{n,k-1-\min\{i-1,k-i\},s}_{K_1,K_2}\right), \tag{8.37}$$

since $\max\{i-1,k-i\} = k-1-\min\{i-1,k-i\}$. This means we have another set of positive integers $(n,k',i') = (n,k-1-\min\{i-1,k-i\},s)$ with $c\left(\oplus^{n,k'}_{K_1,K_2}\right) = c\left(\mathrm{G}^{n,k',i'}_{K_1,K_2}\right)$.

If $i = k/m$, then $i-1 < k-i$ and we find that $s = k/m$ and $k' = k-i = \frac{m-1}{m}k$ and hence $s = k'/(m-1)$. Repeating this process, we obtain $c\left(\oplus^{n,\widetilde{k}}_{K_1,K_2}\right) = c\left(\mathrm{G}^{n,\widetilde{k},\widetilde{i}}_{K_1,K_2}\right)$ for some $\widetilde{i} = \widetilde{k}$, which by the remarks above implies that $c(K_1\#K_2) = c(K_1) + c(K_2)$.

If $i = \frac{m-1}{m}k+1$, then $i-1 > k-i$ and we obtain $s = 2i-k-1 = \frac{m-2}{m}k+1$ and $k' = i-1 = \frac{m-1}{m}k$. Therefore $s = \frac{m-2}{m-1}k'+1$. Repeating this process, we obtain $c\left(\oplus^{n,\widetilde{k}}_{K_1,K_2}\right) = c\left(\mathrm{G}^{n,\widetilde{k},\widetilde{i}}_{K_1,K_2}\right)$ for some $\widetilde{k}$ and $\widetilde{i} = 1$, which again implies $c(K_1\#K_2) = c(K_1) + c(K_2)$. □

At the moment it seems unlikely that one could solve the crossing number conjecture by finding values for n, k and i for which the condition in Proposition 8.17 is satisfied. It is more promising to aim for a pure existence statement. This is of course highly speculative, but the hope is that the situation becomes similar to the one in Section 8.2, where it is very hard for a given n to decide whether $c(\theta^n_{K_1,K_2}) = n(c(K_1)+c(K_2))$, but we know that if n is large enough, then the equality is satisfied.

There are multiple other ways that one could extend the results outlined here to other types of graphs, all of which seem to give some inequalities and conditional results. It is a part of ongoing research, whether the results obtained by studying some of these graphs actually give us something new, something that we cannot find by studying higher degree theta-curves.

Throughout this chapter we have worked under the assumption that K_1 and K_2 are prime. Many of the stated results remain true if we drop this assumption. Notably, for large enough n the minimal crossing number of $\theta^n_{K_1,K_2}$ is equal to $n(c(K_1)+c(K_2))$. The definition of $\Omega^n_{K_1,K_2}$ has to be slightly adjusted. In particular, $x_i \cup x_j$ and $z_i \cup z_j$ are not allowed to be of the form $K\#K$, if K is any summand of $K_1\#K_2\#K_1\#K_2$ other than K_1 or K_2. With this definition we again obtain that for large enough n the crossing number satisfies $c(\Omega^n_{K_1,K_2}) = n(c(K_1)+c(K_2))$.

The results from Section 8.3 also remain largely true. Since the signs in the construction of $\widetilde{D}$ can be chosen in such a way that $x_i \cup x_j$ and $z_i \cup z_j$ are always either a trefoil or the Whitehead double of a non-trivial knot (all of which have genus 1 and are therefore prime), $\widetilde{D}$ is the diagram of a higher degree theta-curve in $c(\Omega^n_{K_1,K_2})$. Thus we again have $c(K_1\#K_2) \geq \frac{1}{n^2}c(\Omega^n_{K_1,K_2})$ for all n.

8.5 Discussion

We can use theta-curves and more general spatial graphs to study the crossing numbers of composite knots. Often there are inequalities relating the crossing number of a composite knot $K_1\#K_2$ to the crossing number of a corresponding spatial graph. This allows us to find conditions that if satisfied imply the additivity of the crossing number.

While it is often still too hard to make any precise statements about the crossing number of a given graph, we can define families such as $\Omega^n_{K_1,K_2}$ for which we can determine the crossing number as n goes to infinity. In particular, we know that for large enough n we have $c(\Omega^n_{K_1,K_2}) = n(c(K_1) + c(K_2))$. It is part of ongoing research to try to find smaller values of n for which this equality holds. By Corollary 8.14 this would lead to new lower bounds of $c(K_1\#K_2)$.

One hope is that we can proceed in a similar fashion with the graphs $\oplus^{m,n}_{K_1,K_2}$ and $G^{m,n,i}_{K_1,K_2}$. Proposition 8.17 gives a conditional result that has a flavour reminiscent of the results obtained for classical theta-curves. Studying the convergence properties of $c(\oplus^{m,n}_{K_1,K_2})/m(n+1)(c(K_1)+c(K_2))$ or $c(\oplus^{m,n}_{K_1,K_2})/(c(K_1^{m(n+1)}\#K_2^{m(n+1)}))$ and similarly for $G^{m,n,i}_{K_1,K_2}$ could lead to a situation where we can apply Proposition 8.17. At the moment, this is still very speculative, but it is a very interesting prospect.

Bibliography

[1] A'Campo N (1973). Le nombre de Lefschetz d'une monodromie. *Indagationes Math. (Proc.)* **76**, 113–118.

[2] A'Campo N (1975). La fonction zêta d'une monodromie. *Comm Math Helv* **50**, 233–248.

[3] A'Campo N (1998). Generic immersions of curves, knots, monodromy and gordian number. *IHES Publ. Math.* **88**, 151—169.

[4] Adams CC (1994). *The knot book*. WH Freeman and Company, New York.

[5] Akbulut S and King H (1981). All knots are algebraic. *Comm Math Helv* **56**, 339–351.

[6] Alexander J (1923). A lemma on a system of knotted curves. *Proc. Nat. Acad. Sci. USA* **9**, 93–95.

[7] Arrayás M and Trueba JL (2014). A class of non-null toroidal electromagnetic fields and its relation to the model of electromagnetic knots. *J Phys A.* **48**, 025203.

[8] Artin E (1925). Theorie der Zöpfe. *Hamburg Abh.* **4**, 47–72.

[9] Atkinson KE (1988). *An Introduction to numerical analysis* 2nd edition. John Wiley and Sons, Hoboken NJ.

[10] Bar-Natan D (2016). The knot atlas. *http://katlas.org/*. (Accessed 27th October 2016).

[11] Beardon AF, Carne TK and Ng TW (2002). The critical values of a polynomial. *Constr Approx* **18**, 343–354.

[12] Bell M (2012). The monodromies of homogeneous links. *(arXiv:1207.0161)*.

[13] Benedetti R and Shiota M (1998). On real algebraic links in S^3. *Bolletino dell'Unione Mathematica Italiana* **1B**(3), 585–609. Serie 8.

[14] Berry M (2001). Knotted zeros in the quantum states of hydrogen. *Found Phys* **31**, 659–667.

[15] Berry M and Dennis MR (2001). Knotted and linked phase singularities in monochromatic waves. *Proc R Soc A* **457**, 2251–2263.

[16] Binysh J and Alexander G (2018). Maxwell's theory of solid angle and the construction of knotted fields. *(arXiv:1805.10358)*.

[17] Birman JS and Brendle TE (2005). Braids: A survey. In Menasco W, Thistleth-

waite MB, editors *Handbook of Knot Theory*, Chapter 2, 19–103.

[18] Birman J, Ko KH and Lee SJ (1998). A new approach to the word and conjugacy problems in the braid groups. *Advances in Math.* **139**, 322–353.

[19] Birman JS (1975). *Braids, links and mapping class groups*. Princeton University Press, Princeton.

[20] Bode B (2017). Constructing links of isolated singularities of polynomials $\mathbb{R}^4 \to \mathbb{R}^2$. *(arXiv:1705.09255)*.

[21] Bode B (2017). Crossing numbers of composite knots and spatial graphs. *(arXiv:1709.05118)*.

[22] Bode B and Dennis MR (2016). Constructing a polynomial whose nodal set is any prescribed knot or link. *(arXiv: 1612.06328)*.

[23] Bode B, Dennis MR, Foster D and King R (2017). Knotted fields and explicit fibrations for lemniscate knots. *Proc R Soc A* **475**, 20160829.

[24] Bogle MGV, Hearst JE, Jones VFR and Stoilov L (1994). Lissajous knots. *Journal of Knot Theory and Its Ramifications* **3**, 121–140.

[25] Boileau M and Orevkov SY (2001). Quasipositivité d'une courbe analytique dans une boule pseudo-convexe. *C. R. Acad. Sci. Paris* **332**, 825–830.

[26] Boileau M and Fourrier L (1998). Knot theory and plane algebraic curves. *Chaos Solitons Fractals* **9**(4-5), 779–792.

[27] Brauner K (1928). Zur Geometrie der Funktionen zweier komplexen Veränderlichen II, III, IV. *Abh Math Sem Hamburg* **6**, 8–54.

[28] Brothers N, Evans S, Taalman L, Van Wyk L, Witczak D and Yarnall C (2010). Spiral knots. *Missouri J Math Sci* **22**(1), 10–18.

[29] Burau K (1933). Kennzeichnung von Schlauchknoten. *Abh Math Sem Hamburg* **9**, 125–133.

[30] Burau K (1934). Kennzeichnung von Schlauchverkettungen. *Abh Math Sem Hamburg* **10**, 285–297.

[31] Cha JC and Livingston C (2016). KnotInfo: Table of knot invariants. http://www.indiana.edu/ knotinfo. (Accessed 27th October 2016).

[32] Cherednik I and Philipp I (2016). DAHA and plane curve singularities. *(arXiv:1605.00978v3)*.

[33] Cisneros-Molina J and dos Santos R A (2010). About the existence of Milnor fibrations. In M Manoel, M R Fuster and C Wall, editors, *Real and complex singularities*, London Mathematical Society Lecture Note Series (380), chapter 6, pages 82–103. Cambridge Univeristy Press, Cambridge.

[34] Cisneros-Molina J, Seade J and Snoussi J (2011). Milnor fibrations for

real and complex singularities. In J Cogolludo-Agustín and E Hironaka, editors, *Topology of algebraic varieties and singularities*, Contemporary Mathematics (538), pages 345–362. AMS.

[35] Conway J (1970). An enumeration of knots and links and some of their algebraic properties. *Computational Problems in Abstract Algebra*, Proc Conf Oxford, 329–358.

[36] Coward A and Lackenby M (2014). An upper bound on Reidemeister moves. *American Journal of Mathematics* **136**(4), 1023–1066.

[37] Coward A (2006). Ordering the Reidemeister moves of a classical knot. *Algebr. Geom. Topol.* **6**, 659–671.

[38] Cromwell PR (2004). *Knots and links*. Cambridge University Press, Cambridge.

[39] de Klerk AAJJM, van der Veen RI, Dalhuisen JW and Bouwmeester D (2017). Knotted optical vortices in exact solutions to Maxwell's equations. *Phys Rev A* **95**, 053820.

[40] Dennis MR and Bode B (2017). Constructing a polynomial whose nodal set is the three-twist knot 5_2. *J Phys A* **50**, 265204.

[41] Dennis MR, King R, Jack B, O'Holleran K and Padgett M (2010). Isolated optical vortex knots. *Nature Physics* **6**, 118–121.

[42] Diao Y (2004). The additivity of the crossing number. *J Knot Theory Ramif* **13**(7), 857–866.

[43] Ehresmann C (1950) Les connexions infinitésimales dans un espace fibré différentiable. *Colloque de Topologie*, Bruxells, 29–55.

[44] Eisenbud D and Neumann W (1985). *Three-dimensional link theory and invariants of plane curve singularities*. Princeton University Press, Princeton.

[45] Elrifai EA and Morton HR (1994). Algorithms for positive braids. *Quart. J. Math. Oxford* **45**, No. 2, 479–497.

[46] Enciso A and Peralta Salas D (2012). Knots and links in steady solutions of the Euler equation. *Annals of Math.* **175**, 345–367.

[47] Enciso A and Peralta Salas D (2015). Existence of knotted vortex tubes in steady Euler flows. *Acta Math.* **214**(1), 61–134.

[48] Epstein DBA (with Cannon, Holt, Levey, Patterson and Thurston) (1992). *Word processing in groups*. Jones and Bartlett, MA.

[49] Faddeev LD (1975). Quantization of solitons. *Princeton Preprint IAS-75-QS70*.

[50] Faddev LD and Niemi AJ (1997). Stable knot-like structures in classical field theories. *Nature* **387**, 58.

[51] Feller P (2018). Private communication. unpublished.

[52] Franco N and González-Meneses J (2003). Conjugacy problem for braid groups and Garside groups. *J of Algebra* **266**(1), 112–132.

[53] Freyd P, Yetter D, Hoste J, Lickorish WB, Millett K and Ocneanu A (1985). A new polynomial invariant of knots and links. *Bull. Amer. Math. Soc.* **12**, 239–246.

[54] Garside FA (1969). The braid group and other groups. *Quart. J. Math. Oxford* **20**, No.78, 235–254

[55] Gittings TA (2004). Minimum braids: A complete invariant of knots and links. *(arXiv:math/0401051)*.

[56] Gold J (2013). A bound for orderings of Reidemeister moves. *Algebr. Geom. Topol.* **13**, 3099–3110.

[57] Goodrick RE (1972). Two bridge knots are alternating knots. *Pacific Journal of Mathematics* **40**(3), 561–564.

[58] Greene J (2013). Combinatorial methods in knot theory. Lecture notes, available at https://www2.bc.edu/joshua-e-greene/MT885S13/Lecture

[59] Gruber H (2003). Estimates for the minimal crossing number. *(arXiv: math/0303273)*.

[60] Hirsch MW (1976). *Differential topology*. Graduate Texts in Mathematics Vol. 33, Springer Verlag, New York.

[61] Hudson SR, Startsev E and Feibush E (2014). A new class of magnetic confinement device in the shape of a knot. *Physics of Plasmas* **21**, 010705.

[62] Ishikawa M (2017). Private communication. unpublished.

[63] Jennings P (2015). Cabling in the Skyrme-Faddeev model. *J Phys A* **48**(31), 315401.

[64] Jones VFR (1985). A polynomial invariant for knots via von Neumann algebras. *Bulletin of the AMS* **12**(1), 103–111.

[65] Kähler E (1929). Über die Verzweigung einer algebraischen Funktion zweier Veränderlichen in der Umgebung einer singulären Stelle. *Math Zeit* **30**, 188-204.

[66] Kamien RD and Mosna RA (2016). The topology of dislocations in smectic liquid crystals. *New J Phys* **18**, 053012.

[67] Kashaev RM (1997). The hyperbolic volume of knots from the quantum dilogarithm. *Letters in Mathematical Physics* **39**(3), 269–275.

[68] Kassel C and Turaev V (2008). *Braid groups*. Graduate Texts in Mathematics, Vol. 247, Springer Verlag, New York.

[69] Kauffman LH (1987). State models and the Jones polynomial. *Topology* **26**(3), 395–407.

[70] Kauffman LH, Simon J, Wolcott K and Zhao P (1993). Invariants of theta-curves and other graphs in 3-space. *Topology and its Applications* **49**, 193–216.

[71] Kauffman LH (1999). Virtual knot theory. *Europen Journal of Combinatorics* **20**(7), 663–690.

[72] Kawauchi A (1996). *A survey of knot theory*. Birkhäuser Verlag, Basel.

[73] Kedia H, Bialynicki-Birula I, Peralta-Salas D and Irvine WTM (2013). Tying knots in light fields. *Phys Rev Lett* **111**, 150404.

[74] Kedia H, Foster D, Dennis MR and Irvine WTM (2016). Weaving knotted vector fields with tunable helicity. *Phys Rev Lett* **117**, 274501.

[75] Kedia H, Peralta-Salas D and Irvine WTM (2017). When do knots in light stay knotted? *J Phys A* **51**(2), 025204.

[76] Khovanov M (2000). A categorification of the Jones polynomial. *Duke Math J* **101**(3), 359–426.

[77] Khovanov M and Rozansky L (2008). Matrix factorizations and link homology II. *Geom. Topol.* **12**(3), 1387–1425.

[78] Kim SJ, Stees R and Taalman L (2016). Sequences of spiral knot determinants. *Journal of Integer Sequences* **19**, 16.1.4.

[79] King RP (2011) *Knotting of optical vortices* PhD Thesis, University of Bristol and Southampton University.

[80] Kleckner D, Kauffman LH and Irvine WTM (2016). How superfluid vortex knots untie. *Nature Physics* **12**, 650–655.

[81] Lackenby M (2009). The crossing number of composite knots. *Journal of Topology* **2**(4), 747–768.

[82] Lax M, Louisell WH and McKnight WB(1975). From Maxwell to paraxial wave optics. *Phys Rev A* **11**(4), 1365–1370.

[83] Lê Dũng Tráng (1972). La monodromie n'a pas de points fixes. *J Fac Sci Univ Tokyo Sect IA Math* textbf22(3), 409–427.

[84] Lee SY and Seo M (2010). A formula for the braid index of links. *Topology and its Applications* **157**, 247–260.

[85] Lee SY (2004) On the Alexander polynomials of periodic links and related topics. *Trends in Mathematics* **7**, 75–86.

[86] Lickorish WB (1997). *An Introduction to knot theory*. Graduate Texts in Mathematics 175, Springer Verlag, New York

[87] Lickorish WB and Thistlewaite M (1988). Some links with non-trivial polynomials and their crossing numbers. *Comment Math Helv* **63**, 527–539.

[88] Liu X and Ricca RL (2012). The Jones polynomial for fluid knots from helicity. *J Phys A* **45**, 205501.

[89] Livingston C (1993). *Knot theory*. Cambridge University Press, Cambridge.

[90] Looijenga E (1971). A note on polynomial isolated singularities. *Ind Math (Proc)* **74**, 418–421.

[91] Machon T and Alexander GP (2014). Knotted defects in nematic liquid crystals. *Phys Rev Lett* **113**, 027801.

[92] Machon T and Alexander G (2016). Global defect topology in nematic liquid crystals. *Proc R Soc A* **472**, 20160265.

[93] Machon T (2015). *Aspects of geometry and topology in liquid crystalline phases*. PhD Thesis, University of Warwick.

[94] Malyutin A (2016). On the question of genericity of hyperbolic knots. *(arXiv:1612.03368)*.

[95] Markov AA (1935). Über die freie Äquivalenz der geschlossenen Zöpfe. *Recueil Math. Moscou* **1**, 73–78.

[96] Matveev S and Turaev V (2011). A semigroup of theta-curves in 3-manifolds. *Mosc Math J* **11**(4), 805–814.

[97] Maulik D (2016). Stable pairs and the HOMFLY polynomial. *Invent. Math.* **204**(3), 787–831.

[98] Menegon Neto A and Seade J (2017). On the Lê-Milnor fibration for real analytic maps. *Math. Nachr.* **209**, no. 2–3, 382–392.

[99] Milnor J (1968). *Singular points of complex hypersurfaces*. Princeton University Press, Princeton.

[100] Moffatt H (1969). The degree of knottedness of tangled vortex lines. *J Fluid Mech* **35**, 117–129.

[101] Murasugi K (1971). On periodic knots. *Comm Math Helv.* **46**, 162–177.

[102] Murasugi K (1987). Jones polynomials and classical conjectures in knot theory. *Topology* **26**, 187–194.

[103] Murasugi K (1987). Jones polynomials and classical conjectures in knot theory II. *Math Proc Camb Phil Soc* **102**, 317–318.

[104] Murasugi K (1991). On the braid index of alternating links. *Trans Am*

Math Soc **326**, 237–260.

[105] Ni Y (2007). Knot Floer homology detects fibred knots. *Invent. Math.* **170**(3), 577–608.

[106] Oblomkov A, Rasmussen J and Shende V (2012). The Hilbert scheme of a plane curve singularity and the HOMFLY homology of its link. *(arXiv:1201.2115)*.

[107] Oblomkov A and Rozansky L (2018). Affine Braid group, JM elements and knot homology. *(arXiv:1702.03569)*.

[108] Oblomkov A and Shende V (2012). The Hilbert scheme of a plane curve singularity and the HOMFLY polynomial of its link. *Duke Math J* **161**(7), 1277-1303.

[109] Ozsváth PS and Szabó Z (2004). Holomorphic disks and knot invariants. *Adv. Math.* **186**(1), 58–116.

[110] Pajitnov A, Rudolph L and Weber LK (2001). The Morse-Novikov number for knots and links. *Algebra i Analiz* **13**, 105–118. Translation in *St Petersburg Math J* **13** (2002), 417–451.

[111] Perron B (1982). Le nœud "huit" est algébrique réel. *Inv Math* **65**, 441–451.

[112] Rañada AF (1989). A topological theory of the electromagnetic field. *Letters in Mathematical Physics* **18**(2), 97–106.

[113] Rañada AF and Trueba JL (1996). Ball lightning an electromagnetic knot? *Nature* **383**, 32.

[114] Reidemeister K (1927). Elementare Begründung der Knotentheorie. *Abh. Math. Sem. Univ. Hamburg* **5**(1), 24-32.

[115] Rolfsen D (2003). *Knots and links.* AMS Chelsea Publishing, Providence, reprinted with corrections, originally published by Berkeley, CA: Publish or Perish in 1976.

[116] Rudolph L (1983). Algebraic functions and and closed braids. *Topology* **22**, 191–202.

[117] Rudolph L (1984). Some topologically-flat surfaces in the complex projective plane. *Comm Math Helv* **59**, 592–599.

[118] Rudolph L (1987). Isolated critical points of mappings from $\mathbb{R}^4$ to $\mathbb{R}^2$ and a natural splitting of the Milnor number of a classical fibred link : 1. Basic theory and examples. *Comm Math Helv* **62**, 630–645.

[119] Rudolph L (1989) Quasipositivity and new knot invariants. *Rev. Mat. Univ. Complutense Madrid* **2**, 85–109.

[120] Rudolph L (2001). Some knot theory of complex plane curves.

(arXiv:math/0106058).

[121] Rudolph L (2005). Knot Theory of complex plane curves. In Menasco W, Thistlethwaite MB, editors *Handbook of Knot Theory*, Chapter 8, 349–428.

[122] Schubert H (1954). Über eine numerische Knoteninvariante. *Math. Zeit.* **61**, 245–288.

[123] Schubert H (1956). Knoten mit zwei Bruecken. *Math. Zeit.* **65**, 133–170.

[124] Seade J (2006). *On the topology of isolated singularities in analytic spaces*. Progress in Mathematics, Volume 241, Birkhäuser Verlag, Basel, Boston, Berlin.

[125] Shapira A (2016). *Extremal graph theory*. Lecture Notes, Tel-Aviv University.

[126] Soret M and Ville M (2016). Lissajous-toric knots. *(arXiv:1610.04418)*.

[127] Stallings JR (1962). On fibering certain 3-manifolds. In Fort MK editor *Topology of 3-manifolds and related topics* Proceedings of the University of Georgia Institute, Prentice-Hall.

[128] Stallings JR (1978). Constructions of fibred knots and links. *Proceedings of Symposia in Pure Mathematics* **32**, 55–60.

[129] Sutcliffe P (2007). Knots in the Skyrme-Faddeev model. *Proc R Soc A* **463**, 3001–3020.

[130] Taylor AJ and Dennis MR (2016). Vortex knots in tangles quantum eigenfunctions. *Nature Comm* **7**, 12346.

[131] Thistlethwaite MB (1987). A spanning tree expansion of the Jones polynomial. *Topology* **26**, 297–309.

[132] Thistlethwaite MB (1988). Kauffman's polynomial and alternating links. *Topology* **27**, 311–318.

[133] Thomson W (Lord Kelvin) (1867). On vortex atoms. *Proceedings of the Royal Society of Edinburgh* **VI**, 94–105.

[134] Turaev V (2012). Knotoids. *Osaka Journal of Mathematics* **49**(1), 195–223.

[135] Viro O (2001). Encomplexing the writhe. In V Turaev and A Vershik, editors, *Topology, Ergodic Theory, Real Algebraic Geometry. Rokhlin's Memorial*, volume 202 of *Transl. Ser. 2*, pages 241–256. AMS.

[136] Witten E (1989). Quantum field theory and the Jones polynomial. *Communications in Mathematical Physics* **121**(3), 351–399.